

Fiscal Year 2016: Second Quarter

Progress Report
**Advanced Battery Materials
Research (BMR) Program**

Released June 2016
for the period of January – March 2016

Approved by

Tien Q. Duong, Advanced Battery Materials Research Program Manager
Vehicle Technologies Office, Energy Efficiency and Renewable Energy

TABLE OF CONTENTS

A Message from the Advanced Battery Materials Research Program Manager.....	1
Task 1 – Advanced Electrode Architectures	3
Task 1.1 – Higher Energy Density via Inactive Components and Processing Conditions (Vincent Battaglia, Lawrence Berkeley National Laboratory)	4
Task 1.2 – Electrode Architecture-Assembly of Battery Materials and Electrodes (Karim Zaghib, HydroQuebec).....	6
Task 1.3 – Design and Scalable Assembly of High-Density, Low-Tortuosity Electrodes (Yet-Ming Chiang, Massachusetts Institute of Technology)	9
Task 1.4 – Hierarchical Assembly of Inorganic/Organic Hybrid Si Negative Electrodes (Gao Liu, Lawrence Berkeley National Laboratory)	11
Task 2 – Silicon Anode Research.....	14
Task 2.0 – Novel Non-Carbonate Based Electrolytes for Silicon Anodes (Dee Strand, Wildcat Discovery Technologies).....	15
Task 2.1 – Development of Silicon-Based High Capacity Anodes (Ji-Guang Zhang and Jun Liu, PNNL; Prashant Kumta, University of Pittsburgh; Jim Zheng, PSU)	18
Task 2.2 – Pre-Lithiation of Silicon Anode for High-Energy Li Ion Batteries (Yi Cui, Stanford University)	20
Task 3 – High-Energy Density Cathodes for Advanced Lithium-ion Batteries.....	23
Task 3.1 – Studies of High Capacity Cathodes for Advanced Lithium-ion Systems (Jagjit Nanda, Oak Ridge National Laboratory)	24
Task 3.2 – High-Energy Density Lithium Battery (Stanley Whittingham, SUNY Binghamton)	27
Task 3.3 – Development of High-Energy Cathode Materials (Ji-Guang Zhang and Jianming Zheng, Pacific Northwest National Laboratory)	30
Task 3.4 – <i>In situ</i> Solvothermal Synthesis of Novel High-Capacity Cathodes (Feng Wang and Jianming Bai, Brookhaven National Laboratory)	33
Task 3.5 – Novel Cathode Materials and Processing Methods (Michael M. Thackeray and Jason R. Croy, Argonne National Laboratory)	36
Task 3.6 – Lithium-bearing Mixed Polyanion (LBMP) Glasses as Cathode Materials (Jim Kiggans and Andrew Kercher, Oak Ridge National Laboratory)	39
Task 3.7 – Advanced Cathode Materials for High-Energy Lithium Ion Batteries (Marca Doeff, Lawrence Berkeley National Laboratory)	41
Task 3.8 – Lithium Batteries with Higher Capacity and Voltage (John B. Goodenough, UT-Austin).....	44
Task 3.9 – Exploiting Co and Ni Spinel in Structurally Integrated Composite Electrodes (Michael M. Thackeray and Jason R. Croy, Argonne National Laboratory).....	46
Task 3.10 – Discovery of High-energy Li ion Battery Materials (Wei Tong, Lawrence Berkeley National Laboratory)	49

Task 4 – Electrolytes for High-Voltage, High-Energy Lithium-Ion Batteries.....52

Note: This task is now closed. The BMR will issue a call in this area later this fiscal year.

Task 5 – Diagnostics53

Task 5.1 – Design and Synthesis of Advanced High-Energy Cathode Materials (Guoying Chen, Lawrence Berkeley National Laboratory) 54

Task 5.2 – Interfacial Processes – Diagnostics (Robert Kostecki, Lawrence Berkeley National Laboratory).....57

Task 5.3 – Advanced *in situ* Diagnostic Techniques for Battery Materials (Xiao-Qing Yang and Xiqian Yu, Brookhaven National Laboratory) 60

Task 5.4 – NMR and Pulse Field Gradient Studies of SEI and Electrode Structure (Clare Grey, Cambridge University)62

Task 5.5 – Optimization of Ion Transport in High-Energy Composite Cathodes (Shirley Meng, UC San Diego)65

Task 5.6 – Analysis of Film Formation Chemistry on Silicon Anodes by Advanced *In situ* and *Operando* Vibrational Spectroscopy (Gabor Somorjai, UC Berkeley, and Phil Ross, Lawrence Berkeley National Laboratory)68

Task 5.7 – Microscopy Investigation on the Fading Mechanism of Electrode Materials (Chongmin Wang, Pacific Northwest National Laboratory).....70

Task 5.8 – Characterization and Computational Modeling of Structurally Integrated Electrodes (Michael M. Thackeray and Jason R. Croy, Argonne National Laboratory)73

Task 6 – Modeling Advanced Electrode Materials76

Task 6.1 – Electrode Materials Design and Failure Prediction (Venkat Srinivasan, Lawrence Berkeley National Laboratory)77

Task 6.2 – Predicting and Understanding Novel Electrode Materials from First-Principles (Kristin Persson, Lawrence Berkeley National Laboratory).....79

Task 6.3 – First Principles Calculations of Existing and Novel Electrode Materials (Gerbrand Ceder, MIT).....82

Task 6.4 – First Principles Modeling of SEI Formation on Bare and Surface/Additive Modified Silicon Anode (Perla Balbuena, Texas A&M University)84

Task 6.5 – A Combined Experimental and Modeling Approach for the Design of High-Current Efficiency Si Electrodes (Xingcheng Xiao, General Motors, and Yue Qi, Michigan State University) 87

Task 6.6 – Predicting Microstructure and Performance for Optimal Cell Fabrication (Dean Wheeler and Brian Mazzeo, Brigham Young University)90

Task 7 – Metallic Lithium and Solid Electrolytes	92
Task 7.1 – Mechanical Properties at the Protected Lithium Interface (Nancy Dudney, ORNL; Erik Herbert, UTK; and Jeff Sakamoto, UM)	94
Task 7.2 – Solid Electrolytes for Solid-State and Lithium-Sulfur Batteries (Jeff Sakamoto, University of Michigan)	97
Task 7.3 – Composite Electrolytes to Stabilize Metallic Lithium Anodes (Nancy Dudney and Frank Delnick, Oak Ridge National Laboratory).....	99
Task 7.4 – Overcoming Interfacial Impedance in Solid-State Batteries (Eric Wachsman, Liangbing Hu, and Yifei Mo, University of Maryland, College Park)	101
Task 7.5 – Nanoscale Interfacial Engineering for Stable Lithium Metal Anodes (Yi Cui, Stanford University)	103
Task 7.6 – Lithium Dendrite Suppression for Lithium-Ion Batteries (Wu Xu and Ji-Guang Zhang, Pacific Northwest National Laboratory)	106
Task 8 – Lithium Sulfur Batteries	109
Task 8.1 – New Lamination and Doping Concepts for Enhanced Li – S Battery Performance (Prashant N. Kumta, University of Pittsburgh).....	111
Task 8.2 – Simulations and X-ray Spectroscopy of Li-S Chemistry (Nitash Balsara, Lawrence Berkeley National Laboratory)	115
Task 8.3 – Novel Chemistry: Lithium Selenium and Selenium Sulfur Couple (Khalil Amine, Argonne National Laboratory)	118
Task 8.4 – Multi-Functional Cathode Additives (MFCA) for Li-S Battery Technology (Hong Gan, Brookhaven National Laboratory, and Co-PI Esther Takeuchi, Brookhaven National Laboratory and Stony Brook University).....	121
Task 8.5 – Development of High-Energy Lithium-Sulfur Batteries (Jie Xiao and Jun Liu, Pacific Northwest National Laboratory)	124
Task 8.6 – Nanostructured Design of Sulfur Cathodes for High-Energy Lithium-Sulfur Batteries (Yi Cui, Stanford University).....	127
Task 8.7 – Addressing Internal “Shuttle” Effect: Electrolyte Design and Cathode Morphology Evolution in Li-S Batteries (Perla Balbuena, Texas A&M University).....	129
Task 8.8 – Mechanistic Investigation for the Rechargeable Li S Batteries (Deyang Qu, U Wisconsin - Milwaukee; Xiao-Qing Yang, BNL)	132
Task 8.9 – Statically and Dynamically Stable Lithium Sulfur Batteries (Arumugam Manthiram, U Texas - Austin).....	134
Task 9 – Li-Air Batteries	137
Task 9.1 – Rechargeable Lithium-Air Batteries (Ji-Guang Zhang and Wu Xu, PNNL).....	138
Task 9.2 – Efficient Rechargeable Li/O ₂ Batteries Utilizing Stable Inorganic Molten Salt Electrolytes (Vincent Giordani, Liox)	141
Task 9.3 – Li-Air Batteries (Khalil Amine, ANL).....	144
Task 10 – Na-ion Batteries	147
Task 10.1 – Exploratory Studies of Novel Sodium-Ion Battery Systems (Xiao-Qing Yang and Xiqian Yu, Brookhaven National Laboratory)	148

LIST OF FIGURES

Figure 1. Scanning electron microscopy of the cross section of electrodes prepared with two different molecular weights: (left) low molecular weight binder, and (right) high molecular weight binder.	5
Figure 2. Energy dispersive X-ray results of the cross section of the two laminates of Figure 1. The numbers embedded in the figures refer to the composition in order from current collector up to the surface. More details will be provided at the Annual Merit Review poster session.	5
Figure 3. Particle size distribution with different milling conditions: (a) 1 mm dia./25%/2200 rpm, (b) 1 mm dia./10%/2200 rpm, (c) 1 mm dia./10%/3000 rpm, and (d) 0.3 mm dia./10%/3000 rpm; bead size/solid content/agitating speed.....	7
Figure 4. Scheme of the nano-Si/C composite processing by the spray dry technique.	7
Figure 5. Scanning electron microscopy images: (a) nano-Si/C composite, and (b) cross section view of nano-Si/C composite.	8
Figure 6. Directional-freeze-cast graphite anode (left) subjected to dynamic stress testing (middle) yielded voltage-area capacity results (right). The voltage limits reached on delithiation (discharge of a Li-ion cell) become limiting as the graphite anode is systematically delithiated. Surprisingly, charge acceptance (lithiation of graphite) appears to have significantly faster kinetics than discharge. The anode tested has 14.7 mAh/cm ² theoretical capacity and is 800 μm thick.	10
Figure 7. Histograms of atomic force microscopy rupture force distribution corresponding to pulling a single polymer chain from a glass surface. Mean rupture forces ± standard deviations. n= number of observations. (a) PVDF, (b) CMC, (c) PPy, (d) PAA, and (e) PPyMAA.	12
Figure 8. Wildcat pouch cells perform similar to high throughput cells on Cycle 1.	16
Figure 9. Cycle life in Wildcat pouch cells is similar to high throughput cells.....	16
Figure 10. Anode delamination is observed after cycling.....	16
Figure 11. Cycled anodes show significant reduction in capacity when re-tested in half cells.	17
Figure 12. Cycled cathode capacity is only slightly reduced when re-tested in half cells.	17
Figure 13. (a) Initial lithiation/delithiation voltage profiles at 0.05C. (b) Specific capacity as a function of cycle number at 0.2C. (c) Rate capability of HC-nSi/G at various discharging C-rates (charging C-rate fixed at 0.2C) for HC-nSi/G. (d) Plot of areal capacity retention of HC-nSi/G with electrode composition ratio (active material:carbon black:binder = 7:1:2).	19
Figure 14. Voltage vs specific capacity plot of (nc-Si+(MM') _n O _x)/carbon nanofiber electrode tested in a Li-ion half-cell. Inset: differential capacity plots of (nc-Si+(MM') _n O _x)/carbon nanofiber electrode.	19

Figure 15. Fabrication and electrochemical characteristics of the N-Co/N-Li ₂ O composite. (a) Schematic of the fabrication process of the N-M/N-Li ₂ O composites. MOs are used as the starting materials and <i>in situ</i> converted into N-M/N-Li ₂ O composites via the chemical reaction with molten Li. (b) The initial charge potential profiles of the electrodes made with various Co/Li ₂ O nanocomposites: Micrometer-sized Co/nanometer-sized Li ₂ O (M-Co/N-Li ₂ O), submicrometer-sized Co/nanometer-sized Li ₂ O (SM-Co/N-Li ₂ O) and N-Co/N-Li ₂ O composites. (c) The charge/discharge potential profiles of the N-Co/N-Li ₂ O electrode after the first charge process. (d) The initial charge potential profiles of the LiFePO ₄ electrodes with different amounts of the N-Co/N-Li ₂ O additive in half cell configurations. (e-f) The initial charge/discharge potential profiles (e) and cycling performance (f) of LiFePO ₄ /graphite full cells with and without the N-Co/N-Li ₂ O additive. The specific capacities of the cathodes are evaluated based on the weight of LiFePO ₄ and the N-Co/N-Li ₂ O additive.	21
Figure 16. (left) X-ray diffraction pattern of pristine Li ₂ CuO ₂ (x = 0.0) and the fluorinated compositions. (right) Scanning electron microscopy of x=0.05 composition showing Cu and F distribution.	25
Figure 17. Comparison of 1 st cycle performance of fluorinated versus pristine Li ₂ CuO ₂ cathodes.	25
Figure 18. (left) Cycling behavior. (right) Rate capability of a LiVOPO ₄ electrode.	28
Figure 19. Cycling of Cu _{0.5} Fe _{0.5} F ₂ using a PEO-based electrolyte	28
Figure 20. (a) Initial voltage profiles versus specific capacity. (b) Cycling performance. (c) Scanning electron microscopy images before cycling. (d) Scanning electron microscopy images after cycling. (e) Electrochemical impedance spectra before cycling. (f) Electrochemical impedance spectra after cycling of LiNi _{0.76} Mn _{0.14} Co _{0.10} O ₂ cathodes prepared at different calcination temperatures and cycled in the voltage range of 2.7-4.5 V. (1C = 200 mA g ⁻¹ , loading: ca. mg cm ⁻²). The scale bars in (c) and (d) are 5 μm and 1 μm, respectively.	31
Figure 21. <i>In situ</i> X-ray diffraction patterns for tracking structural evolution during solid-state synthesis of LiNi _{0.8} Co _{0.2} O ₂	34
Figure 22. Phase evolution (a) and structural ordering (b) with sintering during synthesis of LiNi _{0.8} Co _{0.2} O ₂ obtained from structure refinement of the <i>in situ</i> X-ray diffraction data.	34
Figure 23. (a) First-cycle voltage profiles of LiCoO ₂ (black), 0.95LiCoO ₂ •0.05Li _{1.1} Mn _{1.9} O ₄ (red), and 0.90LiCoO ₂ •0.10Li _{1.1} Mn _{1.9} O ₄ (blue). (b) Corresponding capacity vs. cycle data (4.6-2.0 V, 15 mA/g). (c) 0.95LiCoO ₂ •0.05Li _{1.1} Mn _{1.9} O ₄ coated with ~0.5 nm AlW _x F _y cycled between 4.5-3.0 V. (All data vs. Li/Li ⁺ at 30°C, 15 mA/g). Inset shows dQ/dV plots of cycles 1 (black) and 50 (red). Stars indicate phase transitions in LCO.	37
Figure 24. Antimony-based glasses demonstrated a high-capacity conversion reaction, but not the desired multi-valent intercalation reaction.	40
Figure 25. Ag-based and Ni-based phosphate-borate-vanadate (PBV) glasses were compared to phosphate-vanadate glasses.	40
Figure 26. The 1 st charge curve of NMC-622 materials cycled to 5.0 V vs. Li	42
Figure 27. <i>In situ</i> X-ray diffraction patterns of NMC-622 upon charge to 5.0 V at C/10. The 2θ angles have been converted to those corresponding to the Cu Kα radiation.	42
Figure 28. (left) Ionic conductivity of the Li-glass as a function of temperature. (right) Real (ε') imaginary (ε'') permittivities and permittivity modulus (ε).	45

Figure 29. Results of chronopotentiometry (a galvanostatic direct current, DC, experiment as on a symmetric LiO/Li-glass/LiO cell with calcium-doped Li-glass, $\text{Li}_{2.99}\text{Ca}_{0.005}\text{OCl}$. The cell voltage was reversed every 20 min at a current of 0.10 mAcm^{-2} during 19 days in an argon-filled glove box.	45
Figure 30. Scanning transmission electron microscopy high angle annular dark field images of (a-c) LT- $\text{LiCo}_{0.9}\text{Ni}_{0.1}\text{O}_2$ (400°C) and (d) HT- $\text{LiCo}_{0.9}\text{Ni}_{0.1}\text{O}_2$ (800°C).	47
Figure 31. Scanning transmission electron microscopy high angle annular dark field images of IT- $\text{LiCo}_{0.9}\text{Ni}_{0.1}\text{O}_2$ (600°C) showing atomically integrated ‘layered-spinel’ nano-composite crystals.	47
Figure 32. Cycling performances of LiNiO_2 . Cells were cycled between 4.3 and 2.7 V at C/10 for the first two cycles, followed by C/5 in the subsequent cycles.	50
Figure 33. Synchrotron X-ray diffraction patterns of LiNiO_2 at (a) 4.3 V charging states and (b) 2.7 V discharging states in the selected cycles. The bottom patterns in these two figures are from pristine electrode reference. The green dash line denotes the (003) peak from H3 phase.	50
Figure 34. Extended X-ray absorption fine structure graphs for (a) charging and (b) discharging states.	50
Figure 35. (a) X-ray diffraction patterns of the synthesized $\text{LiM}_x\text{V}_{(1-x)}\text{PO}_4\text{F}$ samples. (b) First-cycle voltage profiles during galvanostatic charge-discharge at 16 mA/g . (c) Long-term cycling performance of the $\text{LiM}_x\text{V}_{(1-x)}\text{PO}_4\text{F}$ cathodes. * indicates peaks from $\text{Li}_3\text{V}_2(\text{PO}_4)_3$ phase.	55
Figure 36. (a) Fluorescence behavior during cycling of NMC-111 cathode. (b) <i>Ex situ</i> fluorescence spectra of NMC-111 electrodes cycled in 1 M LiPF_6 electrolytes with varying solvent. (c) Fluorescence spectra of Mn^{III} and Mn^{II} β -diketone complexes.	59
Figure 37. NMC thin film characterization results. (a) X-ray diffraction (b) Atomic force microscope topography of $4 \mu\text{m}$ area. (c) Topographic profiles from (b).	59
Figure 38. The reconstructed 3D transmission X-ray microscopy image of a particle cluster of fully concentration gradient $\text{LiNi}_{0.6}\text{Mn}_{0.2}\text{Co}_{0.2}\text{O}_2$ sample (left panel) with the color legend indicating the elemental distribution over the investigated 3D volume. By regrouping the voxels as a function of the shortest distance from the corresponding voxel to the outer surface, the project plots the normalized elemental concentration versus the voxel depth. As shown in the right panel, the different slopes in the concentration gradient were clearly observed. Notably, the elemental concentration over tens of millions of voxels were retrieved in this experiment, which provides good statistic of the depth profile as indicated by the color band in right panel.	61
Figure 39. Magnetic resonance imaging time series showing the evolution of the ^7Li electrolyte concentration profile (top) and the ^7Li chemical shift image of the metal (bottom) for the cell charged at 0.76 mA cm^{-2} . The two Li metal electrodes are located at z-positions of approximately, $\pm 4 \text{ mm}$. The intensity increase on the right hand side electrode, seen on passing current indicates the growth of Li microstructure. The onset of dendrite formation is seen in (c) (18.6 hours).	63
Figure 40. (a) Dendrite intensity and (b) electrolyte depletion near the right hand side Li electrode as a function of current (for 0.31 cm^{-1} electrodes). Arbitrary offsets have been applied to the data in the y direction.	63
Figure 41. Comparison between the Sands time and onset of dendrite formation/electrolyte depletion.	63
Figure 42. Scanning transmission electron microscopy/annular bright field images of (a) uncoated Li-rich material and (b) 1 wt% LLTO coated Li-rich. (c) Electron energy loss spectra of 1 wt% LLTO coated Li-rich at different regions. (d) Comparison of capacity and Coulombic efficiency for uncoated and LLTO-coated Li-rich over 190 cycles.	66

Figure 43. Annular dark field scanning transmission electron microscopy images of the Si in conventional electrolyte (a) after 1 cycle, (b) after 5 cycles, (c) after 100 cycles and the Si in electrolyte containing FEC, (d) after 1 cycle, (e) after 5 cycles, and (f) after 100 cycles.	66
Figure 44. This graph shows the SFG signal at open current potential of 1 M LiClO ₄ in EC, and EC : FEC (9:1, w/w) in contact with a-Si anode.	69
Figure 45. Scanning electron microscope scan of a-Si surface after cyclic voltammetry. Micron-sized LiF particles after cycling the anode for 10 CVs, 2.8 V ↔ 0.05 V at 0.1 mV / sec.	69
Figure 46. Scanning transmission electron microscopy high angle annular dark field image revealing the distinctive surface plane selective segregation of Ni and Co in Li-Mn-rich oxide cathodes. Ni exclusively segregates on the (200) type planes and forming a layer of spinel structure, while Co has a strong preference to segregate on (20-2)m plane with minimal on other planes and forms rock salt structure.	71
Figure 47. (a) Nominal (open symbols) and inductively coupled plasma measured (closed symbols) compositions of Li _{1.25-z} (Ni _{0.28} Mn _{0.53} Co _{0.19})O _y layered-layered-spinel, cathode powders. (b) X-ray diffraction patterns of the samples in (a) as a function of targeted spinel contents, x. (c) Simulated structure of composite Li ₂ Co ₂ O ₄ •Li ₂ MnO ₃ after removal of ½ Li from the Co spinel component.	74
Figure 48. (a) Relaxation behavior of Li-S cells previous discharged at different C-rates, which were recorded after the cells reached end of discharge. (b) Relaxation behavior at different C-rates of a Li-S cell that has been previously discharged to 1.5 V by C/10.	78
Figure 49. (a) ln (Eoc-Ess) versus Time (s). (b) Plot of linear region of curves in (b) with fitting line. (c) Extracted slopes of fitting lines at different C-rates.	78
Figure 50. Illustrations of the intra-layer (a) and inter-layer (c) Li migrations in the various local environments and corresponding minimum energy paths of the intra-layer (b) and the inter-layer (d) Li migrations.	80
Figure 51. Screening results for the LiA _{0.5} B _{0.5} O ₂ composition space. A circle represents each combination AB of transition metals. The color of the circle visualizes the predicted stability in terms of the estimated mixing enthalpy (bright green: more stable; dark: less stable), and the size of the circle indicates the tendency to disorder (small circle: strongly ordered; large circle: likely disordered).	83
Figure 52. Unprocessed X-ray diffraction spectrum of as-synthesized LiCo _{0.5} Zr _{0.5} O ₂ (thin black line) and refined spectrum based on the disordered rocksalt structure and the Li ₂ ZrO ₃ impurity phase (thick orange line). Li ₂ ZrO ₃ peaks are indicated with stars. The double-peak intensities are due to signals from Mo Kα1 and Kα2 radiation.	83
Figure 53. (a) Predicted Li ₂ CO ₃ decomposition barriers on Li(100) surfaces. C, O, and Li atoms are in grey, red, blue (orange for excess Li). (b) Same as (a), but for Li _{3.25} Si surfaces.	85
Figure 54. A LiF cluster (F blue, Li purple) is deposited over a Li _x Si slab (Si yellow, bottom layers not shown).	85
Figure 55. Two-dimensional AFM topographs of patterned a-Si electrode during first cycle at (a) 1.5 V, (b) 0.05 V, (c) 1.5 V, and during 2nd cycle at (d) 0.05 V and (e) 1.5 V. The contrast between center and edge regions of island is due to height differences proving the concept.	88
Figure 56. A continuum model established to describe how crack generates in the SEI layer.	88
Figure 57. Example of shape factors produced by the model for different geometries.	91

Figure 58. Standard (top) dynamic indentation with load, hold, and unload. Modified hold and load procedure required for lithium (bottom).....	95
Figure 59. Results for stepwise load and hold on 20 μ m lithium film. The harmonic analysis provides most reliable results at the end of the hold steps indicated by the red circles.....	95
Figure 60. Real (solid symbols) and imaginary (open symbols) of the impedance at room temperature for improved spray coated composite electrolyte.	100
Figure 61. Impedance of a battery with the spray coated composite electrolyte, Li vanadate cathode and Li metal anode. Cell voltage was 1.7 V.	100
Figure 62. Comparison of the cathode/electrolyte interfacial impedance on flat and 3D-structured garnet pellet: (left) electrochemical impedance plot, and (right) reduction of interfacial resistance versus increases in surface area.....	102
Figure 63. Calculated mutual reaction energy, ΔE_D , of garnet and Li-Al alloy interfaces.	102
Figure 64. Surface wetting of molten Li on different carbon materials, including carbon nanotubes film (a, f), carbon fiber paper (b, g), mesoporous carbon coated on Cu foil (c, h), electrospun carbon nanofiber (d, i) and GO film (e, j).	104
Figure 65. Schematic of the material design and the consequent synthetic procedures from a GO film (left) to a sparkled rGO film (middle) to a layered Li-rGO composite film (right). (b–d) Corresponding digital camera images and scanning electron microscopy images of the GO film (b), sparkled rGO film (c) and layered Li-rGO composite film (d). The diameters of the films shown in b–d are ~ 47 μ m.....	104
Figure 66. Rate capability of the LCO/Li-reduced graphene oxide and LCO/Li foil cells at various rates from 0.2 C to 10 C.....	104
Figure 67. Battery performances of Li LFP cells using different electrolytes. (a) Voltage profiles at the first cycle at C/20 rate and room temperature. (b) Cycling performance at C/2 charging and 1C discharging at 60°C. (c) Voltage profiles of the LiTFSI-LiBOB dual-salt electrolyte at selected cycles during cycling at 60°C.....	107
Figure 68. (a) Comparison of long-term cycling stability of Li NMC cells cycled at C/3 charge and C/3 or 1C discharge at room temperature. (b-c) Cross-sectional scanning electron microscopic images of cycled Li metal anodes at C/3 discharge (b) and 1C discharge (c). The thickness of fresh Li anode was about 400 μ m.	107
Figure 69. Schematic illustrations for mechanisms of SEI evolutions on Li metal anodes cycled at (a) low and (b) high discharge C rates.....	107
Figure 70. (a) Binding of infiltrated sulfur onto complex framework network. (b) X-ray photoelectron (XPS) spectroscopy S2p binding energy profile of (i) commercial separator (ii) commercial separator soaked in electrolyte; separators of (iii) commercial sulfur electrode (iv) CFN-1 (v) CFN-2 electrodes; (after 200 cycles at 0.2 C rate). (c) XPS C1s Binding Energy profile of slurry coated electrodes of (i) CFN-1, (ii) CFN-1 after 200 cycles, (iii) CFN-2, and (iv) CFN-2 after 200 cycles at 0.2 C rate.....	113
Figure 71. X-ray absorption spectroscopy of Li ₂ S ₄ in DGM and DMF.....	116
Figure 72. Photograph of <i>in situ</i> cell for X-ray absorption spectroscopy experiments (left) and sulfur K-edge XAS taken during discharge of new Li-S cell (right).	116

Figure 73. <i>In situ</i> high-energy X-ray diffraction study for S_8Se_2/Li cells during cycling with DOL-DME (up) and DOL-TTE (down) electrolytes.....	119
Figure 74. <i>In situ</i> 7Li NMR studies for S_8Se_2/Li cell during cycling with DOL-TTE electrolytes.....	119
Figure 75. Anode discoloration versus FeS_2 activation.....	122
Figure 76. X-ray photoelectron spectroscopy of anode recovered from cycled $S:FeS_2$ hybrid cell (2.6 V to 1.0 V).	122
Figure 77. TiS_2/Li_2S composite cell cycling.	122
Figure 78. Sulfur utilization – first discharge.	122
Figure 79. Hybrid $S:Ti_2S$ cycle life study.	122
Figure 80. (a) Charge/discharge curves of LG/S full cell in 5 M LiTFSI/DOL electrolyte without $LiNO_3$ and (b) corresponding cycling stability and Coulombic efficiency. (c) Transmission electron microscopy image of the graphite after five cycles with 5 M LiTFSI/DOL electrolyte in Li-Graphite half-cell and corresponding electron diffraction pattern (insert). (d) Focused ion beam – scanning electron microscopy cross-sectional image of a single graphite particle after 100 cycles with sulfur cathode. (e-f) Point electron diffraction spectroscopy at the very edge and core area of the graphite particle in (d), respectively.	125
Figure 81. Schematic of the polysulfide adsorption and diffusion on the surface of various nonconductive metal oxides. (a) The metal oxide with weak polysulfide adsorption capability; only few polysulfides can be captured by the oxide. (b) The metal oxide with both strong adsorption and good diffusion, which is favorable for the electrochemical reaction and the controllable deposition of sulfur species. (c) The metal oxide with strong bonding, but without good diffusion; the growth of lithium sulfide and the electrochemical reaction on the oxide/C surface will be impeded.	128
Figure 82. Electrochemical cycling performance and rate capability of Li-S cells. (a) Discharge performance depends strongly on C-rate while charging is weakly independent. (b) Charging behavior depends strongly on the depth of discharge.	130
Figure 83. High performance liquid chromatography / mass spectrometry analysis of the mixture of Na_2S and S_8 (mole ratio 1:3) in acetonitrile.	133
Figure 84. Distribution of polysulfide ions at various depths of discharge of a Li-S cell.....	133
Figure 85. Voltage profiles of carbon nanotube electrodes with LiTFSI-12DMSO electrolyte (a), LiTFSI-4DMSO electrolyte (b), and LiTFSI-3DMSO electrolyte (c), and their cycling performance at 0.1 mA cm^{-2} (d).	139
Figure 86. Scanning electron microscopy images of carbon nanotube based electrodes in charged state after 90 discharge/charge cycles with LiTFSI-3DMSO (a), LiTFSI-4DMSO (b), and LiTFSI-12DMSO (c), as well as the pristine carbon nanotube electrode without cycling (d).....	139
Figure 87. Cross-sectional scanning electron microscopy images of Li metal anodes in charged state after 90 discharge/charge cycles with LiTFSI-3DMSO (a), LiTFSI-4DMSO (b), and LiTFSI-12DMSO (c), as well as the pristine Li metal electrode without cycling (d).	139
Figure 88. (a) Tafel plot for NO_3^- electroreduction at glassy carbon rotating disk electrode (GC RDE) ($A = 0.196\text{ cm}^2$) at 150°C . (b) Tafel slope, charge transfer coefficient α , exchange current density j_0 for NO_3^- reduction reaction ($NO_3^- + 2e^- = NO_2^- + O_2^-$) at a GC RDE, under several different conditions.	142

Figure 89. Scanning electron microscopy image of as prepared Li-doped NiO nanorods used as oxygen reduction reaction cathode in molten nitrate O ₂ cells.	142
Figure 90. TEM Image of Ir nano-particles on an rGO surface. Scale bar is 2 nm.	145
Figure 91. Voltage profiles for (a) Infrared-reduced graphene oxide and (b) reduced graphene oxide cathode materials.....	145
Figure 92. Structure evolution upon Na extraction/insertion. <i>In situ</i> X-ray diffraction patterns collected during the first discharge/charge of the Na _{0.66} [Mn _{0.66} Ti _{0.34}]O ₂ Na half-cell under a current rate of C/10 at a voltage range between 1.5 and 3.9 V. For comparison, the 2 θ angle has been converted to values corresponding to the more common laboratory Cu Ka radiation (λ = 1.54 Å).	149

LIST OF TABLES

Table 1. Concentration of lithium polysulfide radical species in DMF versus TEGDME	116
Table 2. Materials chemistry database for group (i) spherical carbons.....	135
Table 3. Materials chemistry database for group (ii) – (iv) carbon materials.	136

A MESSAGE FROM THE ADVANCED BATTERY MATERIALS RESEARCH PROGRAM MANAGER

While a number of electric drive vehicles are available on the market today, further improvements in battery performance could make them more affordable and extend vehicle range. This document synthesizes recent Advanced Battery Materials Research (BMR) program investigations to identify novel electrode and electrolyte materials that may lead to enhanced battery performance and greater acceptance of electric vehicles. It also includes our efforts to advance diagnostics techniques used to identify degrading battery material mechanisms and provide a path for designing high performance materials. A few selected highlights from the BMR tasks performed during the period from January 2016 through March 2016 are summarized below:

- **Michigan Technological University.** Nanoindentation studies provided the first measure of Li hardness (force/indent area) of 0.015 GPa.
- **Stanford University.** Reduced graphene oxide films were shown to be effective hosts for lithium metal, providing good rate performance for a Li/LiCoO₂ cell.
- **University of Pittsburgh.** Chemical binding of sulfur with carbons generated in complex functional network materials indicated promising polysulfide retention and could lead to ultra-low fade rates in Li/S batteries.
- **Texas A&M University.** Density functional theory (DFT) techniques were used to examine the stability of Li₂CO₃, a prominent anode solid electrolyte interphase (SEI) component. It was shown that Li₂CO₃ decomposition on reactive anode surfaces is to be expected, and the innermost SEI should be composed of Li₂O (or LiF, if fluoride sources are present).
- **Brigham Young University.** Modeling and experiments have shown that standard electrode films have higher conductivity in-plane than out-of-plane by a factor of 1-4. This suggests that further structural optimization is needed to improve utilization of conductive additives in these films.
- **University of Texas, Austin.** A Li⁺ and Na⁺ electrolyte was developed having an ionic conductivity of 10⁻² to 10⁻¹ Scm⁻¹ at room temperature as well as a uniquely high dielectric constant owing to the presence of (OM)- dipoles.

In addition to conducting the research described herein, select BMR investigators periodically hold meetings to brainstorm about the key technical challenges confronting the development of advanced battery electrode and electrolyte materials. On March 15, 2016, BMR investigators held a Cathode Workshop at Oak Ridge National Laboratory. Stable, high-voltage cathode materials are a very important key for affordable, high energy density, lithium-ion batteries of the future. It is therefore important to understand the phenomena limiting their performance. The emphasis of the meeting was on: (1) high voltage redox and anionic stability, (2) irreversible structural transformation, and (3) interfacial stability. Principal Investigators from several institutions worked in a collaborative manner to address these complex issues. As a result of this effort, the Team recommended the following research strategies be undertaken as a path forward:

- Emphasize Ni-rich NMC, substituted excess lithium NMC spinel cathode materials, and promote efforts to ensure high voltage stability.
- Stabilize the structure and composition of multi-lithium polyanionic chemistries containing transition metal cations at higher oxidation state. Address the issue of oxygen evolution at voltages greater than 4.3 V.
- Exploit cation disorder cathode compositions that display no voltage fade or hysteresis (for example, Li_{1.21}Mo_{0.467}Cr_{0.3}O₂). Investigate reversible anionic redox activity.

We encourage you to follow our progress as we proceed. Our next report is expected to be available in October 2016.

Sincerely,

Tien Q. Duong

Manager, Advanced Battery Materials Research (BMR) Program

Energy Storage R&D

Vehicle Technologies Office

Energy Efficiency and Renewable Energy

U.S. Department of Energy

TASK 1 – ADVANCED ELECTRODE ARCHITECTURES

Summary and Highlights

Energy density is a critical characterization parameter for batteries for electric vehicles as there is only so much room for the battery and the vehicle needs to travel over 200 miles. The DOE targets are 500 Wh/L on a system basis and 750 Wh/L on a cell basis. Not only do the batteries need to have high energy density, they must also still deliver 1000 Wh/L for 30 seconds at 80% depth of discharge. To meet these requirements not only entails finding new, high energy density electrochemical couples, but also highly efficient electrode structures that minimize inactive material content, allow for expansion and contraction from one to several thousand cycles, and allow full access to the active materials by the electrolyte during pulse discharges. In that vein, the DOE Vehicle Technology Office (VTO) supports four projects in the BMR Program under Advanced Electrode Architectures: (1) Higher Energy Density via Inactive Components and Processing Conditions, LBNL, (2) Assembly of Battery Materials and Electrodes, HydroQuebec (HQ), (3) Design and Scalable Assembly of High-Density, Low-Tortuosity Electrodes, Massachusetts Institute of Technology (MIT), and (4) Hierarchical Assembly of Inorganic/Organic Hybrid Si Negative Electrodes, LBNL.

The four subtasks take two general engineering approaches to improving the energy density. Subtasks 1 and 3 attempt to increase energy density by making thicker electrodes and reducing the overall amount of inactive components per cell. Subtasks 2 and 4 attempt to increase the energy density of Li-ion cells by replacing graphitic anodes with Si-based active materials. All four attempts are based on determining a suitable binder and a proper methodology for assembling the active material.

The problem being addressed with the first approach is that the salt in the electrolyte must travel a further distance to meet the current throughout the entire discharge. If the salt cannot reach the back of the electrode at the discharge rates required of batteries for automobiles, the battery is said to be running at its limiting current. If the diffusional path through the electrode is tortuous or the volume for electrolyte is too low, the limiting current is reduced. Another problem with thicker electrodes is that they tend to not cycle as well as thinner electrodes and thus reach the end-of-life condition sooner, delivering fewer cycles.

The issue with the second approach is that silicon suffers from two major problems, both associated with the 300% volume change the material experiences as it goes from a fully delithiated state to a fully lithiated one: (1) the change results in freshly exposed surface area to electrolyte during cycling that consumes electrolyte and results in a lithium imbalance between the two electrodes, and (2) the volume change causes the particles to become electrically disconnected, which is further enhanced if particle fracturing also occurs, during cycling.

Highlight. This quarter, Zaghib's group (HQ) developed a series of processes that allows them to go from large chunks of Si to small composite Si/C/binder spheres of 5 to 60 microns diameter.

Task 1.1 – Higher Energy Density via Inactive Components and Processing Conditions (Vincent Battaglia, Lawrence Berkeley National Laboratory)

Project Objective. Thicker electrodes with small levels of inactive components that can still deliver most of their energy at C-rates of C/3 should result in batteries of higher energy density. Higher energy density should translate to more miles per charge or smaller, less expensive batteries. Unfortunately, the limit to making thicker electrodes is not based on power capability but on mechanical capability; for example, thicker electrodes delaminate from the current collector during calendaring and slicing. The objective of this research is to produce a high energy density electrode with typical Li-ion components that does not easily delaminate and still meets the electric vehicle (EV) power requirements through changes to the polymer binder and concomitant changes to the processing conditions.

Project Impact. Today's batteries cost too much on a per kWh basis and have too low of an energy density to allow cars to be driven over 300 miles on a single charge. This research targets both of these problems simultaneously. By developing thicker, higher energy-density electrodes, the fraction of cost relegated to inactive components is reduced, and the amount of energy that can be introduced to a small volume can be increased. Macroscopic modeling suggests that this could have as much as a 20% impact on both numbers.

Out-Year Goals. In the first year, the project will change its binder supplier to a U.S. supplier willing to provide binders of differing molecular weights. The project will then establish the workability of the new binders, establish a baseline binder and processing conditions, and determine how thick an electrode can be made from the project's standard processes for making moderately thick electrodes.

In the outgoing years, changes will be made to the binder molecular weight and electrode processing conditions to whatever degree is necessary to increase the energy density while maintaining power capability. Changes in the processing conditions can include the time of mixing, rate of casting, temperature of the slurry during casting, drying conditions, and hot calendaring. Chemical modifications may include multiple binder molecular weights and changes in the conductive additive.

Collaborations. This project has collaborations with Zaghbi's Group (HQ) for materials and cell testing; Wheeler's Group (Brigham Young University, BYU) for modeling analysis; Liu's group on polymer properties; Arkema for binders; and a commercial cathode material supplier.

Milestones

1. Fabricate laminates of NCM cast to different thicknesses using standard materials and various processing conditions to determine how thick one can cast an electrode that does not display cracking or delamination. (Q1 – Complete)
2. Fabricate laminates of NCM cast to different thicknesses using higher molecular weight binders and various processing conditions to determine how thick one can cast an electrode that does not show cracking or delamination. (Q2 – Complete)
3. Fabricate laminates of NCM cast to different thicknesses using standard materials and various processing conditions on current collectors with a thin layer of binder and conductive additive pre-coated on the current collector to determine how thick one can cast an electrode that does not show cracking or delamination. (Q3)
4. *Go/No-Go.* Determine if a higher molecular weight binder is worth pursuing to achieve thicker electrodes based on ease of processing and level of performance. If no, pursue a path of polymer-coated current collectors. (Q4)

Progress Report

Milestone 2. This quarter, electrodes were cast using a high molecular-weight PVdF binder (HMWB, ca. 1,000,000 g/mol). The difference in preparing a slurry with high molecular weight binder and low molecular weight binder (LMWB) is that more NMP is needed for the former. Despite the need for more NMP, the slurry has a relatively high viscosity. A high viscosity appears beneficial for two reasons: (1) thick castings require higher viscosity to prevent them from collapsing and running off the current collector, and (2) higher viscosities appear to help prevent the accumulation of conductive agent on the surface of the electrode as the laminate dries.

Scanning electron microscopy (SEM) of the cross sections of electrodes fabricated from two molecular weights, each approximately 200 microns thick, are provided in Figure 1. On the left, one observes a thin film (ca. 40 microns thick) on the top of the electrode produced when using a LMWB. The right panel shows no such film with the HMWB.

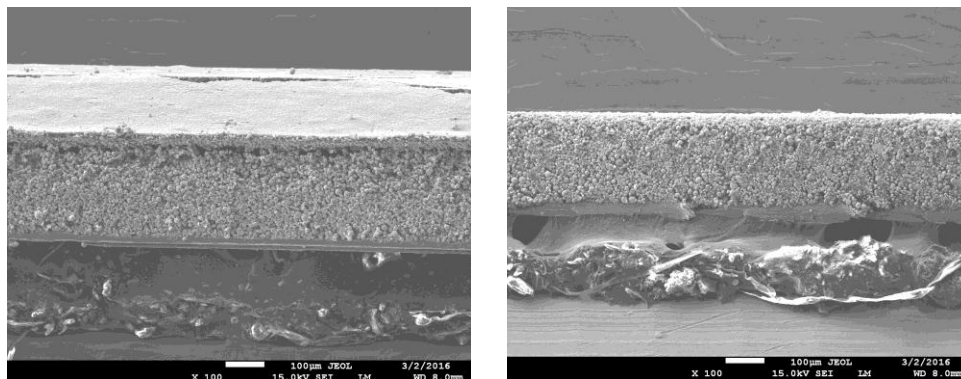


Figure 1. Scanning electron microscopy of the cross section of electrodes prepared with two different molecular weights: (left) low molecular weight binder, and (right) high molecular weight binder.

Figure 2 provides the results of energy dispersive X-ray (EDX) performed on the cross sections of these two electrodes from the current collector up to the surface. Here one observes (left panel, LMWB) a varying distribution, with oxygen (from the cathode) increasing up from the current collector to just before the surface, where it plunges, and carbon content (from conductive carbon and binder) decreasing up from current collector to just below the surface where it escalates. The right panel (HMWB) displays a more uniform distribution from top to bottom.

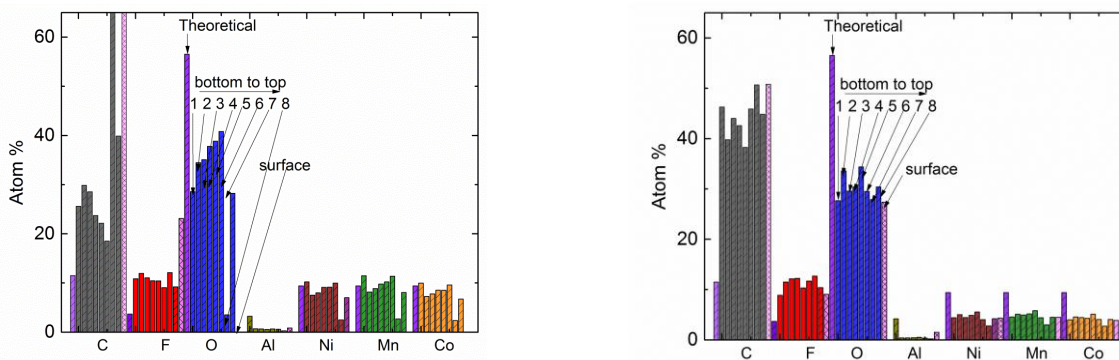


Figure 2. Energy dispersive X-ray results of the cross section of the two laminates of Figure 1. The numbers embedded in the figures refer to the composition in order from current collector up to the surface. More details will be provided at the Annual Merit Review poster session.

Task 1.2 – Electrode Architecture-Assembly of Battery Materials and Electrodes (Karim Zaghib, HydroQuebec)

Project Objective. The project goal is to develop an electrode architecture based on nano-silicon materials and design a full cell having high energy density and long cycle life. To achieve the objective, this project investigates the structure of nano-Si materials that provide acceptable volume change to achieve long cycle life, while still maintaining the high-capacity performance of Si. The project scope includes the control of the particle size distribution of nano-Si materials, crystallinity, Si composition, and surface chemistry of the nano-Si materials. The focus is to develop electrode formulations and electrode architectures based on nano-Si materials that require optimized nano-Si/C composites and functional binders, as well as a controlled pore distribution in the electrode and the related process conditions to fabricate the electrode.

Project Impact. Silicon is a promising alternative anode material with a capacity of ~4200 mAh/g, which is about an order of magnitude higher than that of graphite. However, many challenges inhibiting the commercialization of Si remain unresolved. The primary culprit is viewed as the large volume variations of Si during charge/discharge cycles that result in pulverization of the particle and poor cycling stability. Success in developing highly reversible Si electrodes with acceptable cost will lead to higher energy density and lower cost batteries that are in high demand, especially for expanding the market penetration for EVs.

Out-Year Goals. This project investigates several steps to prepare an optimized composition and electrode structure of Si-based anode. HydroQuebec will use its advanced *in situ* analysis facilities to identify the limitations of the developed Si-based anode materials. *In situ* SEM will be used to monitor crack formations in the particles along with delamination at the binder/particle and current collector/particle interfaces to improve the electrode architecture and cycle life.

Previously, serious gas evolution was observed during the mixing and coating steps of Si-based electrodes. To overcome these technical issues, surface treatment of the nano-Si powder will be considered to utilize the water-based binders. A physical or chemical surface coating to protect the nano-Si powders will be explored. The project will also explore approaches to optimize the particle size distribution (PSD) to achieve better performance.

To achieve high gravimetric energy density (Wh/kg), the electrode loading (mg/cm^2) is a critical parameter in the electrode design. By increasing the anode loading to $2 \text{ mg}/\text{cm}^2$, a higher energy density of more than 300 Wh/kg can be achieved. By utilizing an improved electrode architecture, higher energy cells will be designed with high loading electrodes of $> 3 \text{ mAh}/\text{cm}^2$. The energy density of these cells will be verified in the format of pouch-type full cells ($< 2 \text{ Ah}$); large format cells ($> 40 \text{ Ah}$) will be estimated accordingly.

Collaborations. This project collaborates with BMR members: V. Battaglia and G. Liu from LBNL, C. Wong and Z. Jiguang from PNNL, and J. Goodenough from the University of Texas (UT).

Milestones

1. Failure mode analysis of large-format cells manufactured in 2015. (December 2015 – Complete)
2. Finalize the structure of nano-Si composite. (March 2016 – Complete)
3. Finalize the architecture of nano-Si composite electrode. Go/No-Go: > 300 cycles (80% retention) with loading level of $> 3 \text{ mAh}/\text{cm}^2$ ($3 \text{ mg}/\text{cm}^2$ with 1000 mAh/g). (June 2016 – Ongoing)
4. Verification of performance in pouch-type full cell ($< 2 \text{ Ah}$). (September 2016 – Ongoing)

Progress Report

This quarter, HydroQuebec focused on optimizing the milling process to produce low price nano-Si powders. Several techniques were investigated.

Metallurgical Si is obtained as big chunks, which were crushed by the following steps: jaw crusher ($d_{50} < 13\text{mm}$), roll crusher ($d_{50} < 1\text{mm}$), and jet mill ($d_{50} < 10\mu\text{m}$). Then the powder was sieved with 150 mesh before wet milling. To reduce particle size, we controlled several process parameters such as: bead size (1.0 mm beads size versus 0.3 mm), solid content (25% solid content versus 10%) and milling power (2200 rpm versus 3000 rpm). Organic IPA (isopropyl alcohol) was used as the mixing media for wet milling.

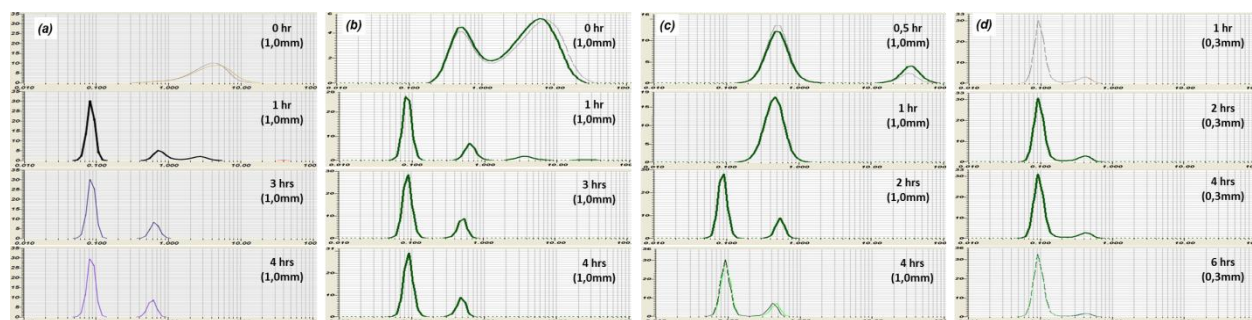


Figure 3. Particle size distribution with different milling conditions: (a) 1 mm dia./25%/2200 rpm, (b) 1 mm dia./10%/2200 rpm, (c) 1 mm dia./10%/3000 rpm, and (d) 0.3 mm dia./10%/3000 rpm; bead size/solid content/agitating speed.

The particle size analysis (Figure 3) shows clearly that at least 2 hours of milling time is required in all conditions. Reducing the solid content or increasing the power speed does not show any improvement in reducing the particle size. Nevertheless, using smaller beads of 0.3 mm shows some improvement regarding the second peak at 0.5 μm . The particles of this size are completely reduced after 6 hours of milling, approaching a monodispersed powder. In general, it seems that there is a limitation for particle reduction of this material around 100 nm.

The nano-Si powder that was milled to 100 nm was added to the solution of a spray-dry process with carbon and PAA (poly acrylic acid) to make secondary particles of the nano-Si/C composite, as described by the process scheme in Figure 4.

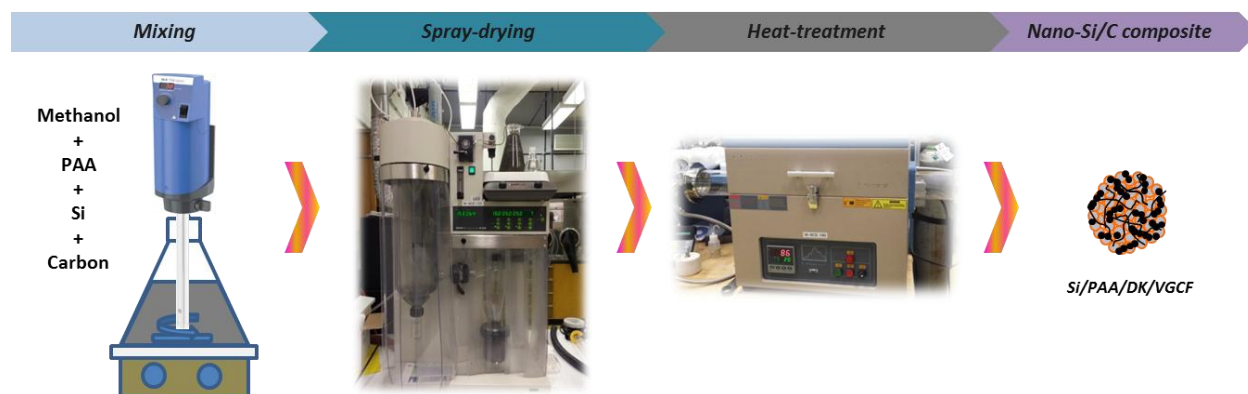


Figure 4. Scheme of the nano-Si/C composite processing by the spray dry technique.

The spray-dry process allows us to produce secondary particles of Si/C composite with 5 to 60 μm particle size (Figure 5a). Based on the cross section, the secondary particles consist of hollow nano-Si particles, with an interior that contains a mixture of polymer, carbon black, and a large fraction of void space (Figure 5b). The electrochemical evaluation will be conducted in the next quarter.

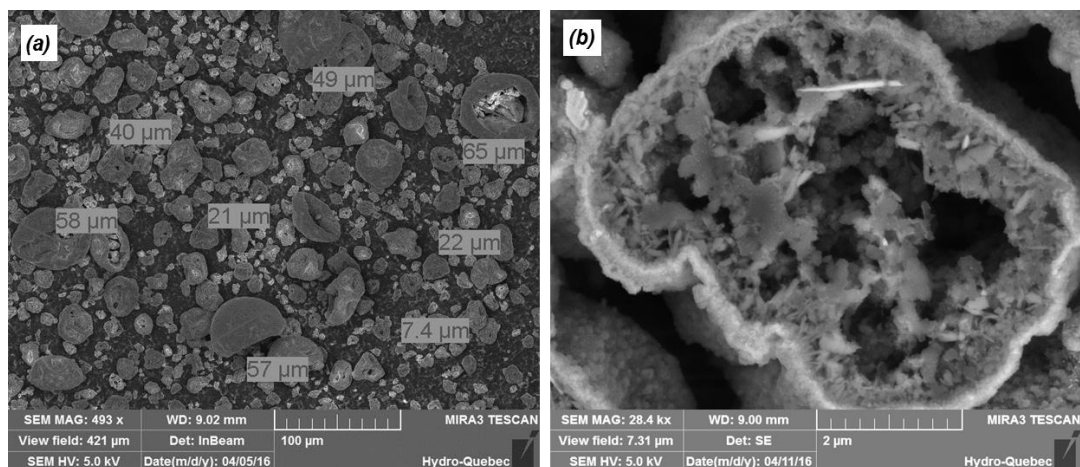


Figure 5. Scanning electron microscopy images: (a) nano-Si/C composite, and (b) cross section view of nano-Si/C composite.

Deliverable. 50 g of nano-Si/C powder made by the spray dry process was supplied as the first deliverable to LBNL for evaluation.

Task 1.3 – Design and Scalable Assembly of High-Density, Low-Tortuosity Electrodes (Yet- Ming Chiang, Massachusetts Institute of Technology)

Project Objective. The project objective is to develop scalable, high-density, low-tortuosity electrode designs and fabrication processes enabling increased cell-level energy density compared to conventional Li-ion technology, and to characterize and optimize the electronic and ionic transport properties of controlled porosity and tortuosity cathodes as well as densely sintered reference samples. Success is measured by the area capacity (mAh/cm^2) that is realized at defined C-rates or current densities.

Project Impact. The high cost (\$/kWh) and low energy density of current automotive lithium-ion technology is in part due to the need for thin electrodes and associated high inactive materials content. If successful, this project will enable use of electrodes based on known families of cathode and anode active compositions, but with at least three times the areal capacity (mAh/cm^2) of current technology while satisfying the duty cycles of vehicle applications. This will be accomplished via new electrode architectures fabricated by scalable methods with higher active materials density and reduced inactive content; this will in turn enable higher energy density and lower-cost EV cells and packs.

Approach. Two techniques are used to fabricate thick, high-density electrodes with low tortuosity porosity oriented normal to the electrode plane: (1) directional freezing of aqueous suspensions; and (2) magnetic alignment. Characterization includes measurement of single-phase material electronic and ionic transport using blocking and non-blocking electrodes with ac and dc techniques, electrokinetic measurements, and drive-cycle tests of electrodes using appropriate battery scaling factors for EVs.

Out-Year Goals. The out-year goals are as follows:

- Identify anodes and fabrication approaches that enable full cells in which both electrodes have high area capacity under EV operating conditions. Anode approach will include identifying compounds amenable to the same fabrication approach as cathode, or use of very high-capacity anodes, such as stabilized lithium or Si-alloys that in conventional form can capacity-match the cathodes.
- Use data from best performing electrochemical couple in techno-economic modeling of EV cell and pack performance parameters.

Collaborations. Within BMR, this project collaborates with Antoni P. Tomsia (LBNL) in fabrication of low-tortuosity, high-density electrodes by directional freeze-casting, and with Gao Liu (LBNL) in evaluating Si anodes. Outside of BMR, the project collaborates with Randall Erb (Northeastern University) on magnetic alignment fabrication methods for low-tortuosity electrodes.

Milestones

1. Obtain 2-, 10- and 30- sec pulse discharge data for an electrode of at least $10 \text{ mAh}/\text{cm}^2$ area capacity. (December 2015 – Revised and complete)
2. Test at least one cathode and one anode, each having at least $10 \text{ mAh}/\text{cm}^2$ area capacity under an accepted EV drive cycle. (March 2016 – Complete)
3. *Go/No-Go:* Demonstrate a cathode or anode having at least $10 \text{ mAh}/\text{cm}^2$ area capacity that passes an accepted EV drive cycle. (June 2016)
4. Construct and obtain test data for full cell in which area capacity of both electrodes is at least $10 \text{ mAh}/\text{cm}^2$. (September 2016)

Progress Report

Milestone 2. This quarter results are reported for Dynamic Stress Tests (DST) of graphite anodes prepared by directional freezing. Unlike cathodes for which results were previously reported, the graphite anodes cannot be sintered in air for densification, and therefore are tested in the lyophilized but nonheat-treated state. Aqueous suspensions were prepared using battery-grade graphite and CMC (carboxymethylcellulose) binder (5 wt% relative to the graphite) and containing no conductive carbon additive. The formulations are otherwise similar to suspensions for an aqueous electrode coating process for Li-ion. Directional freezing experiments were conducted in similar manner to previous experiments for cathodes prepared in this project, except for the absence of sintering. As shown in Figure 6, highly oriented low-tortuosity pore channels were obtained. The final porosity of the electrodes was 58 to 60 vol%. When sectioned to 800 μm thickness, the anodes have a theoretical area capacity of about 15 mAh/cm^2 . Half-cells were built using these anodes and Li-metal counterelectrodes. In the following discussion, “charge” refers to charging of a corresponding Li-ion cell (lithiation of the graphite anode), and “discharge” refers to discharging a corresponding Li-ion cell (delithiation of the graphite anode).

Previously, hybrid pulse power characterization (HPPC) tests of charge acceptance (lithiation) of this anode had shown that 15 mAh/cm^2 area capacity could be achieved without reaching the Li-plating limit. In the present tests, the DST protocol was applied to a half-cell beginning with a fully lithiated anode such that each DST cycle incrementally delithiates the anode (discharge of lithium ion cell). The DST cycle includes a maximum pulse delithiation rate of 2C and maximum pulse lithiation rate of 1C, and was repeated until a discharge voltage of 3V or charge voltage of 10 mV was reached. Figure 6 shows the surprising discovery that the voltage upon discharge is limiting. During the first two DST cycles, the cell voltage on charge did reach the cutoff of 10 mV vs Li/Li^+ , but thereafter remains well above the cutoff. On discharge, the cell voltage reaches the 3.0V cutoff at about 5 mAh/cm^2 , well short of the 15 mAh/cm^2 reached upon charging in the HPPC test. Current efforts are aimed at understanding the origin of the electrode kinetic limitations during discharge.

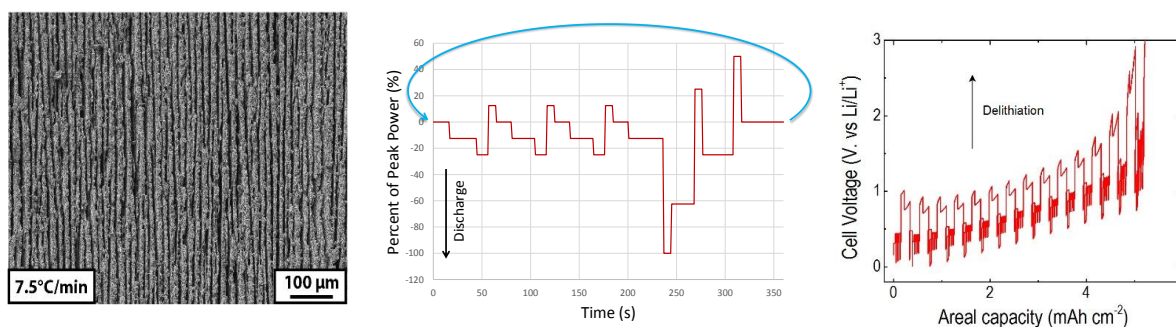


Figure 6. Directional-freeze-cast graphite anode (left) subjected to dynamic stress testing (middle) yielded voltage-area capacity results (right). The voltage limits reached on delithiation (discharge of a Li-ion cell) become limiting as the graphite anode is systematically delithiated. Surprisingly, charge acceptance (lithiation of graphite) appears to have significantly faster kinetics than discharge. The anode tested has 14.7 mAh/cm^2 theoretical capacity and is 800 μm thick.

Task 1.4 – Hierarchical Assembly of Inorganic/Organic Hybrid Si Negative Electrodes (Gao Liu, Lawrence Berkeley National Laboratory)

Project Objective. This work aims to enable silicon as a high-capacity and long cycle-life material for negative electrode to address two of the barriers of lithium-ion chemistry for EV and plug-in hybrid electric vehicle (PHEV) application: insufficient energy density and poor cycle life performance. The proposed work will combine material synthesis and composite particle formation with electrode design and engineering to develop high-capacity, long-life, and low-cost hierarchical Si-based electrode. State of the art Li-ion negative electrodes employ graphitic active materials with theoretical capacities of 372 mAh/g. Silicon, a naturally abundant material, possesses the highest capacity of all Li-ion anode materials. It has a theoretical capacity of 4200 mAh/g for full lithiation to the $\text{Li}_{22}\text{Si}_5$ phase. However, Si volume change disrupts the integrity of electrode and induces excessive side reactions, leading to fast capacity fade.

Project Impact. This work addresses the adverse effects of Si volume change and minimizes the side reactions to significantly improve capacity and lifetime to develop negative electrode with Li-ion storage capacity over 2000 mAh/g (electrode level capacity) and significantly improve the Coulombic efficiency to over 99.9%. The research and development activity will provide an in-depth understanding of the challenges associated with assembling large volume change materials into electrodes and will develop a practical hierarchical assembly approach to enable Si materials as negative electrodes in Li-ion batteries.

Out-Year Goals. The three main aspects of this proposed work (that is, bulk assembly, surface stabilization, and Li enrichment) are formulated into 10 tasks in a four-year period.

- Develop hierarchical electrode structure to maintain electrode mechanical stability and electrical conductivity. (bulk assembly)
- Form *in situ* compliant coating on Si and electrode surface to minimize Si surface reaction. (surface stabilization)
- Use prelithiation to compensate first cycle loss of the Si electrode. (Li enrichment)

The goal is to achieve a Si-based electrode at higher mass loading of Si that can be extensively cycled with minimum capacity loss at high Coulombic efficiency to qualify for vehicle application.

Collaborations. This project collaborates with the following: Vince Battaglia and Venkat Srinivasan of LBNL; Xingcheng Xiao of GM; Jason Zhang and Chongmin Wang of PNNL; and Phillip B. Messersmith of University of California at Berkeley (UC Berkeley).

Milestones

1. Investigate the impact of different side chain conducting moieties to the electric conductivity of the functional conductive binders. (December 2015 – Complete)
2. Quantify the adhesion group impact to the electrode materials and current collector. (March 2016 – Complete)
3. Fabricate higher loading electrode ($> 3 \text{ mAh/cm}^2$) based on the Si electrode materials and select binder; test cycling stability. (June 2016 – On schedule)
4. Fabricate NMC/Si full cell and quantify the performance. (September 2016)

Progress Report

To characterize the binding affinity between polymer binders and Si anode particles, the unbinding forces of different binders when pulling a single polymer chain from a silica substrate were investigated, taking into consideration that the higher the unbinding force of a single attached polymer chain, the stronger its affinity to the substrate. To ensure that the observed force originates from a single molecular event, a novel and complete screening protocol was developed (described in detail in the 2nd Publication) to reject the unbinding force when multiple chains are involved. Figure 7 thus shows the histogram of the averaged unbinding forces of pulling a single PVDF (polyvinylidene fluoride), CMC (carboxymethylcellulose), PPy (polypyrrole), PAA (polyacrylic acid), and PPyMAA (poly[1-pyrenemethyl methacrylate-co-methacrylic acid]) binder from a silica substrate at a constant speed. As shown, a single PPyMAA or PAA was more strongly attached to the silica substrate than the other single polymer chain binders tested. Although PAA has a higher density of carboxylic acid groups compared to PPyMAA, they demonstrate very similar single molecular binding forces. This may be because only limited carboxylic acid groups participate in the adhesion with SiO₂ and because PPyMAA (30% MAA) has already reached the critical number of carboxylic acid groups for the adhesion. PVDF, CMC, and PPy binders demonstrate similar single molecular adhesion forces, but lower than that of the PAA based binder. The binding mechanism between binders of PVDF, CMC, and PPy and SiO₂ differ significantly due to their structure differences. PVDF has C-F polar components, which exert polar-polar interactions with the SiO₂. CMC has both polar bonds, OH polar functional groups, and carboxylate sodium groups. The interaction between CMC with SiO₂ is similar to, but lower than, that of PAA. Although PPy is nonpolar, the binding force between PPy and SiO₂ is similar to CMC, perhaps because of the interaction between the polar surface of the SiO₂ and the extended π conjugation in the pyrene molecules.

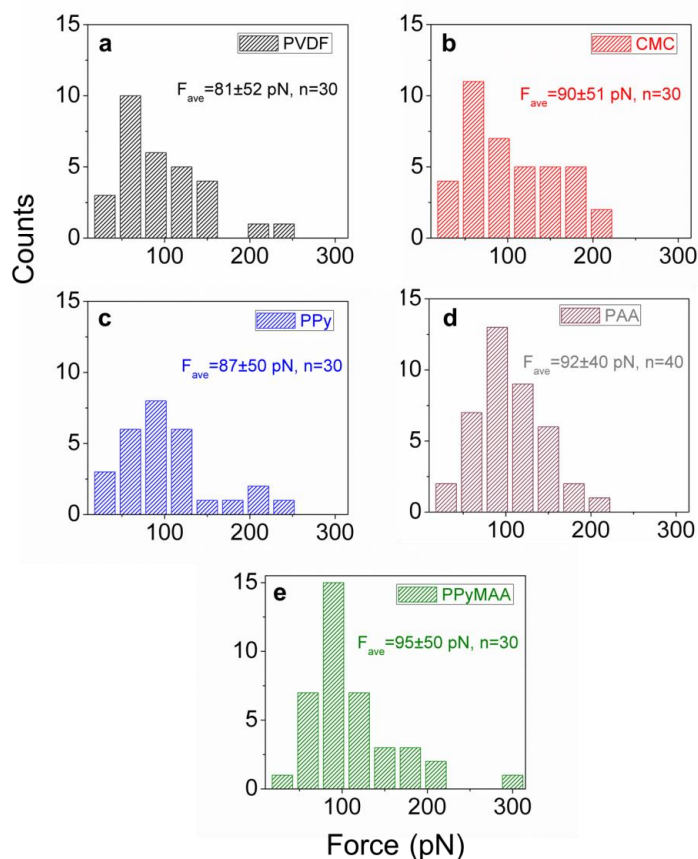


Figure 7. Histograms of atomic force microscopy rupture force distribution corresponding to pulling a single polymer chain from a glass surface. Mean rupture forces \pm standard deviations. n= number of observations. (a) PVDF, (b) CMC, (c) PPy, (d) PAA, and (e) PPyMAA.

Patents/Publications/Presentations

Patents

- Gao Liu, Guo Ai, Zhihui Wang, Donghai Wang, Sergey Lopatin, et al. Scalable Process for Application of Stabilized Lithium Metal Powder (SLMP®) in Li-ion Batteries. Patent application filed by Applied Material Inc. in February 2016.
- Gao Liu, Min Ling, and Changan Yang. Functional Polymer Binder for Sulfur Cathode Fabrication. Patent application filed by LBNL in February 2016; LBNL No. 2016-040.

Publications

- Ai, Guo, and Zhihui Wang, Hui Zhao, Wenfeng Mao, Yanbao Fu, Vincent Battaglia, Sergey Lopatin, and Gao Liu. “Scalable Process for Application of Stabilized Lithium Metal Powder in Li-ion Batteries.” *Journal of Power Sources* 309 (2016): 33-41.
- Zhao, Hui, and Wei Yang, Ruimin Qiao, Chenhui Zhu, Ziyan Zheng, Min Ling, Zhe Jia, Ying Bai, Yanbao Fu, Jinglei Lei, Xiangyun Song, Vincent Battaglia, Wanli Yang, Phillip Messersmith, and Gao Liu. “Conductive Polymer Binder for High-tap-density Nano-silicon Material for Lithium-ion Battery Negative Electrode Application.” *Nano Letters* 15 (2015): 7927-7932.

Presentations

- MRS Meeting, Phoenix, Arizona (March 2016): “High Loading Lithium Sulfur Batteries Achieved Through Multi-Functional Binders”; Min Ling, Changan Yang, Hui Zhao, Zhe Jia, Huali Wang, and Gao Liu. Invited.
- MRS Meeting, Phoenix, Arizona (March 2016): “Conductive Polymer Binder for High-tap-density Nano-silicon Material”; Hui Zhao, Yang Wei, Phillip B. Messersmith, and Gao Liu.

Task 2 – Silicone Anode Research

Summary and Highlights

Most Li-ion batteries used in state-of-the-art EVs contain graphite as their anode material. Limited capacity of graphite (LiC_6 , 372 mAh/g) is one barrier that prevents the long-range operation of EVs required by the EV Everywhere Grand Challenge proposed by the DOE/EERE. In this regard, silicon is one of the most promising candidates as an alternative anode for Li-ion battery applications. Si is environmentally benign and ubiquitous. The theoretical specific capacity of silicon is 4212 mAh/g ($\text{Li}_{21}\text{Si}_5$), which is 10 times greater than the specific capacity of graphite. However, the high specific capacity of silicon is associated with large volume changes (more than 300 percent) when alloyed with lithium. These extreme volume changes can cause severe cracking and disintegration of the electrode and can lead to significant capacity loss.

Significant scientific research has been conducted to circumvent the deterioration of silicon-based anode materials during cycling. Various strategies, such as reduction of particle size, generation of active/inactive composites, fabrication of silicon-based thin films, use of alternative binders, and the synthesis of one-dimensional silicon nanostructures have been implemented by a number of research groups. Fundamental mechanistic research also has been performed to better understand the electrochemical lithiation and delithiation processes during cycling in terms of crystal structure, phase transitions, morphological changes, and reaction kinetics. Although significant progress has been made on developing silicon-based anodes, many obstacles still prevent their practical application. Long-term cycling stability remains the foremost challenge for Si-based anode, especially for the high loading electrode ($> 3\text{mAh/cm}^2$) required for many practical applications. The cyclability of full cells using silicon-based anodes is also complicated by multiple factors, such as diffusion-induced stress and fracture, loss of electrical contact among silicon particles and between silicon and current collector, and the breakdown of SEI layers during volume expansion/contraction processes. The design and engineering of a full cell with a silicon-based anode still needs to be optimized. Critical research remaining in this area includes, but is not limited to, the following:

- Low-cost manufacturing processes have to be found to produce nano-structured silicon with the desired properties.
- The effects of SEI formation and stability on the cyclability of silicon-based anodes need to be further investigated. Electrolytes and additives that can produce a stable SEI layer need to be developed.
- A better binder and a conductive matrix need to be developed. They should provide flexible but stable electrical contacts among silicon particles and between particles and the current collector under repeated volume changes during charge/ discharge processes.
- The performances of full cells using silicon-based anode need to be investigated and optimized.

The main goal of this project is to have a fundamental understanding on the failure mechanism on Si based anode and improve its long-term stability, especially for thick electrode operated at full cell conditions. Success of this project will enable Li-ion batteries with a specific energy of $>350\text{ Wh/kg}$ (in cell level), 1000 deep-discharge cycles, 15-year calendar life, and less than 20% capacity fade over a 10-year to meet the goal of EV everywhere.

Highlight. Kumta reported a flexible nanofiber (NF) electrode based on active-inactive composite comprising of nanocrystalline Si (*nc*-Si) and metal oxide $(\text{MM}')_n\text{O}_x$ [*nc*-Si+ $(\text{MM}')_n\text{O}_x$] impregnated in the carbon nanofiber (CNF) with a specific capacity of $\sim 1325\text{ mAh/g}$.

Task 2.0 – Novel Non-Carbonate Based Electrolytes for Silicon Anodes (Dee Strand, Wildcat Discovery Technologies)

Project Objective. The objective is to develop non-carbonate electrolytes that form a stable SEI on silicon alloy anodes, enabling substantial improvements in energy density and cost relative to current lithium ion batteries. These improvements are vital for mass market adoption of EVs. At present, commercial vehicle batteries employ cells based on LiMO_2 ($M = \text{Mn, Ni, Co}$), LiMn_2O_4 , and/or LiFePO_4 coupled with graphite anodes. Next generation cathode candidates include materials with higher specific capacity or higher operating voltage, with a goal of improving overall cell energy density. However, to achieve substantial increases in cell energy density, a higher energy density anode material is also required. Silicon anodes demonstrate very high specific capacities, with a theoretical limit of 4200 mAh/g and state-of-the-art electrodes exhibiting capacities greater than 1000 mAh/g. While these types of anodes can help achieve target energy densities, their current cycle life is inadequate for automotive applications. In graphite anodes, carbonate electrolyte formulations reductively decompose during the first cycle lithiation, forming a passivation layer that allows lithium transport, yet is electrically insulating to prevent further reduction of bulk electrolyte. However, the volumetric changes in silicon upon cycling are substantially larger than graphite, requiring a much more mechanically robust SEI film.

Project Impact. Silicon alloy anodes enable substantial improvements in energy density and cost relative to current lithium ion batteries. These improvements are vital for mass market adoption of EVs, which would significantly reduce CO_2 emissions as well as eliminate the U.S. dependence on energy imports.

Out-Year Goals. Development of non-carbonate electrolyte formulations that:

- Form stable SEIs on 3M silicon alloy anode, enabling Coulombic efficiency > 99.9% and cycle life > 500 cycles (80% capacity) with NMC cathodes;
- Have comparable ionic conductivity to carbonate formulations, enabling high power at room temperature and low temperature;
- Are oxidatively stable to 4.6 V, enabling the use of high energy NMC cathodes in the future; and
- Do not increase cell costs over today's carbonate formulations.

Collaborations. Wildcat is working with 3M on this project. To date, 3M is supplying the silicon alloy anode films and NMC cathode films for use in Wildcat cells.

Milestones

1. Assemble materials, establish baseline performance with 3M materials. (December 2013 – Complete)
2. Develop initial additive package using non-SEI forming solvent. (March 2014 – Complete)
3. Screen initial solvents with initial additive package. (June 2014 – Complete)
4. Design/build interim cells for the DOE. (September 2014 – Complete)
5. Improve performance with non-carbonate solvents and new SEI additives. (March 2015 – Complete; Continuous to end of project)
6. Optimize formulations. (August 2015 – On track; Continuous to end of project)
7. Design/build final cells for the DOE. (March 2016 – Complete)

Work this quarter focused on two areas. The first area consisted of tasks necessary to select formulations and prepare for the 18650 cell assembly at 3M. Second, the project performed post-mortem testing on cycled cells to help identify the failure mechanisms.

To help ensure translation of results from Wildcat small format cells to larger format cells (such as 18650), the project prepared single layer pouch cells using the same NMC//Si alloy electrodes. Variables such as the electrolyte amount and stack pressure were varied to determine the effect on cell performance for a selection of electrolytes. Samples of the results are shown in Figures 8 and 9.

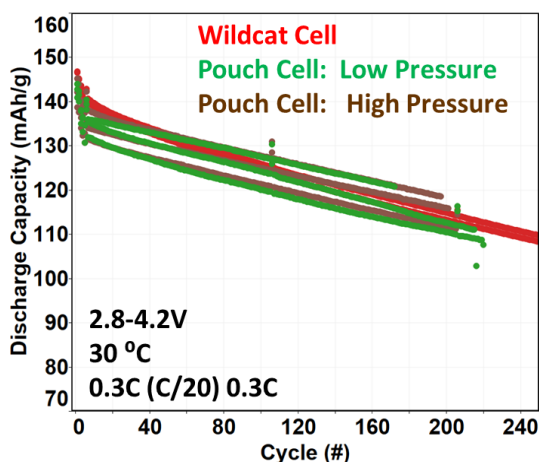


Figure 8. Wildcat pouch cells perform similar to high throughput cells on Cycle 1.

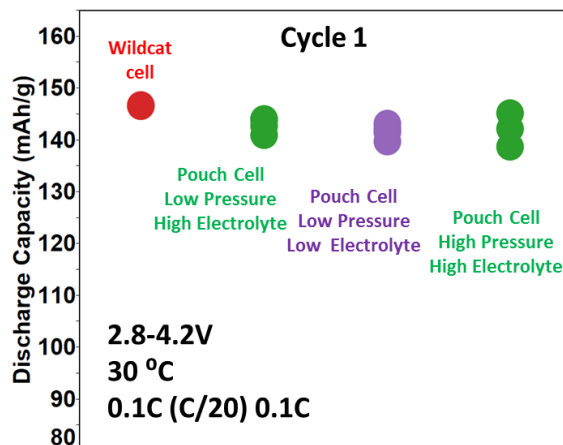


Figure 9. Cycle life in Wildcat pouch cells is similar to high throughput cells.

The project also conducted short shelf life studies on selected electrolyte formulations to ensure that storage during shipment or delay on cell assembly would not negatively affect results. These electrolytes were then shipped to 3M for 18650 cell assembly and formation. Ira Bloom at ANL will receive the cells for testing. The test protocol was reviewed during a phone discussion with Ira on 11 April 2016.

From the cycled pouch cells, the project defined electrochemical experiments to determine if failure mechanism of the cell has changed at the longer cycle life. In general, the anodes show visual flaws and delaminations after cycling (Figure 10).

The cycled cathodes and anodes were harvested, washed, and re-tested in half cells, with results shown in Figures 11 and 12 on the following page. With essentially infinite lithium supply in the half cell testing, loss of capacity on either electrode indicates a reduction in access of the active material.

Significant capacity loss was observed on the anode relative to the cathode. The large loss on the anode can be due either to a large impedance growth on the cycled anode or to actual loss of active material in the electrode. The data were obtained at a fairly low c-rate (C/10), which would indicate active material loss is a big contributor. These experiments are being repeated at a lower c-rate to try to separate contributions.

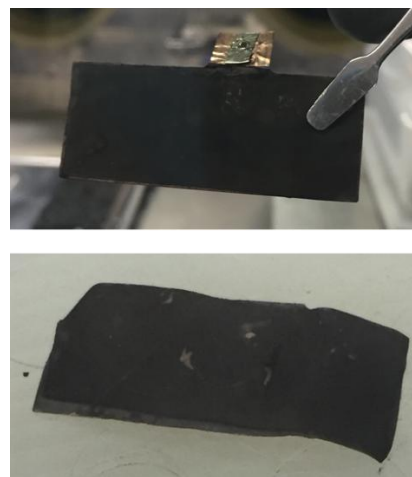


Figure 10. Anode delamination is observed after cycling.

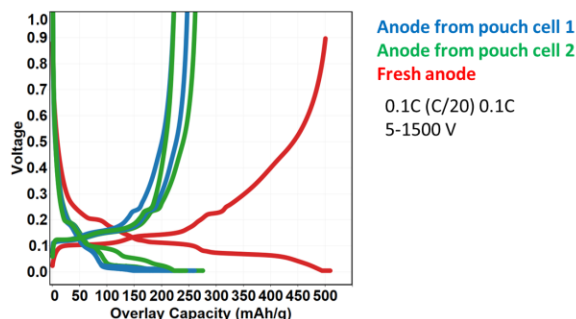


Figure 11. Cycled anodes show significant reduction in capacity when re-tested in half cells.

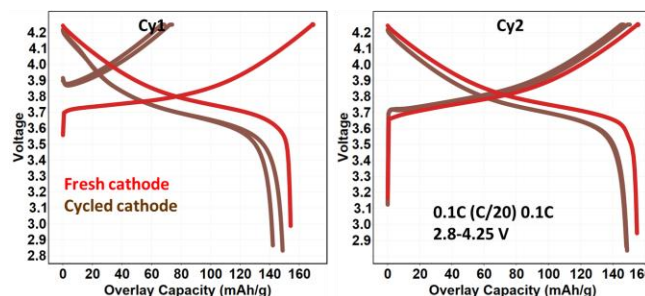


Figure 12. Cycled cathode capacity is only slightly reduced when re-tested in half cells.

Patents/Publications/Presentations

Patents

- Four provisional patent applications have been filed to date.
- One provisional patent application on noncarbonated solvents and combinations filed 6/22/2015.

Presentations

- BMR Program Review Meeting, LBNL, Berkeley, California (January 2015): “Review: Development of Novel Electrolytes for Silicon Anodes”; D. A. Strand, Y. Zhu, G. Cheng, and M. Caldwell.
- 32nd International Battery Conference, Ft. Lauderdale, Florida (March 2015): “Novel Noncarbonate Electrolytes for Silicon Anodes”; D. A. Strand, Y. Zhu, G. Cheng, and M. Caldwell.
- 2nd International Forum on Cathode & Anode Materials for Advanced Batteries, Hangzhou, China (April 2015): “Novel Noncarbonate Electrolytes for Silicon Anodes”; B. Li, D. A. Strand, Y. Zhu, G. Cheng, and M. Caldwell.
- 227th ECS Meeting, Chicago (May 2015): “Development of Novel Lithium Ion Battery Electrolytes for Silicon Anodes”; Y. Zhu, D. A. Strand, and G. Cheng.
- DOE Annual Merit Review, Washington, D. C. (June 2015): “Novel Noncarbonate Electrolytes for Silicon Anodes”; D. A. Strand, Y. Zhu, G. Cheng, and M. Caldwell.
- 4th China LIB Electrolytes Conference, Yangzhou, China (June 2015): “Development of Novel Electrolytes for Silicon Anodes”; G. Cheng, Y. Zhu, and D. A. Strand.
- AABC USA 2015, Troy, Michigan (June 2015): “Novel Noncarbonate Electrolytes for Silicon Anodes”; G. Cheng, Y. Zhu, and D. A. Strand.
- ABAA8, Bilbao, Spain (September 2015): “Development of Novel Electrolytes for Silicon Anodes”; D. A. Strand, Y. Zhu, and G. Cheng.
- Batteries 2015, Nice, France (October 2015): “Development of Novel Electrolytes for Silicon Anodes”; D. A. Strand, Y. Zhu, and G. Cheng.

Task 2.1 – Development of Silicon-Based High Capacity Anodes

(Ji-Guang Zhang/Jun Liu, PNNL; Prashant Kumta, Univ. of Pittsburgh; Jim Zheng, PSU)

Project Objective. The project objective is to develop high-capacity and low-cost silicon-based anodes with good cycle stability and rate capability to replace graphite in lithium-ion batteries. In one approach, the low-cost Si-graphite-carbon (SGC) composite will be developed to improve the long-term cycling performance while maintaining a reasonably high capacity. Si-based secondary particles with a nano-Si content of ~10 to 15 wt% will be embedded in the matrix of active graphite and inactive conductive carbon materials. Controlled void space will be pre-created to accommodate the volume change of Si. A layer of highly graphitized carbon coating at the outside will be developed to minimize the contact between Si and electrolyte, and hence minimize the electrolyte decomposition. New electrolyte additives will be investigated to improve the stability of SEI layer. In another approach, nanoscale silicon and Li-ion conducting lithium oxide composites will be prepared by *in situ* chemical reduction methods. The stability of Si-based anode will be improved by generating the desired nanocomposites containing nanostructured amorphous or nanocrystalline Si as well as amorphous or crystalline lithium oxide (Si+Li₂O) by the direct chemical reduction of a mixture and variety of Si sub oxides (SiO and SiO_x) and/or dioxides. Different synthesis approaches comprising direct chemical reduction using solution, solid-state and liquid-vapor phase methods will be utilized to generate the Si+Li₂O nanocomposites. The electrode structures will be modified to enable high utilization of thick electrode.

Project Impact. Si-based anodes have much larger specific capacities compared with conventional graphite anodes. However, the cyclability of Si-based anodes is limited because of the large volume expansion characteristic of these anodes. This work will develop a low-cost approach to extend the cycle life of high-capacity, Si-based anodes. The success of this work will further increase the energy density of Li-ion batteries and accelerate market acceptance of EVs, especially for the PHEVs required by the EV Everywhere Grand Challenge proposed by the DOE/EERE.

Out-Year Goals. The main goal of the proposed work is to enable Li-ion batteries with a specific energy of > 200 Wh/kg (in cell level for PHEVs), 5000 deep-discharge cycles, 15-year calendar life, improved abuse tolerance, and less than 20% capacity fade over a 10-year period.

Milestones

1. Identify and synthesize the active-inactive Si-based nanocomposite with low-cost approach and a specific capacity ~800 mAh/g. (December 2015 – Complete)
2. Achieve 80% capacity retention over 200 cycles for graphite supported nano Si-carbon shell composite. (March 2016 – Complete)
3. Synthesize the suitable active-inactive nanocomposite with Li₂O as matrix (Si+Li₂O) or intermetallic matrix (Si+ MnBm) of specific capacity ~1000-1200mAh/g. (March 2016 – Ongoing)
4. Develop interface control agents and surface electron conducting additives to reduce the first cycle irreversible loss and improve the CE of Si-based anode. (June 2016 – Ongoing)
5. Optimize the cost-effective, scalable high-energy mechanical milling (HEMM) and solid state synthesis techniques for generation of active-inactive composite with capacities ~1000-1200 mAh/g. (June 2016 – Ongoing)
6. Achieve > 80% capacity retention over 300 cycles for thick electrodes (> 2 mAh cm⁻²) through optimization of the Si electrode structure and binder. (September 2016 – Ongoing)

Progress Report

This quarter, the electrochemical performance of the hard carbon coated nano-Si/graphite (HC-nSi/G) composite was evaluated. Figure 13 shows the charge-discharge curves, cycling stability, and rate performance of the samples. The specific capacity was calculated based on the active material (Si/graphite/hard carbon). The electrode loading was $1.5\sim 2.0\text{ mg cm}^{-2}$. A sample with 10% binder and 14.6% silicon (E2) delivers a capacity of 764.1 mAh g^{-1} with a first-cycle reversible capacity of 78.7%. It is interesting that increasing the binder content to 20% (E3) significantly increased the specific capacity of the electrode (878.6 mAh g^{-1}) and improved first-cycle reversible capacity to 80.5%. Figure 13b presents the effects of binder and silicon content on the cycling performance of the composite electrodes. Sample E3 shows a capacity of 864.1 mAh g^{-1} in the 4th cycle and a capacity retention of 84.1% in 150 cycles. Rate capabilities of the HC-nSi/G composite electrodes with different compositions were further evaluated. A sample of HC-nSi/G with 10% binder and 11.4% silicon (E1) exhibits the higher discharging capacity compared to E2 and E3, delivering 860, 806, 797, 669, and 398 mAh g^{-1} at rates of 0.2, 0.5, 1, 2, and 4 C, respectively. After the rate test, a high discharge capacity of 874.5 mAh g^{-1} can be recovered for the E1 electrode when the discharge current density is returned to 0.2C, further evidencing the good reversibility of the E1 electrode. Moreover, the Coulombic efficiency of the E1 electrode increases to $> 99.0\%$ during long-term cycling.

A flexible nanofiber (NF) electrode based on active-inactive composite comprising of nanocrystalline Si (*nc*-Si) and metal oxide ($(\text{MM}')_n\text{O}_x$ [*nc*-Si+ $(\text{MM}')_n\text{O}_x$]) impregnated in the carbon nanofiber (CNF) has been generated. The nanocomposite powder has been obtained using high energy ball milling of SiO_x with a metal alloy (MM') reductant after 20h of ball milling. The ball milled powder was subsequently heat treated at 550°C to complete the reduction of SiO_x and initiate crystallization of the $(\text{MM}')_n\text{O}_x$ matrix. Flexible nanofiber (*nc*-Si+ $(\text{MM}')_n\text{O}_x$)/CNF electrode was fabricated by impregnating (*nc*-Si+ $(\text{MM}')_n\text{O}_x$) in the polymer derived CNF ($\sim 10\text{wt}\%$) by solution coating method followed by carbonization. The electrochemical performance of (*nc*-Si+ $(\text{MM}')_n\text{O}_x$)/CNF flexible node shows a first cycle discharge and charge capacity of $\sim 1650\text{ mAh/g}$ and $\sim 1045\text{ mAh/g}$, with a first irreversible loss (FIR) of $\sim 35\%$ (Figure 14). The differential capacity plot (inset of Figure 14) shows alloying/dealloying reaction of Si with Li. The flexible NF electrode of (*nc*-Si+ $(\text{MM}')_n\text{O}_x$)/CNF exhibits higher specific capacity on subsequent cycling ($\sim 1325\text{ mAh/g}$ during the 2nd discharge cycle) and lower FIR loss as compared to slurry coated *nc*-Si+ $(\text{MM}')_n\text{O}_x$ composite ($\sim 60\%$). It is expected that the flexible NF (*nc*-Si+ $(\text{MM}')_n\text{O}_x$)/CNF electrode would stabilize the capacity and cycling performance.

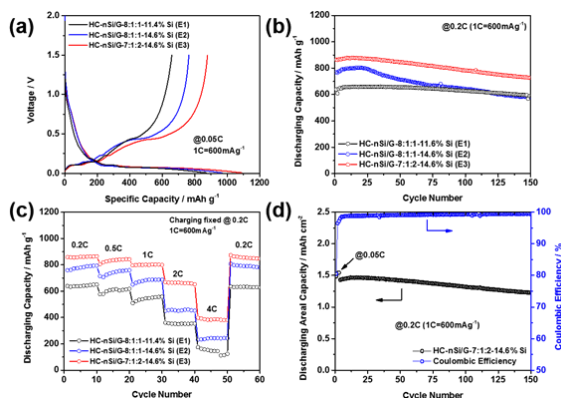


Figure 13. (a) Initial lithiation/delithiation voltage profiles at 0.05C. (b) Specific capacity as a function of cycle number at 0.2C. (c) Rate capability of HC-nSi/G at various discharging C-rates (charging C-rate fixed at 0.2C) for HC-nSi/G. (d) Plot of areal capacity retention of HC-nSi/G with electrode composition ratio (active material:carbon black:binder = 7:1:2).

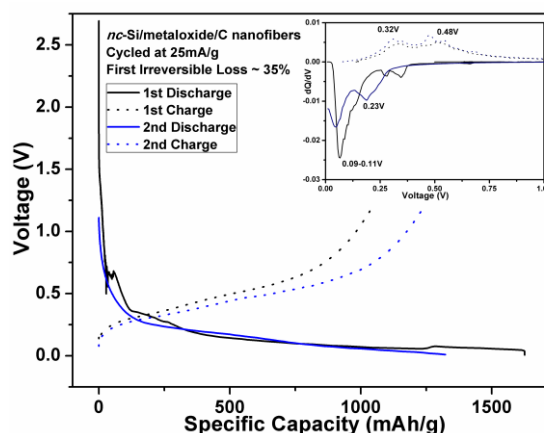


Figure 14. Voltage vs specific capacity plot of (*nc*-Si+ $(\text{MM}')_n\text{O}_x$)/carbon nanofiber electrode tested in a Li-ion half-cell. Inset: differential capacity plots of (*nc*-Si+ $(\text{MM}')_n\text{O}_x$)/carbon nanofiber electrode.

Task 2.2 – Pre-Lithiation of Silicon Anode for High Energy Li Ion Batteries (Yi Cui, Stanford University)

Project Objective. Prelithiation of high-capacity electrode materials such as silicon is an important means to enable those materials in high-energy batteries. This study pursues two main directions: (1) developing facile and practical methods to increase first-cycle CE of Si anodes, and (2) synthesizing fully lithiated Si and other lithium compounds for pre-storing lithium.

Project Impact. The lithium loss for first cycle in existing Li-ion batteries will be compensated by using these cathode prelithiation materials. The cathode prelithiation materials have good compatibility with ambient air, regular solvent, binder, and the thermal processes used in current Li-ion battery manufacturing. This project's success will improve the energy density of existing Li-ion batteries and help to achieve high-energy-density Li-ion batteries for electric vehicles.

Out-Year Goals. Compounds containing a large quantity of Li will be synthesized for pre-storing Li ions inside batteries. First cycle lithium loss will be compensated (for example, ~10%) by prelithiation with the synthesized conversion materials.

Collaborations. The project works with the following collaborators: (1) BMR principal investigators, and (2) SLAC: *in situ* X-ray, Dr. Michael Toney.

Milestones

1. Prelithiate conversion oxides by the reaction between molten Li metal and oxide. (December 2015 – Complete)
2. Synthesize LiF/metal nanocomposite for cathode prelithiation with high capacity and good air stability (> 500 mAh/g). (March 2016 – Ongoing)
3. Synthesize Li₂S/metal nanocomposite for cathode prelithiation with high capacity. (June 2016 – Ongoing)

Progress Report

The cathode prelithiation additives based on nanoscale mixtures of transition metal (M) and lithium oxide (Li_2O) have been developed. These additives are the reaction products of transition metal oxide (M_xO_y) and Li metal via a well-known conversion reaction mechanism (Figure 15a). The composites of nanometer-sized M/nanometer-sized Li_2O (N-M/N- Li_2O) afford a high prelithiation capacity [for example, 619 mAh g^{-1} for the nanometer-sized Co/nanometer-sized Li_2O (N-Co/N- Li_2O ; molar ratio, 3/4) composite, Figure 15b] when converted back to M_xO_y and Li ions during cathode charge. The N-Co/N- Li_2O electrode lost nearly all the capacity after the first cycle, suggesting that after providing Li ion during the first charge, these nanocomposites did not contribute to the active electrochemical process in the cathode (Figure 15c). The response of the additive at different potential ranges is clearly shown by a LiFePO_4 electrode containing different amounts of such additive (Figure 15d). In a full cell configuration, the LiFePO_4 electrode with a 4.8% Co/ Li_2O additive shows 11% higher overall capacity than that of the pristine LiFePO_4 electrode (Figure 15e-f).

To show the generality of using N-M/N- Li_2O composites as high-capacity cathode additives, we also prepared N-Ni/N- Li_2O and N-Fe/N- Li_2O composites using the same synthesis procedure. Similar to the N-Co/N- Li_2O composite, the N-Ni/N- Li_2O and N-Fe/N- Li_2O electrodes possess high initial open circuit voltage (OCV, higher than 1.5 V) and deliver high charge capacities of 506 and 631 mAh g^{-1} , respectively, and very low discharge capacity of 11 and 19 mAh g^{-1} , respectively. The LiFePO_4 electrodes with the two additives were both subject to cycling. As expected, their first-cycle charge capacities are improved significantly. The initial charge capacities are 180 mAh g^{-1} for the electrode with a 4.8% N-Ni/N- Li_2O additive and 178 mAh g^{-1} for that with a 4.8% N-Fe/N- Li_2O composites, respectively. These capacities are ~10% higher than that of LiFePO_4 electrodes without any prelithiation additive. Moreover, these electrodes also show very good cycling stability.

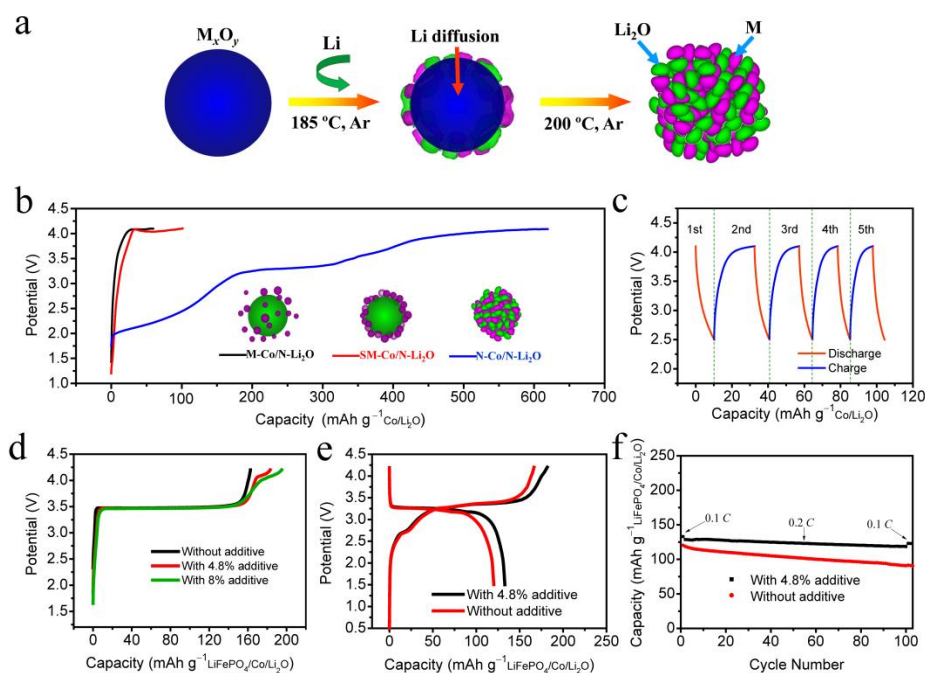


Figure 15. Fabrication and electrochemical characteristics of the N-Co/N- Li_2O composite. (a) Schematic of the fabrication process of the N-M/N- Li_2O composites. MOs are used as the starting materials and *in situ* converted into N-M/N- Li_2O composites *via* the chemical reaction with molten Li. (b) The initial charge potential profiles of the electrodes made with various Co/ Li_2O nanocomposites: Micrometer-sized Co/nanometer-sized Li_2O (M-Co/N- Li_2O), submicrometer-sized Co/nanometer-sized Li_2O (SM-Co/N- Li_2O) and N-Co/N- Li_2O composites. (c) The charge/discharge potential profiles of the N-Co/N- Li_2O electrode after the first charge process. (d) The initial charge potential profiles of the LiFePO_4 electrodes with different amounts of the N-Co/N- Li_2O additive in half cell configurations. (e-f) The initial charge/discharge potential profiles (e) and cycling performance (f) of LiFePO_4 /graphite full cells with and without the N-Co/N- Li_2O additive. The specific capacities of the cathodes are evaluated based on the weight of LiFePO_4 and the N-Co/N- Li_2O additive.

Patents/Publications/Presentations

Patent

- High-capacity Conversion Reaction-based Cathode Additives for Lithium-Ion Batteries; WebDisclosure 197169.

Publication

- Sun, Y. M., and H. -W. Lee, Z. W. Seh, N. Liu, J. Sun, Y. Z. Li and Y. Cui*. “High Capacity Battery Cathode Prelithiation to Offset Initial Lithium Loss.” *Nature Energy* 1 (2016): 15008.

TASK 3 – HIGH-ENERGY DENSITY CATHODES FOR ADVANCED LITHIUM-ION BATTERIES

Summary and Highlights

Developing high energy density, low-cost, thermally stable, and environmentally safe electrode materials is a key enabler for advanced batteries for transportation. High energy density is synonymous with reducing cost per unit weight or volume. Currently, one major technical barrier toward developing high energy density Li-ion batteries is the lack of robust, high-capacity cathodes. As an example, the most commonly used anode material for Li-ion batteries is graphitic carbon, which has a specific capacity of 372 mAh/g, while even the most advanced cathodes like lithium nickel manganese cobalt oxide (NMC) have a maximum capacity of ~180 mAh/g. This indicates an immediate need to develop high-capacity (and voltage) intercalation type cathodes that have stable reversible capacities of 250 mAh/g and beyond. High volumetric density is also critical for transportation applications. Alternative high-capacity cathode chemistries such as those based on conversion mechanisms, Li-S, or metal air chemistries still have fundamental issues that must be addressed before integration into cells for automotive use. Successful demonstration of practical high energy cathodes will enable high energy cells that meet or exceed the DOE cell level targets of 400 Wh/kg and 600 Wh/L with a system level cost target of \$125/kWh.

During the last decade, many high-voltage cathode chemistries were developed under the BATT (now BMR) program, including Li-rich NMC and Ni-Mn spinels. Current efforts are directed toward new syntheses and modifications to improve their stability under high-voltage cycling condition (> 4.4 V) for Ni-rich NMC and Li-Mn-rich NMC (LMR-NMC) [Zhang/Jie, PNNL; Thackeray/Croy, ANL; Doeff and Tong, LBNL]. Three other subtasks are directed towards synthesis and structural stabilization of high-capacity polyanionic cathodes that can have > 1 lithium per transition metal (TM) and can be in crystalline or amorphous phases [Nanda, ORNL; Manthiram, UT Austin; Looney/Wang, BNL; Whittingham, State University of New York (SUNY) at Binghamton; and Kercher/Kiggans, ORNL]. Approaches also include aliovalent or isovalent doping to stabilize cathode structures during delithiation as well as stabilizing oxygen. John Goodenough's group at UT-Austin is developing membranes to stabilize lithium metal anodes and eventually enable high-capacity cathodes in full cell configuration.

Highlights. The highlights for this quarter are as follows:

- **Task 3.1.** Developed and tested a new partial fluorination method for stabilizing Li_2CuO_2 cathodes.
- **Task 3.2.** Demonstrated the rate capability of LiVPO_4 carbon-coated by high-energy ball milling.
- **Task 3.3.** Studied the electrochemical performance of Ni-rich NMC ($\text{LiNi}_{0.76}\text{Mn}_{0.14}\text{Co}_{0.10}\text{O}_2$) cathodes as a function of calcination temperature. The optimal temperature is between 750-775°C.
- **Task 3.4.** Studied the phase transformation and intermediate crystal structure of $\text{LiNi}_{1-x}\text{M}_x\text{O}_2$ using *in situ* synchrotron X-ray diffraction.
- **Task 3.5.** Evaluated the electrochemical performance of a Li-rich spinel ($\text{Li}_{1.1}\text{Mn}_{1.9}\text{O}_4$) coated LiCoO_2 synthesized with wet chemical methods.
- **Task 3.6.** Characterized antimony-based polyanion glass cathodes that showed good conversion capacity but not the desired multivalent intercalation capacity.
- **Task 3.7.** Employed synchrotron *in situ* X-ray diffraction (XRD) to analyze the crystal structure changes of NMC-622 materials during electrochemical cycling.
- **Task 3.8.** Developed Li^+ and Na^+ glass electrolyte with an ionic conductivity $\sigma_i = 10^{-2}$ to 10^{-1} S cm^{-1} at room temperature.
- **Task 3.9.** Using microscopy, showed that annealing temperature controls the phase transition from spinel to layered structure in spinel composite cathodes.
- **Task 3.10.** Analyzed LiNiO_2 electrodes at different state-of-charge using *ex situ* synchrotron XRD (s-XRD) and extended X-ray absorption fine structure (EXAFS).

Task 3.1 – Studies of High Capacity Cathodes for Advanced Lithium-ion Systems (Jagjit Nanda, Oak Ridge National Laboratory)

Project Objective. The overall project goal is to develop high energy density lithium-ion electrodes for EV and PHEV applications that meet and/or exceed the DOE energy density and life cycle targets from the USDRIVE/USABC roadmap. Specifically, this project aims to mitigate the technical barriers associated with high-voltage cathode compositions such as LMR-NMC, and $\text{Li}_2\text{M}_x\text{M}_{1-x}^{\text{II}}\text{O}_2$, where M^{I} and M^{II} are transition metals that do not include Mn or Co. Major emphasis is placed on developing new materials modifications (including synthetic approaches) for high-voltage cathodes that will address issues such as: (i) voltage fade associated with LMR-NMC composition that leads to loss of energy over the cycle life; (ii) transition metal dissolution that leads to capacity and power fade; (iii) thermal and structural stability under the operating state-of-charge (SOC) range; and (iv) voltage hysteresis associated with multivalent transition metal compositions. Another enabling feature of the project is utilizing (and developing) various advanced characterization and diagnostic methods at the electrode and/or cell level for studying cell and/or electrode degradation under abuse conditions. The techniques include electrochemical impedance spectroscopy (EIS), micro-Raman spectroscopy; aberration corrected electron microscopy combined with electron energy loss spectroscopy (EELS), X-ray photoelectron spectroscopy (XPS), inductively coupled plasma – atomic emission spectroscopy (ICP-AES), fluorescence, and X-ray and neutron diffraction.

Project Impact. The project has short- and long- term deliverables directed toward VTO Energy Storage 2015 and 2022 goals. Specifically, work focuses on advanced electrode couples that have cell level energy density targets of 400 Wh/kg and 600 Wh/l for 5000 cycles. Increasing energy density per unit mass or volume reduces the cost of battery packs consistent with the DOE 2022 EV everywhere goal of \$125/kWh.

Out-Year Goals. The project is directed toward developing high-capacity cathodes for advanced lithium-ion batteries. The goal is to develop new cathode materials that have high capacity, are based on low-cost materials, and meet the DOE road map in terms of safety and cycle life. Two kinds of high energy cathode materials are being studied. Over the last few years, the PI has worked on improving cycle life and mitigating energy losses of high-voltage, Li-rich composite cathodes (referred to as LMR-NMC) in collaboration with the voltage fade team at ANL. Since last year, the PI has developed a high-capacity, two-lithium, copper-nickel system ($\text{Li}_2\text{Cu}_x\text{Ni}_{1-x}\text{O}_2$) and similar systems. The plan includes improving the oxygen stability by using anionic substitution. Approaches include fluorination and changing to suitable polyanionic species. The tasks also include working in collaboration with researchers at Stanford Synchrotron Research Laboratory (SSRL) and Advanced Light Source (LBNL) to understand local changes in morphology, microstructure, and chemical composition under *in situ* and *ex situ* conditions.

Collaborations. This project collaborates with Johanna Nelson, SSRL, Stanford Linear Accelerator Center (SLAC): X-ray imaging and X-ray absorption near edge structure (XANES); Guoying Chen, LBNL: *in situ* X-ray absorption spectroscopy (XAS) and XRD; Feng Wang, BNL: X-ray synchrotron spectroscopy and microscopy; and Bryant Polzin, Argonne Research Laboratory: CAMP Facility for electrode fabrication.

Milestones

1. Synthesize three compositions of $\text{Li}_2\text{Cu}_x\text{Ni}_{1-x}\text{O}_2$ cathodes with x between 0.4-0.6 and improve their anionic stability by fluorination. *Subtask 1.1:* Fluorination of Li_2CuO_2 (Q1 – In progress) *Subtask 1.2:* Fluorination of $\text{Li}_2\text{Cu}_x\text{Ni}_{1-x}\text{O}_2$ with x ~ 0.4-0.6. (Q2 – In progress)
2. Identify roles of Ni and F in obtaining reversible redox capacity at higher voltage, and stabilize Ni-rich compositions. *Subtask 2.1:* XANES, microscopy, and X-ray photoelectron spectroscopy (XPS) studies (Q3). *Subtask 2.2:* Gas evolution and electrochemistry (Q4 – Smart Milestone).

Progress Report

Last quarter, the project reported a no-go result on an approach related to partial fluorination of Li_2CuO_2 powders to increase their electrochemical stability when charged to voltages > 3.9 V. The approach was to use commercially available fluorinated polymers (PVDF and Teflon) as fluorinating agents. Reactions carried out in O_2 at $375\text{--}400^\circ\text{C}$ resulted primarily in decomposition of Li_2CuO_2 to LiF and other Cu-containing phases. Deviating from this method, LiF was used as the fluorination source at the precursor level. The chemical reaction is given by:

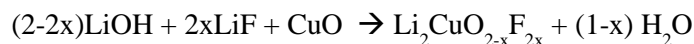


Figure 16 (left panel) shows the XRD pattern of as-synthesized pristine Li_2CuO_2 cathode powder and the top three spectra show the fluorinated compositions. The XRD result does not show any significant impurity phase unlike our earlier approach. The right panel shows the SEM and energy-dispersive X-ray spectroscopy (EDS) maps of the $x = 0.05$ composition. The EDS map shows small domains of F, which could indicate small amount of LiF impurities still present.

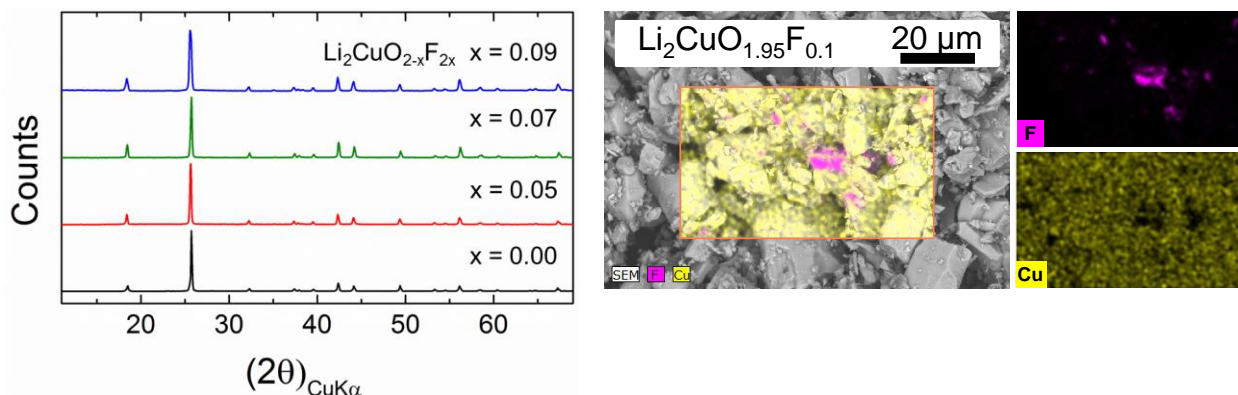


Figure 16. (left) X-ray diffraction pattern of pristine Li_2CuO_2 ($x = 0.0$) and the fluorinated compositions. (right) Scanning electron microscopy of $x=0.05$ composition showing Cu and F distribution.

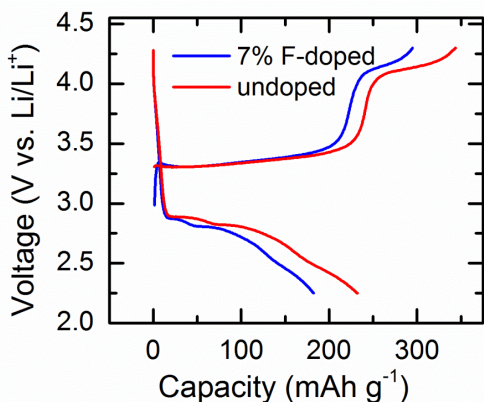


Figure 17. Comparison of 1st cycle performance of fluorinated versus pristine Li_2CuO_2 cathodes.

The project is measuring the electrochemical activity of the various fluorinated composition and trying to obtain a good baseline for comparing with the pristine Li_2CuO_2 . It appears that the electrochemical performance is sensitive to the synthesis and electrode processing conditions. Figure 17 shows a smaller 1st cycle discharge capacity for the fluorinated sample compared to pristine but other batches (not shown) report higher capacity. The project will standardize the process and then report electrochemical performance. Efforts have begun to fluorinate the $\text{Li}_2\text{Cu}_{0.5}\text{Ni}_{0.5}\text{O}_2$ composition.

Patents/Publications/Presentations

Publication

- Sharafi, Asma, and Harry M. Meyer, Jagjit Nanda, Jeff Wolfenstine, and Jeff Sakamoto. “Characterizing the Li-Li₇La₃Zr₂O₁₂ Interface Stability and Kinetics as a Function of Temperature and Current Density. *J. Power Sources* 302 (2016): 135.

Presentations

- IBM Almaden, San Jose, California (February 3, 2016): “Quantifying Chemical and Morphological Heterogeneities in High Capacity Battery Materials: From Micro to Mesoscale”; J. Nanda. Invited.
- BMR Program Review Meeting, LBNL, Berkeley, California (January 21, 2016): “Studies on High Energy Density Cathodes for Advanced Lithium-ion.”

Task 3.2 – High Energy Density Lithium Battery (Stanley Whittingham, SUNY Binghamton)

Project Objective. The project objective is to develop the anode and cathode materials for high energy density cells for use in PHEVs and EVs that offer substantially enhanced performance over current batteries used in PHEVs and with reduced cost. Specifically, the primary objectives are to:

- Increase the volumetric capacity of the anode by a factor of 1.5 over today's carbons
 - Using a SnFeC composite conversion reaction anode
- Increase the capacity of the cathode
 - Using a high-capacity conversion reaction cathode, CuF_2 , and/or
 - Using a high-capacity 2 Li intercalation reaction cathode, VOPO_4
- Enable cells with an energy density exceeding 1 kWh/liter

Project Impact. The volumetric energy density of today's lithium-ion batteries is limited primarily by the low volumetric capacity of the carbon anode. If the volume of the anode could be cut in half, and the capacity of the cathode to over 200 Ah/kg, then the cell energy density can be increased by over 50% to approach 1 kWh/liter (actual cell). This will increase the driving range of vehicles.

Moreover, smaller cells using lower cost manufacturing will lower the cost of tomorrow's batteries.

Out-Year Goals. The long-term goal is to enable cells with an energy density of 1 kWh/liter. This will be accomplished by replacing both the present carbon used in Li-ion batteries with anodes that approach double the volumetric capacity of carbon, and the present intercalation cathodes with materials that significantly exceed 200 Ah/kg. By the end of this project, it is anticipated that cells will be available that can exceed the volumetric energy density of today's Li-ion batteries by 50%.

Collaborations. The Advanced Photon Source at ANL and, when available, the National Synchrotron Light Source II at BNL will be used to determine the phases formed in both *ex situ* and *operando* electrochemical cells. University of Colorado, Boulder, will provide some of the electrolytes to be used.

Milestones

3. Determine the optimum composition Li_xVOPO_4 . (December 2015 – Complete)
4. Demonstrate VOPO_4 rate capability. (March 2016 – Complete)
5. Demonstrate Sn_2Fe rate capability. (June 2016)
6. Demonstrate CuF_2 rate capability. (September 2016)
7. *Go/No-Go*: Demonstrate lithiation method. *Criteria*: A cycling cell containing lithium in one of the intercalation or conversion electrodes must be achieved. (September 2016)

Progress Report

The goal of this project is to synthesize tin-based anodes that have 1.5 times the volumetric capacity of the present carbons, and conversion and intercalation cathodes with capacities over 200 Ah/kg. The major effort this quarter was to complete the cycling evaluation of the intercalation cathode material, Li_xVOPO_4 , and determine its rate capability vs a lithium anode.

Milestone 1. As noted last quarter, the project identified that the optimum composition of the starting cathode is $\Sigma\text{-LiVOPO}_4$, that is, a material containing some lithium rather than the Li-free $\Sigma\text{-VOPO}_4$, and that it be made by a solid state reaction at 750°C . The goal of over 50 cycles at more than 200 Ah/kg has also now been accomplished as indicated in Figure 18 (left).

Milestone 2. The rate capability of the LiVOPO_4 is under evaluation, and the data to date is presented in Figure 1 (right). This cathode is an electronic insulator just like the olivine LiFePO_4 , so must be nanosized and covered with a conductive coating. However, unlike LiFePO_4 it cannot be carbon coated at elevated temperatures using a material such as sucrose, because the oxidation state of the vanadium is reduced under such conditions. Thus, the material was coated by high energy ball-milling with carbon; this ball-milling also resulted in the reduction of the particle size of the LiVOPO_4 . Further efforts will be required to achieve extended discharge cycles at rates exceeding 1C.

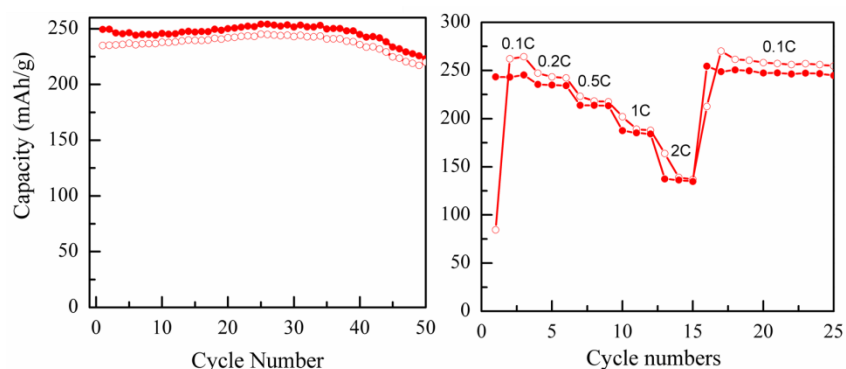


Figure 18. (left) Cycling behavior. (right) Rate capability of a LiVOPO_4 electrode.

Milestone 4. Extended cycling and rate capability studies of the CuF_2 cathode are in progress. A major challenge of this material is almost certainly related to the solubility of the cuprous ions formed on recharging. The project is trying to determine whether this is the critical parameter by using a solid electrolyte where the solubility issue should be eliminated, as was shown by Se Hee et al. at University of Colorado for cycling of FeS_2 . A number of solid electrolytes have been evaluated without great success, but a polyethylene oxide (PEO)-based system did allow the discharge and partial recharge of $\text{Cu}_{1-y}\text{Fe}_y\text{F}_2$. However, there are indications that the Cu^+ ion can replace the Li in the solid electrolyte as observed from electrolyte decomposition on charge at Cu redox potential.

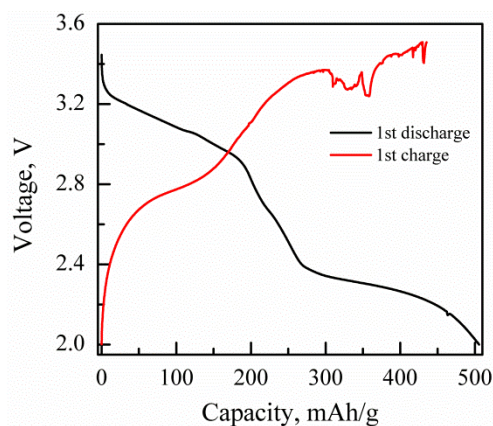


Figure 19. Cycling of $\text{Cu}_{0.5}\text{Fe}_{0.5}\text{F}_2$ using a PEO-based electrolyte

Patents/Publications/Presentations

Publication

- Dong, Zhixin, and R. Zhang, D. Ji, N. A. Chernova, K. Karki, S. Sallis, L. Piper, and M. S. Whittingham. “The Anode Challenge for Lithium-ion Batteries: A Mechanochemically Synthesized Sn-Fe-C Composite Anode Surpasses Graphitic Carbon.” *Advanced Science* 3 (2016): 1500229.

Task 3.3 – Development of High-Energy Cathode Materials (Ji-Guang Zhang and Jianming Zheng, Pacific Northwest National Laboratory)

Project Objective. The project objective is to develop high-energy-density, low-cost, cathode materials with long cycle life. The previous investigation demonstrates that synthesis condition, synthesis approach, and surface modification have significant effects on the performances of high-voltage spinel and LMR-NCM cathodes. These valuable understandings will be used to guide the development of high energy-density, enhanced long-term cycling stability of Ni-rich $\text{LiNi}_x\text{Mn}_y\text{Co}_z\text{O}_2$ (NMC) cathode materials that can deliver a high discharge capacity with long-term cycling stability.

Project Impact. Although state-of-the-art layered structure cathode materials such as $\text{LiNi}_x\text{Mn}_y\text{Co}_z\text{O}_2$ (NMC) have relatively good cycling stability when charged to 4.3 V, their energy densities need to be further improved to meet the requirements of EVs. This work focuses on the two closely integrated parts: (1) Develop the high energy-density NMC layered cathode materials for Li-ion batteries; and (2) characterize the structural properties of the NMC materials by a variety of diagnostic techniques including scanning transmission electron microscopy (STEM)/EELS, EDX mapping and secondary ion mass spectrometry (SIMS), and correlate with part (1). The success of this work will increase the energy density of Li-ion batteries and accelerate market acceptance of EVs, especially for PHEVs required by the EV Everywhere Grand Challenge proposed by DOE/EERE.

Out-Year Goals. The long-term goal of the proposed work is to enable Li-ion batteries with a specific energy of $> 96 \text{ Wh kg}^{-1}$ (for PHEVs), 5000 deep-discharge cycles, 15-year calendar life, improved abuse tolerance, and less than 20% capacity fade over a 10-year period.

Collaborations. This project engages with the following collaborators:

- Dr. Bryant Polzin (ANL) – NMC electrode supply
- Dr. X.Q. Yang (BNL) – *in situ* XRD characterization during cycling
- Dr. Kang Xu (U.S. Army Research Laboratory) – new electrolyte

Milestones

1. Identify NMC candidates that can deliver 190 mAh g^{-1} at high voltages. (December 2015 – Complete)
2. Complete multi-scale quantitative atomic level mapping to identify the behavior of Co, Ni, and Mn in NMC during battery charge/discharge, correlation with battery fading characteristics. (March 2016 – Complete)
3. Identify structural/chemical evolution of modified-composition NMC cathode during cycling. (June 2016 – Ongoing)
4. Optimize compositions of NMC materials to achieve improved electrochemical performance (90% capacity retention in 100 cycles). (September 2016 – Ongoing)

Progress Report

This quarter, the atomic level mapping of Co, Ni, and Mn in NMC during battery charge/discharge was completed. Effects of calcination temperature on the electrochemical performance of a Ni-rich $\text{LiNi}_{0.76}\text{Mn}_{0.14}\text{Co}_{0.10}\text{O}_2$ cathode material were systematically investigated at a high charge cutoff voltage of 4.5 V. The initial charge/discharge voltage profiles showed that high discharge capacities of ca. 215 mAh g^{-1} were achieved at calcination temperatures of 750–850°C (Figure 20a). The long-term cycling performance of the Ni-rich $\text{LiNi}_{0.76}\text{Mn}_{0.14}\text{Co}_{0.10}\text{O}_2$ cathode was found to be very sensitive to the calcination temperature. The capacity retention after 200 cycles decreased with increasing calcination temperature: results are 80.1%, 79.0%, 78.7%, 72.9%, 56.4%, and 41.9% for materials calcined at 725, 750, 775, 800, 850, and 900°C, respectively (Figure 20b). The optimal calcination temperature for $\text{LiNi}_{0.76}\text{Mn}_{0.14}\text{Co}_{0.10}\text{O}_2$ was determined to be 750–775°C based on the achievable discharge capacity and the cyclability.

The cells were disassembled after 200 cycles and the cathode electrodes were retrieved for further characterization, focusing on examination of the micro strain and micro crack formation in the cycled particles. Cross-sectional SEM images of the cycled particles clearly show the formation and growth of micro cracks and void space inside the cycled particles as compared to those of pristine samples (Figure 20c-d). The materials prepared at higher temperatures, that is, 800–900°C, exhibit serious formation of cracks and voids inside the particles due to the substantial micro strain caused by the anisotropic volume variation. This phenomenon is believed to be closely related to the size of primary particles constituting the secondary particles of each material, which is a critical factor affecting the crack formation. Accompanying the crack formation, the electrolyte can penetrate into the interior of secondary particles along the crack network, leading to the formation of a resistive SEI layer at the grain boundaries. Crack formation and the degradation of particle interfacial stability result in the loss of electrical contact between the primary particles, leading to quick buildup of electrode resistance (Figure 20e-f) and fast capacity fading. This is believed to be the primary reason for the poor cycling stability of the materials prepared at calcination temperatures higher than 800°C. In this regard, mitigation of the micro strain and crack formation inside the secondary particles is critically important for achieving improved long-term cycling performance of Ni-rich NMC cathode materials.

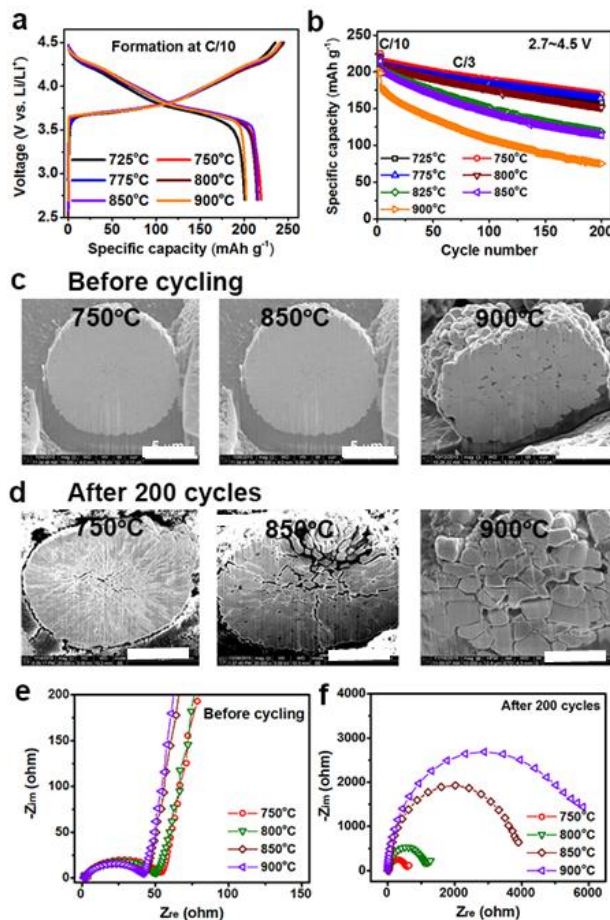


Figure 20. (a) Initial voltage profiles versus specific capacity. (b) Cycling performance. (c) Scanning electron microscopy images before cycling. (d) Scanning electron microscopy images after cycling. (e) Electrochemical impedance spectra before cycling. (f) Electrochemical impedance spectra after cycling of $\text{LiNi}_{0.76}\text{Mn}_{0.14}\text{Co}_{0.10}\text{O}_2$ cathodes prepared at different calcination temperatures and cycled in the voltage range of 2.7–4.5 V. (1C = 200 mA g^{-1} , loading: ca. mg cm^{-2}). The scale bars in (c) and (d) are 5 μm and 1 μm , respectively.

Patents/Publications/Presentations

Publications

- Yan, P., and J. Zheng, Z. Wang, G. Teng, S. Kuppan, J. Xiao, G. Chen, F. Pan, J.-G. Zhang, and C.-M. Wang. “Ni and Co Segregations on Selective Surface Facets and Rational Design of Layered Lithium Transition-Metal Oxide Cathodes.” *Adv. Energy Mater.* (2016). doi: 10.1002/aenm.201502455.
- Yan, P., and J. Zheng, X. Zhang, R. Xu, K. Amine, J. Xiao, J-G. Zhang, and C. Wang. “Atomic to Nanoscale Investigation of Functionalities of Al₂O₃ Coating Layer on Cathode for Enhanced Battery Performance.” *Chem. Mater.* 28 (2016): 857-863.
- Shi, W., and J. Zheng, J. Xiao, X. Chen, B. J. Polzin, and J.-G. Zhang. “The Effect of Entropy and Enthalpy Changes on the Thermal Behavior of Li-Mn-rich Layered Composite Cathode Materials.” *J. Electrochem. Soc.* 163 (2016): A571-A577.
- Shi, Wei, and Jiulin Wang, Jianming Zheng, Jiuchun Jiang, Vilayanur Viswanathan, and Ji-Guang Zhang. “Influence of Memory Effect on the State-of-charge Estimation of Large Format Li-ion Batteries Based on LiFePO₄ Cathode.” *Journal of Power Sources* 312 (2016): 55-59.

Task 3.4 – *In situ* Solvothermal Synthesis of Novel High Capacity Cathodes (Feng Wang and Jianming Bai, Brookhaven National Laboratory)

Project Objective. The goal is to develop novel high-capacity cathodes with precise control of the phase, stoichiometry, and morphology. Despite considerable interest in developing low-cost, high energy cathodes for Li-ion batteries, designing and synthesizing new cathode materials with the desired phases and properties has proven difficult, due to the complexity of the reactions involved in chemical synthesis. Building on established *in situ* capabilities/techniques for synthesizing and characterizing electrode materials, this project will undertake *in situ* studies of synthesis reactions under real conditions to identify the intermediates and to quantify the thermodynamic and kinetic parameters governing the reaction pathways. The results of such studies will enable strategies to “dial in” desired phases and properties, opening up a new avenue for synthetic control of the phase, stoichiometry, and morphology during preparation of novel high-capacity cathodes.

Project Impact. Present-day Li-ion batteries are incapable of meeting the targeted miles of all-electric-range within the weight and volume constraints, as defined by the DOE in the EV Everywhere Grand Challenge. New cathodes with higher energy density are needed for Li-ion batteries so that they can be widely commercialized for plug-in electric vehicle (PEV) applications. The effort will focus on increasing energy density (while maintaining the other performance characteristics of current cathodes) using synthesis methods that have the potential to lower cost.

Out-Year Goals. This project is directed toward developing novel high-capacity cathodes, with a focus on Ni-rich layered oxides. Specifically, synthesis procedures will be developed for making LiNiO_2 and a series of Co/Mn substituted solid solutions, $\text{LiNi}_{1-x}\text{M}_x\text{O}_2$ ($\text{M}=\text{Co}, \text{Mn}$), and through *in situ* studies, this project undertakes systematic investigations of the impact of synthesis conditions on the reaction pathways and cationic ordering processes towards the final layered phases. The structural and electrochemical properties of the synthesized materials will be characterized using s-XRD, neutron scattering, transmission electron microscopy (TEM), EELS, and various electrochemical techniques. The primary goal is to develop a reversible cathode with an energy density of 660 Wh/kg or higher.

Collaborations. This project engages with the following collaborators: Lijun Wu and Yimei Zhu at BNL; Khalil Amine, Zonghai Chen, and Yang Ren at ANL; Jagjit Nanda and Ashfia Huq at ORNL; Nitash Balsara, Wei Tong, and Gerbrand Ceder at LBNL; Arumugam Manthiram at UT-Austin; Scott Misture at Alfred University; Peter Khalifha at SUNY; Kirsuk Kang at Seoul National University; Brett Lucht at University of Rhode Island; and Jason Graetz at HRL Laboratories.

Milestones

1. Develop synthesis procedures for preparing Ni-Mn-Co layered oxides. (December 2015 – Complete)
2. Identify the impact of synthesis conditions on the reaction kinetics and pathways toward forming layered Ni-Mn-Co oxides via *in situ* studies. (March 2016 – Complete)
3. Develop new capabilities for monitoring synthesis parameters (P , T , PH values) in real time during solvothermal synthesis of cathode materials. (June 2016 – On schedule)
4. Identify synthetic approaches for stabilizing the layered structure of Ni-Mn-Co cathodes. (September 2016 – On schedule)

Progress Report

Last quarter, a solid-state method was developed for synthesis of high-capacity Ni-rich layered oxides $\text{LiNi}_{1-x}\text{M}_x\text{O}_2$ ($\text{M}=\text{Co}, \text{Mn}$), in which Co-substitution appears to be crucial for stabilizing the layered structure, and thereby achieving good electrochemical performance. To better understand the impact of synthesis conditions on the reaction kinetics and pathways towards ordered layer oxides, *in situ* XRD studies on solid-state synthesis of LiNiO_2 and $\text{LiNi}_{0.8}\text{Co}_{0.2}\text{O}_2$ were performed. Some of the results are reported here.

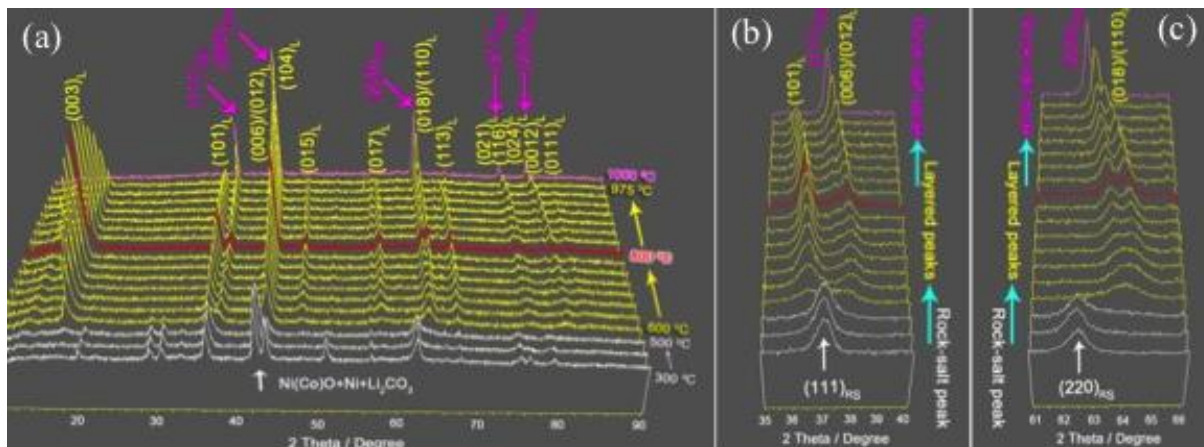


Figure 21. *In situ* X-ray diffraction patterns for tracking structural evolution during solid-state synthesis of $\text{LiNi}_{0.8}\text{Co}_{0.2}\text{O}_2$.

Figure 21a-c shows one set of temperature-resolved XRD patterns recorded during synthesis of $\text{LiNi}_{0.8}\text{Co}_{0.2}\text{O}_2$ under pure O_2 environment. The synthesis process is complex, involving multiple phase transformations along with subtle changes in the local structure. The crystal structure of the intermediates, and evolution towards the final product, may be directly obtained from the changes in the diffraction peaks, for example, changes in the intensity of (003) reflection, the splitting of (006)/(012) and (018)/(110) doublets. As indicated in Figure 21, a solid-solution rock-salt phase $\text{Ni}(\text{Co})\text{O}$ is formed at low temperatures upon decomposition of the precursors, and then transforms directly into a Li-deficient layered phase at about 500°C . Subsequent ordering of the layered structure proceeds with further lithiation at intermediate sintering temperatures, followed by structural degradation and eventual transformation into rock salt due to lithium/oxygen loss at high sintering temperatures.

Quantitative data analysis via structure refinement was made to the diffraction patterns, giving details on the evolutions of cationic ordering, phase concentration, Li occupancy, local bonding (Figure 22). The results provide important insights into thermodynamic and kinetic aspects of synthesis reactions and the reaction pathway during preparing layered oxides under real synthesis conditions. *In situ* XRD studies were also performed on synthesis of quaternary system, $\text{LiNi}_{1-x}(\text{CoMn})_x\text{O}_2$. Results will be reported.

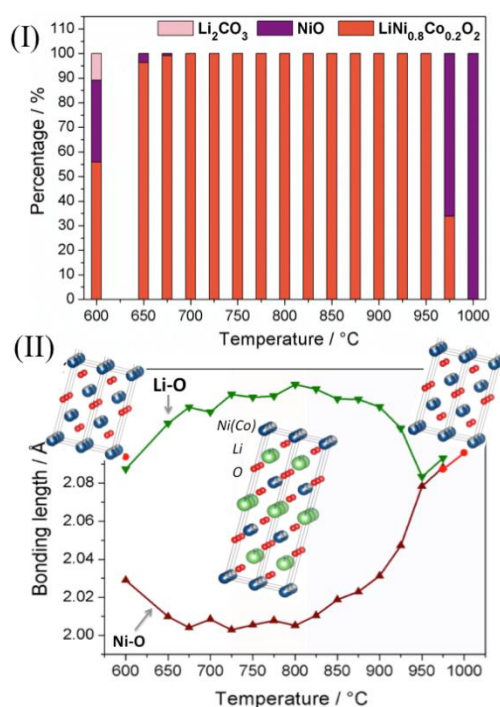


Figure 22. Phase evolution (a) and structural ordering (b) with sintering during synthesis of $\text{LiNi}_{0.8}\text{Co}_{0.2}\text{O}_2$ obtained from structure refinement of the *in situ* X-ray diffraction data.

Patents/Publications/Presentations

Publications

- Xu, J., and F. Lin, D. Nordlund, E. J. Crumlin, F. Wang, J. Bai, M. M. Doeff, and W. Tong. “Elucidation of the Surface Characteristics and Electrochemistry of High-performance LiNiO_2 .” *Chem. Commun.* 52 (2016): 4239.
- Yoo, H. D., and Y. Li, Y. Liang, Y. Lan, F. Wang, and Y. Yao. “Intercalation Pseudocapacitance of Exfoliated Molybdenum Disulphide for Ultrafast Energy Storage.” *ChemNanoMat*. (accepted).

Presentation

- 33rd Annual International Battery Seminar & Exhibits, Fort Lauderdale, Florida (21-23 March 2016): “Ternary Metal Fluorides as High-Energy Cathodes for Rechargeable Lithium Batteries”; F. Wang. Invited.
- PacifiChem 2015, Honolulu, Hawaii, (15-20 December 2015): “Rational Design and Synthesis of New Battery Materials via *in situ* studies”; F. Wang. Invited.

Task 3.5 – Novel Cathode Materials and Processing Methods (Michael M. Thackeray and Jason R. Croy, Argonne National Laboratory)

Project Objective. The project goal is to develop low-cost, high-energy, and high-power Mn-oxide-based cathodes for lithium-ion batteries that will meet the performance requirements of PHEVs and EVs. Improving the design, composition, and performance of advanced electrodes with stable architectures and surfaces, facilitated by an atomic-scale understanding of electrochemical and degradation processes, is a key objective.

Project Impact. Standard lithium-ion battery technologies are unable to meet the demands of the next-generation EVs and PHEVs. Battery developers and scientists will take advantage of both the applied and fundamental knowledge generated from this project to advance the field. In particular, this knowledge should enable progress toward meeting DOE goals for 40-mile, all-electric range PHEVs.

Approach. This project will exploit the concept and optimize the electrochemical properties of structurally integrated “composite” electrode structures with a prime focus on layered-layered-spinel (LLS) materials. Processing routes will be investigated, particularly for scaling up materials for testing by industry; ANL’s comprehensive characterization facilities will be used to explore novel surface and bulk structures by both *in situ* and *ex situ* techniques in pursuit of advancing the electrochemical performance of state-of-the-art cathode materials. A theoretical component will complement the experimental work of this project.

Out-Year Goals. The out-year goals are as follows:

- Identify high-capacity (‘layered-layered’ and ‘layered-spinel’) composite electrode structures and compositions that are stable to electrochemical cycling at high potentials (~4.5 V).
- Identify and characterize surface chemistries and architectures that allow fast Li-ion transport and mitigate or eliminate transition-metal dissolution.
- Scale-up, evaluate, and verify promising cathode materials in conjunction with ANL’s scale-up and cell fabrication facilities.

Collaborators. This project engages with the following collaborators: Joong Sun Park, Bryan Yonemoto, Eungje Lee, and Roy Benedek (Chemical Sciences and Engineering, ANL).

Milestones

1. Optimize the composition, capacity, and cycling stability of structurally integrated cathode materials with a low (~10 – 20%) Li_2MnO_3 content. Target capacity = 200 mAh/g or higher (baseline electrode). (Q1 – In progress)
2. Scale up the most promising materials to batch sizes required for evaluation by industry (10g-100g-1kg). (Q2 – In progress)
3. Synthesize and determine the electrochemical properties of unique surface architectures that enable > 200 mAh/g at a > 1C rate. (Q3 – In progress)

Progress Report

Layered and ‘layered-layered’ lithium transition-metal oxides suffer from degradation mechanisms at high SOC. For example, oxygen loss, surface damage, and the migration of TMs into lithium layers conspire to reduce oxide performance through increased impedance, decreased cell voltage, and loss of cyclable lithium. Past reports have emphasized the strategy of incorporating spinel and/or spinel-type local structures and defects in an attempt to mitigate the above-mentioned degradation mechanisms. Of particular concern is oxygen loss at the surface of particles at high SOC. Large vacancy concentrations (for example, Li) coupled with even small amounts of oxygen loss facilitate migration of the TMs that alters the structure of near-surface layers. Because spinel structures are more stable against oxygen loss and TM migration, and can share a compatible oxygen lattice with their layered counterparts, incorporation of a spinel component at the surface of oxide particles may be an attractive strategy to create more robust cathode surfaces. LiCoO_2 (LCO) is a model system for studying surface-related degradation of cathode electrodes because of its well established electrochemical behavior. Here, the influence of a lithium-rich spinel coating with a targeted composition, $\text{Li}_{1.1}\text{Mn}_{1.9}\text{O}_4$, on the electrochemical properties of LCO is reported.

Figure 23a shows the 1st charge/discharge cycles of a Li/LCO cell before and after wet-chemical treatments of the LCO electrode powder in acidic solutions of Li and Mn nitrates, targeting LCO/spinel concentrations of .95/.05 and .90/.10, followed by firing in air at $\sim 500^\circ\text{C}$. Clearly observed in the 1st-cycle discharge is a plateau at $\sim 2.7\text{V}$ for the treated samples, consistent with the formation of a spinel-type component at the electrode surface. Figure 23b shows cycling data between 4.6–2.0V for the untreated and treated samples. A significant improvement in cell cycling stability was observed for the spinel-coated electrodes relative to the pure LCO electrode, with the 5% targeted spinel electrode delivering more than 200 mAh/g for 20 cycles. To stabilize the surface of the LCO electrode further, a $\sim 0.5\text{ nm}$ coating of AlW_xF_y was deposited directly on the electrode laminates by atomic layer deposition (ALD); this approach to use W- and F-based coatings has been discussed in earlier reports. Figure 23c shows the capacity versus cycle plot of the $\text{Li}/0.95\text{LiCoO}_2 \cdot 0.05\text{Li}_{1.1}\text{Mn}_{1.9}\text{O}_4$ cell in which an AlW_xF_y coating had been applied to the cathode laminate. Cells were cycled between 4.5–3.0V at 15 mA/g and 30°C in Li half-cells. Figure 23c shows that these electrodes delivered an extremely constant capacity ($\sim 185\text{ mAh/g}$) for 50 cycles. The dQ/dV plots (inset in Figure 23c) corresponding to cycles 1 and 50 show two distinct reversible redox peaks (starred), characteristic of a LCO electrode at high potentials; the data illustrate the excellent stability and reversibility of the coated LCO electrodes. Efforts to characterize and understand the surface structures of these electrode materials as well as NMC electrode systems are ongoing.

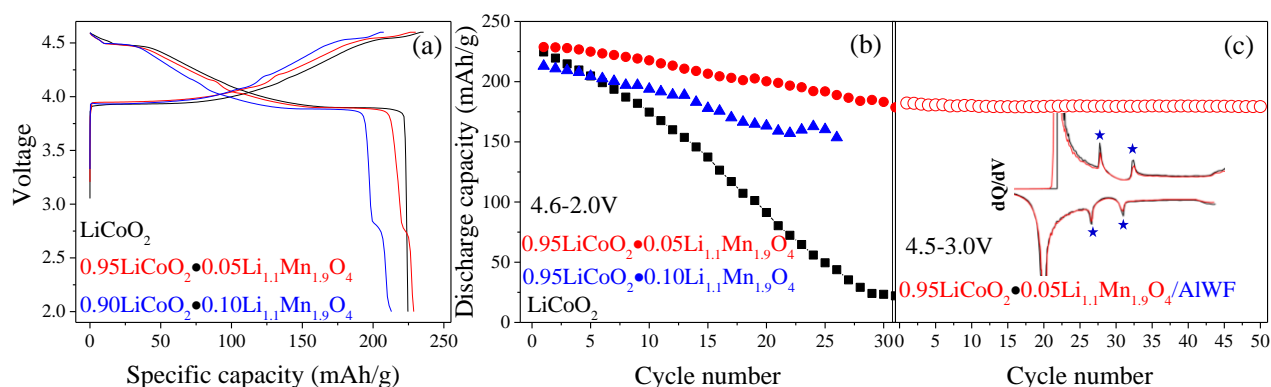


Figure 23. (a) First-cycle voltage profiles of LiCoO_2 (black), $0.95\text{LiCoO}_2 \cdot 0.05\text{Li}_{1.1}\text{Mn}_{1.9}\text{O}_4$ (red), and $0.90\text{LiCoO}_2 \cdot 0.10\text{Li}_{1.1}\text{Mn}_{1.9}\text{O}_4$ (blue). (b) Corresponding capacity vs. cycle data (4.6–2.0 V, 15 mA/g). (c) $0.95\text{LiCoO}_2 \cdot 0.05\text{Li}_{1.1}\text{Mn}_{1.9}\text{O}_4$ coated with $\sim 0.5\text{ nm}$ AlW_xF_y cycled between 4.5–3.0 V. (All data vs. Li/Li^+ at 30°C , 15 mA/g). Inset shows dQ/dV plots of cycles 1 (black) and 50 (red). Stars indicate phase transitions in LCO.

Patents/Publications/Presentations

Presentations

- Gordon Research Conference: Batteries, Ventura, California (February 2016): “Composite ‘Layered-Layered-Spinel’ Electrodes for High Energy Lithium-ion Batteries”; J. S. Park, J. R. Croy, E. Lee, and M. M. Thackeray.
- IMDEA Energy Institute, Madrid, Spain (March 7, 2016): “Energy Storage: Challenges and Opportunities in an Evolving Lithium Economy”; M. M. Thackeray. Invited.
- Metal Air Battery International Congress - MaBIC 16, Santander, Spain (March 9, 2016): “Tapping and Taming the Potential of Lithium-Oxygen Electrochemistry”; M. M. Thackeray. Invited.
- BMW Munich Battery Discussions, Garching, Germany (March 14-15, 2016): “Advances in the Structural Design of Cathodes for High Energy Li-ion Cells”; M. M. Thackeray. Invited.
- BMR Cathode Workshop, ORNL, Oak Ridge, Tennessee (March 15, 2016): “Challenges of High-Energy Cathode Materials”; J. R. Croy.

Task 3.6 – Lithium-bearing Mixed Polyanion (LBMP) Glasses as Cathode Materials (Jim Kiggans and Andrew Kercher, Oak Ridge National Laboratory)

Project Objective. Develop mixed polyanion (MP) glasses as potential cathode materials for lithium-ion batteries with superior performance to lithium iron phosphate for use in EV applications. Modify MP glass compositions to provide higher electrical conductivities, specific capacities, and specific energies than similar crystalline polyanionic materials. Test MP glasses in coin cells for electrochemical performance and cyclability. The final goal is to develop MP glass compositions for cathodes with specific energies up to near 1,000 Wh/kg.

Project Impact. The projected performance of MP glass cathode materials addresses the VTO Multi-Year Program Plan goals of higher energy densities, excellent cycle life, and low cost. MP glasses offer the potential of exceptional cathode energy density up to 1000 Wh/kg, excellent cycle life from a rigid polyanionic framework, and low-cost, conventional glass processing.

Out-Year Goals. MP glass development will focus on compositions with expected multivalent intercalation reactions within a desirable voltage window and/or expected high-energy glass-state conversion reactions.

Polyanion substitution will be further adjusted to improve glass properties to potentially enable multi-valent intercalation reactions and to improve the discharge voltage and cyclability of glass-state conversion reactions. Cathode processing of the most promising mixed polyanion glasses will be refined to obtain desired cycling and rate performance. These optimized glasses will be disseminated to BMR collaborators for further electrochemical testing and validation.

Milestones

1. Produce glass compositions for high-energy cathodes giving maximally oxidized transition metals upon first charge. (March 2016 – Projected completion date is delayed to 30 April 2016 due to equipment refurbishing)
2. Produce unconventional glass cathodes using alternative glass formers or partial crystallinity. (June 2016)

Progress Report

Antimony is theoretically capable of a multivalent intercalation reaction at $\leq 4.5\text{V}$. Lithium antimony borate vanadate and lithium antimony phosphate vanadate glasses were produced with the aim of producing a high-energy, high-capacity intercalation cathode. While both glasses exhibited a high capacity conversion reaction at $\sim 1.2 - 1.4\text{V}$, neither glass had a significant capacity in an intercalation reaction (Figure 24). The phosphate glass conversion reaction was at a higher voltage than the borate glass reaction, because phosphate has a stronger inductive effect than borate. While theoretically very promising, high-capacity intercalation reactions in mixed polyanion glasses (besides iron phosphate vanadate) have continued to be elusive.

A polyanion blend of phosphate, borate, and vanadate (PBV) has shown improved 1st cycle reversibility and round-trip energy efficiency in copper-based glass cathodes. The same PBV blend was used to produce similar silver-based and nickel-based glasses (Figure 25). Near-complete 1st cycle reversibility was observed in the Ag-based PBV glass, but the PBV blend only slightly improved 1st cycle reversibility in the Ni-based PBV glass. Ag- and Ni-based PBV glasses didn't show significant improvements in round-trip efficiency.

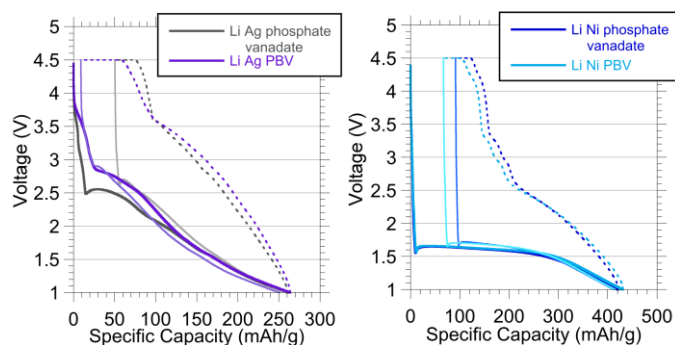


Figure 25. Ag-based and Ni-based phosphate-borate-vanadate (PBV) glasses were compared to phosphate-vanadate glasses.

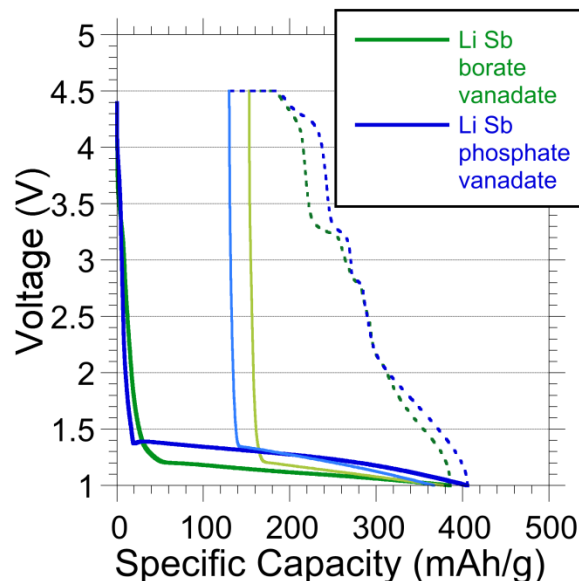


Figure 24. Antimony-based glasses demonstrated a high-capacity conversion reaction, but not the desired multi-valent intercalation reaction.

A copper PBV glass was produced with a higher borate content (15% vs. 10%) to determine if the electrochemical performance could be further improved. The glass with higher borate content had worse 1st cycle reversibility than the original PBV glass, but still had significantly better 1st cycle reversibility than a phosphate/vanadate glass. This result suggests an optimum borate content in PBV glasses to achieve best electrochemical performance. Infrared (IR) and Raman spectroscopy is being used to evaluate the polyanions in PBV glasses that promote the best electrochemical performance.

Task 3.7 – Advanced Cathode Materials for High Energy Lithium Ion Batteries (Marca Doeff, Lawrence Berkeley National Laboratory)

Project Objective. Microscopy and synchrotron X-ray absorption and photoemission techniques will be used to study the phenomenon of surface reconstruction to rock salt on NMC particle surfaces as a function of composition, synthesis method, surface chemistry, and electrochemical history. Because the surface reconstruction is implicated in capacity fading and impedance rise during high-voltage cycling, a thorough understanding of this phenomenon is expected to lead to principles that can be used to design robust, high-capacity NMC materials for Li-ion cells. The emphasis will be on stoichiometric NMCs with high Ni contents such as 622 and 523 compositions.

Project Impact. To increase the energy density of Li-ion batteries, cathode materials with higher voltages and/or higher capacities are required, but safety and cycle life cannot be compromised. Nickel rich NMCs can provide higher capacities and lower cost in comparison with low nickel content NMCs, but surface reactivity is an issue. A systematic evaluation of the effects of synthesis method, composition, and cell history on the surface reconstruction phenomenon will lead to higher capacity, robust and structurally stable positive electrode materials that result in higher energy density Li-ion cells than currently available.

Out-Year Goals. The information generated by the in-depth characterization will be used to design robust NMC materials that can withstand cycling to high potentials and deliver >200 mAh/g.

Collaborations. Transmission X-ray microscopy (TXM) has been used this quarter to characterize NMC materials, with work done in collaboration with Yijin Liu (SSRL). Synchrotron and computational efforts continued in collaboration with Professor M. Asta (UC Berkeley); and Dr. Dennis Nordlund, Dr. Yijin Liu and Dr. Dimosthenis Sokaras (SSRL). The TEM effort is in collaboration with Dr. Huolin Xin (BNL).

Milestones

1. Synthesize baseline NMC-523 and NMC-622 and Ti-substituted variants by spray pyrolysis and co-precipitation. (December 2015 – Completed)
2. Complete surface characterization of pristine materials by XAS and XPS. (March 2016 – Complete).
3. Complete soft XAS experiments on electrodes cycled to high potentials. (June 2016 – On track)
4. *Go/No-Go*: Core-shell composites made by infiltration and re-firing of spray-pyrolyzed hollow spherical particles. (September 2016 – On track)

Progress Report

Evaluation of the electrochemical performance for both spray pyrolyzed and co-precipitated NMC-622 materials continued this quarter. Both materials could deliver first cycle discharge capacities of over 200mAh/g when they were charged to high voltage (4.7 V). Synchrotron *in situ* XRD was employed to investigate the crystal structure change of NMC-622 materials during cycling. The strong X-ray source at synchrotron beamline provides extremely high resolution, where data was collected every 60 seconds without sacrificing the resolution. This capability allows for detailed observation of minor structural changes upon cycling. Here, the project intentionally charged to higher voltage than normal conditions (that is, up to 5.0 V) during the first charge. As shown in Figure 26, a charge capacity of 281 mAh/g was achieved, which is higher than the theoretical capacity (~275mAh/g). The higher capacity is likely due to the decomposition of electrolyte at high voltage. During the cycling, XRD data was collected simultaneously. Figure 27 shows selected data sets from the *in situ* experiment, focusing on the 003 and 104 peaks. It is obvious that NMC-622 undergoes several phase transitions during charge, as indicated with arrows in Figure 27. As with LiNiO_2 , NMC-622 shows phase transitions from H1 (original hexagonal phase 1) to H2 and and H3 at high voltage. The H3 phase, which is thermally unstable, is more pronounced for NMC-622 (our results) and LiNiO_2 (literature) than for NMC-333 (literature). This suggests that higher Ni content will lead to inferior thermal stability during cycling, especially when taken to high voltages. Thermal stability studies using synchrotron TXM and x-ray Raman are in progress to investigate this further.

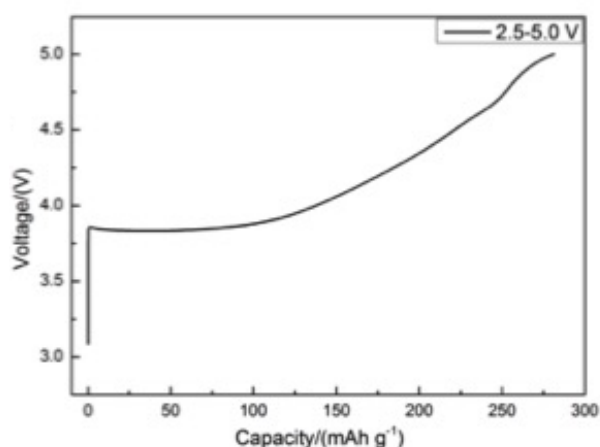


Figure 26. The 1st charge curve of NMC-622 materials cycled to 5.0 V vs. Li

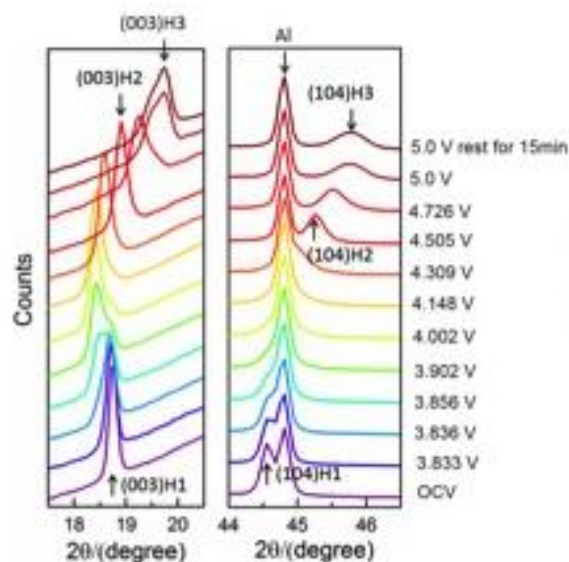


Figure 27. *In situ* X-ray diffraction patterns of NMC-622 upon charge to 5.0 V at C/10. The 2θ angles have been converted to those corresponding to the Cu K α radiation.

Patents/Publications/Presentations

Publications

- Rettenwander, Daniel, and Günther Redhammer, Florian Preishuber-Pflügl, Lei Cheng, Lincoln Miara, Reinhard Wagner, Andreas Welzl, Emmanuel Suard, Marca M. Doeff, Martin Wilkening, Jürgen Fleig, and Georg Amthauer. “Structural and Electrochemical Consequences of Al and Ga Co-substitution in $\text{Li}_7\text{La}_3\text{Zr}_2\text{O}_{12}$ Solid Electrolytes.” *Chem. Mater.* 28 (2016): 2384.
- Catarelli, Samantha, and Daniel Lonsdale, Lei Cheng, Jaroslaw Syzdek, and Marca M. Doeff. “Intermittent Contact Alternating Current Scanning Electrochemical Microscopy: A Method for Mapping Conductivities in Solid Li Ion Conducting Electrolyte Samples.” *Frontiers in Energy Research* (2016). doi: 10.3389/fenrg.2016.00014.
- Xu, J., and F. Lin, D. Nordlund, E. J. Crumlin, F. Wang, J. Bai, M. M. Doeff, and W. Tong. “Elucidating the Surface Characteristics and Electrochemistry of High-Performance LiNiO_2 .” *Chem. Commun.* 52 (2016): 4239.
- Lin, F., and D. Nordlund, Y. Li, M. K. Quan, L. Cheng, T.-C. Weng, Y. Liu, H. L. Xin and M. M. Doeff. “Metal Segregation in Hierarchically Structured Layered Cathode Materials with Improved Lithium Battery Performance.” *Nature Energy* 1, (2016): 1.

Presentation

- 40th International Conference and Expo on Advanced Ceramics and Composites, Daytona Beach, Florida (24-29 January 2016): “Insights into the Structure and Performance of NMC Cathode Materials for Li-ion Batteries”; Marca M. Doeff. Invited.

Task 3.8 – Lithium Batteries with Higher Capacity and Voltage (John B. Goodenough, UT – Austin)

Project Objective. The project objective is to develop an electrochemically stable alkali-metal anode that can avoid the SEI layer formation and the alkali-metal dendrites during charge/discharge. To achieve the goal, a thin and elastic solid electrolyte membrane with a Fermi energy above that of metallic Li and an ionic conductivity $\sigma > 10^{-4} \text{ S cm}^{-1}$ (1) will be tested in contact with alkali-metal surface. (2) The interface between the alkali-metal and the electrolyte membrane should be free from liquid electrolyte, (3) have a low impedance for alkali-metal transport and plating, and (4) keep good mechanical contact during electrochemical reactions.

Project Impact. An alkali-metal anode (Li or Na) would increase the energy density for a given cathode by providing a higher cell voltage. However, lithium is not used as the anode in today's commercial lithium-ion batteries because electrochemical dendrite formation can induce a cell short-circuit and critical safety hazards. This project is to find a way to avoid the formation of alkali-metal dendrites and to develop an electrochemical cell with dendrite-free alkali-metal anode. Therefore, once realized, the project will have a significant impact by an energy-density increase and battery safety; it will enable a commercial lithium-metal rechargeable battery of increased cycle life.

The key approach is to introduce a solid-solid contact between an alkali metal and a solid electrolyte membrane. Where SEI formation occurs, the creation of new anode surface at dendrites with each cycle causes capacity fade and a shortened cycle life. To avoid the SEI formation, a thin and elastic solid electrolyte membrane will be introduced, and liquid electrolyte will be eliminated from the anode surface.

Out-Year Goals. The out-year goals are to increase cell energy density for a given cathode and to allow low-cost, high-capacity rechargeable batteries with cathodes other than insertion compounds.

Collaborations. This project collaborates with A. Manthiram at UT Austin and with Karim Zaghib at HQ.

Milestones

1. Fabricate and test glass-fiber and cross-linked polymer membranes impregnated with Li^+ glass electrolytes. (December 2015 – Complete)
2. Test cycle life of plating/stripping Li across Li^+ glass electrolyte. (March 2016 – Complete)
3. Test and optimize volumetric energy density of all-solid-state cell with Li^+ glass electrolyte. (June 2016).
4. Compare all-solid-state cell with a cell having a similar cathode and a liquid catholyte. (September 2016)

Progress Report

The project has developed a glass Li^+ and Na^+ electrolyte with an ionic conductivity $\sigma_i = 10^{-2}$ to $10^{-1} \text{ S cm}^{-1}$ at room temperature as well as a uniquely high dielectric constant owing to the presence of $(\text{OM})^-$ dipoles (Figure 28).

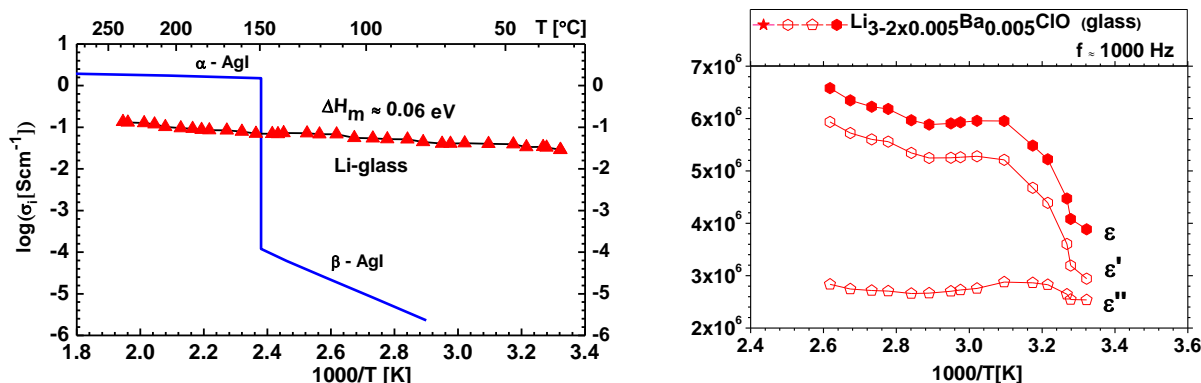


Figure 28. (left) Ionic conductivity of the Li-glass as a function of temperature. (right) Real (ϵ') imaginary (ϵ'') permittivities and permittivity modulus (ϵ).

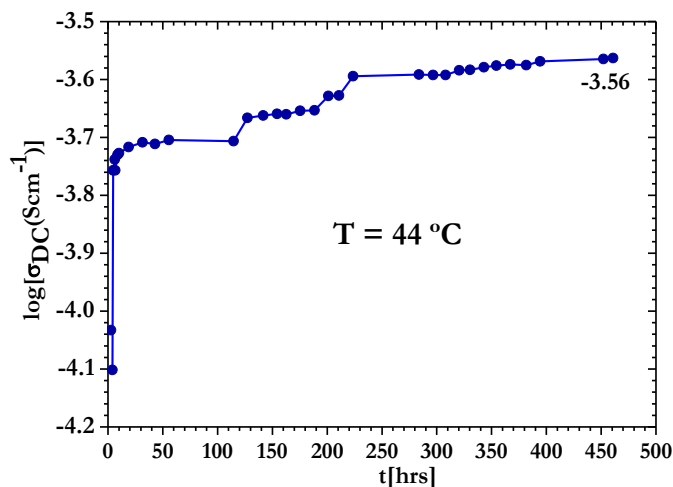


Figure 29. Results of chronopotentiometry (a galvanostatic direct current, DC, experiment) as on a symmetric $\text{Li}^0/\text{Li-glass}/\text{Li}^0$ cell with calcium-doped Li-glass, $\text{Li}_{2.99}\text{Ca}_{0.005}\text{OCl}$. The cell voltage was reversed every 20 min at a current of 0.10 mAcm^{-2} during 19 days in an argon-filled glove box.

It was developed by solvating in little H_2O and adding a small amount of $\text{Ba}(\text{OH})_2$ in a precursor mix of Li_3ClO . On sintering at 250°C , it loses HCl as a gas; and above 230°C an irreversible weight loss is attributed to a loss of water by the reaction $2\text{OH}^- = \text{O}^{2-} + \text{H}_2\text{O}$. Figure 29 demonstrates that the glass plates metallic Li^0 on Li^0 without dendrite formation, but also that the activation energy ΔH_m for Li^+ mobility decreases with time. The evolution of the ΔH_m shows the Li^+ mobility dependence on the orientation of the dipoles; above 75°C , the dipoles rotate freely to allow their rapid orientation and alignment in an electric field to give the $\Delta H_m \approx 0.06 \text{ eV}$.

Task 3.9 – Exploiting Co and Ni Spinel in Structurally Integrated Composite Electrodes (Michael M. Thackeray and Jason R. Croy, Argonne National Laboratory)

Project Objective. The project goal is to stabilize high-capacity, composite ‘layered-layered’ electrode structures with lithium-cobalt-oxide and lithium-nickel-oxide spinel components (referred to as LCO-S and LNO-S, respectively), or solid solutions thereof (LCNO-S), which can accommodate lithium at approximately 3.5 V vs. metallic lithium. This approach and the motivation to use LCO-S and LNO-S spinel components, about which relatively little is known, is novel.

Project Impact. State-of-the-art lithium-ion batteries are unable to satisfy the performance goals for PHEVs and all-electric EVs. If successful, this project will impact the advance of energy storage for electrified transportation as well as other applications, such as portable electronic devices and the electrical grid.

Approach. This work will focus on the design and synthesis of new spinel compositions and structures that operate above 3 V and below 4 V and to determine their structural and electrochemical properties through advanced characterization. This information will subsequently be used to select the most promising spinel materials for integration as stabilizers into high-capacity composite electrode structures.

Out-Year Goals. The electrochemical capacity of most high-potential lithium-metal oxide insertion electrodes is generally severely compromised by their structural instability and surface reactivity with the electrolyte at low lithium loadings (that is, at highly charged states). Although some progress has been made by cation substitution and structural modification, the practical capacity of these electrodes is still restricted to approximately 160-170 mAh/g. This project proposes a new structural and compositional approach with the goal of producing electrode materials that can provide 200-220 mAh/g without significant structural or voltage decay for 500 cycles. If successful, the materials processing technology will be transferred to the Argonne Materials Engineering and Research Facility (MERF) for scale up and further evaluation.

Collaborations. This project collaborates with Eungje Lee, Joong Sun Park (Chemical Sciences and Engineering, ANL), Mali Balasubramanian (Advanced Photon Source, ANL), and V. Dravid and C. Wolverton (Northwestern University).

Milestones

1. Synthesize and optimize spinel compositions and structures with a focus on Co-based systems for use in structurally integrated layered-spinel electrodes. (Q1 – In progress; see text)
2. Determine electrochemical properties of Co-based spinel materials, and when structurally integrated in composite layered-spinel electrodes. (Q2 – In progress; see text)
3. Evaluate the electrochemical migration of transition metal ions in Co-based layered-spinel electrodes. (Q4 – In progress)

Progress Report

Previous reports have emphasized how the synthesis temperature impacts the structure and electrochemistry of $\text{LiCo}_{1-x}\text{Ni}_x\text{O}_2$ materials that are of interest for stabilizing high capacity, lithium- and manganese-rich metal oxide electrodes. X-ray and neutron diffraction data and electrochemical analyses have suggested that $\text{LiCo}_{1-x}\text{Ni}_x\text{O}_2$ structures prepared at a relatively low temperature (LT) are highly complex and that they contain structurally integrated spinel and layered features and intermediate spinel/layered configurations. In this study, TEM imaging was used to gather a more detailed understanding of the atomic arrangements in these complex structures. $\text{LiCo}_{0.9}\text{Ni}_{0.1}\text{O}_2$, synthesized in air between 400°C and 800°C, was selected for the investigation. STEM-high angle annular dark field (STEM-HAADF) image analysis was undertaken in collaboration with Dr. Chongmin Wang's group at PNNL.

Figures 30a-c shows high-resolution TEM images of a LT- $\text{LiCo}_{0.9}\text{Ni}_{0.1}\text{O}_2$ (400°C) sample that reveal both spinel (Figure 30a) and layered (Figure 30b-c) components in an essentially cubic-close-packed (*c*) structure. The existence of a pure layered, cubic $\text{LiCo}_{0.9}\text{Ni}_{0.1}\text{O}_2$ structure (*c*-layered) does not seem likely in view of the stability of conventional layered $\text{LiCo}_{0.9}\text{Ni}_{0.1}\text{O}_2$ structures that crystallize with hexagonal (*h*) symmetry (R-3m) when prepared at high-temperature (HT, ~800°C). Given this anomaly, the d-spacings between the transition metal planes of the *c*-layered (400°C) and *h*-layered (800°C) structures were measured from the TEM images in Figure 30c and 30d, respectively. Figure 30d shows the perfect layering of the transition metal ions in HT- $\text{LiCo}_{0.9}\text{Ni}_{0.1}\text{O}_2$ (bright contrast) in which the d-spacing was determined to be 4.68 Å; by comparison, the corresponding d-spacing in LT- $\text{LiCo}_{0.9}\text{Ni}_{0.1}\text{O}_2$ sample was determined to be slightly smaller, 4.63 Å, consistent with the argument that some of the cobalt and/or nickel ions reside in the lithium layers thereby providing intermediate layered/spinel character and sufficient binding energy in the lithium-rich layers to maintain a cubic-close-packed oxyanion array.

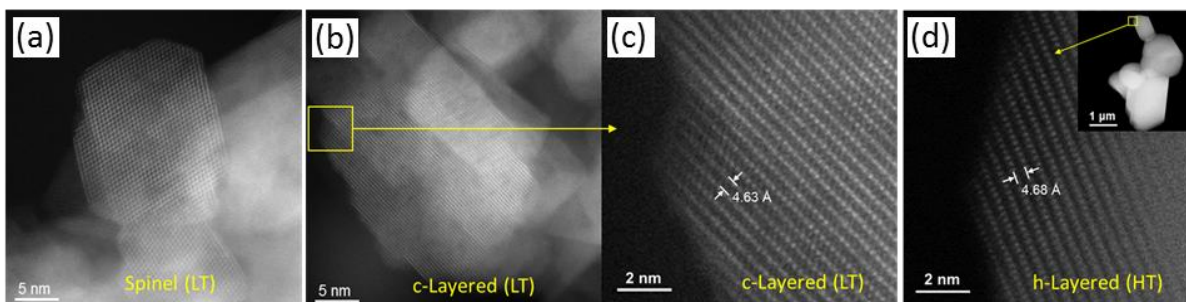


Figure 30. Scanning transmission electron microscopy high angle annular dark field images of (a-c) LT- $\text{LiCo}_{0.9}\text{Ni}_{0.1}\text{O}_2$ (400°C) and (d) HT- $\text{LiCo}_{0.9}\text{Ni}_{0.1}\text{O}_2$ (800°C).

TEM images of a nanocomposite, ‘layered-spinel’ $\text{LiCo}_{0.9}\text{Ni}_{0.1}\text{O}_2$ product prepared at an intermediate temperature (IT, 600°C) show that the structure is composed of spinel and layered domains that are atomically aligned with one another (Figure 31a-b). The images suggest that, on increasing the firing temperature, the phase transition from spinel to a layered configuration occurs at distinct phase boundaries, and that the layered-to-spinel ratio can be controlled by tailoring the annealing temperature. This observation provides compelling evidence to support the strategy of using a Co-based spinel component to stabilize layered and ‘layered-layered’ electrode structures.

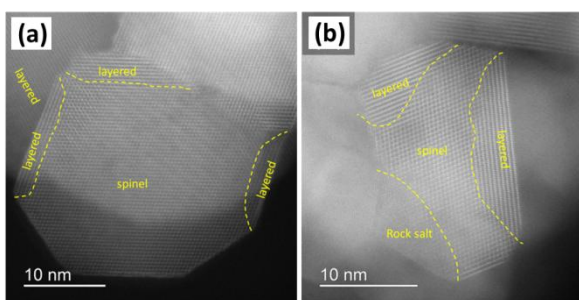


Figure 31. Scanning transmission electron microscopy high angle annular dark field images of IT- $\text{LiCo}_{0.9}\text{Ni}_{0.1}\text{O}_2$ (600°C) showing atomically integrated ‘layered-spinel’ nano-composite crystals.

Patents/Publications/Presentations

Presentation

- BMR Program Review Meeting, LBNL, Berkeley, California (January 20, 2016): “Novel Cathode Materials and Processing Methods”; E. J. Lee, J. R. Croy, and M. M. Thackeray.

Task 3.10 – Discovery of High Energy Li Ion Battery Materials (Wei Tong, Lawrence Berkeley National Laboratory)

Project Objective. This project aims to develop a cathode that can cycle > 200 mAh/g while exhibiting minimal capacity and voltage fade. The emphasis will be on oxides with high nickel contents. This task focuses on the compositions in the Li-Ni-O phase space, which will be explored using a combinatorial materials approach to search for new high-capacity cathodes. The specific objectives of this project are to: (1) investigate and understand the correlation between the synthesis and electrochemical performance of Ni-based compounds, (2) design, synthesize, and evaluate the potential new high-capacity cathodes within Li-Ni-O composition space using the percolation theory as a guideline.

Project Impact. In the commercial Li-ion batteries, the well ordered, close-packed oxides, particularly, layered lithium transition metal oxides (LiTmO_2 , Tm is transition metal) are widely used. However, the energy density needs to be at least doubled to meet the performance requirements of EVs (300 to 400 miles). Although capacities approaching 300 mAh/g have been reported in Li, Mn-rich layered oxide compounds, capacity decay and voltage fading in the long-term cycling are always observed. Therefore, new materials are urgently needed to make the breakthrough in Li-ion battery technology.

Approach. The recent discovery of high-capacity materials with lithium excess provides new insights into design principles for potential high-capacity cathode materials. According to the percolation theory, lithium excess is required to access 1 lithium exchange capacity in LiTmO_2 compounds. This seems to be independent of transition metal species; therefore, it could open up a composition space for the search of new materials with high capacity. The interesting $\text{Ni}^{2+}/\text{Ni}^{4+}$ redox is selected as the electrochemically active component, and combinatorial materials design concept will be used to discover the potential cathode material candidates in the Li-Ni-O phase space.

Out-Year Goals. The long-term goal is to search new high-energy cathodes that can potentially meet the performance requirements of EVs with a 300- to 400-mile range in terms of cost, energy density, and performance. Work will progress from the understanding of the known compounds, LiNiO_2 and Li_2NiO_2 , toward development of new Ni-based, high-energy cathode oxides.

Collaborations. The PI closely collaborates with M. Doeff (LBNL) on soft XAS, C. Ban (NREL) on ALD coating, B. McCloskey (LBNL) for differential electrochemical mass spectrometry (DEMS), and R. Kostecki (LBNL) for Raman spectroscopy. Collaboration is also in progress with other BMR PIs (X.-Q. Yang and F. Wang, BNL; and K. Persson, LBNL) for crystal structure evolution upon cycling and material computation.

Milestones

1. Determine synthetic approach and identify the key synthetic parameters for Ni^{3+} -containing compounds, for example, LiNiO_2 . (Q1 – Complete)
2. Complete the structural and electrochemical characterization of LiNiO_2 . (Q2 – Complete)
3. Determine synthetic approach and identify the key synthetic parameters for Ni^{2+} -containing compounds, for example, Li_2NiO_2 . (Q3 – In progress)
4. Complete the structural and electrochemical characterization of Li_2NiO_2 , and down select the synthetic approach for the phase screening within Li-Ni-O chemical space. (Q4)

Progress Report

LiNiO₂ was synthesized by a conventional solid state method, and characterized after different terms of cycling. As shown in Figure 32, the material exhibited an initial discharge capacity of 205 mAh/g with a Coulombic efficiency of 84.7% during the 1st cycle. In the subsequent cycles, the capacity gradually degraded and only 160 mAh/g remained at the end of the 45th cycle, corresponding to 78% capacity retention with respect to the 1st cycle (Figure 32). *In situ* XRD of highly charged Li_xNiO₂ revealed a series of phase transformations from original hexagonal phase (H1) to monoclinic (M) phase, to another hexagonal (H2), and finally a third hexagonal phase (H3) upon Li removal. The performance decay was ascribed to the bulk structural change. Therefore, SXRD was conducted over the extended cycles.

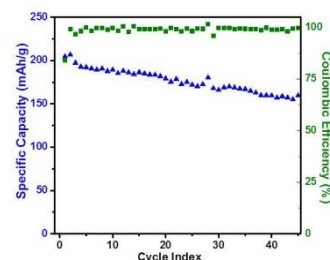


Figure 32. Cycling performances of LiNiO₂. Cells were cycled between 4.3 and 2.7 V at C/10 for the first two cycles, followed by C/5 in the subsequent cycles.

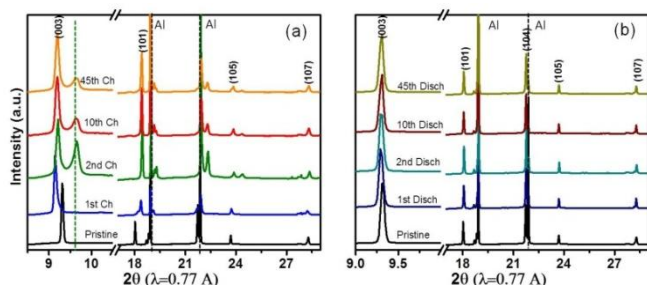


Figure 33. Synchrotron X-ray diffraction patterns of LiNiO₂ at (a) 4.3 V charging states and (b) 2.7 V discharging states in the selected cycles. The bottom patterns in these two figures are from pristine electrode reference. The green dash line denotes the (003) peak from H3 phase.

H3 (003) diffraction peak gradually decreased, suggesting the less H3 phase formation. In addition to the structural change at the charged states, the pristine structure was not completely resumed after the first discharge. As shown in Figure 33b, the (003) peak slightly shifted to the lower angle region, compared to its pristine state, suggesting the lattice expansion along *c* direction likely due to the irreversible Li loss. In the subsequent cycles, the variations were fairly small, indicated by the similar peak positions and intensities in the XRD patterns.

In addition, EXAFS data were collected and analyzed. As shown in Figure 34a, the Ni–O (1.4 Å) and Ni–Ni (2.4 Å) interatomic distances in the pristine state decreased upon charge because of the increase in Ni ion oxidation state. Meanwhile, the increase in intensity of these two shells that are consistent with the absence of Jahn-Teller distortion for Ni⁴⁺ reached to a maximum at Cycle 2 and gradually decreased in the later cycles. As for the discharged states in the subsequent cycles, the Ni local environments were basically recovered (Figure 34b).

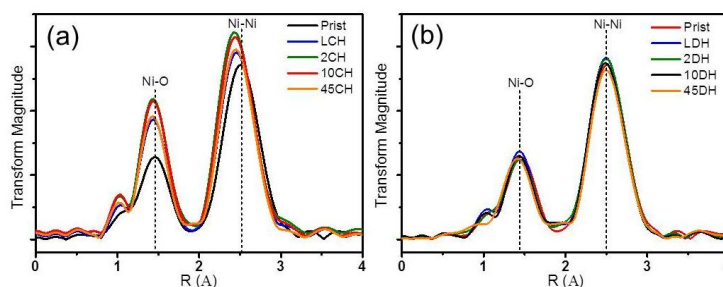


Figure 34. Extended X-ray absorption fine structure graphs for (a) charging and (b) discharging states.

Patents/Publications/Presentations

Publication

- Xu, Jing, and Feng Lin, Wei Tong, Dennis Nordlund, Ethan J. Crumlin, Feng Wang, Jianming Bai, Marca M. Doeff, and Wei Tong. “Elucidation of the Surface Characteristics and Electrochemistry of High-performance LiNiO₂.” *Chemical Communication* 52 (2016): 4239-4242.

TASK 4 – ELECTROLYTES FOR HIGH-VOLTAGE, HIGH-ENERGY LITHIUM-ION BATTERIES

NOTE: This task is now closed, with limited extension work being completed this quarter. The BMR will issue a Call in this area later this fiscal year.

Summary

The current lithium-ion electrolyte technology is based on LiPF_6 solutions in organic carbonate mixtures with one or more functional additives. Lithium-ion battery chemistries with energy density of 175~250 Wh/Kg are the most promising choice. To further increase the energy density, the most efficient way is to raise either the voltage and/or the capacity of the positive materials. Several high-energy materials including high-capacity composite cathode $x\text{Li}_2\text{MnO}_3 \cdot (1-x)\text{LiMO}_2$ and high-voltage cathode materials such as $\text{LiNi}_{0.5}\text{Mn}_{1.5}\text{O}_4$ (4.8 V) and LiCoPO_4 (5.1 V) have been developed. However, their increased operating voltage during activation and charging poses great challenges to the conventional electrolytes, whose organic carbonate-based components tend to oxidatively decompose at the threshold beyond 4.5 V vs Li^+/Li .

Other candidate positive materials for PHEV application that have potential of providing high capacity are the layered Ni-rich NCM materials. When charged to a voltage higher than 4.5 V, they can deliver a much higher capacity. For example, $\text{LiNi}_{0.8}\text{Co}_{0.1}\text{Mn}_{0.1}\text{O}_2$ (NCM 811) only utilizes 50% of its theoretical capacity of 275 mAh/g when operating in a voltage window of 4.2 V – 3.0 V. Operating voltage higher than 4.4 V would significantly increase the capacity to 220 mAh/g; however, the cell cycle life becomes significantly shortened mainly due to the interfacial reactivity of the charged cathode with the conventional electrolyte. The oxidative voltage instability of the conventional electrolyte essentially prevents the practicality to access the extra capacities of these materials.

To address the above challenges, new electrolytes that have substantial high-voltage tolerance at high temperature with improved safety are needed urgently. Organic compounds with low HOMO (highest occupied molecular orbital) energy level are suitable candidates for high-voltage application. An alternative approach to address the electrolyte challenges is to mitigate the surface reactivity of high-voltage cathodes by developing cathode passivating additives. Like the indispensable role of SEI on the carbonaceous anodes, cathode electrolyte interphase (CEI) formation additives could kinetically suppress the thermodynamic reaction of the delithiated cathode and electrolyte, thus significantly improving the cycle life and calendar life of the high energy density lithium-ion battery.

An ideal electrolyte for high-voltage, high-energy cathodes also requires high compatibility with anode materials (graphite or silicon). New anode SEI formation additives tailored for the new high-voltage electrolyte are equally critical for the high-energy lithium-ion battery system. Such an electrolyte should have the following properties: high stability against 4.5 – 5.0 V charging state, particularly with cathodes exhibiting high surface oxygen activity; high compatibility with a strongly reducing anode under high-voltage charging; high Li salt solubility ($> 1.0 \text{ M}$) and ionic conductivity ($> 6 \times 10^{-3} \text{ S/cm}$ @ room temperature); and non-flammability (no flash point) for improved safety and excellent low-temperature performance (-30°C).

TASK 5 – DIAGNOSTICS

Summary and Highlights

To meet the goals of VTO Multi Year Program Plan and develop lower-cost, abuse-tolerant batteries with higher energy density, higher power, better low-temperature operation and longer lifetimes suitable for the next-generation of HEVs, PHEVs and EVs, there is a strong need to identify and understand structure-property-electrochemical performance relationships in materials, life-limiting and performance-limiting processes, and various failure modes to guide battery development activities and scale-up efforts. In the pursuit of batteries with high energy density, high cell operating voltages and demanding cycling requirements lead to unprecedented chemical and mechanical instabilities in cell components. Successful implementation of newer materials such as Si anode and high-voltage cathodes also requires better understanding of fundamental processes, especially those at the solid/electrolyte interface of both anode and cathode.

The BMR Task 5 takes on these challenges by combining model system, *ex situ*, *in situ*, and *operando* approaches with an array of the start-of-the-art analytical and computational tools. Four subtasks are tackling the chemical processes and reactions at the electrode/electrolyte interface. Researchers at LBNL use *in situ* and *ex situ* vibrational spectroscopy, far- and near-field scanning probe spectroscopy and laser-induced breakdown spectroscopy (LIBS) to understand the composition, structure, and formation/degradation mechanisms of the solid electrolyte interface at Si anode and high-voltage cathodes. The University of California at San Diego (UCSD) subtask combines STEM/EELS, XPS, and *ab initio* computation for surface and interface characterization and identification of instability causes at both electrodes. At Cambridge, nuclear magnetic resonance (NMR) is being used to identify major SEI components, their spatial proximity, and how they change with cycling. Subtasks at BNL and PNNL focus on the understanding of fading mechanisms in electrode materials, with the help of synchrotron based X-ray techniques (diffraction and hard/soft X-ray absorption) at BNL and HRTEM and spectroscopy techniques at PNNL. At LBNL, model systems of electrode materials with well defined physical attributes are being developed and used for advanced diagnostic and mechanistic studies at both bulk and single-crystal levels. These controlled studies remove the ambiguity in correlating material physical properties and reaction mechanisms to its performance and stability, which is critical for further optimization. The final subtask takes advantage of the user facilities at ANL that bring together X-ray and neutron diffraction, X-ray absorption, emission and scattering, HRTEM, Raman spectroscopy, and theory to look into the structural, electrochemical, and chemical mechanisms in the complex electrode/electrolyte systems. The diagnostics team not only produces a wealth of knowledge that is key to developing next-generation batteries, it also advances analytical techniques and instrumentation that have a far-reaching effect on material and device development in a range of fields.

Highlights. The highlights this quarter are as follows:

- Cambridge University (Grey's Group) used *in situ* ^7Li magnetic resonance imaging (MRI) on both electrolyte and lithium metal electrodes and revealed a strong correlation between the onset time of dendrite growth and the local depletion of the electrolyte at the surface of the electrode at high currents.
- The UC Berkeley (Somorjai) and LBNL (Ross) team reported that fluoroethylene carbonate (FEC) additive induces better ordering of the adsorbed ethylene carbonate (EC) on the silicon anode surface, which in turn affects the nature of the SEI formed at the interface.
- PNNL (Wang's Group) demonstrated plane selectivity of Ni and Co in building up surface segregation layers and recommended surface tunability through particle morphology and/or oxide composition control.

Task 5.1 – Design and Synthesis of Advanced High-Energy Cathode Materials (Guoying Chen, Lawrence Berkeley National Laboratory)

Project Objective. The successful development of next-generation electrode materials requires particle-level knowledge of the relationships between materials' specific physical properties and reaction mechanisms to their performance and stability. This single-crystal-based project was developed specifically for this purpose, and it has the following objectives: (1) obtain new insights into electrode materials by utilizing state-of-the-art analytical techniques that are mostly inapplicable on conventional, aggregated secondary particles, (2) gain fundamental understanding on structural, chemical, and morphological instabilities during Li extraction/insertion and prolonged cycling, (3) establish and control the interfacial chemistry between the cathode and electrolyte at high operating voltages, (4) determine transport limitations at both particle and electrode levels, and (5) develop next-generation electrode materials based on rational design as opposed to more conventional empirical approaches.

Project Impact. The project will reveal performance-limiting physical properties, phase-transition mechanisms, parasitic reactions, and transport processes based on the advanced diagnostic studies on well formed single crystals. The findings will establish rational, non-empirical design methods that will improve the commercial viability of next-generation $\text{Li}_{1+x}\text{M}_{1-x}\text{O}_2$ (M=Mn, Ni, and Co) and spinel $\text{LiNi}_x\text{Mn}_{2-x}\text{O}_4$ cathode materials.

Approach. This project scope will encompass the following: (1) Prepare crystal samples of Li-rich layered oxides and high-voltage Ni/Mn spinels with well defined physical attributes, (2) Perform advanced diagnostic and mechanistic studies at both bulk and single-crystal levels, and (3) Establish global properties and performance of the samples from the bulk analyses, while, for the single-crystal based studies, utilizing time- and spatial-resolved analytical techniques to probe material redox transformation and failure mechanisms.

Out-Year Goals. This project aims to determine performance and stability limiting fundamental properties and processes in high-energy cathode materials and to outline mitigating approaches. Improved electrode materials will be designed and synthesized.

Collaborations. This project collaborates with Drs. E. Crumlin and P. Ross (LBNL), Drs. Y. Liu and D. Nordlund (SSRL), Prof. C. Grey (Cambridge), Dr. C. Wang (PNNL), and Dr. J. Nanda (ORNL).

Milestones

1. Establish synthesis-structure-electrochemical property relationship in high-voltage Li-TM-oxides. (December 2015 – Complete)
2. *Go/No-Go*: Downselect alternative high-energy cathode materials for further investigation, if the material delivers > 200 mAh/g capacity in the voltage window of 2 – 4.5 V. (March 2016 – Completed with a Go/No-Go decision. A paper summarizing the results is in preparation.)
3. Determine Li concentration and cycling dependent transition-metal movement in and out of oxide particles. Examine the mechanism. (June 2016 – On schedule)
4. Identify key surface properties and features hindering stable high-voltage cycling of Li-TM-oxides. (September 2016 – On schedule)

Progress Report

One of the recognized strategies to improve the energy density of cathode materials is to increase the number of cyclable Li^+ in the compound by introducing multi-electron redox couples. Among the common transition metals, vanadium exhibits several stable oxidation states (+2, +3, +4 and +5) and the $\text{V}^{n+}/\text{V}^{(n-1)+}$ redox couples present a rare opportunity to cycle more than one Li^+ per formula unit. Tavorite-type LiVPO_4F with a triclinic space group $P\bar{1}$ has a three-dimensional framework of distorted $[\text{VO}_4\text{F}_2]$ octahedra and $[\text{PO}_4]$ tetrahedra that form different types of tunnels. The corner-shared chains of Li polyhedra and interconnected interstitial space make the compound a potential fast ionic conductor, while the high ionicity of the M-(O,F) bonds raises operating voltages. This fluorophosphate was initially reported by J. Barker in 2005 as a promising 4 V cathode material, but later studies demonstrated the extraction/reinsertion of one Li^+ at a voltage plateau of ~ 4.25 V ($\text{V}^{3+}/\text{V}^{4+}$ redox process) and another at a much lower plateau of 1.8 V ($\text{V}^{3+}/\text{V}^{2+}$ redox process), yielding theoretical capacities of 156 and 312 mAh/g for one and two removed Li^+ , respectively. As the utilization of two voltage plateaus with such a large gap of 2.4 V presents a major challenge for control electronics in battery systems, most studies on LiVPO_4F so far have been limited to the 4 V region.

In the context of pursuing high-energy cathodes capable of delivering more than 200 mAh/g, the project began investigating whether metal substitution can reduce the voltage gap by manipulating the two-plateau voltage profile into a more sloping one and/or improve the overall cycling stability of the $\text{Li}_2\text{VPO}_4\text{F}$ - LiVPO_4F - VPO_4F system. A series of $\text{LiM}_x\text{V}_{(1-x)}\text{PO}_4\text{F}$ ($\text{M} = \text{Mn}, \text{Co}, \text{Cr}, \text{Fe}$ and Ti , $x=0, 0.05$ or 0.1) was prepared by a two-step carbothermal reduction reaction where $\text{M}_x\text{V}_{(1-x)}\text{PO}_4/\text{C}$ intermediates were first prepared and then reacted with LiF to form the final products. As shown in the XRD patterns (Figure 35a), all samples were phase pure except $\text{LiV}_{0.90}\text{Cr}_{0.1}\text{PO}_4\text{F}$ where the common impurity of monoclinic $\text{Li}_3\text{V}_2(\text{PO}_4)_3$ was also present. Preliminary electrochemical performance was evaluated in 2032-type coin cells with a $\text{LiM}_x\text{V}_{1-x}\text{PO}_4\text{F}$ composite electrode, a Li metal anode, and a 1M LiPF_6 EC : DEC (1:1) electrolyte. Figure 35b shows the first-cycle voltage profiles during galvanostatic charge and discharge at 16 mA/g between 1.5 and 4.5 V. The presence of two plateaus at 4.25 and 1.8 V in LiVPO_4F is consistent with the reported two-phase topotactic reactions, involving significant lattice contractions/expansions and an overall symmetry shift from triclinic $P\bar{1}$ in LiVPO_4F to monoclinic $C2/c$ in VPO_4F and $\text{Li}_2\text{VPO}_4\text{F}$. Mn, Co and Ti substitution resulted in little change in voltage profiles and overall capacity. Although the introduction of Fe or Cr resulted in a more sloping voltage profile that suggests possible involvement of solid solution phases, the discharge capacity was substantially reduced compared to that of the parent LiVPO_4F . The new electrochemical signal around 2.5 V in the Cr substituted version may be attributed to the $\text{Cr}^{3+}/\text{Cr}^{2+}$ redox activity. The long-term cycling performance comparison shows stability improvement in both $\text{LiV}_{0.90}\text{Mn}_{0.05}\text{PO}_4\text{F}$ and $\text{LiV}_{0.90}\text{Co}_{0.05}\text{PO}_4\text{F}$ electrodes (Figure 35c); however, the overall impact of transition metal substitution on the voltage profile and cycling stability of LiVPO_4F was rather trivial. Further work was not justified, and a No-Go decision was made.

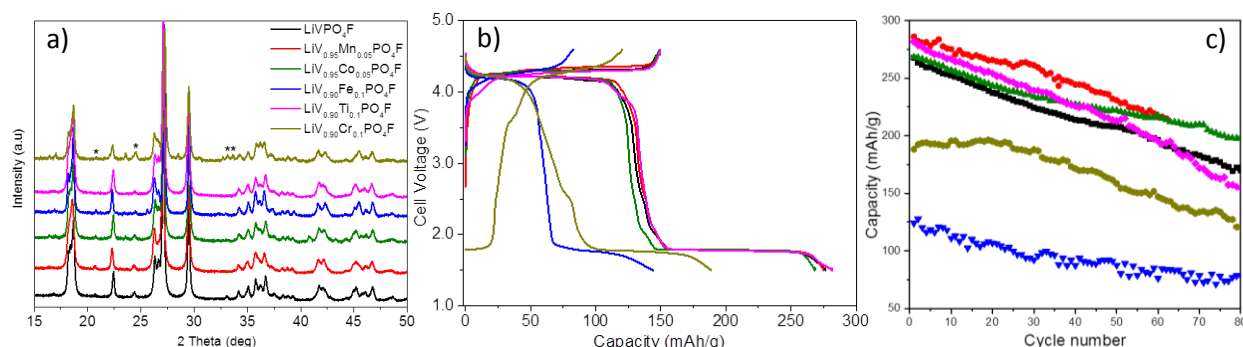


Figure 35. (a) X-ray diffraction patterns of the synthesized $\text{LiM}_x\text{V}_{(1-x)}\text{PO}_4\text{F}$ samples. (b) First-cycle voltage profiles during galvanostatic charge-discharge at 16 mA/g. (c) Long-term cycling performance of the $\text{LiM}_x\text{V}_{(1-x)}\text{PO}_4\text{F}$ cathodes. * indicates peaks from $\text{Li}_3\text{V}_2(\text{PO}_4)_3$ phase.

Patents/Publications/Presentations**Publications**

- Ma, Y., and Y. Zhou, C. Du, P. Zuo, X. Cheng, L. Han, D. Nordlund, Y. Gao, G. Yin, H. L. Xin, M. M. Doeff, F. Lin, and G. Chen. “A New Anion Receptor for Improved Interface between the Lithium- and Manganese-rich Layered Oxide Cathode and the Electrolyte.” Submitted (2016).
- Yan, P., and Jianming Zheng, Jiaxin Zheng, Z. Wang, G. Teng, S. Kuppan, J. Xiao, G. Chen, F. Pan, J.-G. Zhang, and C.-M. Wang. “Ni and Co Segregations on Selective Surface Facets and Their Composition Dependence in Layered Lithium Transition-Metal Oxide Cathodes.” *Advanced Energy Materials* 6, 1502455 (2016).

Presentation

- BMR Program Review Meeting, LBNL, Berkeley, CA (January 2016): “Design and Synthesis of Advanced High-Energy Cathode Materials”; G. Chen.

Task 5.2 – Interfacial Processes – Diagnostics (Robert Kostecki, Lawrence Berkeley National Laboratory)

Project Objective. The main task objective is to obtain detailed insight into the dynamic behavior of molecules, atoms, and electrons at electrode/electrolyte interfaces of high-voltage $\text{Li}[\text{Ni}_x\text{Mn}_y\text{Co}_z]\text{O}_2$ materials at a spatial resolution that corresponds to the size of basic chemical or structural and chemical building blocks. This project focuses on high Ni content NMC compositions such as 523 and 622, which are expected to achieve high discharge capacities even within conservative electrode potential limits. The aim of these studies is to unveil the structure and reactivity at hidden or buried interfaces and interphases that determine material, composite electrode and battery cell performance and failure modes. To accomplish these goals novel far- and near-field optical multifunctional probes must be developed and deployed *in situ*. This work constitutes an integral part of the concerted effort within the BMR Program, and it attempts to establish clear connections between diagnostics, theory/modelling, materials synthesis, and cell development efforts.

Project Impact. This project provides better understanding of the underlying principles that govern the function and operation of battery materials, interfaces, and interphases, which is inextricably linked with successful implementation of high-energy density materials such as $\text{Li}[\text{Ni}_x\text{Mn}_y\text{Co}_z]\text{O}_2$ compounds (NMCs) that can cycle stably to high potentials and deliver $> 200 \text{ mAh/g}$ at Coulombic efficiency close to 100%. This task also involves development and application of novel innovative experimental methodologies to study and understand the basic function and mechanism of operation of materials, composite electrodes, and high-energy Li-ion battery systems for PHEV and EV applications.

Approach. The *in situ/ex situ* investigations of surface reconstruction into rock salt on NMC samples of different morphology and composition will be linked with investigations of interfacial reactivity toward organic electrolytes. Pristine and cycled NMC powders and electrodes will be probed using surface- and bulk-sensitive techniques, including Fourier transform infrared (FTIR), attenuated total reflectance (ATR)-FTIR, near-field IR, and Raman spectroscopy and microscopy and scanning probe microscopy to identify and characterize changes in structure and composition. The effect of electrolyte composition, additives, and protective coatings will be explored to determine the mechanism and kinetics of surface phenomena and implications for long-term electrochemical performance of NMC cathodes in high-energy Li-ion systems.

Out-Year Goals. The requirements for long-term stability of Li-ion batteries are extremely stringent and necessitate control of the chemistry at a wide variety of temporal and structural length scales. Progress toward identifying the most efficient mechanisms for electrical energy storage and the ideal material depends on a fundamental understanding of how battery materials function and what structural/electronic properties limit their performance. This project provides better understanding of the underlying principles that govern the function and operation of battery materials, interfaces, and interphases, which is inextricably linked with successful implementation of high energy density materials in Li-ion cells for PHEVs and EVs.

Collaborations. This project collaborates with Marca Doeff, Vincent Battaglia, Chunmei Ban, Vassilia Zorba, and Bryan D. McCloskey.

Milestones

1. Build and test binder- and carbon-free model NMC electrodes. (December 2015 – Complete)
2. Complete preliminary characterization of interfacial activity of the baseline NMC material in organic carbonate electrolytes. (Q3 – On schedule)
3. Determine relationship between surface reconstruction and surface layer formation during cycling in NMC electrodes. (Q4 – On schedule)
4. *Go/No-Go*: Demonstrate feasibility of *in situ* near-field FTIR microscopy and spectroscopy to study interfacial phenomena at Li-battery electrodes. *Criteria*: Stop development of near-field and LIBS techniques, if the experiments fail to deliver adequate sensitivity. (Q4 – On schedule).

Progress Report

This quarter, the project examined the interfacial activity of NMC in organic carbonate electrolytes. In particular, it investigated the effect of different components of the electrolyte on the NMC particle surface by correlation of surface fluorescence intensity and spectral shape with electrolyte content.

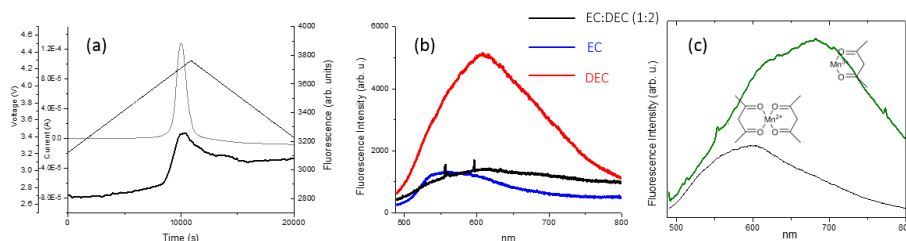


Figure 36. (a) Fluorescence behavior during cycling of NMC-111 cathode. (b) *Ex situ* fluorescence spectra of NMC-111 electrodes cycled in 1 M LiPF₆ electrolytes with varying solvent. (c) Fluorescence spectra of Mn^{III} and Mn^{II} β-diketone complexes.

It was established previously that fluorescence occurs at the surface of transition metal oxide cathodes during high-potential cycling. Figure 36a demonstrates this phenomenon in LiNi_{0.33}Mn_{0.33}Co_{0.33}O₂. The fluorescence rise coincides with Li⁺ removal and results in solvent oxidation and metal dissolution. To further understand the mechanisms of metal dissolution and fluorescence, binder- and carbon-free electrodes of NMC-111 were cycled at 0.05 mV/s in electrolyte composed of 1 M LiPF₆ in three different solvents: standard EC:DEC 1:2, pure EC, and pure DEC (diethyl carbonate). *Ex situ* fluorescence spectra, shown in Figure 36b, were taken of each electrode and compared. The fluorescence yield of the DEC electrode was substantially higher than the other two, indicating that DEC oxidation is the principal origin of fluorescence in the electrolyte.

Oxidation of EC and DEC leads to the formation of Metal(β-diketone) fluorescence complexes. EC oxidation produces high molecular weight Metal^{II}(β-diketone) complexes which contribute to the build-up of a surface film at the cathode surface. DEC oxidation leads to the formation of Metal^{III}(β-diketone) fluorescent complexes with short side chains which dissolve in the electrolyte. Figure 36c shows the fluorescence yield of Mn^{III}(β-diketone)₃ and Mn^{II}(β-diketone)₂ complexes, with the former producing a much stronger fluorescence signal. These results demonstrate that the DEC oxidation produces most of the soluble fluorescent complexes seen in *in situ* fluorescent results, while the Mn^{II}-based products of EC oxidation precipitate at the surface and prevent further dissolution and fluorescence. ICP measurements also revealed that the rate of metal dissolution was twice as fast in DEC electrolyte as in EC.

The project continued investigating thin-film NMC cathodes as model electrodes to understand interfacial processes during cycling. It procured from the Wang group, at Texas A&M University (TAMU), NMC-532 cathodes deposited by pulse laser deposition on Au/stainless steel substrates. XRD data (Figure 37a) show they are highly crystalline, while atomic force microscope (AFM) results (Figure 37b-c) demonstrate film thickness on the order of 200 nm with roughly 20 nm roughness. Although 1 μm outgrowths appear on the surface, these are not expected to affect the localized characterization methods planned for these samples. Preparations for investigation by *in situ* AFM followed by near- and far-field vibrational spectroscopies are in progress.

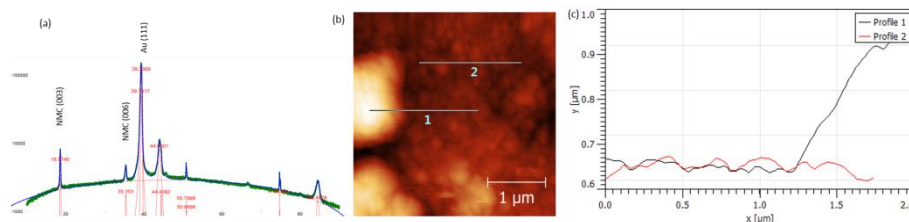


Figure 37. NMC thin film characterization results. (a) X-ray diffraction (b) Atomic force microscope topography of 4 μm area. (c) Topographic profiles from (b).

Task 5.3 – Advanced *in situ* Diagnostic Techniques for Battery Materials (Xiao-Qing Yang and Xiqian Yu, Brookhaven National Laboratory)

Project Objective. The primary project objective is to develop new advanced *in situ* material characterization techniques and to apply these techniques to support development of new cathode and anode materials for the next generation of Li-ion batteries for PHEVs. To meet the challenges of powering the PHEV, Li-ion batteries with high energy and power density, low cost, good abuse tolerance, and long calendar and cycle life must be developed.

Project Impact. The VTO Multi Year Program Plan describes the goals for battery: “Specifically, lower-cost, abuse-tolerant batteries with higher energy density, higher power, better low-temperature operation, and longer lifetimes are needed for the development of the next-generation of HEVs, PHEVs, and EVs.” The knowledge gained from diagnostic studies through this project will help U.S. industries develop new materials and processes for new generation Li-ion batteries in the effort to reach these VTO goals.

Approach. This project will use the combined synchrotron based *in situ* X-ray techniques (XRD, and hard and soft X-ray absorption) with other imaging and spectroscopic tools such as HRTEM and mass spectroscopy (MS) to study the mechanisms governing the performance of electrode materials and provide guidance for new material and new technology development regarding Li-ion battery systems.

Out-Year Goals. Complete the first stage development of diagnostic technique to study kinetic property of advanced Li-ion electrode materials using time resolved XRD (TR-XRD) and X-ray absorption (TR-XAS) combined with STEM imaging and transmission X-ray microscopy (TXM). Apply this technique to study the structural changes of new cathode materials including various NCM and high-voltage spinel materials during high rate cycling.

Collaborations. The BNL team will work closely with material synthesis groups at ANL (Drs. Thackeray and Amine) for the high-energy composite; and at PNNL for the Si-based anode materials. Such interaction between the diagnostic team at BNL and synthesis groups of these other BMR members will catalyze innovative design and synthesis of advanced cathode and anode materials. The project will also collaborate with industrial partners at General Motors and Johnson Controls, as well as with international collaborators.

Milestones

1. Complete the thermal stability studies of Fe substituted high-voltage spinel cathode materials $\text{LiNi}_{1/3}\text{Mn}_{4/3}\text{Fe}_{1/3}\text{O}_4$ in comparison with un-substituted $\text{LiNi}_{0.5}\text{Mn}_{1.5}\text{O}_4$ using *in situ* TR-XRD and MS techniques. (December 2015 – Complete)
2. Complete the energy resolved TXM investigation on new concentration gradient NCM cathode sample particles in a noninvasive manner with 3D reconstructed by images through tomography scans to study the 3D Ni, Co, and Mn elemental distribution from surface to the bulk. (March 2016 – Complete)
3. Complete the *in situ* TR-XRD studies of the structural changes of $\text{Li}_{1-x}\text{Ni}_{1/3}\text{Co}_{1/3}\text{Mn}_{1/3}\text{O}_2$ from $x=0$ to $x=0.7$ during high rate charge process at different C rates at 10C, 30C, and 60C. (June 2016 – In progress)
4. Complete the *in situ* TR- XAS of $\text{Li}_{1-x}\text{Ni}_{1/3}\text{Co}_{1/3}\text{Mn}_{1/3}\text{O}_2$ cathode material at Ni, Co and Mn K-edge during 30C high rate charge. (September 2016 – In progress)

Progress Report

The second milestones are complete. BNL has focused the energy resolved TXM investigation on new concentration gradient NCM cathode sample particles in a noninvasive manner with 3D reconstructed by images through tomography scans to study the 3D Ni, Co, and Mn elemental distribution from surface to the bulk. In Figure 38 (left), the 3D distribution of Ni, Mn, and Co is clearly displayed using red, blue, and green colors. On the right panel, using the same color code, the concentrations of Ni, Mn, and Co as functions of distance from surface (0 μm) toward the core (up to -5 μm) are plotted. It can be seen that the concentration gradient nature of the material is well demonstrated (higher Mn concentration at surface than in the bulk; lower Ni concentration at surface than in the bulk, to get both better thermal stability and higher capacity).

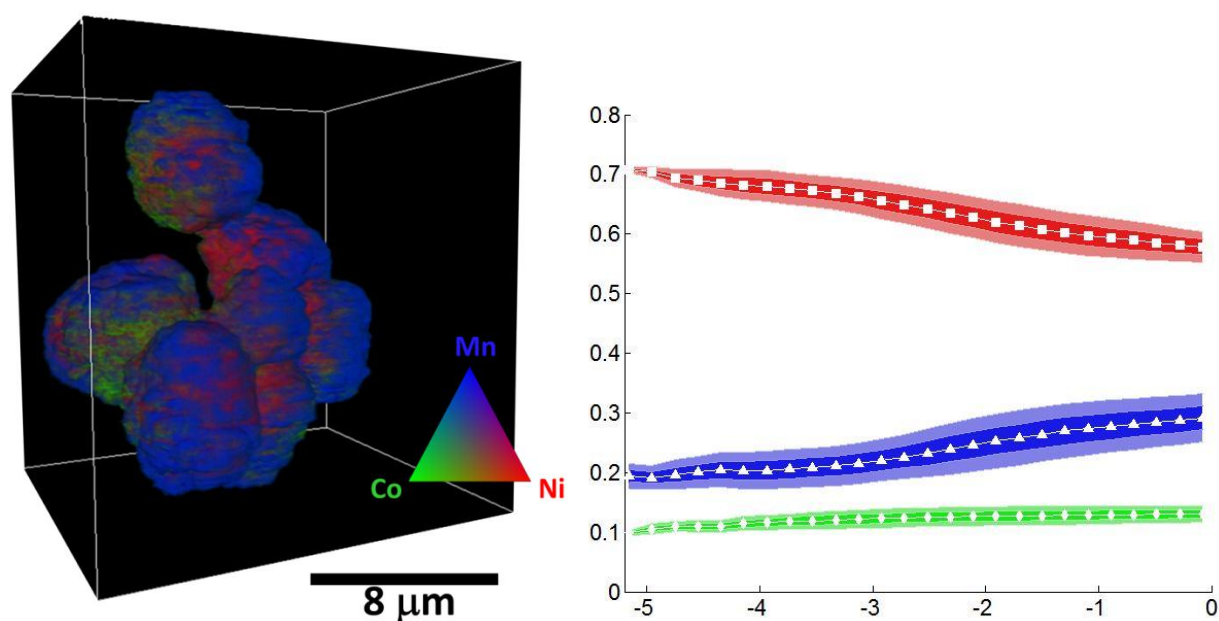


Figure 38. The reconstructed 3D transmission X-ray microscopy image of a particle cluster of fully concentration gradient $\text{LiNi}_{0.6}\text{Mn}_{0.2}\text{Co}_{0.2}\text{O}_2$ sample (left panel) with the color legend indicating the elemental distribution over the investigated 3D volume. By regrouping the voxels as a function of the shortest distance from the corresponding voxel to the outer surface, the project plots the normalized elemental concentration versus the voxel depth. As shown in the right panel, the different slopes in the concentration gradient were clearly observed. Notably, the elemental concentration over tens of millions of voxels were retrieved in this experiment, which provides good statistic of the depth profile as indicated by the color band in right panel.

Patents/Publications/Presentations

Publication

- Kim, Hyun-Kyung, and **Seong-Min Bak**, Suk Woo Lee, Myeong-Seong Kim, Byeongho Park, Su Chan Lee, Yeon Jun Choi, Seong Chan Jun, Joong Tark Han, Kyung-Wan Nam, Kyung Yoon Chung, Jian Wang, Jigang Zhou, **Xiao-Qing Yang**, Kwang Chul Roh, and Kwang-Bum Kim. “Scalable Fabrication of Micron-Scale Graphene Nanomeshes for High-Performance Supercapacitor Applications.” *Energy & Environmental Science* (2016). doi: 10.1039/c5ee03580e.

Task 5.4 – NMR and Pulse Field Gradient Studies of SEI and Electrode Structure (Clare Grey, Cambridge University)

Project Objective. The formation of a stable SEI is critical to the long-term performance of a battery, since the continued growth of the SEI on cycling/aging results in capacity fade (due to Li consumption) and reduced rate performance due to increased interfacial resistance. Although arguably a (largely) solved problem with graphitic anodes/lower voltage cathodes, this is not the case for newer, much higher capacity anodes such as silicon, which suffer from large volume expansions on lithiation, and for cathodes operating above 4.3 V. Thus it is essential to identify how to design a stable SEI. The objectives are to identify major SEI components, and their spatial proximity, and how they change with cycling. SEI formation on Si versus graphite and high-voltage cathodes will be contrasted. Li⁺ diffusivity in particles and composite electrodes will be correlated with rate. The SEI study will be complemented by investigations of local structural changes of high-voltage/high-capacity electrodes on cycling.

Project Impact. The first impact of this project will be an improved, molecular based understanding of the surface passivation (SEI) layers that form on electrode materials, which are critical to the operation of the battery. Second, the project will provide direct evidence for how additives to the electrolyte modify the SEI. Third, it will provide insight to guide and optimize the design of more stable SEIs on electrodes beyond LiCoO₂/graphite.

Out-Year Goals. The project goals are to identify the major components of the SEI as a function of state of charge and cycle number on different forms of silicon. The project will determine how the surface oxide coating affects the SEI structure and will establish how the SEI on Si differs from that on graphite and high-voltage cathodes. The project will determine how the additives that have been shown to improve SEI stability affect the SEI structure and will explore the effect of different additives that react directly with exposed fresh silicon surfaces on SEI structure. Via this program, the project will develop new NMR-based methods for identifying different components in the SEI and their spatial proximities within the SEI, which will be broadly applicable to the study of SEI formation on a much wider range of electrodes. These studies will be complemented by studies of electrode bulk and surface structure to develop a fuller model with which to describe how these electrodes function.

Collaborations. This project collaborates with B. Lucht (Rhode Island); E. McCord and W. Holstein (DuPont); J. Cabana, (University of Illinois at Chicago); G. Chen and K. Persson (LBNL); S. Whittingham (SUNY Binghamton); P. Bruce (St. Andrews); R. Seshadri and A. Van der Ven (UCSB); S. Hoffman and A. Morris (University of Cambridge); N. Brandon (Imperial); and P. Shearing (University College London).

Milestones

1. Identify the major carbon-containing break down products that form on graphene platelets. (December 2015 – Ongoing. Decision made to complete Si studies from Q3 milestone first since student is graduating.)
2. *Go/No-Go:* Establish the difference between extrinsic and P-doped silicon nanowires. *Criteria:* If no difference in performance of P-doped wires established after the first cycle, terminate project. (March 2016 – Ongoing. No clear differences under conditions used to date. In process of terminating project and writing results.)
3. Complete SEI study of silicon nanoparticles by NMR spectroscopy. (6/30/16 – Complete, with papers in preparation.) Develop NMR methodology to examine cathode SEI. (Ongoing)
4. Produce first optimized coating for Si electrode. (September 2016 – Ongoing)

Progress Report

Lithium dendrite growth in lithium-ion and lithium rechargeable batteries is associated with severe safety concerns. To overcome these problems, a fundamental understanding of the growth mechanism of dendrites under working conditions is needed. The project used *in situ* ^7Li MRI on both the electrolyte and lithium metal electrodes in symmetric lithium cells, allowing the behavior of the electrolyte concentration gradient to be studied and correlated with the type and rate of microstructure growth on the Li metal electrode. A standard EC / dimethyl carbonate (DMC) / LiPF_6 electrolyte was used. Chemical shift (CS) imaging was used because the project has shown that it can resolve different types of Li microstructures, the mossy types of microstructure growing close to the surface of the anode from the beginning of charge in every cell studied, from high to low currents, while dendritic growth is triggered much later (Figure 39).

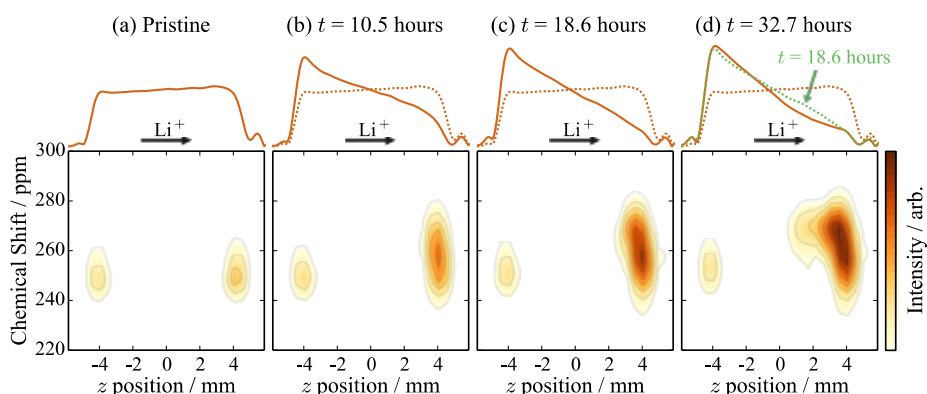


Figure 39. Magnetic resonance imaging time series showing the evolution of the ^7Li electrolyte concentration profile (top) and the ^7Li chemical shift image of the metal (bottom) for the cell charged at 0.76 mA cm^{-2} . The two Li metal electrodes are located at z-positions of approximately, $\pm 4 \text{ mm}$. The intensity increase on the right hand side electrode, seen on passing current indicates the growth of Li microstructure. The onset of dendrite formation is seen in (c) (18.6 hours).

Simple metrics have been developed to interpret the MRI data sets and compare results from a series of cells charged at different current densities (Figure 40). The results show that at high charge rates, there is a strong correlation between the onset time of dendrite growth and the local depletion of the electrolyte at the surface of the electrode observed both experimentally and predicted theoretical (via the Sand's time model) (Figure 41). A separate mechanism of dendrite growth is observed at low currents, which is not governed by salt depletion in the *bulk* liquid electrolyte. Experiments are in progress to correlate the onset of dendrite formation with SEI formation.

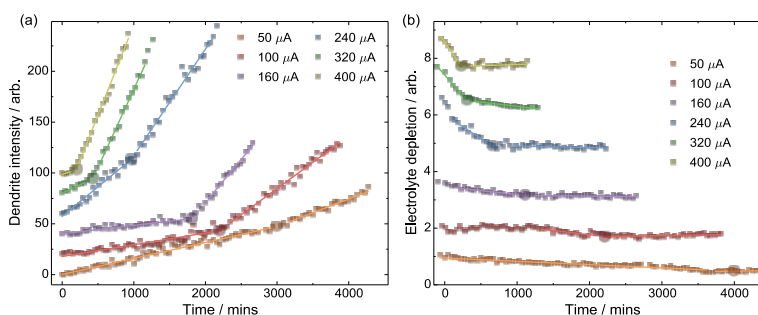


Figure 40. (a) Dendrite intensity and (b) electrolyte depletion near the right hand side Li electrode as a function of current (for 0.31 cm^{-1} electrodes). Arbitrary offsets have been applied to the data in the y direction.

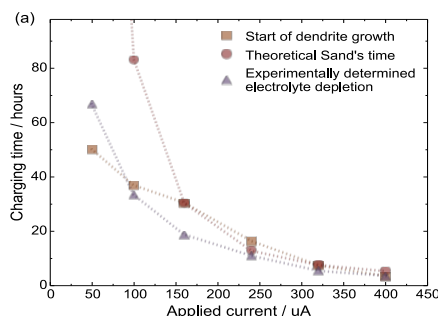


Figure 41. Comparison between the Sands time and onset of dendrite formation/electrolyte depletion.

Patents/Publications/Presentations

Publication

- Bayley, P. M., and N. M. Trease, and C. P. Grey. “Insights into Electrochemical Sodium Metal Deposition as Probed with *In Situ* ^{23}Na NMR.” *J. Am. Chem. Soc.* 138 (2016): 1955.

Presentations

- Ludwig-Maximilians-Universität, Chemistry Department, Munich, Germany (January 2016). Invited talk.
- 17th Israel Materials Engineering Conference (IMEC 17), Bar-Ilan University, Israel (February 2016).
- International Battery Association 2016, Nantes, France (March 2016).

Task 5.5 – Optimization of Ion Transport in High-Energy Composite Cathodes (Shirley Meng, UC – San Diego)

Project Objective. This project aims to probe and control the atomic-level kinetic processes that govern the performance limitations (rate capability and voltage stability) in a class of high-energy composite electrodes. A systematic study with powerful suite of analytical tools [including atomic resolution scanning transmission electron microscopy (a-STEM) and EELS, neutron, XPS and first principles (FP) computation] will elucidate approaches to optimize ion transport. Ultimately, this will hone in on the optimum bulk compositions and surface characteristics to improve the mechanistic rate and cycling performance of high-energy composite electrodes. Moreover, it aims to develop the large-scale synthesis efforts in order to produce materials with consistent performance. The surface-sensitive characterization tools will be extended to diagnose various silicon anode types.

Project Impact. If successful, this research will provide a major breakthrough in commercial applications of the class of high energy density cathode material for lithium ion batteries. Additionally, it will provide in-depth understanding of the role of surface modifications and bulk substitution in the high-voltage composite materials. The diagnostic tools developed here can also be leveraged to study a wide variety of cathode and anode materials for rechargeable batteries.

Approach. This unique approach combines STEM/EELS, XPS, and *ab initio* computation as diagnostic tools for surface and interface characterization. This allows for rapid identification of surface interphases that provide surface instability or stability in various types of electrode materials including both high-voltage cathodes and low-voltage anodes. Neutron enables the characterization of bulk material properties to enhance and further optimize high-energy electrode materials.

Out-Year Goals. The goal is to control and optimize Li-ion transport, TM migration, and oxygen activity in the high-energy composite cathodes and to optimize electrode/electrolyte interface in silicon anodes so that their power performance and cycle life can be significantly improved.

Collaborations. This work funds collaborations on silicon thin film fabrication (Nancy Dudney, ORNL); molecular layer deposition (MLD) (Chunmei Ban, NREL); neutron diffraction (Ken An, ORNL); and XPS, TOF-SIMS characterization (Keith Stevenson, UT Austin). It supports collaborative work with Zhaoping Liu and Yonggao Xia at Ningbo Institute of Materials Technology and Engineering China.

Milestones

1. Quantify the SEI characteristics of MLD coated silicon anode upon long cycling with a combination of STEM/EELS and XPS. (March 2016 – Complete)
2. Obtain the optimum nanoscale uniform crystalline lithium-lanthanum-titanium-oxide surface coating in Li-rich layered oxides when charged up to 4.8 V (or 5.0 V). (March 2016 – Complete)
3. Complete investigation of coating and morphology control for Li-rich, Mn-rich, layered oxides. (June 2016 – Ongoing)

Progress Report

Nanoscale LLTO (Lithium Lanthanum Titanium Oxide) surface coating for Li-rich LNMO

The surface of Li-rich LNMO was coated with LLTO to enhance the electrochemical performance. XRD determined that crystallized LLTO existed in the coated Li-rich material. To identify the uniformity of the LLTO coating, bright field STEM coupled with EELS was applied to the uncoated and coated LLTO Li-rich material. Figure 42a-b compares the STEM images of the uncoated and coated Li-rich material. The uncoated particles have a clean surface with Li and TM layers extending to the outermost surface. After LLTO coating, there is a uniform nanoscale layer (<1 nm in thickness) found on the particle surface. The EELS experiments were carried out on both bulk and surface region of LLTO coated Li-rich (Figure 42c). The data points are aligned with the BF image to illustrate where each spectrum was taken (shown in red and black). There is a clear Ti-L edge peak in the spectra obtained on the surface region where Ti-L3 and Ti-L2 were induced by the electron transitions from $2p^{3/2}$ and $2p^{1/2}$, respectively, to unoccupied 3D orbitals. This Ti-L edge disappears in the bulk region of the material, which indicates LLTO is only on the surface. Both materials were cycled at a slow rate of 25 mA g^{-1} between 2 - 4.8 V. The uncoated Li-rich material shows only 74.2% capacity retention after 190 cycles, while the LLTO coating improves the capacity retention to 82.3%. In addition, the LLTO coated Li-rich delivers higher Coulombic efficiency than the uncoated upon the long term cycling.

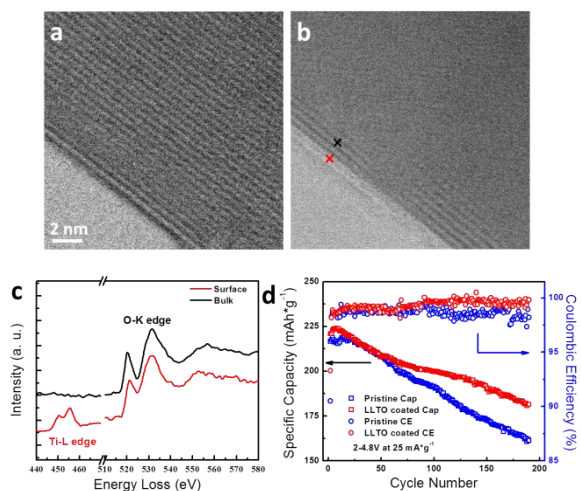


Figure 42. Scanning transmission electron microscopy/annular bright field images of (a) uncoated Li-rich material and (b) 1 wt% LLTO coated Li-rich. (c) Electron energy loss spectra of 1 wt% LLTO coated Li-rich at different regions. (d) Comparison of capacity and Coulombic efficiency for uncoated and LLTO-coated Li-rich over 190 cycles.

Direct visualization of the SEI morphology on Si using STEM EELS

For the first time this project presents direct visualization on how FEC affects the SEI morphology throughout electrochemical cycling. Figure 43 shows ADF-STEM images of SEI with progressive cycling, where the electrode cycled in EC/DEC after the first delithiation forms an inhomogeneous porous SEI. Moreover, this SEI is intermixed with the silicon nanoparticles as the cycle number increases (up to 100 cycles). Conversely, the electrode cycled in EC/DEC/FEC is covered with a dense, uniform SEI layer. The silicon nanoparticles preserved its morphology and are covered in a homogenous, dense SEI, as first hypothesized. Surprisingly, after 100 cycles the electrode cycled in EC/DEC/FEC had similar SEI morphology as that of the SEI generated by EC/DEC.

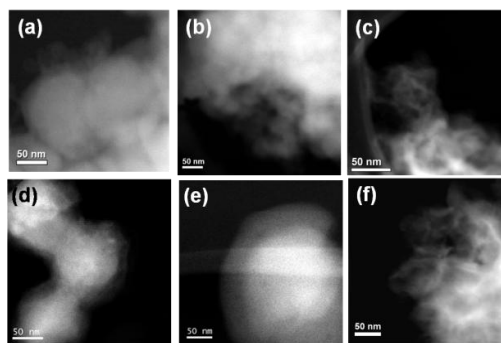


Figure 43. Annular dark field scanning transmission electron microscopy images of the Si in conventional electrolyte (a) after 1 cycle, (b) after 5 cycles, (c) after 100 cycles and the Si in electrolyte containing FEC, (d) after 1 cycle, (e) after 5 cycles, and (f) after 100 cycles.

Aluminum hydroquinone coated Si amorphous thin film using MLD

Amorphous Si thin film (50 nm) was coated with varying cycles of aluminum hydroquinone using the MLD process. The thin films were cycled using the traditional electrolyte (1M LiPF₆ in EC:DEC) to focus on the effects of the coating. Optimization of coating type and coating thickness is ongoing in order to see the significant coating effect on capacity retention.

Patents/Publications/Presentations**Publications**

- Hy, S., and H. Liu, D. Qian, M. Zhang, B. J. Hwang, and Y. S. Meng. *Energy Environ. Sci.* (2016). doi: 10.1039/C5EE03573B.
- Liu, H. D., and J. Huang, D. Qian, S. Hy, C. Fang, J. Luo, and Y. S. Meng. *J. Electrochem. Soc.* 163, no. 6 (2016): A971.
- Liu, H. D., and Y. Chen, S. Hy, K. An, S. Venkatachalam, D. Qian, M. Zhang, and Y. S. Meng, *Adv. Energy Mater.* (2016): 1502143.

Presentation

- International Battery Association 2016, Nantes, France (March 2016): “Interface Optimization Principles of Si Anode for Li-ion Batteries”; J. Alvarado, M. Sina, H. Shobukawa, and Y. S. Meng. Invited.

Task 5.6 – Analysis of Film Formation Chemistry on Silicon Anodes by Advanced *In situ* and *Operando* Vibrational Spectroscopy

(Gabor Somorjai, UC – Berkeley; Phil Ross, Lawrence Berkeley National Laboratory)

Project Objective. Understand the composition, structure, and formation/degradation mechanisms of the SEI on the surfaces of Si anodes during charge/discharge cycles by applying advanced *in situ* vibrational spectroscopies. Determine how the properties of the SEI contribute to failure of Si anodes in Li-ion batteries in vehicular applications. Use this understanding to develop electrolyte additives and/or surface modification methods to improve Si anode capacity loss and cycling behavior.

Project Impact. A high-capacity alternative to graphitic carbon anodes is Si, which stores 3.75 Li per Si versus 1 Li per 6 C yielding a theoretical capacity of 4008 mAh/g versus 372 mAh/g for C. But Si anodes suffer from large first-cycle irreversible capacity loss and continued parasitic capacity loss upon cycling leading to battery failure. Electrolyte additives and/or surface modification developed from new understanding of failure modes will be applied to reduce irreversible capacity loss, and to improve long-term stability and cyclability of Si anodes for vehicular applications.

Approach. Model Si anode materials including single crystals, e-beam deposited polycrystalline films, and nanostructures are studied using baseline electrolyte and promising electrolyte variations. A combination of *in situ* and *operando* FTIR, Sum Frequency Generation (SFG), and UV-Raman vibrational spectroscopies are used to directly monitor the composition and structure of electrolyte reduction compounds formed on the Si anodes. Pre-natal and post-mortem chemical composition is identified using XPS. The Si films and nanostructures are imaged using SEM.

Out-Year Goals. Extend study of interfacial processes with advanced vibrational spectroscopies to high-voltage oxide cathode materials. The particular oxide to study will be chosen based on materials of interest and availability of the material in a form suitable for these studies (for example, sufficiently large crystals or sufficiently smooth/reflective thin films). The effect of electrolyte composition, electrolyte additives, and surface coatings will be determined, and new strategies for improving cycle life developed.

Milestones

1. Modifying the SFG apparatus to obtain high-resolution SFG spectra further allowing particles, thin film, and microstructures of Si and the electrolyte interface research. (December 2015 – Complete)
2. Performing ps-SFG measurement under constant and dynamic potentials (-0.01 V, 0.5 V, and 1.0 V vs Li/Li⁺) of 1 M LiPF₆ in EC without DEC to probe the SEI formed on amorphous silicon anodes. (January 2016 – Complete)
3. *Go/No-Go*: Can this task distinguish between the various SEI products in the C-H stretch mode (2800 – 3200 cm⁻¹)? If not, proceed to conventional C-O region (1700 – 1800 cm⁻¹). (June 2016 - Ongoing)
4. Performing fs-SFG measurement in tandem with CV (potential sweep) to find the ring opening kinetics of EC. (September 2016)

Progress Report

The project has synthesized the following electrolyte solutions: 1.0 M LiClO₄ in EC : 1.0 M LiClO₄ in FEC, and their mixture EC:FEC in a 9:1 w/w ratio to investigate the effect of fluorinated additives (FEC) on chemical composition of the SEI and surface ordering of electrolytes at electrolyte/amorphous silicon (a-Si) interface. The main conclusion this quarter is that FEC induces ordering of the adsorbed EC on a-Si anode. The results may explain the unique role of FEC as a known stabilizing additive in Li-ion batteries. The project has decided to use lithium perchlorate (LiClO₄) instead of lithium-hexafluorophosphate (LiPF₆) to minimize the creation of inorganic fluorine compounds related to lithium salt dissociation (for example, LiF). When the project probed the a-Si / FEC based electrolyte interphase at open circuit potential (OCP), no prominent SFG features corresponding to FEC were detected from the interface. Presumably FEC molecules are either isotropic, well ordered in an up-down orientation, or flat in respect to the Si surface. With EC electrolyte, the project observes two prominent peaks in SFG spectrum at OCP (black curve) in the frequency range of 2960 to 3075 cm⁻¹. The SFG of the EC : FEC carbonate mixture reveals that FEC induces better EC surface ordering (blue curve). This conclusion was reached by analyzing the origin of the new peaks at 2880 cm⁻¹ and 2930 cm⁻¹. The project suggests that the s-CH₂ at 2880 cm⁻¹ is red shifted due to Van der Waals interactions with the a-Si surface. The peaks at 2930 cm⁻¹, 2990 cm⁻¹ are associated with pure EC FTIR spectra. It is assumed that this intensification results from a more perpendicular orientation in respect to the silicon surface, which is detectable by tuning the SFG sensitivity to perpendicular dipoles under SSP polarization configuration. When an external potential was applied to reach lithiation, the SFG spectra showed different SEI compositions for FEC and EC/FEC mixtures. Further investigation is needed. In Figure 45, an SEM scan shows an a-Si electrode surface after cyclic-voltammetry of 1.0 M LiClO₄ in FEC. The surface of the a-Si is intact and, according to EDS (not shown), micron-sized LiF particles are evident on its surface. It is assumed that the F⁻ ion originated due to FEC conversion to vinylene carbonate (VC) through the removal of HF to form the carbon-carbon double bond.

In conclusion, the project has observed that FEC on a-Si induces better ordering of the adsorbed EC on the silicon anode and also affects the SEI composition at interface. SEM scans show that a smooth a-Si surface is obtained with micron sized particles after cycling the anode for 10 CVs, between 2.8-0.05 V at 0.1 mV / sec.

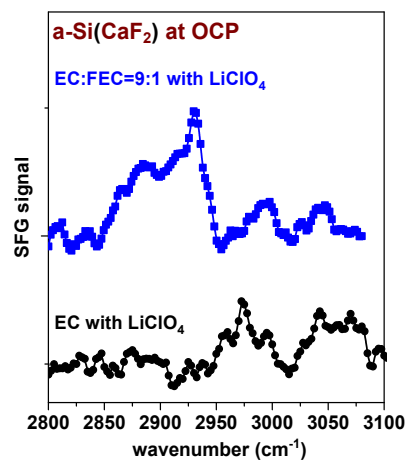


Figure 44. This graph shows the SFG signal at open current potential of 1 M LiClO₄ in EC, and EC : FEC (9:1, w/w) in contact with a-Si anode.



Figure 45. Scanning electron microscope scan of a-Si surface after cyclic voltammetry. Micron-sized LiF particles after cycling the anode for 10 CVs, 2.8 V ↔ 0.05 V at 0.1 mV / sec.

Task 5.7 – Microscopy Investigation on the Fading Mechanism of Electrode Materials (Chongmin Wang, Pacific Northwest National Laboratory)

Project Objective. The overall objective is to develop low-cost, high-energy cathode materials with long cycle life. This part is focused on microscopy investigation on the fading mechanism of the electrode materials. The focus will be on using *ex situ*, *in situ*, and *operando* HR-TEM and spectroscopy to probe the structural evolution of electrodes and interfaces between the electrode and electrolyte and correlate this structural and chemical evolution with battery performance.

Project Impact. Both *ex situ* and *in situ* TEM have been demonstrated to be critical for probing the structure and chemistry of electrode and SEI layer. Recently, this task developed new *operando* characterization tools to characterize SEI formation and electrode/electrolyte interaction using a practical electrolyte, which is critical for making new breakthroughs in the battery field. The success of this work will increase the energy density of Li-ion batteries and accelerate market acceptance of EV, especially for PHEV required by the EV Everywhere Grand Challenge proposed by the DOE/EERE.

Approach. Extend and enhance the unique *ex situ* and *in situ* TEM methods for probing the structure of Li-ion batteries, especially for developing a biasing liquid electrochemical cell that uses a real electrolyte in a nano-battery configuration. Use various microscopic techniques, including *ex situ*, *in situ*, and especially the *operando* TEM system, to study the fading mechanism of electrode materials in batteries. This project will be closely integrated with other research and development efforts on high-capacity cathode and anode projects in the BMR Program to (1) discover the origins of voltage and capacity fading in high-capacity layered cathodes and (2) provide guidance for overcoming barriers to long cycle stability of electrode materials.

Out-Year Goals. The out-year goals are as follows:

- Multi-scale (ranging from atomic scale to meso-scale) *ex situ/in situ* and *operando* TEM investigation of failure mechanisms for energy-storage materials and devices. Atomic-level *in situ* TEM and STEM imaging to help develop a fundamental understanding of electrochemical energy storage processes and kinetics of electrodes.
- Extension of the *in situ* TEM capability for energy storage technology beyond Li ions, such as Li-S, Li-air, Li-metal, sodium ions, and multi-valence ions.

Collaborations. The project is collaborating with the following principal investigators: Michael M. Thackeray (ANL); Guoying Chen (LBNL); Chunmei Ban (NREL); Khalil Amine (ANL); Donghai Wang (Pennsylvania State University); Arumugam Manthiram (UT-Austin); Gao Liu (LBNL); Yi Cui (Stanford University); Jason Zhang (PNNL); Jun Liu (PNNL); and Xingcheng Xiao (GM).

Milestones

1. Complete multi-scale quantitative atomic level mapping to identify the behavior of Co, Ni, and Mn in NCM during battery charge/discharge. (March 2016 – Complete)
2. Complete quantitative measurement of structural/chemical evolution of modified-composition NCM cathode during cycling of battery. (June 2016 – Ongoing)
3. Complete the correlation between structure stability and charge voltage of NCM for optimized charge voltage. (September 2016)

Progress Report

Through intensive aberration corrected STEM investigation on ten layered oxide cathode materials, two important observations were made (Figure 46). Firstly, Ni and Co show strong plane selectivity when building up their respective surface segregation layers (SSL). Specifically, Ni-SSL is exclusively developed on (200)_m facet in Li-Mn-rich oxides (monoclinic C2/m symmetry) and (012)_h facet in Mn-Ni equally rich oxides (hexagonal R-3m symmetry), while Co-SSL has a strong preference to (20-2)_m plane with minimal Co-SSL also developed on some other planes in Li-Mn-rich cathodes. Structurally, Ni-SSLs tend to form spinel-like lattice while Co-SSLs are in a rock-salt-like structure. Secondly, by increasing Ni concentration in these layered oxides, Ni and Co SSLs can be suppressed and even eliminated. These observations indicate that Ni and Co SSLs are tunable through controlling particle morphology and oxide composition, which opens up a new way for future rational design and synthesis of cathode materials.

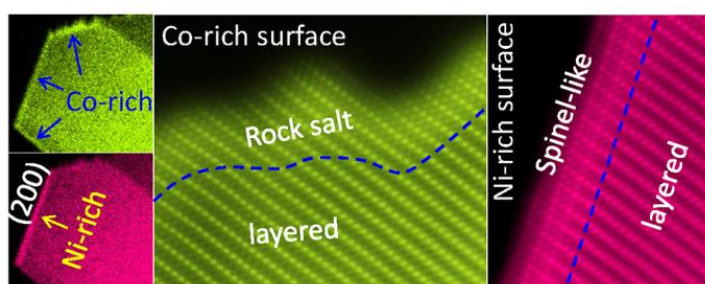


Figure 46. Scanning transmission electron microscopy high angle annular dark field image revealing the distinctive surface plane selective segregation of Ni and Co in Li-Mn-rich oxide cathodes. Ni exclusively segregates on the (200) type planes and forming a layer of spinel structure, while Co has a strong preference to segregate on (20-2)_m plane with minimal on other planes and forms rock salt structure.

When cathode materials are subjected to battery cycling, material degradation often initiates from the surface layer, as evidenced by recent characterization studies. For example, surface reconstruction layer (SRL) was frequently observed on cathode particle surface after battery cycling, which was believed to act as a barrier for Li-ion transport and thus contribute to battery high polarization and poor rate capability. Moreover, such SRL keeps growing from particle surface into inner bulk as battery cycling continues, which is believed to contribute to battery capacity and voltage decay. The nature of the surface layer also influences the SEI, particle corrosion and side reactions with the electrolyte, all of which are critical to Li-ion battery performance. The project has used aberration corrected STEM and high efficient spectroscopy to probe the atomic level structural and chemical features LMR layered oxide: $\text{Li}_{1.2}\text{Ni}_{0.13}\text{Co}_{0.13}\text{Mn}_{0.54}\text{O}_2$ (MS-NC-LMR) synthesized by using a molten salt method; $\text{Li}_{1.2}\text{Ni}_{0.13}\text{Co}_{0.13}\text{Mn}_{0.54}\text{O}_2$ (CP-NC-LMR), $\text{Li}_{1.2}\text{Ni}_{0.2}\text{Mn}_{0.6}\text{O}_2$ (20N-LMR), $\text{LiNi}_{0.5}\text{Mn}_{0.5}\text{O}_2$ (NM-55), $\text{LiNi}_{0.6}\text{Co}_{0.2}\text{Mn}_{0.2}\text{O}_2$ (NMC-622) and $\text{LiNi}_{0.8}\text{Co}_{0.1}\text{Mn}_{0.1}\text{O}_2$ (NMC-811) synthesized via a coprecipitation method; $\text{Li}_{1.05}\text{Ni}_{0.43}\text{Mn}_{0.52}\text{O}_2$ and $\text{Li}_{1.17}\text{Ni}_{0.25}\text{Mn}_{0.58}\text{O}_2$ synthesized by hydrothermal assisted method; $\text{LiNi}_{0.4}\text{Co}_{0.2}\text{Mn}_{0.4}\text{O}_2$ (NMC-442) and $\text{LiNi}_{0.8}\text{Co}_{0.15}\text{Al}_{0.05}\text{O}_2$ (NCA) are commercially available materials manufactured by TODA KOGYO company. It is found that on one hand, Ni and Co show distinctive plane selectivity while forming SSLs on particle surface as evidenced in several LMR oxides regardless of the synthesis methods: Ni exclusively segregates to (200)_m plane and Co prefer to

(20-2)_m plane. On the other hand, such Ni and Co SSLs show composition dependence of cathode materials. The project found that both Ni and Co SSLs can be eliminated by increasing Ni concentration to Ni-rich layered oxides. These findings indicate that Ni and Co SSLs are adjustable through two strategies. One is by controlling surface morphology and the other one is by controlling material compositions. Structurally, it has been found Ni-SSLs tend to form a spinel-like structure while Co-SSLs form a rock-salt-like structure. In Ni-rich cathodes, surface layers were found to transform into rock-salt-like structure even without any transition metal segregation. The systematical investigation in this work will facilitate fundamental understanding on Ni-Co-Mn-based layered cathode oxides and provide valuable guidelines for cathode material design and synthesis.

Patents/Publications/Presentations

Publication

- Yan, Pengfei, and Jianming Zheng, Xiaofeng Zhang, Rui Xu, Khalil Amine, Jie Xiao, Ji-Guang Zhang, and Chong-Min Wang. “Atomic to Nanoscale Investigation of Functionalities of an Al₂O₃ Coating Layer on a Cathode for Enhanced Battery Performance.” *Chem. Mater.* 28 (2016): 857–863.

Presentation

- 2016 Materials Research Society (MRS) Spring Meeting, Phoenix, Arizona (March 29, 2016): “Mitigating Capacity Fading of Lithium ion Battery by Surface Coating of Electrode Materials: The Beneficial and Detrimental Effect”; Chongmin Wang, Pengfei Yan, Langli Luo, Jianming Zheng, Jie Xiao, and Ji-Guang Zhang.

Task 5.8 – Characterization and Computational Modeling of Structurally Integrated Electrode (Michael M. Thackeray and Jason R. Croy, Argonne National Laboratory)

Project Objective. The primary project objective is to explore the fundamental, atomic-scale processes that are most relevant to the challenges of next-generation, energy-storage technologies, in particular, high-capacity, structurally integrated electrode materials. A deeper understanding of these materials relies on novel and challenging experiments that are only possible through unique facilities and resources. The goal is to capitalize on a broad range of facilities to advance the field through cutting-edge science, collaborations, and multi-disciplinary efforts to characterize and model structurally integrated electrode systems, notably those with both layered and spinel character.

Project Impact. This project capitalizes on and exploits DOE user facilities and other accessible national and international facilities (including skilled and trained personnel) to produce knowledge to advance lithium-ion battery materials. Specifically, furthering the understanding of structure-electrochemical property relationships and degradation mechanisms will contribute significantly to meeting the near- to long- term goals of PHEV and EV battery technologies.

Approach. A wide array of characterization techniques including X-ray and neutron diffraction, X-ray absorption, emission and scattering, HR-TEM, Raman spectroscopy, and theory will be brought together to focus on challenging experimental problems. Combined, these resources promise an unparalleled look into the structural, electrochemical, and chemical mechanisms at play in novel, complex electrode/electrolyte systems being explored at ANL.

Out-Year Goals. The out-year goals are as follows:

- Gain new, fundamental insights into complex structures and degradation mechanisms of high-capacity composite cathode materials from novel, probing experiments carried out at user facilities and beyond.
- Investigate structure-property relationships that will provide insight into the design of improved cathode materials.
- Use knowledge and understanding gained from this project to develop and scale up advanced cathode materials in practical lithium-ion prototype cells.

Collaborators. This project engages in collaboration with Eungje Lee, Joong Sun Park, Joel Blauwkamp, and Roy Benedek (Chemical Sciences and Engineering, ANL).

Milestones

1. Characterize bulk and surface properties of structurally integrated electrode materials using DOE user facilities at Argonne (Advanced Photon Source, Electron Microscopy Center, and Argonne Leadership Computing Facility) and facilities elsewhere, for example, Spallation Neutron Source (ORNL) and the Northwestern University Atomic and Nanoscale Characterization Experimental Center (NUANCE). (September 2016 – In progress)
2. Use complementary theoretical approaches to further the understanding of the structural and electrochemical properties of layered-spinel electrodes and protective surface layers. (September 2016 – In progress)
3. Analyze, interpret, and disseminate collected data for publication and presentation. (September 2016 – In progress)

Progress Report

Structurally integrated $y[x\text{Li}_2\text{M}'\text{O}_3 \cdot (1-x)\text{LiMO}_2] \cdot (1-y)\text{LiM}_2\text{O}_4$ LLS electrodes present a unique, though extremely complex, compositional and structural design space. Past reports have shown this class of electrodes to possess novel attributes such as high capacities and first-cycle efficiencies despite relatively high lithium and manganese contents. However, methods of controlling the structural and elemental compositions of these materials to a high degree are currently not well developed or understood. To further complicate understanding and optimization of these electrodes, small changes to lithium and TM ratios have observable effects on both structure and electrochemical performance. It is hypothesized that the local domain structures of these systems possess both spinel and spinel-type character. For example, spinel domains on the order of ~ 5 nm and larger have been clearly identified by electron microscopy and diffraction. However, XRD and XAS have also suggested TM occupation of tetrahedral sites and NiO-like structures, though these materials can possess good electrochemical performance. Therefore, understanding subtle changes in structure as a function of composition and, in particular, the tendencies for TM occupation of lithium-layer sites as a function of Li:TM ratios, have been identified as priorities for understanding the structure-property-electrochemical relationships of ‘LLS’ cathodes.

A systematic study of structure and electrochemistry was initiated on a series of LLS materials as a function of Li:TM ratios by keeping the TMs constant and varying the Li content. Nominally, in the complex LLS notation, samples with various, targeted spinel contents were synthesized belonging to the series $(1-x)[0.25\text{Li}_2\text{MnO}_3 \cdot 0.75\text{LiNi}_{0.375}\text{Mn}_{0.375}\text{Co}_{0.25}\text{O}_2] \cdot x[\text{Li}_{0.5}\text{Ni}_{0.28125}\text{Mn}_{0.53125}\text{Co}_{0.1875}\text{O}_2]$, with $x=0, 0.025, 0.05, 0.075, 0.1$. Figure 47a shows a comparison of the targeted and ICP-measured elemental compositions for the series. Excellent agreement was obtained, and the targeted Li:TM ratios confirmed. Figure 47b shows XRD patterns of the series. Although, as shown in Figure 47a, only a modest range of lithium contents was targeted, continual differences in the XRD patterns emerged as a function of x ; particularly associated with the peaks near $\sim 44^\circ$ 2θ associated with the cubic (400) reflections, where the $x=0.1$ sample clearly showed the presence of a second phase. Interestingly, this sample achieved a stable capacity of ~ 200 mAh/g and a first-cycle efficiency of $\sim 90\%$ (not shown). Neutron diffraction data of this series has recently been acquired at the SNS at ORNL and are being analyzed.

Parallel to experimental efforts, ongoing simulations are exploring the incorporation of Co-based spinels into integrated systems. Co-based spinels are of interest due to their operation $>3\text{V}$ and stability of Co against migration. Figure 47c shows integrated domains of Li_2MnO_3 and lithiated spinel $\text{Li}_2\text{Co}_2\text{O}_4$, where one half of the Li was removed from the $\text{Li}_2\text{Co}_2\text{O}_4$ component. On delithiation, it was found that some of the lithium spontaneously migrated to empty tetrahedral sites. These studies are shedding light on the voltage profiles and stabilities of experimentally explored and structurally integrated systems.

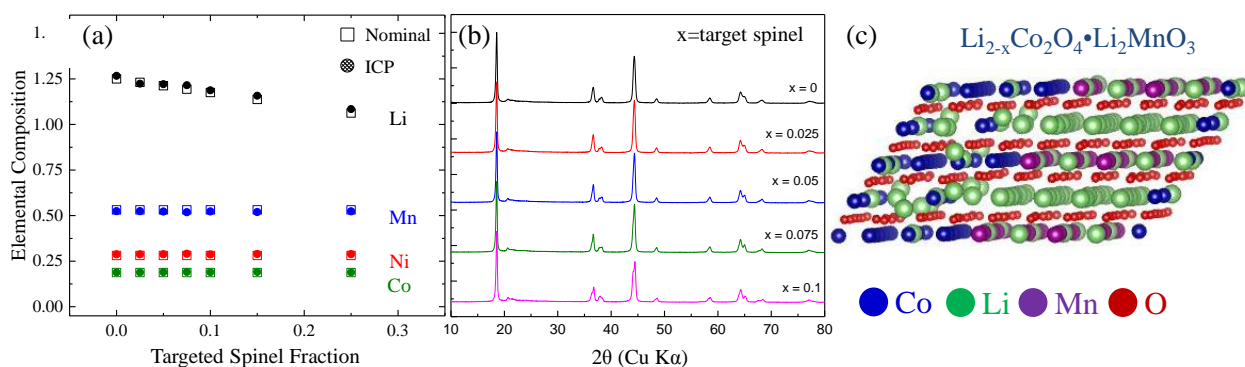


Figure 47. (a) Nominal (open symbols) and inductively coupled plasma measured (closed symbols) compositions of $\text{Li}_{1.25-x}(\text{Ni}_{0.28}\text{Mn}_{0.53}\text{Co}_{0.19})\text{O}_y$ layered-layered-spinel, cathode powders. (b) X-ray diffraction patterns of the samples in (a) as a function of targeted spinel contents, x . (c) Simulated structure of composite $\text{Li}_2\text{Co}_2\text{O}_4 \cdot \text{Li}_2\text{MnO}_3$ after removal of $\frac{1}{2}$ Li from the Co spinel component.

Patents/Publications/Presentations

Presentations

- International Battery Association Meeting, Nantes, France (March 24, 2016): “Lithium- and Manganese-Rich Cathodes: A Deep Dive and A Look Forward”; Jason R. Croy, K. G. Gallagher, M. Balasubramanian, J. S. Park, E. J. Lee, A. K. Burrell, and M. M. Thackeray. Invited.
- Energy Materials Nanotechnology, Orlando, Florida (February 24, 2016): “Atomic-Scale Degradation Mechanisms in High-Capacity, Lithium- and Manganese Rich Cathode Materials”; Jason R. Croy. Invited.
- BMR Program Review Meeting, LBNL, Berkeley, California (January 20, 2016): “Processing and Characterization of High Capacity, Composite Electrode Structures”; Jason R. Croy and M. M. Thackeray.

TASK 6 – MODELING ADVANCED ELECTRODE MATERIALS

Summary and Highlights

Achieving the performance, life, and cost targets outlined in the EV Everywhere Grand Challenge will require moving to next generation chemistries, such as higher capacity Li-ion intercalation cathodes, silicon and other alloy-based anodes, lithium metal anode, and sulfur cathodes. However, numerous problems plague the development of these systems, from material level challenges in ensuring reversibility to electrode level issues in accommodating volume changes, to cell-level challenges in preventing cross talk between the electrodes. In this task, a mathematical perspective is applied to these challenges to provide an understanding of the underlying phenomenon and to suggest solutions that can be implemented by the material synthesis and electrode architecture groups.

The effort spans multiple length scales from *ab initio* methods to continuum-scale techniques. Models are combined with experiments and extensive collaborations are established with experimental groups to ensure that the predictions match reality. Efforts are also focused on obtaining the parameters needed for the models either from lower length scale methods or from experiments. Projects also emphasize pushing the boundaries of the modeling techniques used to ensure that the task stays at the cutting edge.

In the area of intercalation cathodes, the effort is focused on understanding the working principles of the high Ni layered materials with an aim of understanding structural changes and the associated changes in transport properties. In addition, focus is paid to the assembling of porous electrodes with particles to predict the conduction behavior and developing tools to measure electronic conduction. This quarter, the lithium diffusion process in the excess-lithium material was studied. In the area of new disordered materials, the project has devised an efficient screening methodology for the computational prediction of synthesizable cation-disordered materials. Finally, to measure anisotropic conductivity in cathodes, a new numerical procedure was implemented with the required robustness that can now be compared to experimental four-probe-type measurements.

In the area of silicon anodes, the effort is in trying to understand the interfacial instability and suggest ways to improve the cyclability of the system. In addition, effort is focused on designing artificial SEI layers that can accommodate the volume change, and in understanding the ideal properties for a binder to accommodate the volume change without delamination. Simulations show that lithium carbonate decomposition on reactive anode surfaces is expected, and the innermost SEI should be composed of Li_2O or LiF . In addition, for the first time, *in situ* AFM studies show that SEI cracking generates and propagates normal to the surface. Continuum modeling shows that the SEI layer near the edge of the island is under pronounced in-plane tensile stress, consistent with the experiments.

In the area of sulfur cathodes, the focus is on developing better models for the chemistry with the aim of describing the precipitation reactions accurately. Efforts are focused on performing the necessary experiments to obtain a physical picture of the phase transformations in the system and in measuring the relevant thermodynamic, transport, and kinetic properties. In addition, changes in the morphology of the electrode are described and tested experimentally. In this quarter, the transport across the film of Li_2S was quantified using potential relaxation methods. The values of the time constant for diffusion shows that transport across the film could very well limit performance during discharge.

Task 6.1 – Electrode Materials Design and Failure Prediction (Venkat Srinivasan, Lawrence Berkeley National Laboratory)

Project Objective. The project goal is to use continuum-level mathematical models along with controlled experiments on model cells to (i) understand the performance and failure models associated with next-generation battery materials, and (ii) design battery materials and electrodes to alleviate these challenges. The research will focus on the Li-S battery chemistry and on microscale modeling of electrodes. Initial work on the Li-S system will develop a mathematical model for the chemistry along with obtaining the necessary experimental data, using a single ion conductor (SIC) as a protective layer to prevent polysulfide migration to the Li anode. The initial work on microscale modeling will use the well understood $\text{Li}(\text{NiMnCo})_{1/3}\text{O}_2$ (NMC) electrode to establish a baseline for modeling next-generation electrodes.

Project Impact. Li-S cells promise to increase the energy density and decrease the cost of batteries compared to the state of the art. If the performance and cycling challenges can be alleviated, these systems hold the promise for meeting the EV Everywhere targets.

Out-Year Goals. At the end of this project, a mathematical model will be developed that can address the power and cycling performance of next-generation battery systems. The present focus is on microscale modeling of electrodes and Li-S cells, although the project will adapt to newer systems, if appropriate. The models will serve as a guide for better design of materials, such as in the kinetics and solubility needed to decrease the morphological changes in sulfur cells and increase the power performance.

Milestones

1. Replace parameters (porosity gradient and tortuosity) in macroscale NMC model with corresponding values or functions obtained from tomography data. (December 2015 – Complete)
2. Measure the relationship of film growth to electrochemical response and develop a model to interpret the relationship. (March 2016 – Complete)
3. Measure transport properties of polysulfide solutions using electrochemical methods. If unsuccessful at obtaining concentration-dependent diffusion coefficient, use fixed diffusion coefficient value in upcoming simulations. (June 2016 – In progress)
4. Incorporate measured properties into porous-electrode model of Li-S cell and compare to data (September 2016 – In progress)

Progress Report

Measurement of the relationship of film growth to electrochemical response. This project has investigated physical processes by observing relaxation behavior of Li-S batteries. Figure 48a shows relaxation behavior of Li-S cells at different C-rates, recorded after the cells reached end of discharge. The relaxation kinetics clearly depend on rate of discharge. The slow relaxation with a long time constant might be attributed to a combination of electrochemical reaction and double-layer capacitance effects; the different C-rates might lead to different amount of discharge product and different capacitance, resulting in different relaxation kinetics. Alternatively, transport phenomena, including those within the film formed on the reaction surface during discharge, suggest another possible explanation for the relaxation behavior wherein concentration gradients build up within the cell when current is applied and relaxes after interrupting the applied current, leading to the relaxation of voltage.

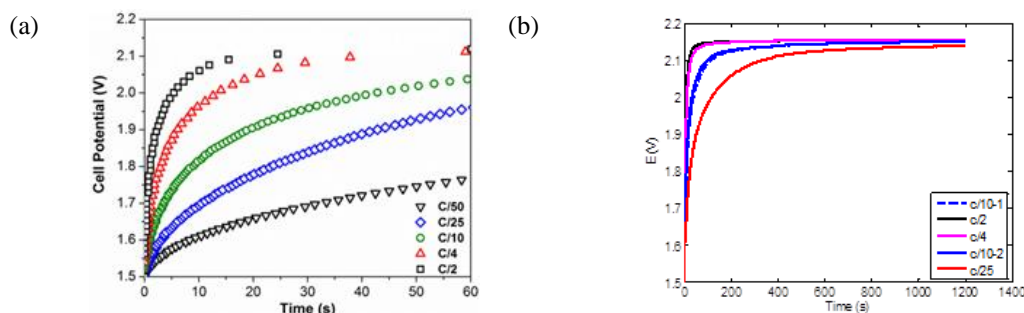


Figure 48. (a) Relaxation behavior of Li-S cells previously discharged at different C-rates, which were recorded after the cells reached end of discharge. (b) Relaxation behavior at different C-rates of a Li-S cell that has been previously discharged to 1.5 V by C/10.

To explore these possible explanations, the project examined the relaxation behavior at different C-rates of a Li-S cell, discharged initially to 1.5 V at a C/10 rate to set a reference film thickness. After the initial discharge step, the cell underwent a sequence of rest and discharge steps at different C-rates. Relatively small amounts of current were passed during the discharge steps. In Figure 48b, the curve labeled “C/10-1” shows the relaxation after the initial C/10 discharge step and “C/10-2” is from the subsequent C/10 discharge. The relaxation behavior is rate-dependent despite the fixed film thickness, indicating that relaxation is more like a transport-limited process than a double-layer capacitance effect. Figure 49a shows a plot of $\ln(E_{oc} - E_{ss})$ versus Time (s). A linear region at the later stage of relaxation (Figure 49b) confirms the transport-limited process. The extracted slopes of linear lines (Figure 49c) are quite similar at different C-rates due to the essentially fixed film thickness. The calculated characteristic transport time (L^2/D) is around 1.23×10^4 s. When these extracted values are incorporated into a model that describes film transport, the model suggests that transport across the film could limit cell performance. This model describing the relation of the electrochemical response to film presence completes the Q2 milestone.

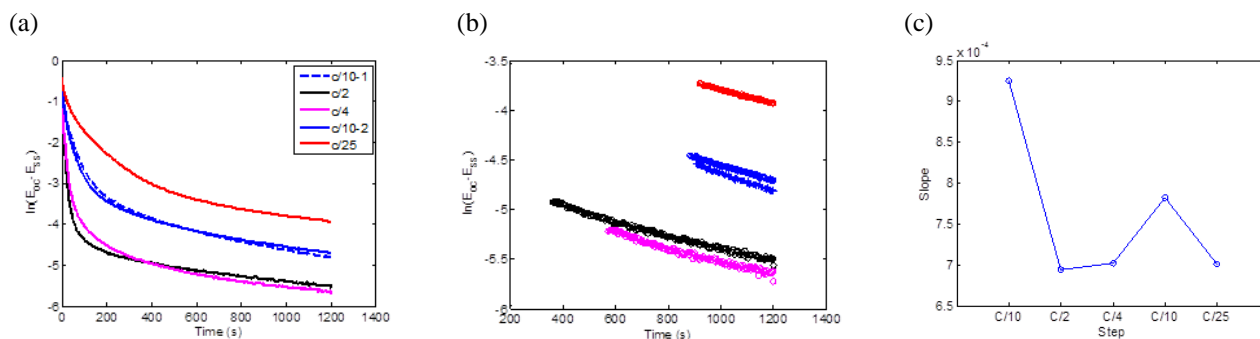


Figure 49. (a) $\ln(E_{oc} - E_{ss})$ versus Time (s). (b) Plot of linear region of curves in (b) with fitting line. (c) Extracted slopes of fitting lines at different C-rates.

Task 6.2 – Predicting and Understanding Novel Electrode Materials from First-Principles (Kristin Persson, Lawrence Berkeley National Laboratory)

Project Objective. The project aim is to model and predict novel electrode materials from first-principles focusing on (1) understanding the atomistic interactions behind the behavior and performance of the high-capacity lithium excess and related composite cathode materials, and (2) predicting new materials using the recently developed Materials Project high throughput computational capabilities at LBNL. More materials and new capabilities will be added to the Materials Project Lithium Battery Explorer App (www.materialsproject.org/apps/battery_explorer/).

Project Impact. The project will result in a profound understanding of the atomistic mechanisms underlying the behavior and performance of the Li-excess as well as related composite cathode materials. The models of the composite materials will result in prediction of voltage profiles and structural stability—the ultimate goal being to suggest improvements based on the fundamental understanding that will increase the life and safety of these materials. The Materials Project aspect of the work will result in improved data and electrode properties being calculated to aid predictions of new materials for target chemistries relevant for ongoing BMR experimental research.

Out-Year Goals. During years one and two, the bulk phase diagram will be established, including bulk defect phases in layered Li_2MnO_3 , layered LiMO_2 ($\text{M} = \text{Co}, \text{Ni}, \text{and Mn}$), and LiMn_2O_4 spinel to map out the stable defect intermediate phases as a function of possible transition metal rearrangements. Modeling of defect materials (mainly Li_2MnO_3) under stress/strain will be undertaken to simulate effect of composite nano-domains. The composite voltage profiles as function of structural change and Li content will be obtained. In years two to four, the project will focus on obtaining Li activation barriers for the most favorable TM migration paths as a function of Li content, as well as electronic DOS as a function of Li content for the most stable defect structures identified in years one to two. Furthermore, stable crystal facets of the layered and spinel phases will be explored, as a function of O_2 release from surface and oxygen chemical potential. Within the project, hundreds of novel Li intercalation materials will be calculated and made available.

Collaborations. This project engages in collaboration with Gerbrand Ceder (MIT), Clare Grey (Cambridge, UK), Mike Thackeray (ANL), and Guoying Chen (LBNL).

Milestones

1. Mn mobilities as a function of Li content in layered Li_xMnO_3 and related defect spinel and layered phases. (March 2015 – Complete)
2. Surface facets calculated and validated for Li_2MnO_3 . (March 2016 – Complete)
3. Calculate stable crystal facets. Determine whether facet stabilization is possible through morphology tuning. (March 2016 – Complete)
4. *Go/No-Go*: Stop this approach if facet stabilization cannot be achieved. (March 2016 – Ongoing)
5. Li mobilities as a function of Li content in layered Li_xMnO_3 and related defect spinel and layered phases. (September 2015 – Complete)

Progress Report

The project is finishing its study of lithium-ion diffusion mechanisms in Li-excess layered materials using first-principle calculations. Taking Li_2MnO_3 as the ‘worst case’ scenario in the family of Li-excess materials, the project systematically investigated the Li migrations in various local vacancy environments in both the intra-layer as well as inter-layer Li migrations. The different vacancy populations will occur as a function of Li content in the material with certain statistics during cycling. Using the results obtained, the calculations show that the Li-diffusion in *pristine bulk* Li_2MnO_3 is comparable to commercialized cathode materials, which suggests that the observed low rate behavior of this class of materials is due to other factors such as first charge surface modification and/or electrode-level particle-particle transport.

The migration energy barriers are calculated with the Nudged Elastic Band method using first principle density functional theory. The mobile Li-ions migrate through an activated, intermediate tetrahedral site between the initial and final stable octahedral sites. The project investigates three possible local vacancy topologies for Li-migration in both intra- and inter-layer Li-migration: (1) *single vacancy*: the mobile Li move from the initial octahedral site to the nearest, only vacant, octahedral site; (2) *di-vacancy*; the mobile Li move into one of the two available nearest vacant octahedral sites; and (3) *tri-vacancy*; the mobile Li move into one of the three available nearest vacant octahedral sites.

For intra-layer Li migration, there are two types of tetrahedral sites (saddle points) where the tetrahedral site face 1 Mn- and 3 Li-ions ($\text{T}_{4g}^{\text{Li}}$; purple tetrahedron in Figure 50a) or 4 Li-ions ($\text{T}_{2b}^{\text{Li}}$; green tetrahedron in Figure 50a) that connect the initial and final octahedral sites. During cycling, the population of Li vacancies vary, and the project finds that the number of local vacancies around a mobile Li greatly influences both the activation barrier as well as the preferred migration path (see Figure 50b).

Hence, the mobile Li-ion moves into the $\text{T}_{4g}^{\text{Li}}$ site for single- and tri-vacancies, and the $\text{T}_{2b}^{\text{Li}}$ site for di-vacancy (see Figure 50a) scenarios. For inter-layer migration, there are two possible activated, tetrahedral sites; facing either 2 Mn- and 2 Li-ions ($\text{T}_{2c}^{\text{Mn}}$ or $\text{T}_{4h}^{\text{Mn}}$; cyan tetrahedron in Figure 50c) or 4 Li-ions ($\text{T}_{2b}^{\text{Li}}$; green tetrahedron in Figure 50a). For both single- and di-vacancy environments, the mobile Li in the transition metal layer moves through the $\text{T}_{2b}^{\text{Li}}$ site (see Figure 50c). The project observes that the di-vacancy stabilizes the saddle point tetrahedral site and dramatically reduces the Li migration energy (see Figure 50d). If a tri-vacancy environment is formed, the mobile Li in transition metal layer spontaneously migrate into the Li-layer without an energy barrier.

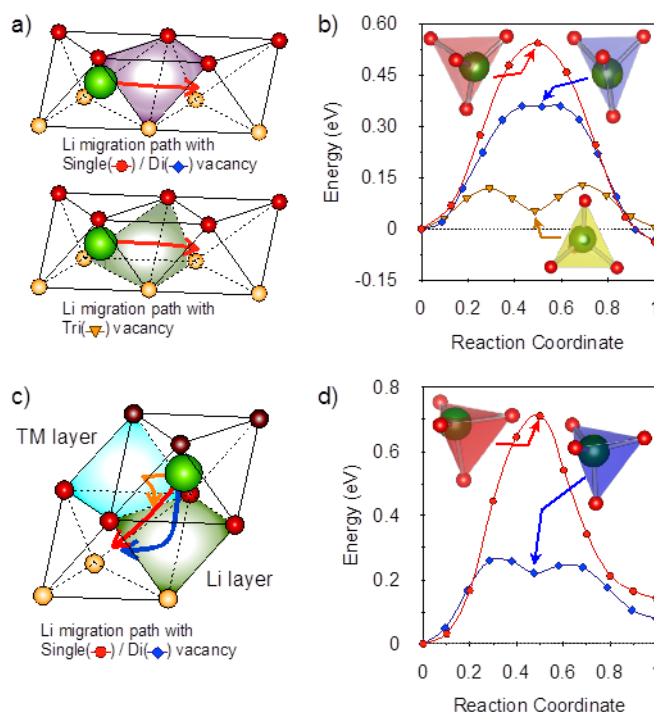


Figure 50. Illustrations of the intra-layer (a) and inter-layer (c) Li migrations in the various local environments and corresponding minimum energy paths of the intra-layer (b) and the inter-layer (d) Li migrations.

Patents/Publications/Presentations

Publication

- Shin, Yongwoo, and Hong Ding, and Kristin A. Persson. “Revealing the Intrinsic Li Mobility in the Li_2MnO_3 Lithium-Excess Materials.” *Chemistry of Materials, Articles ASAP* (2016). doi: 0.1021/acs.chemmater.5b04862.

Task 6.3 – First Principles Calculations of Existing and Novel Electrode Materials (Gerbrand Ceder, MIT)

Project Objective. Identify the structure of layered cathodes that leads to high capacity. Clarify the role of the initial structure as well as structural changes upon first charge and discharge. Give insight into the role of Li-excess and develop methods to predict ion migration in layered cathodes upon cycling and during overcharge. Develop predictive modeling of oxygen charge transfer and oxygen loss. Give insight into the factors that control the capacity and rate of Na-intercalation electrodes, as well as Na-vacancy ordering. Develop very high-capacity layered cathodes with high structural stability (> 250 mAh/g).

Project Impact. The project will lead to insight in how Li excess materials work and ultimately to higher capacity cathode materials for Li-ion batteries. The project will help in the design of high-capacity cathode materials that are tolerant to transition metal migration.

Out-Year Goals. The out-year goals are as follows:

- Higher capacity Li-ion cathode materials
- Novel chemistries for higher energy density storage devices
- Guidance for the field in search for higher energy density Li-ion materials

Collaborations. This project collaborates with K. Persson (LBNL) and C. Grey (Cambridge).

Milestones

1. Model to predict compositions that will disorder as synthesized. (December 2015 – Complete)
2. At least one Ti-based compound with high capacity. (March 2016 – Complete)
3. Predictive model for the voltage curve (slope) of cation-disordered materials. (June 2016)
4. Modeling capability for materials with substantial oxygen redox capability. (September 2016)

Progress Report

Cathode materials based on cation-disordered Li transition-metal (TM) oxides have recently been demonstrated to deliver high capacities and sustain efficient Li transport, provided an excess of at least 10% of Li compared to the transition metal concentration [1,2]. In addition, cation disorder has been credited with the improved structural stability of $\text{Li}_{1.211}\text{Mo}_{0.467}\text{Cr}_{0.3}\text{O}_2$, which undergoes only negligible volume changes during cycling [1]. Similarly, cation-disordered $\text{Li}_{1.25}\text{Nb}_{0.25}\text{Mn}_{0.5}\text{O}_2$ with a large capacity of 287 mAh/g from TM and O^{2-}/O^- redox activity has been reported without indications of material decay through oxygen release [3]. However, the discovery of novel cation-disordered cathode materials has so far either been by chance or through the modification of known disordered materials.

To aid the systematic design of new cation-disordered cathode materials, an efficient screening methodology for the computational prediction of synthesizable cation-disordered materials was devised. Previously, it was determined that the energy of the random (disordered) state of a hypothetical oxide cathode material can be well approximated based on *special quasi-random structures* (SQS), so that only two first principles calculations, the ground state structure and the SQS, are required to estimate the likeliness of cation disorder in any given composition. Using this, an automated computational search for new cation-disordered cathode materials was conducted for binary combinations of transition metals, with the results visualized in Figure 51. In the figure, every TM combination is represented by a circle, and the radius of the circle indicates the cation ordering strength. In addition, the color of each circle in Figure 51 encodes the mixing enthalpy with respect to oxides with transition-metal oxidation states between 2 and 4.

To confirm the accuracy of the presented computational results, $\text{LiCo}_{0.5}\text{Zr}_{0.5}\text{O}_2$ was selected for experimental investigation. While this chemistry is predicted to form the disordered rocksalt structure from the calculations presented in Figure 51, it has never been reported. Solid-state synthesis methods have yielded samples of cation-disordered $\text{LiCo}_{0.5}\text{Zr}_{0.5}\text{O}_2$ of ~95% purity, confirming the validity of this computational methodology (Figure 52).

- [1] Lee, J., et al., *Science* 343 (2014): 519-522.
- [2] Urban, A., et al., *Adv. Energy Mater.* 4 (2014): 1400478.
- [3] Wang, R., et al., *Electrochem. Commun.* 60 (2015): 70–73.

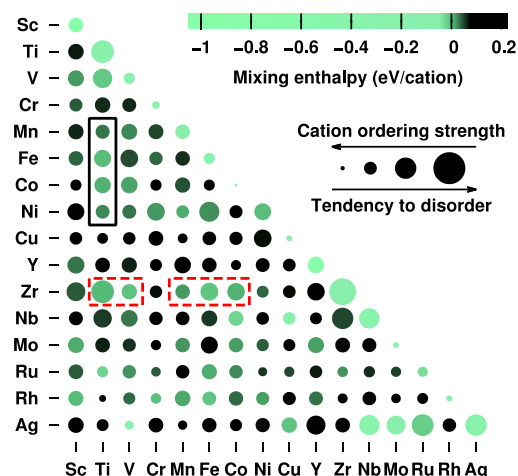


Figure 51. Screening results for the $\text{LiA}_{0.5}\text{B}_{0.5}\text{O}_2$ composition space. A circle represents each combination AB of transition metals. The color of the circle visualizes the predicted stability in terms of the estimated mixing enthalpy (bright green: more stable; dark: less stable), and the size of the circle indicates the tendency to disorder (small circle: strongly ordered; large circle: likely disordered).

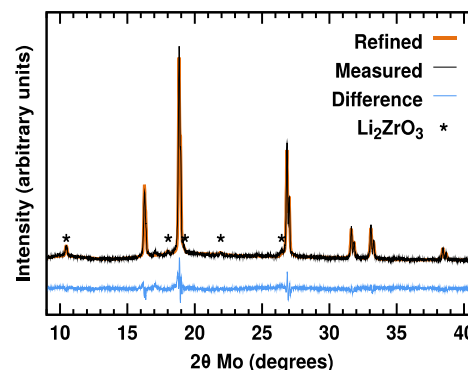


Figure 52. Unprocessed X-ray diffraction spectrum of as-synthesized $\text{LiCo}_{0.5}\text{Zr}_{0.5}\text{O}_2$ (thin black line) and refined spectrum based on the disordered rocksalt structure and the Li_2ZrO_3 impurity phase (thick orange line). Li_2ZrO_3 peaks are indicated with stars. The double-peak intensities are due to signals from Mo $\text{K}\alpha_1$ and $\text{K}\alpha_2$ radiation.

Task 6.4 – First Principles Modeling of SEI Formation on Bare and Surface/Additive Modified Silicon Anode (Perla Balbuena, Texas A&M University)

Project Objective. This project aims to develop fundamental understanding of the molecular processes that lead to the formation of a SEI layer due to electrolyte decomposition on Si anodes, and to use such new knowledge in a rational selection of additives and/or coatings. The focus is on SEI layer formation and evolution during cycling and subsequent effects on capacity fade through two concatenated problems: (1) SEI layers formed on lithiated Si surfaces, and (2) SEI layers formed on coated surfaces. Key issues being addressed include the dynamic evolution of the system and electron transfer through solid-liquid interfaces.

Project Impact. Finding the correspondence between electrolyte molecular properties and SEI formation mechanism, structure, and properties will allow the identification of new/improved additives. Studies of SEI layer formation on modified surfaces will allow the identification of effective coatings able to overcome the intrinsic deficiencies of SEI layers on bare surfaces.

Approach. Investigating the SEI layer formed on modified Si surfaces involves analysis of the interfacial structure and properties of specific coating(s) deposited over the Si anode surface, characterization of the corresponding surface properties before and after lithiation, especially how such modified surfaces may interact with electrolyte systems (solvent/salt/additive), and what SEI layer structure, composition, and properties may result from such interaction. This study will allow identification of effective additives and coatings able to overcome the intrinsic deficiencies of SEI layers on bare surfaces. Once the SEI layer is formed on bare or modified surfaces, it is exposed to cycling effects that influence its overall structure (including the anode), chemical, and mechanical stability.

Out-Year Goals. Elucidating SEI nucleation and electron transfer mechanisms leading to growth processes using a molecular level approach will help establish their relationship with capacity fading, which will lead to revisiting additive and/or coating design.

Collaborations. Work with Chunmei Ban (NREL) consists in modeling the deposition-reaction of alucon coating on Si surfaces and their reactivity. Reduction of solvents and additives on Si surfaces were studied in collaboration with K. Leung and S. Rempe, from SNL. Collaborations with Prof. Jorge Seminario (TAMU) on electron and ion transfer reactions, and Dr. Partha Mukherjee (TAMU) focusing on the development of a multi-scale model to describe the SEI growth on Si anodes.

Milestones

1. Identify SEI nucleation and growth on Si surfaces modified by deposition of alucone coatings as a function of degree of lithiation of the film. (December 2015 – Complete)
2. Quantify chemical and electrochemical stability of various SEI components: competition among polymerization, aggregation, and dissolution reactions. Evaluate voltage effects on SEI products stability. (March 2016 – Complete)
3. Identify alternative candidate electrolyte and coating formulations. (June 2016)
4. *Go/No-Go*: Test potential candidate electrolyte and coating formulations using coarse-grained model and experimentally via collaborations. (September 2016)

Progress Report

Stability of SEI components. Density functional theory (DFT) techniques were used to examine the stability of Li_2CO_3 , a prominent anode SEI component, on $\text{Li}(001)$ and $\text{Li}_{3.25}\text{Si}$ (010) surfaces. Li_2CO_3 is thermodynamically unstable versus Li metal. The question becomes whether kinetics permit electrochemical reduction of Li_2CO_3 . In a BMR-funded publication [Leung et al., *J. Phys. Chem. C* 120:6302 (2016)], it was shown that adding two extra surface Li atoms at the interface (orange labeled in Figure 53a), equivalent to a small excess -0.07 V overpotential or an extra 0.14 eV barrier, lead to deformation of the CO_3^{2-} unit and subsequent C-O bond-breaking which takes place in O(1) second time scales. Ongoing study of this reaction at $\text{Li}_{3.25}\text{Si}$ (010) interfaces shows that two excess Li at the interfaces lead to even faster (millisecond time scale) Li_2CO_3 decomposition there (Figure 53b). This shows that lithium carbonate decomposition on reactive anode surfaces is to be expected, and the innermost SEI should be composed of Li_2O (or LiF if fluoride sources are present). The implications of this innermost SEI structure on Li transport and dendrite formation are being explored.

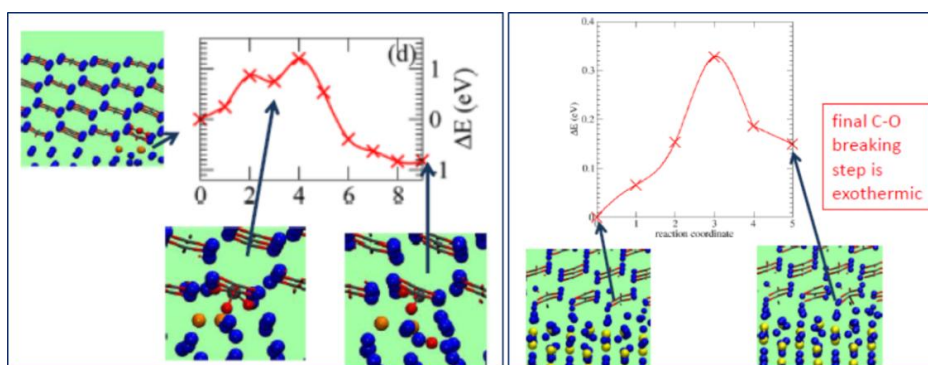


Figure 53. (a) Predicted Li_2CO_3 decomposition barriers on $\text{Li}(100)$ surfaces. C, O, and Li atoms are in grey, red, blue (orange for excess Li). (b) Same as (a), but for $\text{Li}_{3.25}\text{Si}$ surfaces.

Dynamics and free energy studies of electrolyte solvation. The structural results from molecular simulations showed that partial charge on an electrolyte molecule affects solvent structure around an ion. Starting with the partial charges calculated with the electronic structure Hartree-Fock (HF) method and 6-31G** basis sets, those atomic partial charges were reduced to 90% and 80% to determine the effect of partial charges on ion solvation and mobility properties. With full partial charges, it was found that the radial distribution function (rdf) around Li^+ ion is comparable to experimental results, but has an overly tight first solvation shell. The first solvation shell peak broadens as the partial charge on EC and propylene carbonate (PC) is decreased, and an additional two solvent molecules interact with the ion. The diffusion constants and transference numbers for various partial charges on PC and EC are comparable to the experimental values. Accordingly, it was concluded that certain sets of partial charges give optimal agreement with specific experimental measurements. Next, the cluster-quasichemical theory (QCT) approach coupled with electronic structure methods was applied to obtain benchmark values for comparison with classical molecular dynamics (MD) results. It was found that non-polarizable all-atom optimized potentials for liquid simulations (OPLS-AA) force field parameters can predict both structural and transport properties of Li^+ , and also match solvation free energy trends compared to the QCT-based electronic structure calculations.

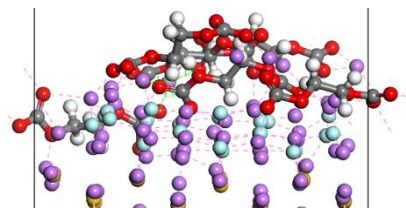


Figure 54. A LiF cluster (F blue, Li purple) is deposited over a Li_xSi slab (Si yellow, bottom layers not shown).

SEI structure and growth. Nucleation of Li_2EDC , Li_2VDC , LiF , and Li_2O is being studied using DFT and AIMD analyses. In Figure 54, a LiF cluster (F blue, Li purple) is deposited over a Li_xSi slab (Si yellow, bottom layers not shown). Adsorption of Li_2EDC is evaluated by sequentially depositing molecules on the surface of the LiF or Li_xSi (the most stable location). Packing and interactions of the organic layer is evaluated for Li_2EDC vs. Li_2VDC .

Patents/Publications/Presentations**Publications**

- Perez-Beltrán, S., and G. E. Ramirez-Caballero, and P. B. Balbuena. “First Principles Calculations of Lithiation of a Hydroxylated Surface of Amorphous Silicon Dioxide.” *J. Phys. Chem. C* 119 (2015): 16424-16431.
- Ma, Y., and J. M. Martinez de la Hoz, I. Angarita, J. M. Berrio-Sanchez, L. Benitez, J. M. Seminario, S.-B. Son, S.-H. Lee, S. M. George, C. M. Ban, and P. B. Balbuena. “Structure and Reactivity of Alucone-Coated Films on Si and Li_xSi_y Surfaces.” *ACS Appl. Mater. Inter.* 7 (2015): 11948-11955.
- Martinez de la Hoz, J. M., and F. A. Soto, and P. B. Balbuena. “Effect of the Electrolyte Composition on SEI Reactions at Si Anodes of Li-ion Batteries.” *J. Phys. Chem. C* 119 (2015): 7060-7068. doi: 10.1021/acs.jpcc.5b01228.
- Soto, F. A., and Y. Ma, J. M. Martinez de la Hoz, J. M. Seminario, and P. B. Balbuena. “Formation and Growth Mechanisms of Solid-Electrolyte Interphase Layers in Rechargeable Batteries.” *Chem. Mater.* 27, no. 23 (2015): 7990-8000.
- You, X., and M. I. Chaudhari, S. B. Rempe, and L. R. Pratt. “Dielectric Relaxation of Ethylene Carbonate and Propylene Carbonate from Molecular Dynamics Simulations.” *J. Phys. Chem. B*. doi: 10.1021/acs.jpcb.5b09561.
- Leung, K., and F. A. Soto, K. Hankins, P. B. Balbuena, and K. L. Harrison. “Stability of Solid Electrolyte Interphase Components on Reactive Anode Surfaces.” *J. Phys. Chem. C* 120 (2016): 6302-6313.

Task 6.5 – A Combined Experimental and Modeling Approach for the Design of High Current Efficiency Si Electrodes

(Xingcheng Xiao, General Motors; Yue Qi, Michigan State University)

Project Objective. The use of high-capacity, Si-based electrode has been hampered by its mechanical degradation due to large volume expansion/contraction during cycling. Nanostructured Si can effectively avoid Si cracking/fracture. Unfortunately, the high surface to volume ratio in nanostructures leads to an amount of SEI formation and growth, and thereby low current/CE and short life. Based on mechanics models, the project demonstrates that the artificial SEI coating can be mechanically stable despite the volume change in Si, if the material properties, thickness of SEI, and the size/shape of Si are optimized. Therefore, the project objective is to develop an integrated modeling and experimental approach to understand, design, and make coated Si anode structures with high current efficiency and stability.

Project Impact. The validated model will ultimately be used to guide the synthesis of surface coatings and the optimization of Si size/geometry that can mitigate SEI breakdown. The optimized structures will eventually enable a negative electrode with a 10x improvement in capacity (compared to graphite), while providing a > 99.99% Coulombic efficiency; this could significantly improve the energy/power density of current lithium-ion batteries.

Out-Year Goals. The out-year goal is to develop a well validated mechanics model that directly imports material properties either measured from experiments or computed from atomic simulations. The predicted SEI induced stress evolution and other critical phenomena will be validated against *in situ* experiments in a simplified thin-film system. This comparison will also allow fundamental understanding of the mechanical and chemical stability of artificial SEI in electrochemical environments and the correlation between the Coulombic efficiency and the dynamic process of SEI evolution. Thus, the size and geometry of coated Si nanostructures can be optimized to mitigate SEI breakdown, providing high current efficiency.

Collaborations. This project engages in collaboration with LBNL, PNNL, and NREL.

Milestones

1. Identify critical mechanical and electrochemical properties of the SEI coating that can enable high current efficiency. (December 2015 – Complete)
2. Design a practically useful Si electrode where degradation of the SEI layer is minimized during lithiation and delithiation. (March 2016 – Complete)
3. Construct an artificial SEI design map for Si electrodes, based on critical mechanical and transport properties of desirable SEI for a given Si architecture. (June 2016)
4. Validated design guidance on how to combine the SEI coating with a variety of Si nano/microstructures. *Go/No-Go:* Decision based on whether the modeling guided electrode design can lead to high Coulombic efficiency > 99.9%. (September 2016 – Complete; identified the desirable SEI component)

Progress Report

First-time observation of the failure mechanisms of SEI using *in situ* AFM. SEI surface topographs on a patterned monocrystalline Si electrode system at the initial, fully lithiated and delithiated states during the first (Figure 55a-c) and second (Figure 55d-e) cycles were recorded. It is the first direct observation that the crack generates and propagates normal to the surface, which is associated with tensile stress during lithiation (but not in the underlying Si). The lateral sliding of patterned island puts SEI layer in tension and compression during lithiation and delithiation respectively. During first cycle lithiation, at 0.1V hold, cracking begins to occur in the edge and corner regions due to tensile stress buildup in the SEI layer. This tensile state is further substantiated when these cracks open further as the Si expansion continues. More surface cracks appear in the edge region and other corners of the island during further insertion of Li at 0.05V (Figure 55b).

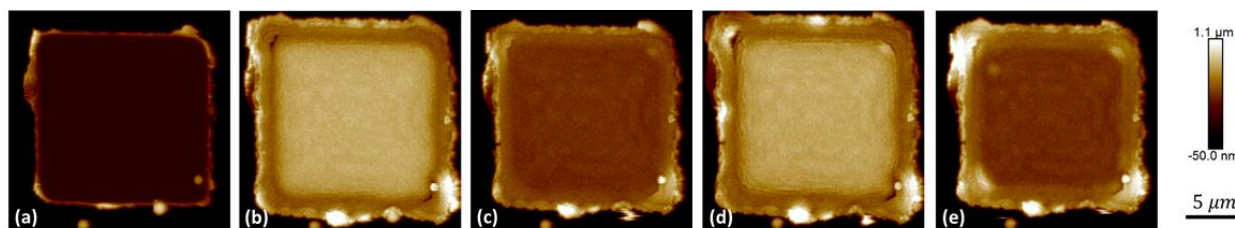


Figure 55. Two-dimensional AFM topographs of patterned a-Si electrode during first cycle at (a) 1.5 V, (b) 0.05 V, (c) 1.5 V, and during 2nd cycle at (d) 0.05 V and (e) 1.5 V. The contrast between center and edge regions of island is due to height differences proving the concept.

Two possible mechanisms proposed to explain SEI failure based on a bilayer SEI structure. One of the possible explanations is that the crack only runs through the top organic layer and does not reach the interface of SEI and Si to cause further SEI formation. Another explanation could be that the cracks run all the way to the interface of SEI and Si, but crack filling only occurs at the bottom of the crack and is not enough to fill the entire crack. During delithiation, there is compressive stress buildup in the SEI layer, and at first these cracks become narrower at 0.4V. With further removal of Li, it is observed that there is a huge buildup of material at the edge crack site. The material buildup at the crack site is a result of compressive stress that causes buckling of the SEI layer.

Established a continuum modeling of growth and crack formation of SEI on lithiated a-Si. As shown in Figure 56, the model shows that the SEI layer near the edge of the island is under pronounced in-plane tensile stress, which is consistent with the region where surface cracks were observed in experiments. The model predicts that the energy release rate for the growth of the surface crack increases with the length of the crack until it reaches a maximum value as the crack approaches the SEI/Si interface. This result suggests that a surface crack in the SEI layer would propagate unstably toward the interface, but it will stop or change to a path parallel to the interface in the later stage.

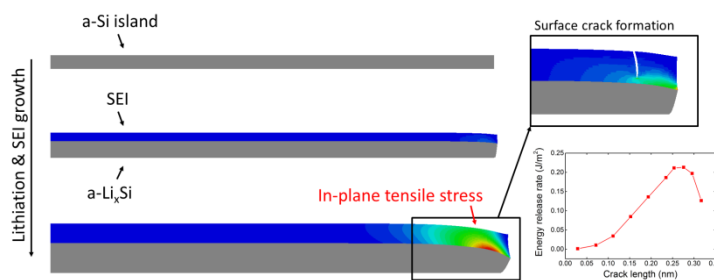


Figure 56. A continuum model established to describe how crack generates in the SEI layer.

Patents/Publications/Presentations

Publications

- Kim, S., and A. Ostadhossein, A. van Duin, X. Xiao, H. Gao, and Y. Qi. “Self-generated Concentration and Modulus Gradients Coating Design to Protect Si Nano-wire Electrodes during Lithiation.” *Phys. Chem. Chem. Phys.* (2016). doi: 10.1039/C5CP07219K.
- Pan, J., and Q. Zhang, X. Xiao, Y. Cheng, and Y. Qi. “Design of Nanostructured Heterogeneous Solid Ionic Coatings through a Multiscale Defect Model.” *ACS Appl. Mater. Interfaces* 8, no. 8 (2016): 5687–5693.
- Tokranov, A., and R. Kumar, C. Li, S. Minne, X. Xiao, and B. W. Sheldon. “Control and Optimization of the Electrochemical and Mechanical Properties of the Solid Electrolyte Interphase on Silicon Electrodes in Lithium Ion Batteries.” *Advanced Energy Materials*. doi: 10.1002/aenm.201502302.
- Zhang, Q., and J. Pan, P. Lu, Z. Liu, M. W. Verbrugge, B. W. Sheldon, Y. Cheng, Y. Qi, and X. Xiao. “Synergetic Effects of Inorganic Components in Solid Electrolyte Interphase on High Cycle Efficiency of Lithium Ion Batteries.” *Nano Letters* 16, no. 3 (2016): 2011–2016.
- Ostadhossein, A., and S. Y. Kim, E. D. Cubuk, Y. Qi, and A. van Duin. “Atomic Insight into the Lithium Storage and Diffusion Mechanism of SiO₂/Al₂O₃ Electrodes of Li-ion Batteries: ReaxFF Reactive Force Field Modeling.” *J. Phys. Chem. A* 120, no. 13 (2016): 2114–2127.
- Kim, K. J., and Y. Qi. “Vacancies in Si Can Improve the Concentration-Dependent Lithiation Rate: Molecular Dynamics Studies of Lithiation Dynamics of Si Electrodes.” *J. Phys. Chem. C* 119, no. 43 (2015): 24265–24275.

Presentations

- International Symposium on Advanced Materials and Structures (ISAMS 2016), Hong Kong University of Science and Technology (3 January 2016): “Brittle vs Ductile Fracture in Amorphous Alloys: From Metallic Glasses to Lithiated Si Electrodes”; Huajian Gao. Plenary Lecture.
- Rice University, Houston, Texas (February 11, 2016): “Stress Evolution and Degradation Mechanisms in Energy Materials”; Brian W. Sheldon.

Task 6.6 – Predicting Microstructure and Performance for Optimal Cell Fabrication (Dean Wheeler and Brian Mazzeo, Brigham Young University)

Project Objective. This work uses microstructural modeling coupled with extensive experimental validation and diagnostics to understand and optimize fabrication processes for composite particle-based electrodes. The first main outcome will be revolutionary methods to assess electronic and ionic conductivities of porous electrodes attached to current collectors, including heterogeneities and anisotropic effects. The second main outcome is a particle-dynamics model parameterized with fundamental physical properties that can predict electrode morphology and transport pathways resulting from particular fabrication steps. These two outcomes will enable the third, which is an understanding of the effects of processing conditions on microscopic and macroscopic properties of electrodes.

Project Impact. This work will result in new diagnostic tools for rapidly and conveniently interrogating electronic and ionic pathways in porous electrodes. A new mesoscale 3D microstructure prediction model, validated by experimental structures and electrode-performance metrics, will be developed. The model will enable virtual exploration of process improvements that currently can only be explored empirically.

Out-Year Goals. This project was initiated April 2013 and concludes March 2017. Goals by fiscal year are as follows.

- 2013: Fabricate first-generation micro-four-line probe, and complete associated computer model.
- 2014: Assess conductivity variability in electrodes; characterize microstructures of multiple electrodes.
- 2015: Fabricate first-gen ionic conductivity probe, N-line probe, and dynamic particle packing (DPP) model.
- 2016: Improve robustness of N-line probe and DPP model; assess structure correlation to conductivity.
- 2017: Using model and probe, evaluate effect of processing conditions.

Collaborations. Bryant Polzin (ANL) and Karim Zaghbi (HydroQuebec) provided battery materials. Transfer of technology to A123 to improve their electrode production process took place in FY15. There are ongoing collaborations with Simon Thiele (IMTEK, University of Freiburg) and Mårten Behm (KTH, Sweden).

Milestones

1. Demonstrate that the DPP model can accurately imitate the mechanical calendaring process for a representative electrode film. (December 2015 – Complete)
2. Develop a robust numerical routine for interpreting N-line conductivity measurements. (March 2016 – Complete)
3. *Go/No-Go:* Continue work on N-line probe and inversion routine if they can accurately determine anisotropic conductivity for test materials. (June 2016 – Ongoing)
4. *Go/No-Go:* Demonstrate correlations between DPP modeled conductivities and those determined by FIB/SEM and N-line probe. (September 2016 – Ongoing)

Progress Report

Milestone 2 (Complete). The second milestone was to develop a robust numerical routine for interpreting N-line conductivity measurements. A model is necessary to invert the conductivity measurements because (1) conductivity measurements are performed by placing electrical probes on the external surface of a sample, (2) the geometry of the probes and sample are complex and include 3D effects, and (3) multiple experiments are being used to regress multiple properties simultaneously. The model is formulated to produce shape factors that account for these complexities and are used to convert the voltage and current measurements into geometry-independent material properties of the battery electrode sample film. At the same time, the model must include a least-squares or optimization routine to produce the simultaneous properties. A previously developed a numerical routine worked, but was not robust enough to automate the interpretation of the additional experiments possible with the new 6-line probe produced in FY 2015.

The new numerical routine has been completed. The new routine uses a specialized quadrature algorithm and Fourier transforms to solve the underlying partial differential equation for the required geometry. The code also includes an implementation of a generalized Newton's method to do the inversion of the multiple experiments. The routine was initially implemented as VBA code inside a spreadsheet. It was found to be at least 100 times faster than the previous code and is considered fast enough for general purpose use. The code can also be implemented in other platforms for additional speed advantages. This means that the inversion model will not be the limiting factor as we seek to do real-time interpretation of the conductivity experiments.

One goal of the new code was to enable determination of anisotropic conductivity parameters from the N-line probe data. The model is robust in this respect, but it was found that a small amount of experimental noise makes it difficult to accurately determine the degree of anisotropy in practice. The model and experiments are clearly showing that standard electrode films have higher conductivity in-plane than out-of-plane (the direction in which it is most desirable for battery performance) by a factor of 1-4, meaning that further structural optimization is needed to improve utilization of conductive additives in these films. However, the experiments must be modified to get a more exact determination of the magnitude of this problem. Work will continue in the next quarter to see if the experiment can be adapted to make more-reliable anisotropic measurements possible (Go/No-Go Decision).

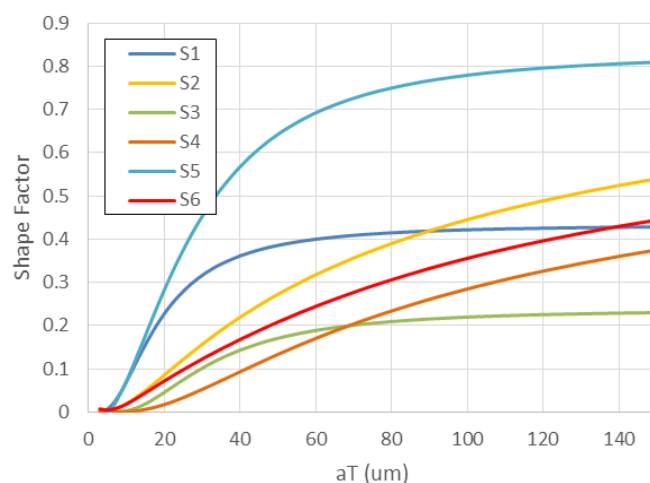


Figure 57. Example of shape factors produced by the model for different geometries

Patents/Publications/Presentations

Publication

- Forouzan, M. M., and C.-W. Chao, D. Bustamante, B. A. Mazzeo, and D. R. Wheeler. "Experiment and Simulation of the Fabrication Process of Lithium-ion Battery Cathodes for Determining Microstructure and Mechanical Properties." *J. Power Sources* 312 (2016): 172-183.

TASK 7 – METALLIC LITHIUM AND SOLID ELECTROLYTES

Summary and Highlights

The use of a metallic lithium anode is required for advanced battery chemistries like Li-air and Li-S to realize dramatic improvements in energy density, vehicle range, cost economy, and safety. However, the use of metallic Li with liquid and polymer electrolytes has been so far limited due to parasitic SEI reactions and dendrite formation. Adding excess lithium to compensate for such losses effectively negates the high energy density for lithium in the first place. For a long lifetime and safe anode, it is essential that no lithium capacity is lost to physical isolation from roughening, to dendrites or delamination processes, or to chemical isolation from side reactions. The key risk and current limitation for this technology is the gradual loss of lithium over the cycle life of the battery.

To date there are no examples of battery materials and architectures that realize such highly efficient cycling of metallic lithium anodes for a lifetime of 1000 cycles due to degradation of the Li-electrolyte interface. A much deeper analysis of the degradation processes is needed, so that materials can be engineered to fulfill the target level of performance for EV, namely 1000 cycles and a 15-year lifetime, with adequate pulse power. Projecting the performance required in terms of just the Li anode, this requires a high rate of lithium deposition and stripping reactions, specifically about 40µm Li per cycle, with pulse rates up to 10 and 20 nm/s charge and discharge, respectively. This is a conservative estimate, yet daunting in the total mass and rate of material transport. While such cycling has been achieved for state-of-the-art batteries using *molten* Na in Na-S and zebra cells, solid Na and Li anodes are proving more difficult.

The efficient and safe use of metallic lithium for rechargeable batteries is then a great challenge, and one that has eluded research and development efforts for many years. The BMR Task 7 takes a broad look at this challenge for both solid state batteries and batteries continuing to use liquid electrolytes. Four of the projects are new endeavors; two are ongoing. For the liquid electrolyte batteries, PNNL researchers are examining the use of cesium salts and organic additives to the typical organic carbonate electrolytes to impede dendrite formation at both the lithium and graphite anodes. If successful, this is the simplest approach to implement. At Stanford, novel coatings of carbon and boron nitride with a 3D structure are applied to the lithium surface and appear to suppress roughening and lengthen cycle life. A relatively new family of solid electrolytes with a garnet crystal structure shows superionic conductivity and good electrochemical stability. Four programs chose this family of solid electrolytes for investigation. Aspects of the processing of this ceramic garnet electrolyte are addressed at the University of Maryland and at the University of Michigan (UM), with attention to effect of flaws and composition. Computational models will complement their experiments to better understand interfaces and reduce the electrode area specific resistance (ASR). At ORNL, composite electrolytes composed of ceramic and polymer phases are being investigated, anticipating that the mixed phase structures may provide additional means to adjust the mechanical and transport properties. The last project takes on the challenge to use nano-indentation methods to measure the mechanical properties of the solid electrolyte, the lithium metal anode, and the interface of an active electrode. Each of these projects involves a collaborative team of experts with the skills needed to address the challenging materials studies of this dynamic electrochemical system.

Highlights. The highlights for this quarter are as follows:

- Nanoindentation studies provide the first measure of Li hardness (force/indent area) of 0.015 GPa. (Task 7.1)
- Though it has been believed that porosity may affect the stability of ceramic electrolytes, no observation was made when correlating the porosity (1 - 15%) with the critical current density. (Task 7.2)
- The first result for a spray coated polymer-ceramic electrolyte lithium battery was stable, although too resistive. (Task 7.3)

- A 3D structured garnet surface reduced the interfacial resistance for contact to a LiFePO_4 cathode slurry by 50%. (Task 7.4)
- Reduced graphene oxide films were shown to be effective hosts for lithium metal providing good rate performance for a Li-LiCoO₂ cell. (Task 7.5)
- Dual salt electrolytes improved the stability of Li||LFP batteries cycled to 500 cycles at 60°C, but the lithium stability depends on the current density as shown for C/3 cycles of Li||NMC cells. (Task 7.6)

Task 7.1 – Mechanical Properties at the Protected Lithium Interface (Nancy Dudney, ORNL; Erik Herbert, UT – Knoxville; Jeff Sakamoto UM)

Project Objective. This project will develop understanding of the Li metal SEI through state-of-the-art mechanical nano-indentation methods coupled with solid electrolyte fabrication and electrochemical cycling. The goal is to provide the critical information that will enable transformative insights into the complex coupling between the microstructure, its defects, and the mechanical behavior of Li metal anodes.

Project Impact. Instability and/or high resistance at the interface of lithium metal with various solid electrolytes limit the use of the metallic anode for batteries with high-energy density batteries, such as Li-air and Li-S. The critical impact of this endeavor will be a much deeper analysis of the degradation, so that materials can be engineered to fulfill the target level of performance for EV batteries, namely 1000 cycles and a 15-year lifetime, with adequate pulse power.

Approach. Mechanical properties studies through state-of-the-art nano-indentation techniques will be used to probe the surface properties of the solid electrolyte and the changes to the lithium that result from prolonged electrodeposition and dissolution at the interface. An understanding of the degradation processes will guide future electrolyte and anode designs for robust performance. In the first year, the team will address the two critical and poorly understood aspects of the protected Li metal anode assembly: (1) the mechanical properties of the solid electrolyte and (2) the morphology of the cycled Li metal.

Out-Year Goals. Work will progress toward study of the electrode assembly during electrochemical cycling of the anode. This project hopes to capture the formation and annealing of vacancies and other defects in the lithium and correlate this with the properties of the solid electrolyte and the interface.

Collaborations. This project funds work at ORNL, Michigan Technological University (MTU), and UM. Asma Sharafi (UM, Ph. D. student), Dr. Robert Schmidt (UM) also contribute to the project. Steve Visco (PolyPlus) will serve as a technical advisor.

Milestones

1. Determine elastic properties of battery grade lithium from different sources and preparation, comparing to values from the reference literature. (September 2015 – Complete)
2. Compare lithium properties, uncycled versus cycled, using thin film battery architecture. (June 2016 – On schedule)
3. View annealing of defects following a single stripping and plating half cycle, using thin film battery architecture. (September 2016 – On schedule)

Progress Report

New methods were developed for analyzing and conducting the nano-indentation tests of the lithium metal films. Films of 5 and 20 μm thicknesses were prepared on substrates of glass and kapton. The major challenge with testing lithium, besides preparing a pure material, is the extreme plasticity. This makes analysis of the intensive mechanical properties (elastic modulus and hardness) very uncertain. For most materials the elastic response is evaluated using a dynamic indentation method where a small 1nm modulation of the tip at 100Hz provides a measure of the elastic response as a function of depth from the surface. But this does not work well for lithium even at low strain rates and low frequency.

The original indentation mode and the new approach are shown in Figure 58. At top, the indenter is driven at two different strain rates then held while the tip continues to sink into the lithium. The harmonic response was measured all along, but was greatly distorted by the plasticity. At bottom of Figure 58, the new mode is a much slower stepwise load and hold, and the harmonic response at the end of each hold, when the tip is moving very slowly, is used to determine the modulus and hardness. Examples are shown in Figure 59. At these holds, the phase angle is only about 1-2°. The modulus and hardness (maximum load per contact area) are higher near the surface, likely reflecting the reacted surface of the lithium, but then are constant for holds at larger displacement. This is believed to be the first report of such hardness for lithium metal. Not surprisingly, ~15 MPa is low; in comparison for Al this hardness is 250 MPa. Changes in the firmware will provide automation of this new test mode.

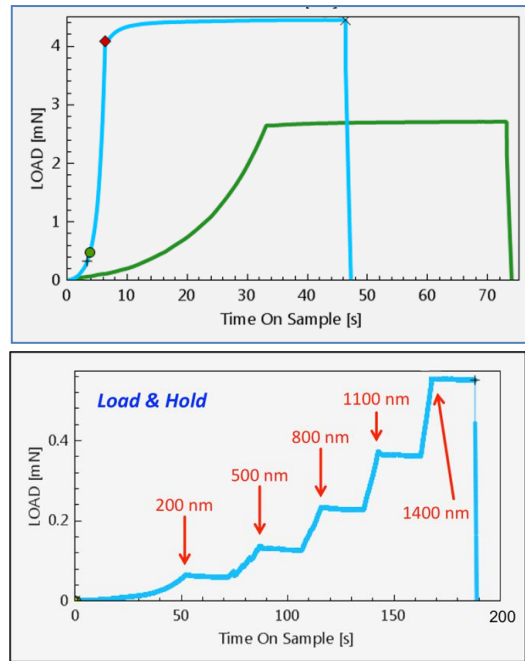


Figure 58. Standard (top) dynamic indentation with load, hold, and unload. Modified hold and load procedure required for lithium (bottom).

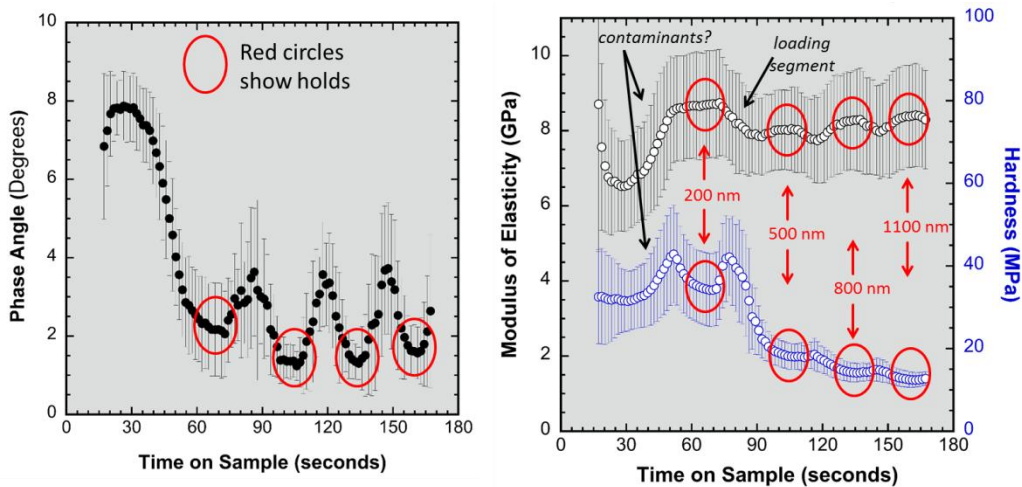


Figure 59. Results for stepwise load and hold on 20 μm lithium film. The harmonic analysis provides most reliable results at the end of the hold steps indicated by the red circles.

Patents/Publications/Presentations

Publication

- Yu, Seungho, and Robert D. Schmidt, Regina Garcia-Mendez, Erik Herbert, Nancy J. Dudney, Jeffrey B. Wolfenstine, Jeff Sakamoto, and Donald J. Siegel. “Elastic Properties of the Solid Electrolyte $\text{Li}_7\text{La}_3\text{Zr}_2\text{O}_{12}$ (LLZO).” *Chem. Mat.* 28, no. 197: (2016).

Task 7.2 – Solid Electrolytes for Solid-State and Lithium-Sulfur Batteries (Jeff Sakamoto, University of Michigan)

Project Objectives. *Enable advanced Li-ion solid-state and lithium-sulfur EV batteries using LLZO solid-electrolyte membrane technology.* Owing to its combination of fast ion conductivity, stability, and high elastic modulus, LLZO exhibits promise as an advanced solid-state electrolyte. To demonstrate relevance in EV battery technology, several objectives must be met. First, LLZO membranes must withstand current densities approaching $\sim 1 \text{ mA/cm}^2$ (commensurate with EV battery charging and discharging rates). Second, low ASR between Li and LLZO must be achieved to achieve cell impedance comparable to conventional Li-ion technology ($\sim 10 \text{ Ohms/cm}^2$). Third, low ASR and stability between LLZO and sulfur cathodes must be demonstrated.

Project Impact. The expected outcomes will: (i) enable Li metal protection, (ii) augment DOE access to fast ion conductors and/or hybrid electrolytes, (iii) mitigate Li-polysulfide dissolution and deleterious passivation of Li metal anodes, and (iv) prevent dendrite formation. Demonstrating these aspects could enable Li-S batteries with unprecedented end-of-life, cell-level performance: $> 500 \text{ Wh/kg}$, $> 1080 \text{ Wh/l}$, > 1000 cycles, lasting > 15 years.

Approach. This effort will focus on the promising new electrolyte known as LLZO ($\text{Li}_7\text{La}_3\text{Zr}_2\text{O}_{12}$). LLZO is the first bulk-scale ceramic electrolyte to simultaneously exhibit the favorable combination of high conductivity ($\sim 1 \text{ mS/cm}$ at 298K), high shear modulus (61 GPa) to suppress Li dendrite penetration, and apparent electrochemical stability (0-6 V vs Li/Li⁺). While these attributes are encouraging, additional research and development is needed to demonstrate that LLZO can tolerate current densities in excess of 1 mA/cm^2 , thereby establishing its relevance for PHEV/EV applications. This project hypothesizes that defects and the polycrystalline nature of realistic LLZO membranes can limit the critical current density. However, the relative importance of the many possible defect types (porosity, grain boundaries, interfaces, surface and bulk impurities), and the mechanisms by which they impact current density, have not been identified. Using experience with the synthesis and processing of LLZO (Sakamoto and Wolfenstine), combined with sophisticated materials characterization (Nanda), this project will precisely control atomic and microstructural defects and correlate their concentration with the critical current density. These data will inform multi-scale computation models (Siegel and Monroe), which will isolate and quantify the role(s) that each defect plays in controlling the current density. By bridging the knowledge gap between composition, structure, and performance, this project will determine if LLZO can achieve the current densities required for vehicle applications.

Collaborations. This project collaborates with Don Siegel (UM atomistic modeling), Chuck Monroe (UM, continuum scale modeling), Jagjit Nanda (ORNL, sulfur chemical and electrochemical spectroscopy), and Jeff Wolfenstine (ARL, atomic force microscopy of Li-LLZO interfaces).

Milestones

1. Correlate the critical current density based on the pore size and volume of porosity (UM). (February 2015 – Completed ahead of schedule)

Progress Report

Progress from the University of Michigan

Sakamoto Group. The Sakamoto group controlled microstructural defects by modifying LLZO processing conditions. Attempts were made to correlate the fraction of microstructural defects with the critical current density. No clear trend is apparent at this time; however, key Li metal propagation phenomena were elucidated with electron microscopy, XPS, and auger spectroscopy.

Siegel Group. The Siegel group calculated rates of reaction and free energy of formations to elucidate the reaction between LLZO and ambient air. The data agree very well with the experimental data. This analysis will quantify the stability between LLZO membranes and air.

Progress from ORNL

Dr. Jagjit Nanda's group completed XPS analysis on LLZO to quantify the rate of reaction between LLZO and ambient air. The results of the study elucidate the reaction pathway that leads to a relatively thin (nm - 10 nm) and benign passivation layer on LLZO.

Progress from ARL

Dr. Jeff Wolfenstine and the Sakamoto group completed analysis to determine if a Zr-based PO_4^- polyanion solid electrolyte (NASICON) is as stable as the O anion in LLZO garnet. The Zr-NASICON was synthesized at ARL and hot pressed at UM. A suite of mechanical and electrochemical characterization analyses were conducted. The results are included in a manuscript under preparation.

Patents/Publications/Presentations

Presentations

- International Battery Seminar, Ft. Lauderdale, Florida (March 21, 2016): "Ceramic Electrolytes Enabling All Solid-state Batteries"; J. Sakamoto. Invited tutorial.
- Material Challenges in Renewable Energy, Clearwater, Florida (April 10, 2016): "Cubic $\text{Li}_7\text{La}_3\text{Zr}_2\text{O}_{12}$ as a Solid Electrolyte"; J. Wolfenstine. Talk.

Task 7.3 – Composite Electrolytes to Stabilize Metallic Lithium Anodes (Nancy Dudney and Frank Delnick, Oak Ridge National Laboratory)

Project Objective. Prepare composites of representative polymer and ceramic electrolyte materials to achieve thin membranes that have the unique combination of electrochemical and mechanical properties required to stabilize the metallic lithium anode while providing for good power performance and long cycle life. Understand the lithium-ion transport at the interface between polymer and ceramic solid electrolytes, which is critical to the effective conductivity of the composite membrane. Identify key features of the composite composition, architecture, and fabrication that optimize the performance. Fabricate thin electrolyte membranes to use with a thin metallic lithium anode to provide good power performance and long cycle life.

Project Impact. A stable lithium anode is critical to achieve high energy density with excellent safety, lifetime, and cycling efficiency. This study will identify the key design strategies that should be used to prepare composite electrolytes to meet the challenging combination of physical, chemical, and manufacturing requirements to protect and stabilize the lithium metal anode for advanced batteries. By utilizing well characterized and controlled component phases, the design rules developed for the composite structures will be generally applicable toward the substitution of alternative and improved solid electrolyte component phases as they become available. Success in this program will enable these specific DOE technical targets: 500-700 Wh/kg, 3000-5000 deep discharge cycles, and robust operation.

Approach. This project seeks to develop practical solid electrolytes that will provide stable and long-lived protection for the lithium metal anode. Current electrolytes all have serious challenges when used alone: oxide ceramics are brittle, sulfide ceramics are air sensitive, polymers are too resistive and soft, and many electrolytes react with lithium. Composites provide a clear route to address these issues. This project does not seek discovery of new electrolytes; rather, the goal is to study combinations of current well known electrolytes. The project emphasizes the investigation of polymer-ceramic interfaces formed as bilayers and as simple composite mixtures where the effects of the interface properties can be readily isolated. In general, the ceramic phase is several orders of magnitude more conductive than the polymer electrolyte, and interfaces can contribute an additional source of resistance. Using finite element simulations as a guide, composites with promising compositions and architectures are fabricated and evaluated for lithium transport properties using ac impedance and dc cycling with lithium in symmetric or half cells. General design rules will be determined that can be widely applied to other combinations of solid electrolytes.

Out-Year Goal. Use advanced manufacturing processes where the architecture of the composite membrane can be developed and tailored to maximize performance and cost-effective manufacturing.

Collaborations. Electrolytes under investigation include a garnet electrolyte from Jeff Sakamoto (UM) and ceramic powder from Ohara. Staff at Corning Corporation will serve as the industrial consultant. Student intern, Cara Herwig, from Virginia Technological University assisted this quarter.

Milestones

1. Measure the removal of solvent molecules introduced via solution synthesis or gas absorption from ceramic-polymer composite sheets under vacuum and heating conditions. (March 2016 – Complete)
2. Prepare ceramic-polymer electrolyte sheets with a coating, and map the uniformity with nano-indentation and by profiling the Li plating. (September 2016 – On schedule)

Progress Report

This quarter, the project continued to improve techniques to form stable aqueous suspensions and sprayed coatings of Ohara LATP powders in PEO with lithium triflate salt with various additives. The slurry is coated using an air brush onto aluminum and copper foils and also onto aluminum foils coated with a lithium vanadate cathode. For impedance tests, two disks of the composite electrolyte coated foil are pressed face to face and sealed in a coin cell. While previously there was indication of some shorting or shuttle transport at low frequencies, now the impedance has the expected shape for an electrolyte with blocking electrodes (Figure 60). This is attributed to a more homogeneous mixture of salt and ceramic (~50 vol.%) in the PEO matrix, which may lead to more complete drying when heated under vacuum. The temperature dependence of the composite electrolyte is also more reproducible. It is clear that the tetraethylene glycol dimethyl ether (TEGDME) additive both improves the adhesion and the uniformity of the coatings on the foils and plasticizes the polymer to inhibit crystallization of the PEO at low temperatures. Unfortunately the conductivity at room temperature at $\sim 2 \mu\text{S}/\text{cm}$ is lower than required and the LATP particles are not participating in the conductivity. The conductivity is almost 2 orders of magnitude lower than the earlier melt processed composites with a similar concentration DMC rather than the TEGDME. This will be confirmed for spray coated composites.

The stability of the spray coated composite under vacuum and with lithium was tested by fabricating a battery. The composite electrolyte was sprayed over a thin vanadate electrolyte, thoroughly dried and pressed before loading into the vacuum chamber for Lithium deposition. When the lithium anode film was limited to only $1 \mu\text{m}$ thickness, it was clear that the lithium had reacted and was not conductive. With a thicker lithium anode, the battery was functional and did not self discharge. But it was obviously too resistive. Figure 61 shows the impedance of this battery compared to a similar thickness of the electrolyte alone.

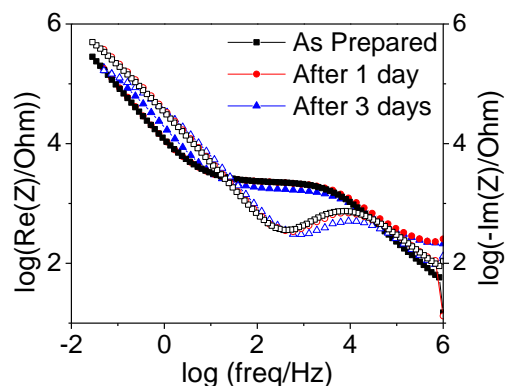


Figure 60. Real (solid symbols) and imaginary (open symbols) of the impedance at room temperature for improved spray coated composite

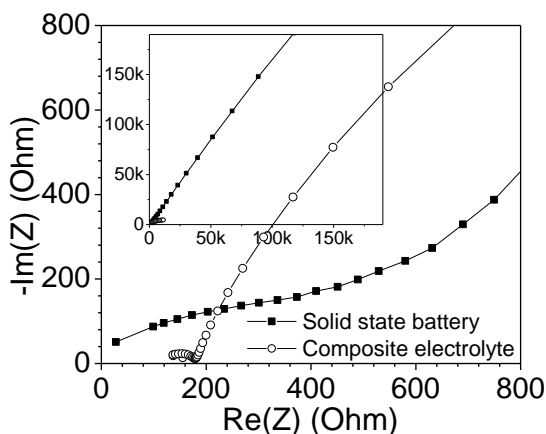


Figure 61. Impedance of a battery with the spray coated composite electrolyte, Li vanadate cathode and Li metal anode. Cell voltage was 1.7 V.

Task 7.4 – Overcoming Interfacial Impedance in Solid-State Batteries (Eric Wachsman, Liangbing Hu, and Yifei Mo, University of Maryland – College Park)

Project Objective. Develop a multifaceted and integrated (experimental and computational) approach to solve the key issue in solid-state, Li-ion batteries (SSLIBs), interfacial impedance, with a focus on garnet-based solid-state electrolytes (SSEs), the knowledge of which can be applied to other SSE chemistries. The focus is to develop methods to decrease the impedance across interfaces with the solid electrolyte, and ultimately demonstrate a high power/energy density battery employing the best of these methods.

Project Impact. Garnet electrolytes have shown great promise for safer and high-energy density batteries. The success of the proposed research can lead to dramatic progress on the development of SSLIBs based on garnet electrolytes. With regard to the fundamental science, the project methodology by combining computations and experiments can lead to an understanding of the thermodynamics, kinetics and structural stability, and evolution of SSLIBs with the garnet electrolytes. Due to the ceramic nature of garnet electrolyte, being brittle and hard, garnet electrolyte particles intrinsically lead to poor contacts among themselves or with electrode materials. A fundamental understanding at the nanoscale and through computations, especially with interface layers, can guide improvements to their design and eventually lead to the commercial use of such technologies.

Approach. SSLIB interfaces are typically planar, resulting in high impedance due to low specific surface area, and attempts to make 3D high surface area interfaces can also result in high impedance due to poor contact (for example, pores) at the electrode-electrolyte interface that hinder ion transport or degrade due to expansion/contraction with voltage cycling. This project will experimentally and computationally determine the interfacial structure-impedance relationship in SSLIBs to obtain fundamental insight into design parameters to overcome this issue. Furthermore, it will investigate interfacial modification (layers between SSE and electrode) to see if it can extend these structure-property relationships to higher performance.

Collaborations. This project is in collaboration with Dr. Venkataraman Thangadurai on garnet synthesis. It will collaborate with Dr. Leonid A. Bendersky (Leader, Materials for Energy Storage Program at NIST) and use neutron scattering to investigate the lithium profile across the bilayer interface with different charge-discharge rates. The project is in collaboration with Dr. Kang Xu in ARL with preparation of PFPE electrolyte.

Milestones

1. Identify compositions of gel electrolyte to achieve $100 \Omega \cdot \text{cm}^2$. (Milestone 1 – Complete)
2. Determination of interfacial impedance in layered and 3D controlled solid state structures. (Milestone 2 – Complete)
3. Develop computation models to investigate interfacial ion transport with interlayers. (Milestone 3 – Ongoing)
4. Identify compositions out of 4 types of interlayers and processing with electrolyte/electrode interfacial impedance of $\sim 10 \Omega \cdot \text{cm}^2$. (Milestone 4 - Ongoing)

Progress Report

Determine interfacial impedance in layered and 3D controlled solid state structures

3D structured garnet line patterns were printed on surface polished garnet pellets and sintered to form structured ionic conductive paths with varying line spacing (Figure 62). Cathode slurry (LiFePO_4 , CNT, and PVDF-HFP) was coated on both flat and structured garnet surfaces. Impedance (EIS) of the symmetrical cells was obtained at room temperature. The 3D printed structures reduced the cathode-electrolyte interfacial resistance. The depressed arcs, which can be assigned to

Li^+ diffusion and charge transfer steps, became much smaller after effective extension of surface area. The 3D printed lines ($40\mu\text{m}$ height and $70\mu\text{m}$ width) increased the effective sample surface areas from 36 mm^2 for polished pellet to 39.9 , 42.3 and 48 mm^2 with increasing line density, resulting in 22%, 35% and 52% reduction of interfacial resistance (from the intercept of real axis high frequency arc) proportional to the increase in effective surface area. Further impedance reduction is anticipated with further increase in line density (using smaller printing tips and reduced particle size).

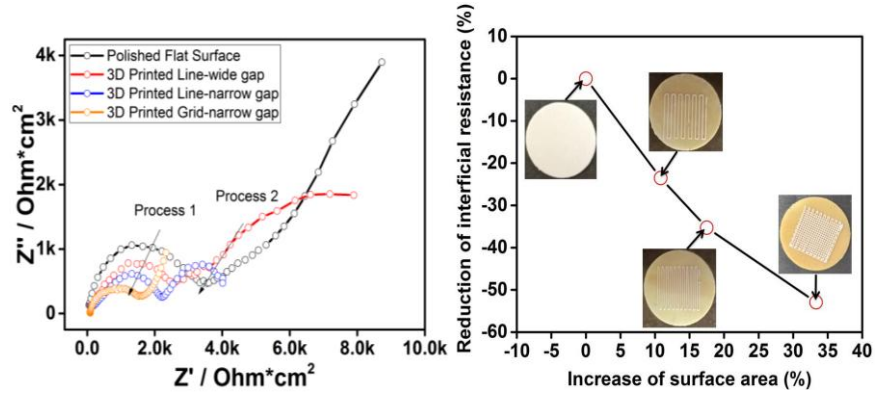


Figure 62. Comparison of the cathode/electrolyte interfacial impedance on flat and 3D-structured garnet pellet: (left) electrochemical impedance plot, and (right) reduction of interfacial resistance versus increases in surface area.

Modeling of interfacial coating layers on garnet-electrode interfaces

The project applied first principles calculations to investigate the interface stability between garnet and formed Li-Al alloys. It also considered the interface as a pseudo-binary of Li-Al alloy and garnet, then constructed the related phase diagram to identify possible thermodynamically favorable reactions. The compositional phase diagrams were constructed, and the mutual reaction energy of the pseudo-binary calculated using same approach defined in previous work. Three kinds of Li-Al alloy showed mutual reactions with garnet because of the slightly thermodynamic “welding” at their interface. Since the calculated reaction enthalpy is only around $-60 \sim -40$ meV/atom, the small reaction energy indicates that the interfacial reactions are likely to be limited and the formed interface could be relatively thermodynamic stable. Therefore, the interface between Li-Al alloy and garnet may exhibit good chemical stability, which might facilitate Li ion transport through.

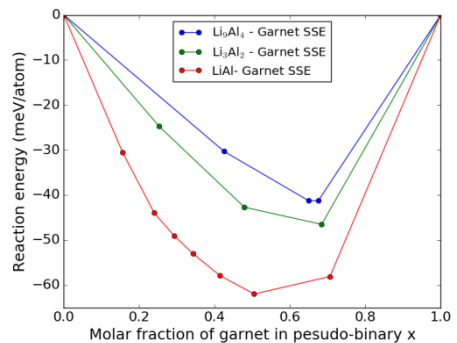


Figure 63. Calculated mutual reaction energy, ΔE_D , of garnet and Li-Al alloy interfaces.

Patents/Publications/Presentations

Presentation

- BMR Program Review Meeting, LBNL, Berkeley, California (January 20-21, 2016): “Overcoming Interfacial Impedance in Solid State Batteries”; Eric Wachsman.

Task 7.5 – Nanoscale Interfacial Engineering for Stable Lithium Metal Anodes (Yi Cui, Stanford University)

Project Objective. This study aims to render lithium metal anode with high capacity and reliability by developing chemically and mechanically stable interfacial layers between lithium metal and electrolytes, which is essential to couple with sulfur cathode for high-energy, lithium-sulfur batteries. With the nanoscale interfacial engineering approach, various kinds of advanced thin films will be introduced to overcome issues related to dendritic growth, reactive surface, and virtually “infinite” volume expansion of lithium metal anode.

Project Impact. Cycling life and stability of lithium metal anode will be dramatically increased. The success of this project, together with breakthroughs of sulfur cathode, will significantly increase the specific capacity of lithium batteries and decrease cost as well, therefore stimulating the popularity of EVs.

Out-Year Goals. Along with suppressing dendrite growth, the cycle life, Coulombic efficiency, and current density of lithium metal anode will be greatly improved (No dendrite growth for current density up to 3.0 mA/cm^2 , with $\text{CE} > 99.5\%$) by choosing the appropriate interfacial nanomaterial along with rational electrode material design.

Milestones

1. Study the relative affinity of lithium for different materials. (March 2016 – Complete)
2. Demonstrate facile, low-cost, scalable fabrication of porous host-lithium composite electrodes. (March 2016 – Complete)

Progress Report

Previously, the project demonstrated fabrication of Li-host composites via molten lithium (Li) infusion into host materials, which successfully achieved minimum volume change during Li metal cycling and improved electrochemical performance. Nevertheless, the hosts (carbon nanofibers and polyimide nanofibers) need to be coated with a layer of material that can chemically react with Li (Si and ZnO, respectively) to make the surface ‘lithiophilic’ for molten Li infusion. It is thus imperative to find a material that has intrinsic ‘lithiophilicity’ for more practical, facile synthesis of Li composite electrodes.

Carbon-based materials are the ideal host candidates for Li metal. Carbon is among the lightest materials available for scaffold construction and can be engineered to have appealingly high surface area with excellent mechanical strength. Moreover, carbon materials are generally stable under the redox environment in Li batteries. Thus, the project studied the relative affinity of Li for different carbon materials (Figure 64). While most of the carbon materials have relatively weak binding with Li, reduced graphene oxide (rGO) exhibits surprisingly high lithiophilicity, which is attributed to the synergistic effect of the chemical reactions between Li and its oxygen-containing functional groups and the nano-capillary force from the nanoscale gaps between the rGO flakes.

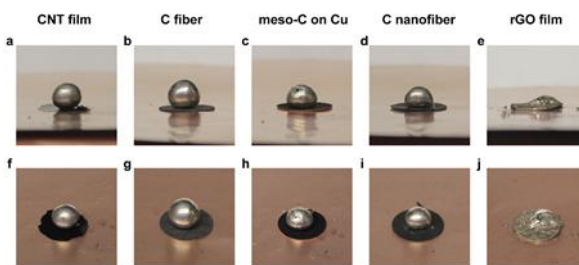


Figure 64. Surface wetting of molten Li on different carbon materials, including carbon nanotubes film (a, f), carbon fiber paper (b, g), mesoporous carbon coated on Cu foil (c, h), electrospun carbon nanofiber (d, i) and GO film (e, j).

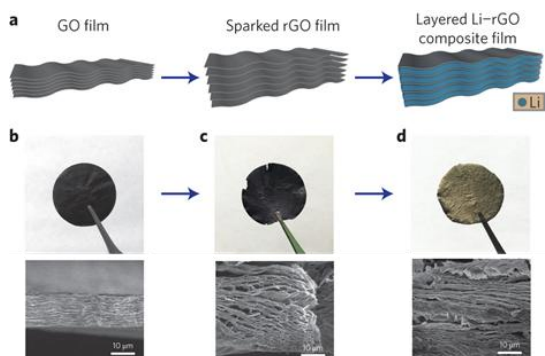


Figure 65. Schematic of the material design and the consequent synthetic procedures from a GO film (left) to a sparkled rGO film (middle) to a layered Li-rGO composite film (right). (b–d) Corresponding digital camera images and scanning electron microscopy images of the GO film (b), sparkled rGO film (c) and layered Li-rGO composite film (d). The diameters of the films shown in b–d are ~ 47 mm.

The intrinsic lithiophilicity of GO was utilized by directly contacting vacuum-filtrated GO film with molten Li, and Li can be drawn rapidly into the matrix without any additional surface modification (Figure 65). The resulting electrode can be described as a layered structure with Li uniformly infused into the nanogaps between rGO layers. This layered Li-rGO composite electrode can not only realize highly reduced dimension change during electrochemical cycling, effective dendrite suppression due to increased surface area and lithiophilic surface, but also the rGO cap layer can serve as a scaffold for SEI stabilization, improving the cycling Coulombic efficiency.

When paired with lithium cobalt oxide (LiCoO_2 , LCO) cathode, the layered Li-rGO anodes consistently exhibited a much better rate capability and lower hysteresis compared to Li foil (Figure 66). With Li-rGO anodes, a much higher LCO capacity can be retained especially at a high rate ($\sim 110 \text{ mAh g}^{-1}$ at 4 C and $\sim 70 \text{ mAh g}^{-1}$ at 10 C; x C = fully discharge within 1/x hours).

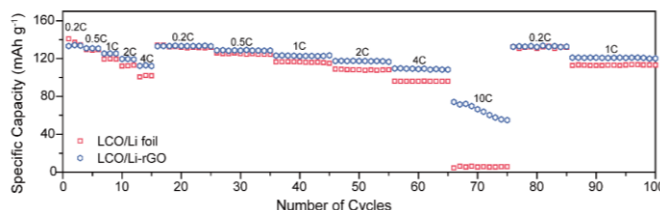


Figure 66. Rate capability of the LCO/Li-reduced graphene oxide and LCO/Li foil cells at various rates from 0.2 C to 10 C.

Patents/Publications/Presentations

Publication

- Lin, D., et al. “Layered Reduced Graphene Oxide with Nanoscale Interlayer Gaps as a Stable Host for Lithium Metal Anodes.” *Nat. Nanotechnol.* (2016).

Task 7.6 – Lithium Dendrite Suppression for Lithium-Ion Batteries (Wu Xu and Ji-Guang Zhang, Pacific Northwest National Laboratory)

Project Objective. The project objective is to enable lithium metal to be used as an effective anode in rechargeable Li-metal batteries for long cycle life at a reasonably high current density. The investigation will focus on the effects of various lithium salts, additives, and carbonate-based electrolyte formulations on Li anode morphology, Li Coulombic efficiency, and battery performances in terms of long-term cycling stability at room temperature and elevated temperatures and at various current density conditions, rate capability, and low-temperature discharge behavior. The surface layers on Li anode and cathode will be systematically analyzed. The properties of solvates of cation-solvent molecules will also be calculated to help explain the obtained battery performances.

Project Impact. Li metal is an ideal anode material for rechargeable batteries. Unfortunately, uncontrollable dendritic Li growth and limited CE during Li deposition/stripping inherent in these batteries have prevented their practical applications. This work will explore the new electrolyte additives that can lead to dendrite-free Li deposition with high CE. The success of this work will increase energy density of Li and Li-ion batteries and accelerate market acceptance of EVs, especially for PHEVs required by the EV Everywhere Grand Challenge proposed by the DOE/EERE.

Out-Year Goals. The long-term goal of the work is to enable Li and Li-ion batteries with >120 Wh/kg (for PHEVs), 1000 deep-discharge cycles, a 10-year calendar life, improved abuse tolerance, and less than 20% capacity fade over a 10-year period.

Collaborations. This project engages in collaboration with the following:

- Bryant Polzin (ANL) – NCA, NMC, and graphite electrodes
- Vincent Battaglia (LBNL) – LFP electrode
- Chongmin Wang (PNNL) – Characterization by TEM/SEM

Milestones

1. Develop mixed salts electrolytes to protect Al substrate and Li metal anode, and to maintain Li Coulombic efficiency over 98%. (December 2015 – Complete)
2. Demonstrate over 500 cycles for Li|LFP cells with high LFP loading and at high current density cycling. (March 2016 – Complete)
3. Demonstrate over 200 cycles for 4-V Li-metal batteries with high cathode loading and at high current density cycling. (June 2016 – Ongoing)
4. Achieve over 500 cycles for 4-V Li-metal batteries with high cathode loading and at high current density cycling. (September 2016 – Ongoing)

Progress Report

This quarter, the battery performances of Li||LFP coin cells with high LFP loading of 3.0 mAh/cm^2 using different dual-salt electrolytes were tested at a high charging current density (1.5 mA/cm^2). The dual-salt mixtures are LiTFSI-LiBOB and LiTFSI-LiDFOB in EC-EMC solvent mixture and the control electrolyte is 1.0 M LiPF_6 in EC-EMC. As shown in Figure 67a, these dual-salt electrolytes have similar voltage profiles that are slightly higher capacity than the control electrolyte (E256). However, when cycling, these electrolytes behave quite differently (Figure 67b). Only the LiTFSI-LiBOB electrolyte (E319) could lead the cells to be cycled at high charging rate (1.5 mAh/cm^2) and at elevated temperatures in high loading Li||LFP cells—70% capacity retention after 500 cycles. This is because the LiTFSI-LiBOB dual-salt electrolyte has good film-formation ability on Li metal surface and the interface layer enriched with boron and sulfur species is highly conductive. The effect of discharging current density on cycling performance of Li metal cells was further studied in Li||NMC coin cells with an areal capacity of 2.0 mAh/cm^2 for NMC cathode using conventional $1.0 \text{ M LiPF}_6/\text{EC-DMC}$ electrolyte. Figure 68a shows that the cycling protocol of C/3 charge and 1C discharge can result in stable cycling for at least 500 cycles, while the C/3 rate for both charge and discharge can only lead to stable cycling for less than 80 cycles. The difference is mainly from the Li metal anode side. Slow discharge rate yields serious corrosion of Li metal anode (Figure 68b) while fast discharge rate leads to well protected Li metal anode (Figure 68c). As shown in Figure 69, a transient high concentration electrolyte layer forms near the surface of Li metal anode during high rate discharge process. The highly concentrated Li^+ ions immediately coordinate with the available organic solvent molecules around the Li metal surface to form more stable solvates which facilitate the formation of a stable and flexible protection SEI film, which largely suppresses the corrosion of Li metal anode by free organic solvents and enables stable operation of Li metal batteries. However, the slow discharge rate cannot supply such protection, thus the Li metal anode is seriously corroded by free organic solvents during repeated cycling, leading to fast capacity fade and short cycle life.

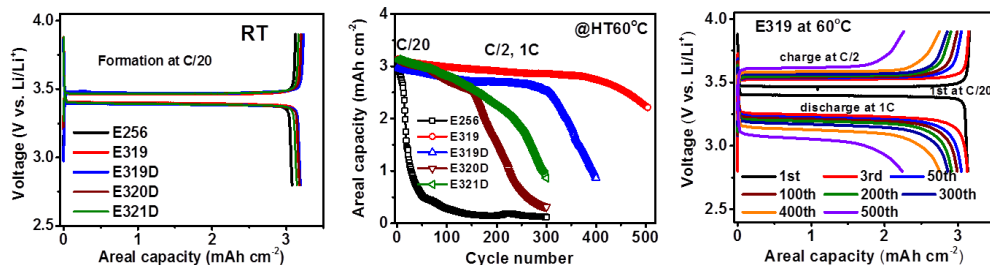


Figure 67. Battery performances of Li||LFP cells using different electrolytes. (a) Voltage profiles at the first cycle at C/20 rate and room temperature. (b) Cycling performance at C/2 charging and 1C discharging at 60°C. (c) Voltage profiles of the LiTFSI-LiBOB dual-salt electrolyte at selected cycles during cycling at 60°C.

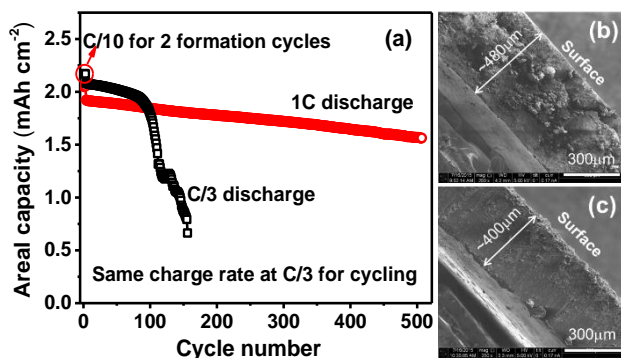


Figure 68. (a) Comparison of long-term cycling stability of Li||NMC cells cycled at C/3 charge and C/3 or 1C discharge at room temperature. (b-c) Cross-sectional scanning electron microscopic images of cycled Li metal anodes at C/3 discharge (b) and 1C discharge (c). The thickness of fresh Li anode was about $400 \mu\text{m}$.

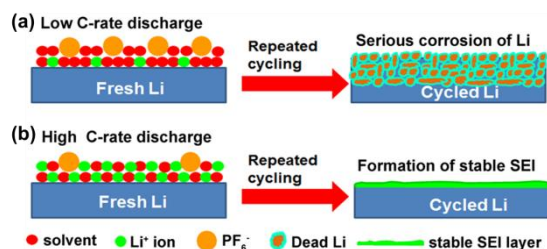


Figure 69. Schematic illustrations for mechanisms of SEI evolutions on Li metal anodes cycled at (a) low and (b) high discharge C rates.

Patents/Publications/Presentations

Publications

- Zheng, J., and P. Yan, R. Cao, H. Xiang, M. H. Engelhard, B. J. Polzin, C. Wang, J.-G., Zhang,* and W. Xu.* “Effects of Propylene Carbonate Content in CsPF₆-containing Electrolytes on the Enhanced Performances of Graphite Electrode for Lithium-ion Batteries.” *ACS Appl. Mater. Interfaces* 8 (2016): 5715-5722.
- J. Zheng, P. Yan, D. Mei, M. H. Engelhard, S. S. Cartmell, B. J. Polzin, C. Wang, J.-G. Zhang,* and W. Xu.* “Highly Stable Operation of Lithium Metal Batteries Enabled by the Formation of a Transient High-concentration Electrolyte Layer.” *Advanced Energy Materials* 6 (2016): 1502151.
- Xiang, H., and P. Shi, P. Bhattacharya, X. Chen, D. Mei, M. E. Bowden, J. Zheng, J.-G. Zhang, and W. Xu.* “Enhanced Charging Capability of Lithium Metal Batteries based on Lithium bis(trifluoromethanesulfonyl)imide-lithium bis(oxalato)borate Dual-salt Electrolytes.” *Journal of Power Sources* (2016). doi:10.1016/j.jpowsour.2016.04.017 (in press).

TASK 8 – LITHIUM SULFUR BATTERIES

Summary and Highlights

Advances in Li-ion technology have been stymied by challenges involved in developing high reversible capacity cathodes and stable anodes. Hence, there is a critical need for development of alternate battery technologies with superior energy densities and cycling capabilities. In this regard, lithium-sulfur batteries have been identified as the next flagship technology, holding much promise due to the attractive theoretical specific energy densities of 2,567 Wh/kg. In addition, realization of the high theoretical specific capacity of 1,675 mAh/g corresponding to formation of Li_2S using earth-abundant sulfur renders the system highly promising compared to other available cathode systems. Thus, the research focus has shifted to developing Li-S batteries. This system, however, suffers from major drawbacks, as elucidated below.

- Limited inherent electronic conductivity of sulfur and sulfur compound based cathodes.
- Volumetric expansion and contraction of both the sulfur cathode and lithium anode.
- Soluble polysulfide formation/dissolution and sluggish kinetics of subsequent conversion of polysulfides to Li_2S resulting in poor cycling life.
- Particle fracture and delamination as a result of the repeated volumetric expansion and contraction.
- Irreversible loss of lithium at the sulfur cathode, resulting in poor Coulombic efficiency.
- High diffusivity of polysulfides in the electrolyte, resulting in plating at the anode and consequent loss of driving force (that is, drop in cell voltage).

These major issues cause sulfur loss from the cathode, leading to mechanical disintegration. Additionally, surface passivation of anode and cathode systems results in a decrease in the overall specific capacity and Coulombic efficiency upon cycling. As a result, the battery becomes inactive within the first few charge-discharge cycles. Achievement of stable high capacity in Li-S batteries requires execution of fundamental studies to understand the degradation mechanisms in conjunction with engineered solutions. The BMR Task 8 addresses both aspects with execution of esoteric, fundamental *in situ* XAS and *in situ* electron paramagnetic resonance (EPR) studies juxtaposed with applied research comprising use of suitable additives, coatings, and exploration of composite morphologies. Both ANL and LBNL use X-ray based techniques to study phase evolution and loss of Coulombic efficiency in Se_8 during lithiation/delithiation, while understanding polysulfide formation in sulfur and polysulfides (PSL) in oligomeric polyethylene oxide (PEO) solvent, respectively. Work from PNNL, University of Pittsburgh (U Pitts), and Stanford University demonstrates high areal capacity electrodes in excess of 2 mAh/cm². Following loading studies reported in the first quarter, PNNL has performed *in situ* EPR to study reaction pathways mediated by sulfur radical formation. Coating/encapsulation approaches adopted by U Pitts and Stanford comprise flexible sulfur wire (FSW) electrodes coated with Li-ion conductors, and TiS_2 encapsulation of Li_2S in the latter, both ensuring polysulfide retention at sulfur cathodes. BNL work has focused on benchmarking of pouch cell testing by optimization of the voltage window and study of additives such as LiI and LiNO_3 . *Ab initio* studies at Stanford and U Pitts involving calculation of binding energies and reaction pathways, respectively, augment the experimental results. *Ab initio* molecular dynamics (AIMD) simulations performed at TAMU reveal multiple details regarding electrolyte decomposition reactions and the role of soluble polysulfides (PS) on such reactions. Using KMC simulations, electrode morphology evolution and mesostructured transport interaction studies were also executed. Each of these projects has a collaborative team of experts with the required skill set needed to address the EV Everywhere Grand Challenge of 350 Wh/kg and 750 Wh/l, and cycle life of at least 1000 cycles.

Highlights. The highlights from this quarter are as follows:

- Discharge performance in Li-S batteries shown to exhibit significant variation with C-rates, while charging behavior exhibits weak dependence on C-rates (Balbuena-TAMU). Electrochemical memory effect or the “shuttle effect” in sulfur batteries was also shown; that is, charging overpotential is less when discharge is partial and also the charging capacity is higher.
- Chemical binding of sulfur with carbon species and unique pore size (~2nm) generated in complex functional network (CFN) materials indicate promising propensity to ensure polysulfide retention and hence lead to ultra-low fade rates of 0.0014% fade/cycle (Kumta-Pitt).

Task 8.1 – New Lamination and Doping Concepts for Enhanced Li – S Battery Performance (Prashant N. Kumta, University of Pittsburgh)

Project Objective. The project objective is to successfully demonstrate generation of novel sulfur cathodes for Li-S batteries meeting the targeted gravimetric energy densities ≥ 350 Wh/kg and ≥ 750 Wh/l with a cost target \$125/kWh and cycle life of at least 1000 cycles for meeting the EV Everywhere blueprint. The proposed approach will yield sulfur cathodes with specific capacity ≥ 1400 mAh/g, at ≥ 2.2 V, generating ~ 460 Wh/kg energy density higher than the target. Full cells meeting the required deliverables will also be made.

Project Impact. Identification of new laminated Sulfur cathode based systems displaying higher gravimetric and volumetric energy densities than conventional Li-ion batteries will likely result in new commercial battery systems that are more robust, capable of delivering better energy and power densities, and more lightweight than current Li-ion battery packs. Strategies and configurations based on new lithium-ion conductor (LIC)-coated sulfur cathodes will also lead to more compact battery designs for the same energy and power density specifications as current Li-ion systems. Commercialization of these new S cathode based Li-ion battery packs will represent, fundamentally, a major hallmark contribution of the DOE VTO and the battery community.

Out-Year Goals. This is a multi-year project comprising of three major phases to be successfully completed in three years. Phase 1 (Year 1): Synthesis, Characterization, and Scale up of suitable LIC matrix materials and multilayer composite sulfur cathodes. This phase is completed. Phase 2 (Year 2): Development of LIC-coated sulfur nanoparticles, scale up of high-capacity engineered LIC-coated multilayer composite electrodes and doping strategies for improving electronic conductivity of sulfur. Phase 3 (Year 3): Advanced high energy density, high rate, extremely cyclable cell development.

Collaborations. The project collaborates with the following members with the corresponding expertise:

- Dr. Spandan Maiti (U Pitts): for mechanical stability and multi-scale modeling
- Dr. A. Manivannan (NETL): for XPS for surface characterization
- Dr. D. Krishnan Achary (U Pitts): for solid-state magic angle spinning NMR (MAS-NMR) characterization

Milestones

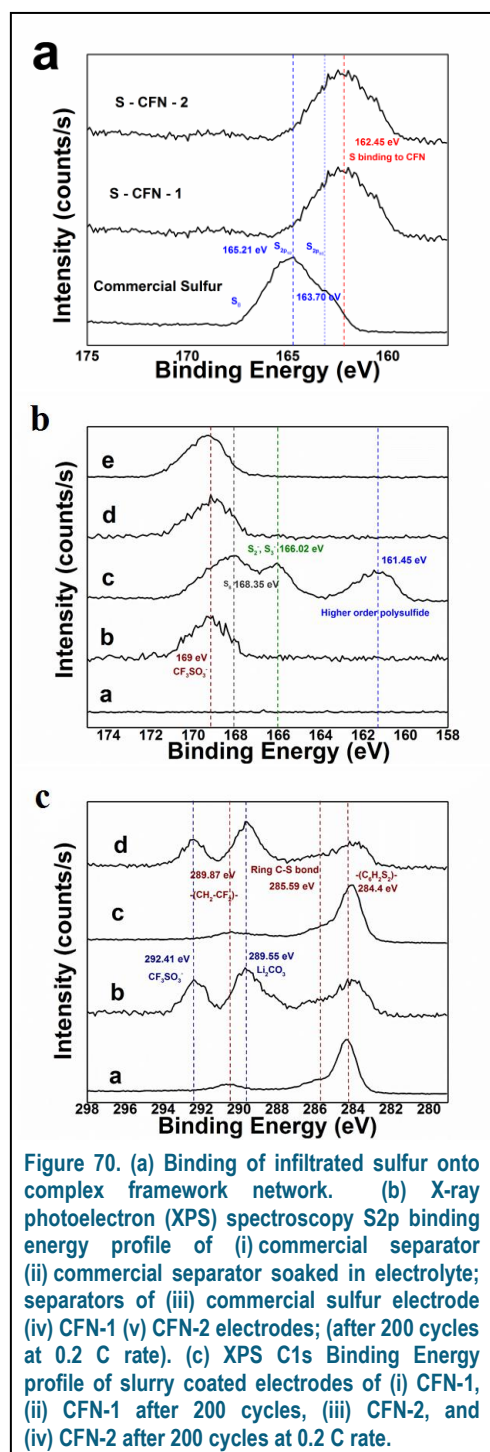
1. Identification of suitable dopants and dopant compositions to improve electronic conductivity of sulfur. (October 2015 – Complete)
2. Fundamental electrochemical study to understand the reaction kinetics, mechanism and charge transfer kinetics. (October 2015 – Complete)
3. Preparing doped LIC with improved ionic conductivity. (January 2016 – Complete)
4. Demonstrated synthesis of doped LIC membrane with improved Lithium-ion conductivity. (January 2016 – Complete)
5. Development of CFN morphology with a stable cycling performance of ~ 650 mAh/g for over 300 cycles with $< 0.02\%$ fade rate. (April 2016 – Complete)
6. Demonstration of binding of polysulfide with CFN results in polysulfide retention and hence, improved cycling stability. (April 2016 – Complete)

7. Demonstrated the effect of the unique pore size (~2nm) of CFN preventing dissolution of polysulfide from the liquid electrolyte. (April 2016 – Complete)
8. Application of TMPM improved the specific capacity of commercial sulfur demonstrating stable capacity of ~550 mAh/g over 100 cycles. (April 2016 – Complete)
9. Develop multiwall carbon nanotube (MWCNT) and LIC incorporated layer morphologies that demonstrate enhanced stability. (Ongoing)

Progress Report

Phase 1 of the project concluded with the successful identification of effective LIC membrane and demonstration of its ability to shield polysulfide from dissolving into the electrolyte. The principal aim of Phase 2 was to synthesize LIC materials identified in Phase 1 and to develop effective coating strategies of

these materials and to generate hetero-structured composites of sulfur with CNT. The LIC was synthesized using a high temperature – solid state synthesis. In Q1 of Phase 2, doping of the LIC with dopants identified during FY 2015 using DFT showed a threefold increase in ionic conductivity. This quarter, different strategies were investigated to coat the LIC onto sulfur cathodes effectively, and sputtering technique was selected due to the unique properties of sputter coating. A detailed investigation of sputtering of LIC onto sulfur cathodes is in progress. As a Q2 subtask, a detailed fundamental electrochemical investigation was performed on Complex Framework Network (CFN) materials that were developed and tested in Q1. The CFN material has pore size (~2 nm) comparable to the molecular size of PS. Hence it serves to prevent dissolution of PS into organic electrolyte and a very high pore volume. CFN electrodes were cycled with respect to lithium, and very low fade (<0.02% fade/cycle) was demonstrated in Q1. Figure 70a shows the XPS pattern of CFN before and after sulfur infiltration suggesting binding of sulfur with the CFN. XPS analysis of the post cycled CFN material shows no observable polysulfide species in the electrolyte as shown by Figure 70b indicating prevention of the formation of any soluble polysulfides and associated losses. XPS results also show chemical binding of the polysulfide species with the CFN as shown in Figure 70c, indicating that improvement in cycling stability (0.0014%/cycle) is owing to masking of PS dissolution in the organic electrolyte. As another subtask of Q2, a free standing transition metal oxide incorporated polymer membrane (TMPM) was used as a sieve to restrain polysulfides reaching the anode. The TMPM was used in addition to a commercial separator to test with commercial sulfur cathode. Incorporation of the TMPM improved the specific capacity of commercial sulfur to ~550 mAh/g for over 100 cycles. This improvement in specific capacity arises from the binding of polysulfide onto the transition metal oxide.



Patents/Publications/Presentations

Publication

- Shanthi, P. M; and P. H. Jampani, B. Gattu, M. Sweeney, M. K. Datta, and P. N. Kumta. “Nanoporous Non-carbonized Metal Organic Frameworks (MOFs): Effective Sulfur Hosts for High Performance Li-S Batteries.” *Journal of Materials Chemistry A* (2016). Under review.

Task 8.2 – Simulations and X-ray Spectroscopy of Li-S Chemistry (Nitash Balsara, Lawrence Berkeley National Laboratory)

Project Objective. Lithium-sulfur cells are attractive targets for energy storage applications as their theoretical specific energy of 2600 Wh/kg is much greater than the theoretical specific energy of current lithium-ion batteries. Unfortunately, the cycle-life of lithium-sulfur cells is limited due to migration of species generated at the sulfur cathode. These species, collectively known as polysulfides, can transform spontaneously, depending on the environment, and it has thus proven difficult to determine the nature of redox reactions that occur at the sulfur electrode. The project objective is to use X-ray spectroscopy to track species formation and consumption during charge-discharge reactions in a lithium-sulfur cell. Molecular simulations will be used to obtain X-ray spectroscopy signatures of different polysulfide species, and to determine reaction pathways and diffusion in the sulfur cathode. The long-term objective is to use mechanistic information to build high specific energy lithium-sulfur cells.

Project Impact. Enabling rechargeable Li-S cells has potential to change the landscape of rechargeable batteries for large-scale applications beyond personal electronics due to: (1) high specific energy, (2) simplicity and low cost of cathode (the most expensive component of Li-ion batteries), and (3) earth abundance of sulfur. The proposed diagnostic approach also has significant potential impact as it represents a new path for determining the species that form during charge-discharge reactions in a battery electrode.

Approach. Experimental XAS of charging/discharging lithium sulfur batteries will be used to examine battery reaction mechanisms *in situ*. Theoretical XAS calculations and molecular dynamics simulations will be used to provide a molecular level understanding and conclusive interpretation of experimental observations.

Out-Year Goals. The out-year goals are as follows:

- Year 1: Simulations of sulfur and polysulfides (PSL) in oligomeric PEO solvent. Prediction of X-ray spectroscopy signatures of PSL/PEO mixtures. Measurement of X-ray spectroscopy signatures of PSL/PEO mixtures.
- Year 2: Use comparisons between theory and experiment to refine simulation parameters. Determine speciation in PSL/PEO mixtures without resorting to adhoc assumptions.
- Year 3: Build an all-solid lithium-sulfur cell that enables measurement of X-ray spectra *in situ*. Conduct simulations of reduction of sulfur cathode.
- Year 4: Use comparisons between theory and experiment to determine the mechanism of sulfur reduction and Li₂S oxidation in all-solid lithium-sulfur cell. Use this information to build lithium-sulfur cells with improved life-time.

Collaborations. This project collaborates with Tsu-Chien Weng, Dimosthenis Sokaras, and Dennis Nordlund at SSRL, SLAC National Accelerator Laboratory in Stanford, California.

Milestones

1. Establish disproportionation thermodynamics in solvents with high and low electron pair donor (EPD) numbers using theoretical calculations. (December 2015 – Complete)
2. Extend theoretical calculations of XAS to dimethylformamide, a model solvent for high electron pair donor number solvents that stabilize radical polysulfide anions. (February 2016 – Complete)
3. Perform *in situ* XAS tests of Li-S charge/discharge. (May 2016 – On schedule)
4. Vary charge/discharge rate for *in situ* XAS testing; compare reaction pathways. (August 2016 – On schedule)

Progress Report

Ultraviolet-visible (UV-vis) spectroscopy was performed on dimethylformamide (DMF) and tetraethylene glycol dimethyl ether (TEGDME) lithium polysulfide solutions. The results showed that radical polysulfide species are present in both systems. The UV-vis signature of radical species in TEGDME was confirmed to be 617 nm through EPR experiments. This result confirms that radical polysulfide species may exist in Li-S batteries that contain ether-based solvents. The concentration of radical species in TEGDME and DMF was determined using Beer's Law. Concentrations for $\text{Li}_2\text{S}_{x_{\text{mix}}}$, $x_{\text{mix}} = 4, 6, 8$ and 10 at a solution sulfur concentration of 10 mM are shown in Table 1. The concentration of radical species in DMF is an order of magnitude higher in DMF solutions, in agreement with previous thermodynamic calculations.

Table 1. Concentration of lithium polysulfide radical species in DMF versus TEGDME.

$\text{Li}_2\text{S}_{x_{\text{mix}}}$	Sulfur concentration (mM)	Radical concentration (mM)	
		DMF	TEGDME
10	10	0.61	0.05
8		0.91	0.06
6		2.35	0.12
4		2.61	0.25

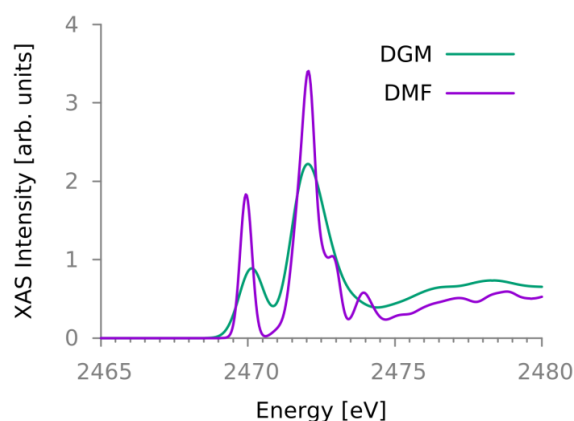
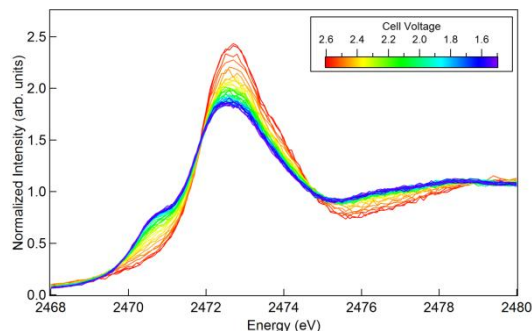
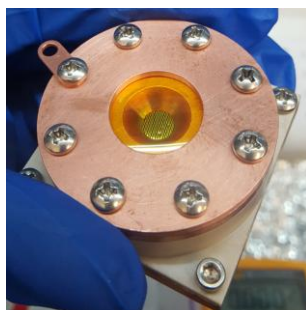


Figure 71. X-ray absorption spectroscopy of Li_2S_4 in DGM and DMF.

The sulfur K-edge X-ray absorption spectra were calculated for lithium polysulfide species in DMF and compared to that obtained for diglyme (DGM). Figure 71 shows the calculated spectrum of Li_2S_4 in DMF and DGM. The spectral features of DMF polysulfides are more distinct than what is obtained for ether-based electrolytes, because there is less structural fluctuation and electronic confinement.

Lastly, a new *in situ* cell was built for XAS experiments that will allow the cathode to be probed during discharge/charge. An image of the cell is shown in Figure 72. The cell was used at SSRL to probe a cathode as discharge took place. The resultant spectra, also shown in Figure 72, are now being interpreted using the theoretically calculated X-ray spectra.

Figure 72. Photograph of *in situ* cell for X-ray absorption spectroscopy experiments (left) and sulfur K-edge XAS taken during discharge of new Li-S cell (right).



Patents/Publications/Presentations

Presentations

- APS Spring Meeting, Baltimore, Maryland (March 2016): “Structure, Spectroscopy, and Thermodynamics at the Carbon-Sulfur Interface”; T. A. Pascal and D. Prendergast.
- 1st International Conference on Hydrophobic Interfaces, King Abdullah University of Science and Technology, Jeddah, Saudi Arabia (February 2016): “Quantum Effects, Structure, and Thermodynamics at the Carbon-Sulfur Interface of Lithium Sulfur Batteries”; T. A. Pascal.

Task 8.3 – Novel Chemistry: Lithium Selenium and Selenium Sulfur Couple (Khalil Amine, Argonne National Laboratory)

Project Objective. The project objective is to develop a novel S_xSe_y cathode material for rechargeable lithium batteries with high energy density and long life, as well as low cost and high safety.

Project Impact. Development of a new battery chemistry is promising to support the goal of PHEV and EV applications.

Approach. The dissolution of lithium polysulfides in nonaqueous electrolytes has been the major contribution to the low energy efficiency and short life of Li/S batteries. In addition, the insulating characteristics of both end members during charge/discharge (S and Li_2S) limit their rate capacity. To overcome this problem, S or Li_2S are generally impregnated in a carbon conducting matrix for better electronic conductivity. However this makes it difficult to increase the loading density of practical electrodes. It is proposed here to solve the above barriers using the following approaches: (1) partially replace S with Se and (2) nano-confine the S_xSe_y in a nanoporous conductive matrix.

Out-Year Goals. When this new cathode is optimized, the following result can be achieved:

- A cell with nominal voltage of 2 V and energy density of 600 Wh/kg.
- A battery capable of operating for 500 cycles with low capacity fade.

Collaborations. This project engages in collaboration with the following:

- Prof. Chunsheng Wang of University of Maryland
- Dr. Yang Ren and Dr. Chengjun Sun of Advanced Photon Source at ANL

Milestones

1. Investigate the phase diagram of S_xSe_y system. (Q1 – Complete)
2. Encapsulating Se_2S_5 in nanoporous carbon. (Q1 – Complete)
3. Investigating the impact of fluorinated solvents. (Ongoing)
4. Stabilizing materials with a higher S content for a higher energy density. (Initiation in Q3)
5. Investigating the impact of the pore structure of carbon matrix. (Initiation in Q4)

Progress Report

Last quarter, the project reported the addition of fluoroether 1,1,2,2-tetrafluoroethyl-2,2,3,3-tetrafluoropropyl ether (TTE) as a co-solvent to improve the reversible specific capacity and the capacity retention as well as Coulombic efficiency during continuous cycling of S_5Se_2/Li cells. To unravel the detailed function mechanism of TTE on the electrochemical performance, synchrotron *in situ*, high-energy X-ray diffraction (HEXRD) and *in situ* nuclear magnetic resonance (NMR) were conducted.

Figure 73 shows the *in situ* HEXRD patterns of S_5Se_2/Li cells during cycling with DME-based (up) and TTE-based electrolytes (down) together with their 1st discharge/charge curve at 0.1 C, respectively. Four discharge plateaus related to the transformation of long-chain polysulfides and polyselenides to short chain polysulfides and polyselenides and further Li_2S and Li_2Se can be seen in the DME-based electrolytes, while only one long plateau was seen in the TTE-based electrolytes, indicating a different reaction pathway. *In situ* HEXRD results indicated that Li_2S and Li_2Se were formed during the discharge process; however, much Li_2S and Li_2Se remained during the charge process in the case of DME-based electrolytes. The formation of Li_2Se and Li_2S was also confirmed in the TTE-based electrolytes, while very little residue of Li_2Se and Li_2S can be seen during the charge process. The information of soluble polysulfides and polyselenides cannot be identified by XRD as most of them are amorphous.

To elucidate the structure and information of both soluble polysulfides or polyselenides and Li_2S and Li_2Se , 7Li NMR studies were further conducted.

Figure 74 shows the *in situ* 7Li NMR study for of S_5Se_2/Li cells during cycling with TTE-based electrolytes. Generally, the sharp peaks at chemical shift about 5 ppm were attributed to soluble polysulfides and polyselenides, lithium salts and $LiNO_3$ additive, while the broad peaks at chemical shift around ± 15 ppm were attributed to solid Li_2S and Li_2Se . As shown in the contour plot (left), the signals of solid Li_2S and Li_2Se were gradually increased upon discharge and largely decreased at the end of charge. However, there is very little peak variation for the polysulfides and polyselenides through the whole charge/discharge process, which can be further seen in the NMR spectra at different charge/discharge states. The results suggested that there may be very little formation of soluble polysulfides and polyselenides during cycling in TTE-based electrolytes, which coincides with their voltage profile and hence results in good cycle stability. *In situ* NMR study for the DME electrolytes is also ongoing to see the information change of soluble polysulfides and polyselenides during cycling.

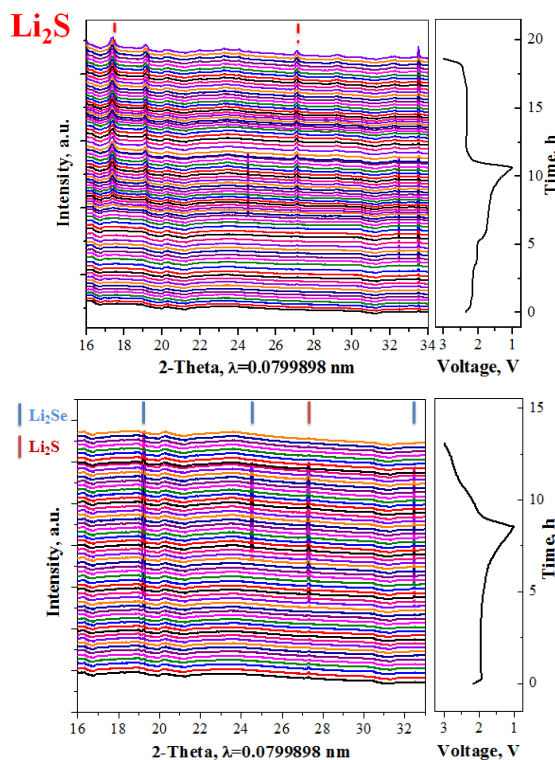


Figure 73. *In situ* high-energy X-ray diffraction study for S_5Se_2/Li cells during cycling with DOL-DME (up) and DOL-TTE (down) electrolytes.

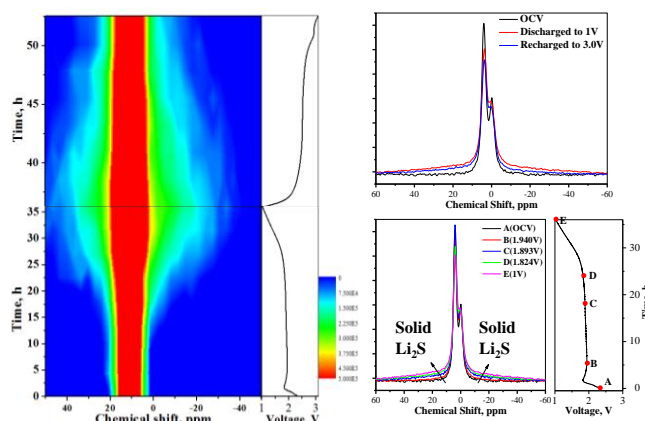


Figure 74. *In situ* 7Li NMR studies for S_5Se_2/Li cell during cycling with DOL-TTE electrolytes.

Patents/Publications/Presentations

Publication

- Xu, G. L., and T. Y. Ma, C. J. Sun, C. Luo, L. Cheng, Y. Ren, S. M. Heald, C. S. Wang, L. Curtiss, J. G. Wen, D. J. Miller, T. Li, X. B. Zuo, V. Petkov, Z. H. Chen and K. Amine. “Insights into the Capacity Fading Mechanism of Amorphous Se₂₅ Confined in the Micro/Mesoporous Carbon Matrix in Ether-based Electrolytes. *Nano Letters* (2016). doi:10.1021/acs.nanolett.6b00318.

Task 8.4 – Multi-Functional Cathode Additives (MFCA) for Li-S Battery Technology (Hong Gan, Brookhaven National Laboratory; and Co-PI Esther Takeuchi, Brookhaven National Laboratory and Stony Brook University)

Project Objective. Develop a low-cost battery technology for PEV application utilizing Li-S electrochemical system by incorporating multifunctional cathode additives (MFCA), consistent with the long-term goals of the DOE EV Everywhere Grand Challenge.

Project Impact. The Li-S battery system has gained significant interest due to its low material cost potential (35% cathode cost reduction over Li-ion) and its attractive 2.8x (volumetric) to 6.4x (gravimetric) higher theoretical energy density compared to conventional Li-ion benchmark systems. Commercialization of this technology requires overcoming several technical challenges. This effort will focus on improving the cathode energy density, power capability, and cycling stability by introducing MFCA. The primary deliverable is to identify and characterize the best MFCA for Li-S cell technology development.

Approach. Transition metal sulfides are evaluated as cathode additives in sulfur cathode due to their high electronic conductivity and chemical compatibility to the sulfur cell system. Electrochemically active additives are also selected for this investigation to further improve energy density of the sulfur cell system. In the first year, the team has established the individual baseline sulfur and transition metal sulfide coin cell performances, and demonstrated the strong interactions between sulfur and various MFCA within the hybrid electrode. TiS_2 and FeS_2 were selected as the leading candidates for additional optimization studies with synthetic method developed. During the second year, leading candidates for the cathode optimization studies will be further narrowed down. More attention will be directed into electrode optimization and cell system optimization for improved electrode integrity, energy density and electrochemical charge/discharge cycling performance. Examples for these efforts include electrode components (binder, carbon), electrode formulation optimization, and electrolyte optimization.

Out-Year Goals. This is a multi-year project comprised of two major phases to be successfully completed in three years. Phase 1 includes cathode and MFCA proof of concept investigations to be mostly completed during year 1 investigations. Phase 2 will include cell component interaction studies and full cell optimization. The work scope for year 2 will focus on the leading MFCA candidate selection, followed by hybrid electrode processing, material and formulation studies for optimized energy density, and cell electrochemical performance testing. The mechanistic studies of MFCA and sulfur interaction will continue throughout the year to advance fundamental understanding of the system.

Collaborations. This project collaborates with Dong Su at BNL, Xiao Tong (BNL), Yu-chen Karen Chen-Wiegart (BNL), Amy Marschilok (SBU), and Kenneth Takeuchi (SBU).

Milestones

1. Synthesized MFCA evaluation and selection. (Q1 – Complete)
2. MFCA particle size effect study and best candidate selection. (Q2 – Complete)
3. Cathode process and material optimization. (Q3 – On schedule)
4. Cathode formulation optimization. (Q4 – On schedule)

Progress Report

Sulfur-FeS₂ interaction. Several issues were uncovered for FeS₂ activation in the hybrid cathode system that resulted in either high cell internal impedance growth (with LiNO₃ in electrolyte) or severe shuttling effect (without LiNO₃ in electrolyte). Without

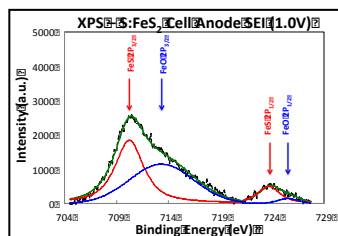


Figure 76. X-ray photoelectron spectroscopy of anode recovered from cycled S:FeS₂ hybrid cell (2.6 V to 1.0 V).

activation, the presence of FeS₂ (either commercial or synthesized) in the sulfur cathode showed no obvious impact on cell cycling performance. This quarter, effort focused on the mechanistic understanding of these observed phenomena. It was found that the severe shuttling effect of the S:FeS₂ hybrid cathode cell system without LiNO₃ electrolyte additive is linked to the dissolution of Fe species. Interestingly more severe dissolution happens for the cells with FeS₂ activation (cycled between 2.6V to 1.0V), as evidenced by the anode discoloration (Figure 75). EDS and XPS prove the existence of Fe on the anode recovered from cycled S:FeS₂ hybrid cathode cell in the



Figure 75. Anode discoloration versus FeS₂ activation.

form of FeS and FeO (Figure 76). Alternative methods to prevent this Fe dissolution induced shuttling effect are needed. Since FeS₂ is not stable after activation, its morphology and particle size effects on sulfur cell performance were not pursued.

Synthesized TiS₂ evaluation. The synthesized TiS₂ sample is a composite mixture of 43.4% Li₂S and 56.6% TiS₂ based on the quantitative analysis of Li and Ti via ICP-OES. This material results in reasonable cycling performance at C/2 rate (Figure 77). Hybrid cathodes with this composite were tested in coin cells in comparison with the sulfur control cells and cells made from hybrid cathode using the commercial TiS₂. Figure 78 shows the first discharge voltage

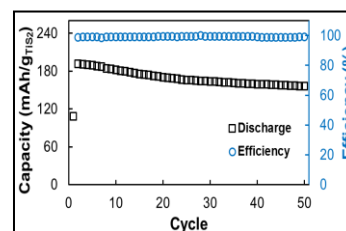


Figure 77. TiS₂/Li₂S composite cell cycling.

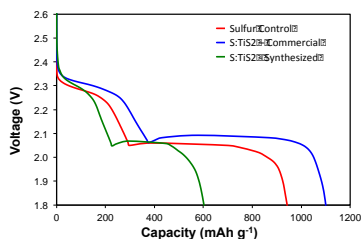


Figure 78. Sulfur utilization – first discharge.

profiles and sulfur utilization of the three cathodes at C/5 rate. Cells containing both types TiS₂ additives exhibited higher initial voltages than the sulfur cells. However, cells with synthesized Li₂S/TiS₂ composite sample exhibited much lower sulfur utilization. This trend also holds during cell cycling at 1C discharge rate. The poor performance of synthesized TiS₂ composite sample is more likely due to the presence of a significant amount of Li₂S, which is non-conductive and introduces more impedance within the hybrid cathode.

Milled commercial TiS₂ additive. Hybrid cathode with milled commercial TiS₂ was tested to confirm the previous finding from the group. Figure 79 shows the hybrid S:TiS₂ electrode cycling test at

1C rate with intermittent C/5 rate discharge at every 51st cycle. The hybrid cell exhibited low capacity fade rate over 500 cycles (0.039% per cycle at 1C) – confirming the beneficial effect of milled TiS₂.

Phase 1 studies have been completed with multiple MFCA evaluations, including CuS, Cu₂S, FeS, FeS₂, CoS₂ and TiS₂. Milled commercial TiS₂ with smaller particle size is identified as the leading MFCA for improved sulfur cell cycle life. Future studies will focus on S:TiS₂ hybrid electrode optimization using commercial TiS₂. Fundamental understanding of sulfur-TiS₂ interaction will continue to aid in the determination of future MFCA research direction.

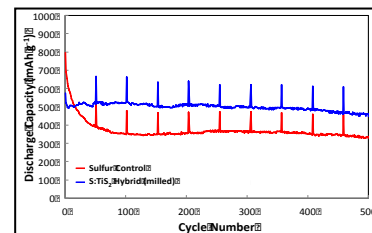


Figure 79. Hybrid S:TiS₂ cycle life study.

Patents/Publications/Presentations

Publication

- He, Kai, and Sen Zhang, Jing Li, Xiqian Yu, Qingping Meng, Yizhou Zhu, Enyuan Hu, Ke Sun, Hongseok Yun, Xiao-Qing Yang, Yimei Zhu, Hong Gan, Yifei Mo, Eric A. Stach, Christopher B. Murray, and Dong Su. “Visualizing Non-equilibrium Lithiation of Spinel Oxide via *in situ* Transmission Electron Microscopy.” Accepted for publication in *Nature Comm.* doi: 10.1038/ncomms11441.

Task 8.5 – Development of High-Energy Lithium-Sulfur Batteries (Jie Xiao and Jun Liu, Pacific Northwest National Laboratory)

Project Objective. The project objective is to develop high-energy, low-cost lithium sulfur (Li-S) batteries with long lifespan. All proposed work will employ thick sulfur cathode (≥ 2 mAh/cm² of sulfur) at a relevant scale for practical applications. The diffusion process of soluble polysulfide out of thick cathode will be revisited to investigate cell failure mechanism at different cycling. Alternative anode will be explored to address the lithium anode issue. The fundamental reaction mechanism of polysulfide under the electrical field will be explored by applying advanced characterization techniques to accelerate development of Li-S battery technology.

Project Impact. The theoretical specific energy of Li-S batteries is ~2300 Wh/kg, which is almost three times higher than that of state-of-the-art Li-ion batteries. The major challenge for Li-S batteries is polysulfide shuttle reactions, which initiate a series of chain reactions that significantly shorten battery life. The proposed work will design novel approaches to enable Li-S battery technology and accelerate market acceptance of long-range EVs required by the EV Everywhere Grand Challenge.

Out-Year Goals. This project has the following out-year goals:

- Fabricate Li-S pouch cells with thick electrodes to understand sulfur chemistry/electrochemistry in the environments similar to the real application.
- Leverage the Li-metal protection project funded by the DOE and PNNL advanced characterization facilities to accelerate development of Li-S battery technology.
- Develop Li-S batteries with a specific energy of 400 Wh/kg at cell level, 1000 deep-discharge cycles, improved abuse tolerance, and less than 20% capacity fade over a 10-year period to accelerate commercialization of electrical vehicles.

Collaborations. This project engages in collaboration with the following:

- Dr. Xiao-Qing Yang (LBNL) – *In situ* characterization
- Dr. Bryant Polzin (ANL) – Electrode fabrication
- Dr. Xingcheng Xiao (GM) – Materials testing
- Dr. Jim De Yoreo (PNNL) – *In situ* characterization

Milestones

1. SEI study on graphite surface in the new EC-free electrolyte. (December 2015 – Complete)
2. Demonstrate prototype Li-ion sulfur cells with > 95% Coulombic efficiency (no additive) and > 80% capacity retention for 100 cycles. (March 2016 – Complete)
3. Identify effective approaches to facilitate electrolyte penetration within thick sulfur cathode (≥ 4 mg/cm²). (June 2016 – In progress)
4. Complete pouch cell assembly and testing by using optimized electrode and electrolyte. (September 2016 – In progress)

Progress Report

Previous study indicated that the corrosion of Li anode is a key degradation mechanism for Li-S batteries, especially for the long-term cycling of thick sulfur cathode. To decouple the influences from Li anode side and study the intrinsic properties of cathode, lithiated graphite (LG) has been used to replace Li anode and to investigate the performance of Li-ion sulfur (LG/S) batteries. However, it is found that LiC_6 is not stable in the conventional 1M LiTFSI/DOL-DME electrolyte. Further investigation indicated that graphite can be cycled stably in the 5M LiTFSI-DOL (M refers to mol salt/liter solvent) electrolyte, which forms a reversible protection layer on graphite during charging process (Li^+ intercalation). These findings enable a platform to study the fundamental properties of sulfur cathode including materials development and mechanism understanding.

This quarter, the electrochemical performance of sulfur battery with lithiated graphite as anode (LG/S full cell) was systematically studied. Promising electrochemical properties are demonstrated from the full cell data in terms of reversible capacity, Coulombic efficiency, and cycling stability. At a low rate of 0.1 C, the LG/S cell exhibits a high capacity of 980 mAh g^{-1} (2 mAh cm^{-2}) with two flat discharge plateaus at 2.2 and 2.0 V, respectively (Figure 80a). In the first charging process, a capacity around 1080 mAh g^{-1} is obtained, delivering a high Coulombic efficiency of 90.7% without LiNO_3 additive in the electrolyte. When the rate is elevated to 0.5 C after 5 cycles at 0.1C, a capacity as high as 815 mAh g^{-1} is delivered. After 100 cycles, a capacity retention of 81.3% can be achieved at 0.5 C with a high Coulombic efficiency of above 97% (Figure 80b). The high performance of LG/S cell is attributed to both bulk and interfacial stability of graphite anode in the concentrated electrolyte. Figure 80c shows smooth surface and well maintained graphite particle after 5 cycles with the electrolyte in Li-graphite half-cell. In addition, the interfacial properties of graphite are studied after being cycled in LG/S full cell. Figure 80d exhibits a cross-sectional image of a single graphite particle by focused ion beam (FIB)-SEM after 100 cycles in sulfur battery. The particle shows a solid dark core with a thin layer of coating outside (ca. 100-200 nm). The EDS analysis (Figure 80e-f) was performed at the very surface and core area of the selected particle. It is clear that the core of graphite is dominated by carbon with a trace amount of oxygen. The surface layer is coated by the byproducts from polysulfide depositions. This means the graphite interface is stable enough to endure the attack from polysulfides and maintains its structural integrity. Therefore, the irreversible loss of polysulfides and SEI accumulation on the anode side are both alleviated, which greatly improves the cycling stability of the Li-ion sulfur cell. The interfacial properties of graphite/electrolyte will be tuned to further suppress the self-discharge of LG/S batteries.

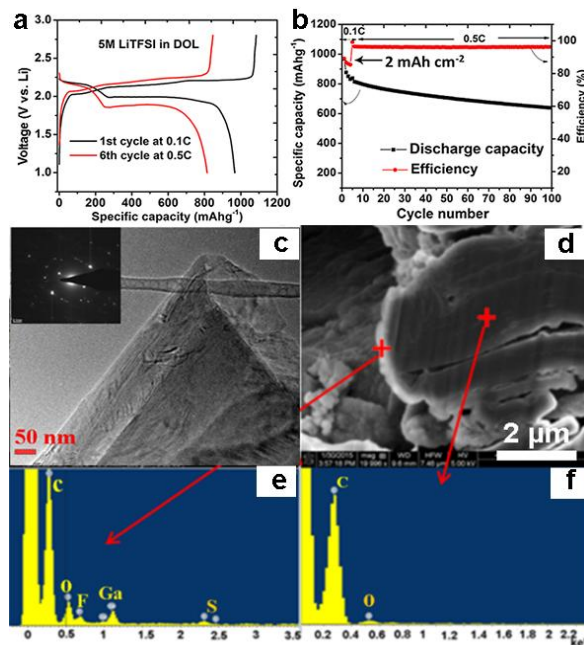


Figure 80. (a) Charge/discharge curves of LG/S full cell in 5 M LiTFSI/DOL electrolyte without LiNO_3 and (b) corresponding cycling stability and Coulombic efficiency. (c) Transmission electron microscopy image of the graphite after five cycles with 5 M LiTFSI/DOL electrolyte in Li-Graphite half-cell and corresponding electron diffraction pattern (insert). (d) Focused ion beam – scanning electron microscopy cross-sectional image of a single graphite particle after 100 cycles with sulfur cathode. (e-f) Point electron diffraction spectroscopy at the very edge and core area of the graphite particle in (d), respectively.

Patents/Publications/Presentations

Publication

- D. Lv, J. Tao, P. Yan, W. A. Henderson, Q. Li, Y. Shao, G. L. Graff, B. Polzin, C. Wang, J. Zhang, J. D. Yoreo, J. Liu, and J. Xiao. “Reversible Shielding of Electrodes.” Submitted for publication.

Task 8.6 – Nanostructured Design of Sulfur Cathodes for High Energy Lithium-Sulfur Batteries (Yi Cui, Stanford University)

Project Objective. The charge capacity limitations of conventional transition metal oxide cathodes are overcome by designing optimized nano-architected sulfur cathodes.

This study aims to enable sulfur cathodes with high capacity and long cycle life by developing sulfur cathodes from the perspective of nanostructured materials design, which will be used to combine with lithium metal anodes to generate high-energy lithium-sulfur batteries. Novel sulfur nanostructures as well as multifunctional coatings will be designed and fabricated to overcome issues related to volume expansion, polysulfide dissolution, and the insulating nature of sulfur.

Project Impact. The capacity and the cycling stability of sulfur cathode will be dramatically increased. This project's success will make lithium-sulfur batteries to power electric vehicles and decrease the high cost of batteries.

Out-Year Goals. The cycle life, capacity retention, and capacity loading of sulfur cathodes will be greatly improved (200 cycles with 80% capacity retention, $>0.3 \text{ mAh/cm}^2$ capacity loading) by optimizing material design, synthesis, and electrode assembly.

Collaborations. This project engages in collaboration with the following:

- BMR program principal investigators
- SLAC: *In situ* X-ray, Dr. Michael Toney
- Stanford: Prof. Nix, mechanics; Prof. Bao, materials

Milestones

1. Demonstrate synthesis to generate monodisperse sulfur nanoparticles with/without hollow space. (October 2013 – Complete)
2. Develop surface coating with one type of polymers and one type of inorganic materials. (January 2014 – Complete)
3. Develop surface coating with several types of polymers; Understand amphiphilic interaction of sulfur and sulfide species. (April 2014 – Complete)
4. Demonstrate sulfur cathodes with 200 cycles with 80% capacity retention and 0.3 mAh/cm^2 capacity loading. (July 2014 – Complete)
5. Demonstrate Li_2S cathodes capped by layered metal disulfides. (December 2014 – Complete)
6. Identify the interaction mechanism between sulfur species and different types of sulfides/oxides/metals, and find the optimal material to improve the capacity and cycling of sulfur cathode. (July 2015 – Complete)
7. Demonstrate the balance of surface adsorption and diffusion of Li_2S_x species on nonconductive metal oxides. (December 15 – Complete)
8. The selection criterion of metal oxide is proposed to guide the rational design of cathode materials for advanced Li-S batteries. (April-2016 – Complete)

Progress Report

Last quarter, the diffusion of lithium on the surface of various metal oxides was investigated by DFT calculation, including $\text{Al}_2\text{O}_3/\text{C}$, CeO_2/C , $\text{La}_2\text{O}_3/\text{C}$, MgO/C , CaO/C composites. Results indicate that an optimized balance between lithium polysulfides adsorption and surface diffusion is favorable for the lithium sulfide species deposition on the surface of oxide/carbon matrix, keeping materials active during the cycling and ensuring the final good cycling performance of batteries. This quarter, results were summarized, and the selection criterion of metal oxide is proposed to guide the rational design of cathode materials for advanced Li-S batteries.

Based on experimental results, three functions of these oxides were clarified (Figure 81). The first basic function of these metal oxides is the polysulfide adsorption. DFT calculation and temperature swing adsorption experiments confirm that the monolayer chemisorption is dominant during the polysulfide capture. The second role of these metal oxides, especially some nonconductive oxides, is the Li_2S_x transfer station, which transports the Li_2S_x from the poorly conductive oxide surface to high conductive carbon matrix to ensure the full electrochemical conversion. The third role is to induce the controlled growth of Li_2S_x species on the surface instead of random deposition. Based on these functions of nonconductive metals oxides, an oxide selection criterion for in Li-S batteries can be proposed. Because the first role of oxides is adsorption, the binding between the sulfides species and the matrix should be strong, which can both suppress the shuttle effect and enable the full utilization of active materials. Considering that the polysulfide capture is the monolayer chemisorption and the adsorption amount will depend on the surface area of oxides, uniformly distributed oxides nanostructures with high surface area are essential. Although strong binding and high surface area are preconditions, the surface diffusion properties of oxides are also very important, which affect the distribution and structure of lithium sulfides. An optimized balance between lithium polysulfides adsorption and surface diffusion is favorable for the lithium sulfide species to deposit on the surface of oxide/carbon matrix, keep active during the cycling and ensure the final good cycling performance of batteries. In addition, some other factors such as electric conductivities, chemical stability, and lithiation/delithiation of the oxides also need to be considered.

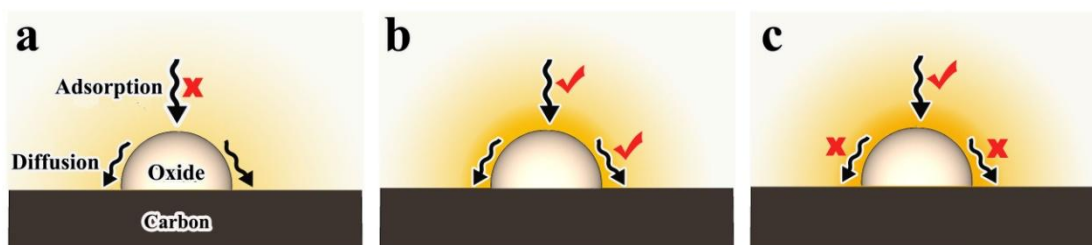


Figure 81. Schematic of the polysulfide adsorption and diffusion on the surface of various nonconductive metal oxides. (a) The metal oxide with weak polysulfide adsorption capability; only few polysulfides can be captured by the oxide. (b) The metal oxide with both strong adsorption and good diffusion, which is favorable for the electrochemical reaction and the controllable deposition of sulfur species. (c) The metal oxide with strong bonding, but without good diffusion; the growth of lithium sulfide and the electrochemical reaction on the oxide/C surface will be impeded.

Patents/Publications/Presentations

Publication

- Tao, Xinyong, and Jianguo Wang, Chong Liu, Haotian Wang, Hongbin Yao, Guangyuan Zheng, Zhi Wei Seh, Qiuxia Cai, Weiyang Li, Guangmin Zhou, Chenxi Zu, and Yi Cui. "Balancing Surface Adsorption and Diffusion of Lithium-polysulfides on Nonconductive Oxides for Lithium-sulfur Battery Design." *Nature Comm.* 7 (2016): 11203.

Task 8.7 – Addressing Internal “Shuttle” Effect: Electrolyte Design and Cathode Morphology Evolution in Li-S Batteries (Perla Balbuena, Texas A&M University)

Project Objective. The project objective is to overcome the lithium-metal anode deterioration issues through advanced Li-anode protection/stabilization strategies including (i) *in situ* chemical formation of a protective passivation layer and (ii) alleviation of the “aggressiveness” of the environment at the anode by minimizing the polysulfide shuttle with advanced cathode structure design.

Project Impact. Through formulation of alternative electrolyte chemistries as well as design, fabrication, and test of improved cathode architectures, it is expected that this project will deliver Li/S cells operating for 500 cycles at efficiency greater than 80%.

Approach. A mesoscale model including different realizations of electrode mesoporous structures generated based on a stochastic reconstruction method will allow virtual screening of the cathode microstructural features and the corresponding effects on electronic/ionic conductivity and morphological evolution. Interfacial reactions at the anode due to the presence of polysulfide species will be characterized with *ab initio* methods. For the cathode interfacial reactions, data and detailed structural and energetic information obtained from atomistic-level studies will be used in a mesoscopic-level analysis. A novel sonochemical fabrication method is expected to generate controlled cathode mesoporous structures that will be tested along with new electrolyte formulations based on the knowledge gained from the mesoscale and atomistic modeling efforts.

Out-Year Goals. By determining reasons for successes or failures of specific electrolyte chemistries, and assessing relative effects of composite cathode microstructure and internal shuttle chemistry versus that of electrolyte chemistry on cell performance, expected results are : (1) develop an improved understanding of the Li/S chemistry and ways to control it; (2) develop electrolyte formulations able to stabilize the Li anode; (3) develop new composite cathode microstructures with enhanced cathode performance; and (4) develop a Li/S cell operating for 500 cycles at an efficiency > 80%.

Collaborations. This is a collaborative work combining first-principles modeling (Perla Balbuena, TAMU), mesoscopic level modelling (Partha Mukherjee, TAMU), and synthesis, fabrication, and test of Li/S materials and cells (Vilas Pol, Purdue University).

Milestones

1. Complete coin cell testing of various C/S electrodes. (December 2015 – Complete)
2. Using electrochemical and transport modeling gain an understanding of the mesoscopic interfacial reactions. (March 2016 – Complete)
3. Complete evaluation of deposition-induced stress and mechanical interplay. (June 2016)
4. Determination of SEI nucleation and growth at the PS/Li anode interface. *Go/No-Go*: Determine reasons for electrolyte failure or success. (September 2016)

Progress Report

Electrochemical Modeling to Understand Mesoscopic Interactions in Li-S Battery. The current study seeks to explore the effect of electrochemical memory in the Li-S battery performance and cycling behavior. The reported meso-/macroscale model has been extended to study the charge-discharge and cycling behavior. Toward the end of discharge of a typical Li-S cell, the electroactive polysulfide ions in the electrolyte are reduced to S^{2-} , which eventually precipitates as Li_2S . Hence, at the start of charging, these solid precipitates need to dissolve to produce S^{2-} ions which can then be electrochemically oxidized. This proves to be quite a stringent criterion for the cell rate capability and cycling behavior. Figure 82 demonstrates that the discharge performance shows significant variation with C-rates, while charging behavior exhibits weak dependence on C-rates. The discharge was stopped at 1000 mAh/g of S_8 to have electroactive polysulfide ions in the electrolyte.

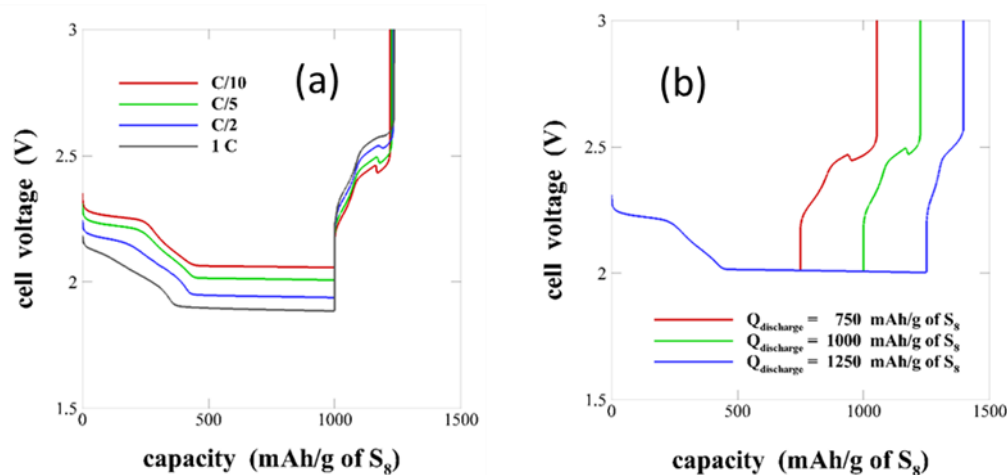


Figure 82. Electrochemical cycling performance and rate capability of Li-S cells. (a) Discharge performance depends strongly on C-rate while charging is weakly independent. (b) Charging behavior depends strongly on the depth of discharge.

If the discharge is carried out further (for example, until full capacity), the electroactive sulfide ions are already sufficiently consumed to begin charging with acceptable overpotential. This fact is more apparent from Figure 82b, where performance predictions are reported for different values of cut-off discharge capacities. The results show that the charging overpotential is less when discharge is partial and also the charging capacity is higher. This interesting electrochemical memory effect is another important aspect of the “shuttle effect.”

Reactivity of the Li anode. Current work focuses on developing an understanding of the effect of high salt molarity on the reactivity of the Li anode. AIMD simulations are being performed in 1M and 4M solutions of two different salts: LiTFSI and LiFSI with DME and DOL solvents and Li_2S_8 molecules (1M). The different reactivities of the salts are characterized in terms of the electron transfer from the surface, and the reaction mechanisms have been identified. It is found that LiFSI decomposes completely in the constituent atoms and much faster than LiTFSI, with the main product being LiF. On the other hand, LiTFSI decomposition products are much larger and remain undecomposed for longer times. Interestingly, highly coordinated networks are found present in the bulk electrolyte, where Li ions are acting as “glue” among several fragments and/or intact molecules of salt, polysulfides, and solvents.

Experimental tests to control PS dissolution at the C/S cathode. The electrochemical cycling performance of three graphene-sulfur composites was tested with different substrates. The highest capacity is shown with the undecorated material; however, there is a significant drop in capacity between cycles 1 and 2. Future work will demonstrate the long-term performance of these materials.

Patents/Publications/Presentations

Publications

- Liu, Z., and D. Hubble, P. B. Balbuena, and P. P. Mukherjee. “Adsorption of Insoluble Polysulfides Li_2S_x ($x = 1, 2$) on Li_2S Surfaces.” *Phys. Chem. Chem. Phys.* 17 (2015): 9032-9039.
- Camacho-Forero, Luis E., and Taylor W. Smith, Samuel Bertolini, and Perla B. Balbuena. “Reactivity at the Lithium-Metal Anode Surface of Lithium-Sulfur Batteries.” *J. Phys. Chem. C* 119, no. 48 (2015): 26828-26839.
- Tsai, C. S. J., and A. D. Dysart, J. H. Beltz, and V. G. Pol. “Identification and Mitigation of Generated Solid By-Products during Advanced Electrode Materials Processing.” *Environ. Sci. Technol.* 50, no. 5 (2016): 2627-2634.
- Dysart, Arthur A., and Juan C. Burgos, Aashutosh Mistry, Chien-Fan Chen, Zhixiao Liu, Perla B. Balbuena, Partha P. Mukherjee, and Vilas G. Pol. “Towards Next Generation Lithium-Sulfur Batteries: Non-Conventional Carbon Compartments/Sulfur Electrodes and Multi-scale Analysis.” *J. Electrochem. Soc.* 163, no. 5 (2016): A730-741.
- Liu, Zhixiao, and Samuel Bertolini, Partha Mukherjee, and Perla B. Balbuena. “ Li_2S Film Formation on Lithium Anode Surface of Li-S batteries.” *ACS Appl. Mat. & Interfaces* 8, no. 7 (2016): 4700-4708.
- Kamphaus, Ethan, and Perla B. Balbuena. “Long-Chain Polysulfide Retention at the Cathode of Li-S Batteries.” *J. Phys. Chem. C* 120, no. 8 (2016): 4296-4305.
- Liu, Zhixiao, and Perla B. Balbuena, and Partha P. Mukherjee. “Evaluating Silicene as a Potential Cathode Host to Immobilize Polysulfides in Lithium-Sulfur Batteries.” *J. Coord. Chem.* In press.

Presentation

- BMR Program Review Meeting, LBNL, Berkeley, California (January 22, 2016): “Addressing Internal ‘Shuttle’ Effect: Electrolyte Design and Cathode Morphology Evolution in Li-S Batteries DE-EE-0006832”; P. B. Balbuena.

Task 8.8 – Mechanistic Investigation for the Rechargeable Li S Batteries (Deyang Qu, University of Wisconsin - Milwaukee; Xiao-Qing Yang, BNL)

Project Objective. The primary objectives are to conduct focused fundamental research on the mechanism for Li-S batteries, investigate the kinetics of the sulfur redox reaction, develop electrolyte and additives to increase the solubility of Li_2S , and optimize the sulfur electrode design. In this objective, special attention will be paid to the investigation of highly soluble polysulfide species including both ions and radicals, and the potential chemical equilibrium among them. Through such investigation, the detail pathway for polysulfide shuttle will be better understood, and alleviation of the obstacle will be explored.

Project Impact. Rechargeable Li-S battery is a potential candidate to meet the demand of high energy density for next generation rechargeable Li battery. Through the fundamental mechanistic investigation, the mechanism of Li-S batteries can be better understood, which will lead to the material design and battery engineering to materialize the potential of Li-S chemistry. Li-S batteries could enable competitive market entry of EVs by reducing the cost and extending the driving distance per charge.

One-Year Goals. The project has the following goals: (1) complete development of an analytical method for the quantitative and qualitative determination of all polysulfide ions in nonaqueous electrolytes, and (2) complete the initial design of an *in situ* electrochemical study for the sulfur reduction reaction.

Collaborations. The principal investigator is the Johnson Control Endowed Chair Professor; the University of Wisconsin Milwaukee and BNL team has close collaboration with Johnson Controls' scientists and engineers. The collaboration enables the team to validate the outcomes of fundamental research in pilot-scale cells. This team has been working closely with top scientists on new material synthesis at ANL, LBNL, and PNNL, with U.S. industrial collaborators at General Motor, Duracell, and Johnson Control, as well as international collaborators in Japan and South Korea. These collaborations will be strengthened and expanded to give this project a vision both on today's state-of-the-art technology and on tomorrow's technology in development, with feedback from the material designer and synthesizers upstream as well as from the industrial end users downstream.

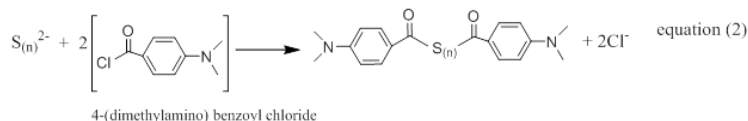
Milestones

1. Complete literature review and feasibility study of the methods for polysulfide determination. (December 2015 – Complete)
2. Complete development of the essay to determine all polysulfide ions. (March 2016 – Complete)
3. Complete design qualification for an *in situ* electrochemical high performance liquid chromatography / mass spectrometry (HPLC-MS) cell for Li-S investigation. (June 2016 – In progress)
4. Complete identification of polysulfide ions formed from elemental sulfur. (September 2016 – In progress)

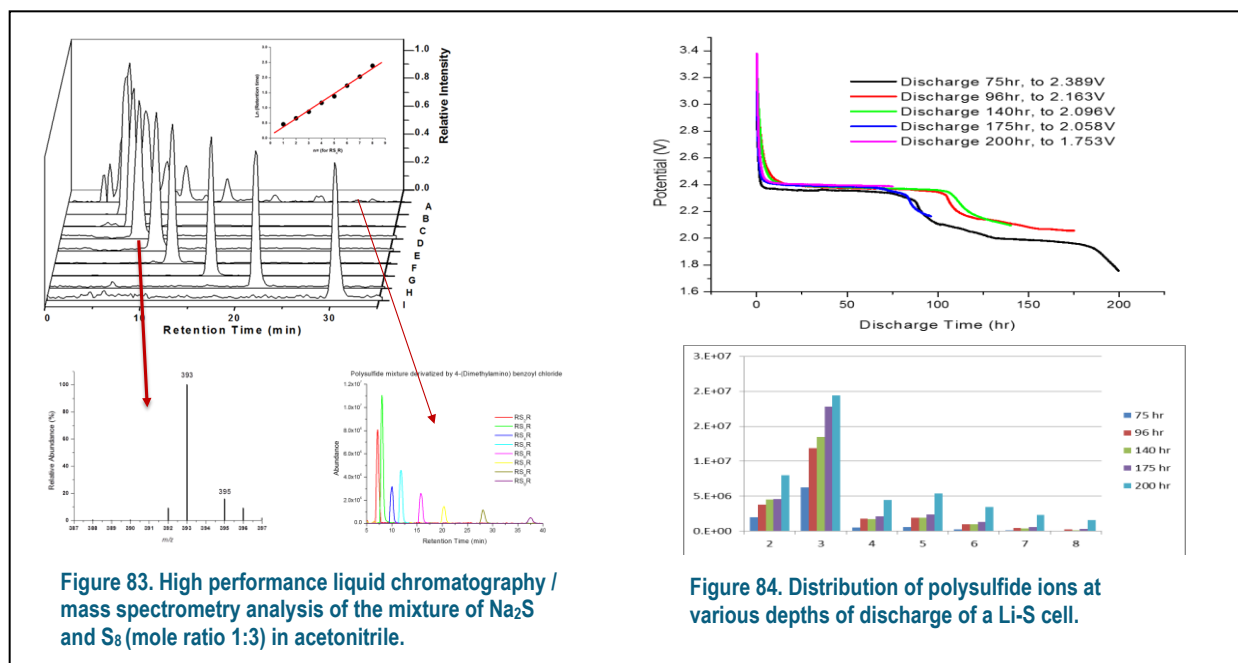
Progress Report

This quarter, a reliable analytical method for quantitative and qualitative analysis of the dissolved elemental sulfur and polysulfides has been developed based on the HPLC / MS technique. The technique is the first (perhaps the only) technique for accurate determination of dissolved polysulfide formed during the discharge and recharge of Li-S batteries.

It has been proven that polysulfide ions by themselves cannot be separated in a HPLC column due to the lack of retention mechanism with the solid phase. The dissolved polysulfide ions have to be derivatized first before being separated in HPLC. Several essays have been developed and tested; one example is shown below:



The derivatized species can be identified by MS according to the mass/charge ratio. Since the formula of each derivatized polysulfide species is known, they can be quantitatively determined. The distribution of all eight polysulfide ions were separated by HPLC and identified by MS successfully after derivatization as shown in Figure 83. The relative abundance can be calculated from the HPLC peak area, and actual concentration can be determined after the measurement of total sulfur content in the electrolyte.



Using the technique, the polysulfide ions formed at the various stage of discharge and recharge of a Li-S battery can be determined. One example is shown in Figure 84. Apparently, most polysulfide ions in the electrolyte at different depths of discharge were short chain polysulfide ions. The mechanism of the sulfur redox reaction can now be investigated more reliably.

Task 8.9 – Statically and Dynamically Stable Lithium Sulfur Batteries (Arumugam Manthiram, U Texas – Austin)

Project Objective. The project objective is to develop statically and dynamically stable lithium-sulfur batteries by integrating polysulfide-filter-coated separators with a protected lithium-metal anode through additives or a modified Li_2S cathode with little or no charge barrier during first charge. The project includes demonstration of electrochemically stable cells with sulfur capacities of $> 1,000 \text{ mA h g}^{-1}$ and cycle life in excess of 500 cycles (dynamic stability) along with positive storage properties (static stability) at $> 70 \text{ wt\%}$ sulfur content and $\sim 5 \text{ mg cm}^{-2}$ loading that will make the Li-S technology superior to the present-day Li-ion technology in terms of cost and cell performance.

Project Impact. The combination of polysulfide-filter-coated separator, lithium-metal-protection additives, and Li_2S cathode modifications offers a viable approach to overcome the persistent problems of Li-S batteries. This project is systematically integrating the basic science understanding gained in its laboratory of these three aspects to develop the Li-S technology as the next-generation power source for EVs. The project targets demonstrating cells with sulfur capacities of over $1,000 \text{ mA h g}^{-1}$ and cycle life in excess of 500 cycles along with good storage properties at high sulfur content and loading that will make the Li-S technology superior to the present-day Li-ion technology in terms of cost and cell performance.

Approach. Electrochemical stability of the Li-S cells is improved by three complementary approaches. (i) The first approach focuses on the establishment of an electrochemically stable cathode environment by employing PS-filter-coated separators. The PS-filter coatings aim to suppress the severe polysulfide diffusion and improve the redox capability of the Li-S cells with high-sulfur loadings. The study includes an understanding of the materials characteristics, fabrication parameters, electrochemical properties, and battery performance of the PS-filter-coated separators. (ii) The second approach focuses on electrode engineering from two aspects. First, the investigation of a Li-metal anode with coating- and additive-supporting approaches is aimed at improving the safety of Li-S cells. Second, the research on activated- Li_2S cathode with little or no charge-barrier will promote the performance and safety of the C- Li_2S cells. (iii) The integration of approaches (i) and (ii) would create statically and dynamically stable Li-S batteries for EVs.

Out-Year Goals. The overall goal is to develop statically and dynamically stable Li-S batteries with custom cathode and stabilized anode active materials. In addition to developing a high-performance battery system, a fundamental understanding of the structure-configuration-performance relationships will be established. Specifically, optimization of the electrochemical and engineering parameters of polysulfide-filter-coated separators aims at comprehensively investigating different coating materials and their corresponding coating techniques for realizing various high-performance custom separators. The developed polysulfide-filter-coated separators can be coupled with pure sulfur cathodes and allow pure sulfur cathodes to attain high sulfur loading and content. Multifunctional polysulfide-filter-coated separators, high-loading sulfur cathodes, stabilized-Li-metal anodes, activated- Li_2S cathodes, and novel approaches on the cell design and optimization are anticipated to provide an in-depth understanding of the full-cell battery chemistry and to realize statically and dynamically stable Li-S batteries for EVs.

Collaborations. This project collaborates with ORNL.

Milestones

1. Database of coating materials and polysulfide-filter coatings established. (December 2015 – Complete)
2. Database of fabrication parameters and S-filter-coated separators established. (March 16 – Complete)
3. Low-capacity fade rate and self-discharge testing completed. (June 2016 – Ongoing)
4. *Go/No-Go*: Lightweight design and electrochemical stability demonstrated. (September 2016 – Ongoing)

Progress Report

This quarter, the physical/chemical characteristics of the coating materials were updated to create a more comprehensive database as compared to that completed under Milestone 1 last quarter. The following were developed: (i) optimal coating methods for the carbon materials with different morphologies, and (ii) advanced polysulfide-filter (PS-filter) coatings with new configurations. These studies complete Milestone 2.

The detailed study of different carbon materials allows one to select and focus on the 12 unique carbon materials with various morphologies and microstructures. The morphological study involves (i) spherical, (ii) fibrous, (iii) tubular, and (iv) flaky carbon materials. The spherical carbon materials in group (i) include both nonporous and porous carbon materials. The porous carbon spheres allow detailed studies on micro-, meso-, and macro-porous structures as well as surface area and pore volume studies for Li-S battery chemistries. On the other hand, the nonporous carbon nanofibers in group (ii) allow the study of the role of coating configuration on the electrochemical performance of Li-S cells by excluding any enhancement in cell performance contributed by high porosity and micropores. To study the morphology and microstructure of different carbon materials toward the Li-S battery chemistries, corresponding fabrication processes were developed to coat these carbon materials onto a Celgard separator as the PS-filter coating. The fabrication processes and optimal coating methods, including the layer-by-layer technique and the carbon-nanotube supporting, are also designed to further improve the electrochemical characteristics of Li-S cells. The database indicating the materials characteristics of the 12 carbon materials and their optimal coating methods are summarized in Tables 2 and 3.

Table 2. Materials chemistry database for group (i) spherical carbons.

(Coating material): coating methods	Carbon sample	Surface area [m ² g ⁻¹]	Pore volume [cm ³ g ⁻¹]	Pore size [nm]	Microporosity	
					Surface area [m ² g ⁻¹]	Pore volume [cm ³ g ⁻¹]
(i-i): T&B, V*	Acetylene Black	82	0.29	14	0	0
(i-i): T&B, V*	Super P Carbon	89	0.44	19	0	0
(i-i): T&B, V*	Carbon Black (Lampblack)	30	0.22	29	0	0
(i-ii): T&B, V*	Carbon Black (Vulcan)	298	1.03	14	85	0.04
(i-ii): T&B, V*	Activated Carbon	732	0.53	3	585	0.31
(i-ii): T&B, V*	Activated Charcoal	1002	0.70	3	754	0.40
(i-ii): T&B, V*	Microporous Carbon	1321	3.62	10	753	0.41
(i-ii): T&B, V*	Ketjen Black	950	2.92	12	58	0.02
Coating materials: (i) spherical carbons: (i-i) nonporous carbon and (i-ii) porous carbon Coating methods: (T) tape-casting, (B) binder-supporting, and (V*) vacuum-filtration process with carbon nanotube (CNT) as the framework						

Table 3. Materials chemistry database for group (ii) – (iv) carbon materials.

(Coating material): coating methods	Carbon sample	Surface area [m ² g ⁻¹]	Pore volume [cm ³ g ⁻¹]	Pore size [nm]	Microporosity	
					Surface area [m ² g ⁻¹]	Pore volume [cm ³ g ⁻¹]
(ii): T&B, V, V&B	CNF	26	0.09	14	0	0
(iii): V	CNT	279	2.48	36	0	0
(iv): T, B, V	R-GO	272	0.57	8	11	0.003
(iv): T, B, V	EO-GO	251	0.43	7	36	0.017
Coating materials: (ii) carbon nanofibers (CNF), (iii) carbon nanotubes (CNT), and (iv) graphene: edge-oxidized graphene oxide (EO-GO) and reduced graphene oxide (R-GO) Coating methods: tape-casting (T), binder-supporting (B), or vacuum-filtration process (V)						

Patents/Publications/Presentations

Presentations

- 2016 Spring Meeting of the Materials Research Society, Phoenix, Arizona (March 28, 2016): “Tutorial on Electrode Materials and Electrolytes for Next Generation Rechargeable Batteries”; A. Manthiram.
- 2016 Energy Week, Austin, Texas (February 16 - 19, 2016): “From Trash to Treasure: Transforming Waste Newspapers into an Interlayer of Lithium-Sulfur Battery for Improving Electrochemical Performance”; C.-H. Chang, S.-H. Chung, and A. Manthiram.
- 2016 Graduate and Industry Networking, Austin, Texas (January 28 – February 2, 2016): “Tandem Pure Sulfur Cathodes for Li-S Batteries with High Areal Capacities”; C.-H. Chang, S.-H. Chung, and A. Manthiram.

TASK 9 – LI-AIR BATTERIES

Summary and Highlights

High-density energy storage systems are critical for EVs required by the EV Everywhere Grand Challenge. Conventional Li-ion batteries still cannot fully satisfy the ever-increasing needs because of their limited energy density, high cost, and safety concerns. As an alternative, the rechargeable Li-O₂ battery has the potential to be used for long-range EVs. The practical energy density of a Li-O₂ battery is expected to be ~ 800 Wh kg⁻¹. The advantages of Li-O₂ batteries come from their open structure; that is, they can absorb the active cathode material (oxygen) from the surrounding environment instead of carrying it within the batteries. However, the open structure of Li-O₂ batteries also leads to several disadvantages. The energy density of Li-O₂ batteries will be much lower if oxygen has to be provided by an onboard container. Although significant progress has been made in recent years on the fundamental properties of Li-O₂ batteries, the research in this field is still in an early stage, and many barriers must be overcome before practical applications. The main barriers include:

- Instability of electrolytes. Superoxide species generated during discharge or O₂ reduction process is highly reactive with electrolyte and other components in the battery. Electrolyte decomposition during charge or O₂ evolution process is also significant due to high over-potentials.
- Instability of air electrode (dominated by carbonaceous materials) and other battery components (such as separators and binders) during charge/discharge processes in an oxygen-rich environment.
- Limited cyclability of the battery associated with instability of the electrolyte and other components of the batteries.
- Low energy efficiency associated with large over-potential and poor cyclability of Li-O₂ batteries.
- Low power rate capability due to electrode blocking by the reaction products.
- Absence of a low-cost, high-efficiency oxygen supply system (such as oxygen selective membrane).

The main goal of the PNNL Task is to provide a better understanding on the fundamental reaction mechanisms of Li-O₂ batteries and identify the required components (especially electrolytes and electrodes) for stable operation of Li-O₂ batteries. The PNNL researchers will investigate stable electrolytes and oxygen evolution reaction (OER) catalysts to reduce the charging overvoltage of Li-O₂ batteries and improve their cycling stability. New electrolytes will be combined with stable air electrodes to ensure their stability during Li-O₂ reaction. Considering the difficulties in maintaining the stability of conventional liquid electrolyte, the Liox team will explore the use of a nonvolatile, inorganic molten salt comprising nitrate anions and operating Li-O₂ cells at elevated temperature (> 80°C). It is expected that these Li-O₂ cells will have a long cycle life, low over potential, and improved robustness under ambient air compared to current Li-air batteries. At ANL, new cathode materials and electrolytes for lithium-air batteries will be developed for Li-O₂ batteries with long cycle life, high capacity, and high efficiency. The state-of-the-art characterization techniques and computational methodologies will be used to understand the charge and discharge chemistries. The University of Massachusetts/BNL team will investigate the root causes of the major obstacles of the air cathode in the Li-air batteries. Special attention will be paid to optimizing high surface carbon material used in the gas diffusion electrode, catalysts, electrolyte, and additives stable in Li-air system and with capability to dissolve Li oxide and peroxide. Success of this project will establish a solid foundation for further development of Li-O₂ batteries toward practical applications for long-range EVs. The fundamental understanding and breakthrough in Li-O₂ batteries may also provide insight on improving the performance of Li-S batteries and other energy storage systems based on chemical conversion processes.

Highlight. Amine et al. of the ANL team reported that crystalline LiO₂ can be stabilized in a Li-O₂ battery by using a suitable graphene-based cathode. They anticipate that this discovery will lead to methods of synthesizing and stabilizing LiO₂, which could open the way to high-energy-density batteries based on LiO₂ as well as to other possible uses of this compound, such as oxygen storage.

Task 9.1 – Rechargeable Lithium-Air Batteries (Ji-Guang Zhang and Wu Xu, PNNL)

Project Objective. The project objective is to develop stable electrolyte and air electrode to reduce the charging overvoltage and improve the cycling stability of rechargeable lithium-oxygen (Li-O₂) batteries. New air electrode will be synthesized to improve the capacity and cycling stability of Li-O₂ batteries. New electrolytes will be investigated to ensure their stability during Li-O₂ reaction.

Project Impact. Li-air batteries have a theoretical specific energy that is more than five times that of state-of-the-art Li-ion batteries and are potential candidates for use in next-generation, long-range EVs. Unfortunately, the poor cycling stability and low CE of Li-air batteries have prevented practical application to date. This work will explore a new electrolyte and electrode that could lead to long cyclability and high Coulombic efficiency in Li-air batteries that can be used in the next generation EVs required by the EV Everywhere Grand Challenge.

Out-Year Goals. The long-term goal of the proposed work is to enable rechargeable Li-air batteries with a specific energy of 800 Wh/kg at cell level, 1000 deep-discharge cycles, improved abuse tolerance, and less than 20% capacity fade over a 10-year period to accelerate commercialization of long-range EVs.

Collaborations. This project engages in collaboration with the following:

- Chunmei Ben (NREL) – Metal oxide coated glassy carbon electrode
- Chongmin Wang (PNNL) – Characterization of cycled air electrodes by TEM/SEM

Milestones

1. Synthesize and characterize the modified solvent and the transition metal oxide catalyst coated carbon material. (December 2015 – Complete)
2. Identify a modified carbon air electrode that is stable in a Li-O₂ battery by using conventional glyme solvent. (June 2016 – Ongoing)
3. Demonstrate stable operation of Li-O₂ battery by employing the new electrolyte and modified air electrode. (September 2016 – Ongoing)

Progress Report

This quarter, the effect of the concentration of $\text{LiN}(\text{SO}_2\text{CF}_3)_2$ -dimethyl sulfoxide (LiTFSI-DMSO) electrolytes on the cycling performance of Li- O_2 batteries has been investigated using CNTs/PVDF/carbon-paper as the air electrodes. Three LiTFSI/DMSO mole ratios of 1:12 (1.0 M), 1:4, and 1:3 were used to make the electrolytes. The cycling capacity was limited to 600 mAh g^{-1} during these tests. As shown in Figure 85, the LiTFSI-3DMSO electrolyte leads to stable cycling for at least 90 cycles. The stable cycling behavior can be attributed to the lack of free DMSO solvent molecules in this highly concentrated electrolyte. The optimized air electrode preparation process also further enhanced the cell performance. With a decrease in salt concentration, the cycling stability of the Li- O_2 cells deteriorates. Computational calculations show that the Gibbs activation energy barriers for C-H bond scission in DMSO, $\text{Li}^+(\text{DMSO})_4$, and $\text{TFSI}^-\text{Li}^+(\text{DMSO})_3$ by the attack of $\text{O}_2^{\bullet-}$ are 192, 210, and 216 kJ mol^{-1} , respectively, indicating that the free DMSO solvent is not stable against $\text{O}_2^{\bullet-}$, but the DMSO in solvates or complexes is greatly stabilized.

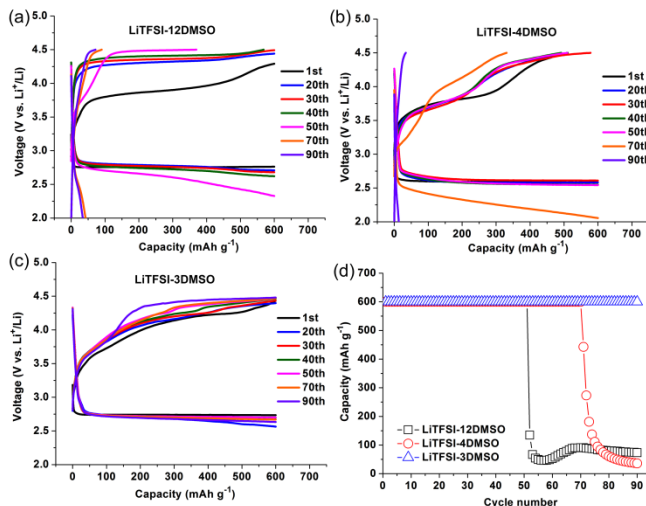


Figure 85. Voltage profiles of carbon nanotube electrodes with LiTFSI-12DMSO electrolyte (a), LiTFSI-4DMSO electrolyte (b), and LiTFSI-3DMSO electrolyte (c), and their cycling performance at 0.1 mA cm^{-2} (d).

The air electrodes and Li metal anodes from cycled cells were analyzed after cleaning. Figures 86 and 87 show that the LiTFSI-3DMSO leads to well protected CNT-electrode and Li metal anode, while the other two electrolytes result in thick deposits on the air electrode and more extensive corrosion of the Li anode; these effects are due to the decomposition of free DMSO by the attack of $\text{O}_2^{\bullet-}$ and the reaction of free DMSO with Li metal, respectively.

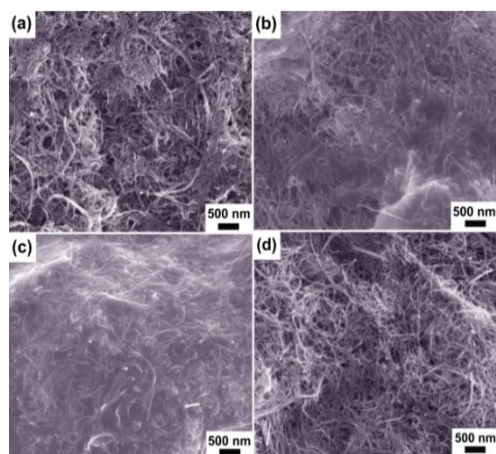


Figure 86. Scanning electron microscopy images of carbon nanotube based electrodes in charged state after 90 discharge/charge cycles with LiTFSI-3DMSO (a), LiTFSI-4DMSO (b), and LiTFSI-12DMSO (c), as well as the pristine carbon nanotube electrode without cycling (d).

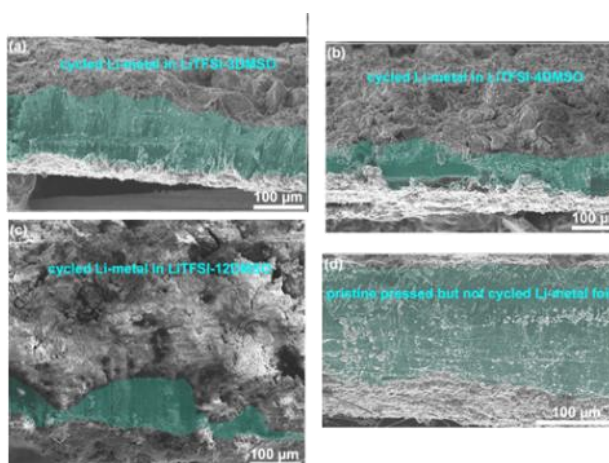


Figure 87. Cross-sectional scanning electron microscopy images of Li metal anodes in charged state after 90 discharge/charge cycles with LiTFSI-3DMSO (a), LiTFSI-4DMSO (b), and LiTFSI-12DMSO (c), as well as the pristine Li metal electrode without cycling (d).

Patents/Publications/Presentations**Publications**

- Liu, B., and W. Xu,* P. Yan, X. Sun, M. E. Bowden, J. Read, J. Qian, D. Mei, C.-M. Wang, J.-G. Zhang.* “Enhanced Cycling Stability of Rechargeable Li-O₂ Batteries Using High-Concentration Electrolytes.” *Adv. Funct. Mater.* 26 (2016): 605-613.
- Liu, B., and P. Yan, W. Xu,* J. Zheng, Y. He, L. Luo, C.-M. Wang,* and J.-G. Zhang.* “Electrochemically Formed Ultrafine Metal Oxide Nano-Catalysts for High-Performance Lithium-oxygen Batteries.” Submitted for publication.

Task 9.2 – Efficient Rechargeable Li/O₂ Batteries Utilizing Stable Inorganic Molten Salt Electrolytes (Vincent Giordani, Liox)

Project Objective. The project objective is to develop high specific energy, rechargeable Li-air batteries having lower overpotential and improved robustness under ambient air compared to current Li-air batteries. The technical approach involves replacing traditional organic and aqueous electrolytes with a nonvolatile, inorganic molten salt comprising nitrate anions and operating the cell at elevated temperature (> 80°C). The research methodology includes powerful *in situ* spectroscopic techniques coupled to electrochemical measurements (for example, electrochemical MS) designed to provide quantitative information about the nature of chemical and electrochemical reactions occurring in the air electrode.

Project Impact. If successful, this project will solve particularly intractable problems relating to air electrode efficiency, stability, and tolerance to the ambient environment. Furthermore, these solutions may translate into reduced complexity in the design of a Li-air stack and system, which in turn may improve prospects for use of Li-air batteries in EVs. Additionally, the project will provide materials and technical concepts relevant for developing other medium temperature molten salt Li battery systems of high specific energy, which may also have attractive features for EVs.

Out-Year Goals. The long-term goal is to develop Li-air batteries comprising inorganic molten salt electrolytes and protected Li anodes that demonstrate high (> 500 Wh/kg) specific energy and efficient cyclability in ambient air. By the end of the project, it is anticipated that problems hindering use of both the Li anode and air electrode will be overcome due to materials advances and strategies enabled within the intermediate (> 80°C) operating temperature range of the system under development.

Collaborations. This project engages in collaboration with the following:

- Bryan McCloskey (LBNL): Analysis of air electrode and electrolyte
- Julia Greer (Caltech): Design of air electrode materials and structures

Milestones

1. Quantify e^-/O_2 and oxygen evolution reaction / oxygen reduction reaction (OER/ORR) ratio for metals and metal alloys in half cells under pure O₂. (December 2015 – Complete)
2. Determine the kinetics and mechanisms of electrochemical nitrate reduction in the presence of O₂, H₂O, and CO₂. (March 2016 – Complete)
3. Synthesize electronically conductive ceramics and cermets. (March 2016 – Complete)
4. Quantify e^-/O_2 and OER/ORR ratio for electronically conductive ceramics and cermets in half cells under pure O₂. (June 2016 – Ongoing)
5. Demonstrate $e^-/\text{O}_2=2$ and OER/ORR ratio=1, +/- 5% and correcting for the effect of Li₂O₂ crossover. (June 2016 – Ongoing)
6. Demonstrate Li₂O yield=1, $e^-/\text{O}_2=4$ and OER/ORR ratio=1, +/- 5%. (September 2016 – Ongoing)
7. Demonstrate discharge specific power and power density ≥ 800 W/kg and ≥ 1600 W/L, respectively, based on air electrode mass and volume. (September 2016 – Ongoing)
8. Demonstrate solid electrolytes that are stable to molten nitrate electrolytes over a temperature range of 100°C to 150°C for 6 months or greater. (September 2016 – Ongoing)

Progress Report

The kinetics parameters such as exchange current density j_0 and Tafel slope for the electroreduction of NO_3^- have determined at a glassy carbon rotating disk electrode, in the presence of O_2 , water, and CO_2 . The following cell reaction (1) $2\text{Li} + (\text{Li/K})\text{NO}_3 \rightleftharpoons \text{Li}_2\text{O} + (\text{Li/K})\text{NO}_2$ has an equilibrium potential $E^0 = 2.43 \text{ V}$ and a specific capacity of 612 mAh per gram of eutectic $(\text{Li/K})\text{NO}_3$. Practical discharge capacities are limited by the amount of solid Li_2O the positive electrode can accommodate within its porous volume, typically around 15 mAh at 0.1 mA discharge current, for 0.01 g of cathode material (that is, 1500 mAh/g_{cathode}). While the main challenge for Li/O_2 chemistry is to develop chemically stable air cathodes, understanding the reversibility of the nitrate reduction reaction (Figure 88) could enable a “condensed-phase” electrochemical system where O_2 is drawn directly from the electrolyte material and not the environment, provided one can make such electrochemical process kinetically reversible.

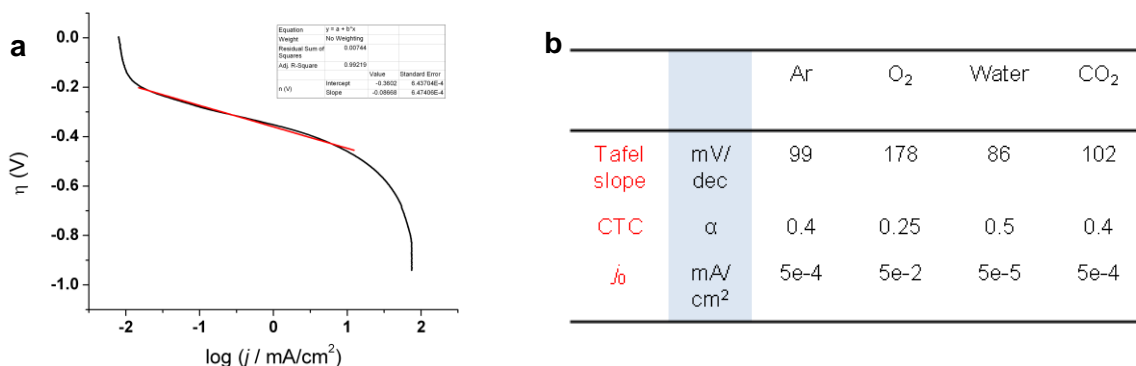


Figure 88. (a) Tafel plot for NO_3^- electroreduction at glassy carbon rotating disk electrode (GC RDE) ($A = 0.196 \text{ cm}^2$) at 150°C . (b) Tafel slope, charge transfer coefficient α , exchange current density j_0 for NO_3^- reduction reaction ($\text{NO}_3^- + 2\text{e}^- = \text{NO}_2^- + \text{O}_2$) at a GC RDE, under several different conditions.

The second milestone consisted in preparing electronically conducting ceramics and cermets. Li-doped NiO is used as ORR cathode material in high temperature molten carbonate fuel cells given its good oxidative stability and electrical conductivity. Nickel oxides were prepared following two different procedures. (1) Li-doped NiO was synthesized from mixing LiOH and nanopowder $\text{Ni}(\text{OH})_2$ in H_2O /isopropanol, then dried at 70°C on a hot plate. The mix was subsequently annealed at 500°C for 3 h to enhance crystallinity. Li doping level was 10% by stoichiometry; BET (Brunauer–Emmett–Teller) surface area (N_2 adsorption) was found to be $18 \text{ m}^2/\text{g}$. (2) NiO/Graphene hybrid material was prepared as follows: 15 mL of graphene oxide suspension (3 mg/mL) in H_2O was dissolved in 45 mL of deionized water (DI). To this solution was added 10 mL of 50 mM $\text{Ni}(\text{NO}_3)_2 \cdot 6\text{H}_2\text{O}$ aqueous solution drop by drop. The solution was stirred for 30 min. The pH of the solution was adjusted to 8.0 by adding 1 M NH_4HCO_3 solution. The reaction mixture was stirred at room temperature for 18 h. The precipitate was obtained by vacuum filtration, washed with EtOH and DI water three times, respectively. The precipitate was dried at 80°C overnight. The hybrid NiO/Graphene was produced by pyrolysis of the precursor at 400°C for 4 h in an argon atmosphere. BET surface area was $125 \text{ m}^2/\text{g}$. Electrochemical testing in molten nitrate Li/O_2 cells is in progress.

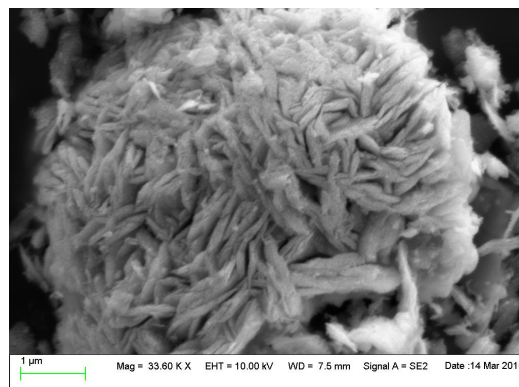


Figure 89. Scanning electron microscopy image of as prepared Li-doped NiO nanorods used as oxygen reduction reaction cathode in molten nitrate O_2 cells.

Patents/Publications/Presentations

Publication

- Giordani, Vincent, and Dylan Tozier, Hongjin Tan, Colin Burke, Betar Gallant, Jasim Uddin, Julia Greer, Bryan McCloskey, Gregory Chase, and Addison. "A Molten Salt Lithium-Oxygen Battery." *J. Am. Chem. Soc.* 138, no. 8 (2016): 2656–2663.

Task 9.3 – Li-Air Batteries (Khalil Amine, ANL)

Project Objective. This project will develop new cathode materials and electrolytes for lithium-air batteries for long cycle life, high capacity, and high efficiency. The goal is to obtain critical insight that will provide information on the charge and discharge processes in lithium-air batteries to enable new advances to be made in their performance. This will be done using state-of-the-art characterization techniques combined with state-of-the-art computational methodologies to understand and design new materials and electrolytes for lithium-air batteries.

Project Impact. The instability of current nonaqueous electrolytes and degradation of cathode materials limits the performance of lithium air batteries. The project impact will be to develop new electrolytes and cathode materials that are stable and can increase cycle life and improve efficiency of lithium-air batteries.

Approach. The project is using a joint theoretical/experimental approach for design and discovery of new cathode and electrolyte materials that act synergistically to reduce charge overpotentials and increase cycle life. Synthesis methods, in combination with design principles developed from computations, are used to make new cathode architectures. Computational studies are used to help understand decomposition mechanisms of electrolytes and how to design electrolytes with improved stability. The new cathodes and electrolytes are tested in Li-O₂ cells. Characterization along with theory is used to understand the performance of the materials used in the cell and make improved materials.

Out-Year Goals. The out-year goals are to find catalysts that promote discharge product morphologies that reduce charge potentials and find electrolytes for long cycle life through testing and design.

Collaborations. This project engages in collaboration with Professor Amin Salehi (University of Illinois-Chicago), Professor Yang-Kook Sun (Hanyang University), Professor Yiying Wu (Ohio State University), and Dr. Dengyun Zhai (China).

Milestones

1. Development of new cathode materials based on Pd nanoparticles and ZnO coated carbon that can improve efficiency of Li-O₂ batteries through control of morphology and oxygen evolution catalysis. (December 2015 – Complete)
2. Investigation of catalyst to control the lithium superoxide content of discharge products of Li-O₂ batteries to help improve efficiency and cycling. (March 2016 – Ongoing)
3. Investigations of mixed K/Li salts and salt concentration on the performance of Li-O₂ batteries with goal of increasing cycle life. (June 2016 – Ongoing)
4. Computational studies of electrolyte stability with respect to superoxide species and salt concentrations for understanding and guiding experiment. (September 2016 – Initiated)

Progress Report

Two cathode materials were studied: one based on rGO and the other based on rGO with added Ir nanoparticles. Initially graphene oxide (GO) was prepared by a modified Hummer's method. The Ir-rGO composite was then made by a hydrothermal reduction method and characterized. SEM images of the pristine rGO and Ir-rGO composite reveal porous 3D networks of rGO composed of wrinkled 2D rGO sheets. TEM image of the Ir nanoparticles on rGO is shown in Figure 90 and indicate that the well-dispersed Ir nanoparticles decorated on rGO are very small (< 2 nm) with evidence for the presence of some small Ir clusters. A backscattering image shows some scattered larger Ir particles of about 500 nm in size, which may be due to agglomeration of the smaller nanoparticles, and Fast Fourier Transform analysis of HR-TEM images show that the nanoparticles are Ir. An XPS analysis indicates the Ir surface is only partially oxidized.

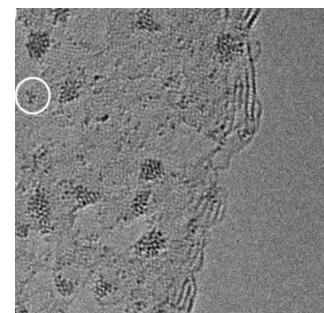


Figure 90. TEM Image of Ir nanoparticles on an rGO surface. Scale bar is 2 nm.

The performance of the rGO and Ir-rGO cathodes was examined using a Swagelok-type cell composed of a lithium metal anode, electrolyte 1M LiCF_3SO_3 in TEGDME impregnated into a glass fiber separator, and a porous cathode. A current density of 100 mA/g is used for both discharge and charge, and the cell was run under time control (capacity of 1000 mAh/g). Figure 91a-b shows voltage profiles for the Ir-rGO and rGO cathode architectures, respectively. The Ir-rGO discharge product shows a very low charge potential of ~ 3.2 V that rises to 3.5 V over 40 cycles leading to over 85% efficiency in this system. The voltage profile of the rGO cathode shows a much larger charge potential of ~ 4.2 V with lower efficiency of $\sim 67\%$.

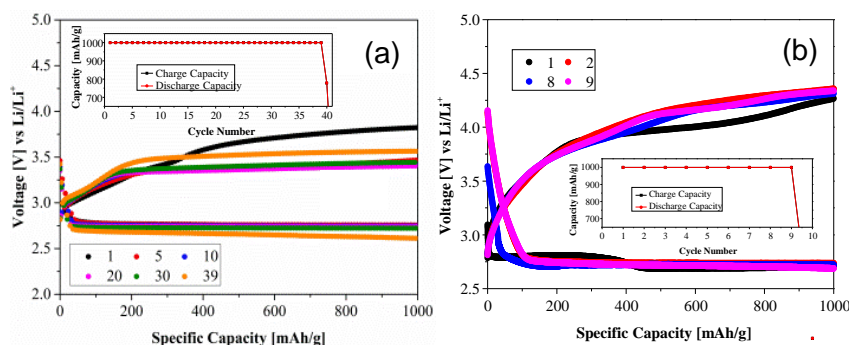


Figure 91. Voltage profiles for (a) Infrared-reduced graphene oxide and (b) reduced graphene oxide cathode materials.

identification of the LiO_2 peaks is based on a theoretical XRD pattern derived from our DFT predicted crystalline LiO_2 structure since no experimental XRD pattern has been reported. The LiO_2 structure is orthorhombic. For comparison, NaO_2 is cubic at room temperature and orthorhombic at < 196 K, while KO_2 is tetragonal at room temperature. Some amorphous LiO_2 cannot be ruled out on the basis of the XRD results. The standard Li_2O_2 XRD pattern was used to determine the absence of Li_2O_2 . Further evidence for the presence of LiO_2 was obtained from Raman, EPR, and differential electrochemical mass spectrometry (DEMS) measurements.

The work has shown for the first time that crystalline LiO_2 can be stabilized in a Li- O_2 battery by using a suitable cathode material, with no evidence for the presence of Li_2O_2 from various characterization techniques. Our results demonstrate that the LiO_2 formed in the Li- O_2 battery is stable enough that it can be repeatedly charged and discharged with a very low charge potential (~ 3.2 V). This can open the avenue for high-energy density lithium superoxide-based batteries as well as other potential uses such as a source of oxygen storage.

Patents/Publications/Presentations**Publication**

- Lu, J., and Y. J. Lee, X. Luo, K. C. Lau, M. Asadi, H.-H. Wang, S. Brombosz, J. G. Wen, D. Zhai, Z. Chen, D. J. Miller, Y. S. Jeong, J.-B. Park, Z. Z. Fang, B. Kumar, A. Salehi-Khojin, Y.-K. Sun, L. A. Curtiss, K. Amine. *Nature* 529 (2016): 377.

Presentations

- Austin Symposium, Dallas, Texas (March 5-7, 2016): “Insight into the Role of Lithium Superoxide in Li-O₂ Electrochemistry from Spectroscopic Studies”; L. A. Curtiss.

TASK 10 – NA-ION BATTERIES

Summary and Highlights

To meet the challenges of powering the PHEV, the next generation of rechargeable battery systems with higher energy and power density, lower cost, better safety characteristics, and longer calendar and cycle life (beyond lithium-ion batteries, which represent today's state-of-the-art technology) must be developed. Recently, Na-ion battery systems have attracted increasing attention due to the more abundant and less expensive nature of the Na resource. The issue is not insufficient lithium on a global scale, but what fraction can be used in an economically effective manner. Most untapped lithium reserves occur in remote or politically sensitive areas. Scale-up will require a long lead time, involve heavy capital investment in mining, and may require the extraction and processing of lower quality resources, which could drive extraction costs higher. Currently, high costs remain a critical barrier to the widespread scale-up of battery energy storage. Recent computational studies on voltage, stability, and diffusion barriers of Na-ion and Li-ion materials indicate that Na-ion systems can be competitive with Li-ion systems.

The primary barriers and limitations of current state-of-the-art of Na-ion systems are as follows:

- Building a sodium battery requires redesigning battery technology to accommodate the chemical reactivity and larger size of sodium ions.
- Lithium batteries pack more energy than sodium batteries per unit mass. Therefore, for sodium batteries to reach energy densities similar to lithium batteries, the positive electrodes in the sodium battery need to hold more ions.
- Since Na-ion batteries are an emerging technology, new materials to enable Na electrochemistry and the discovery of new redox couples along with the diagnostic studies of these new materials and redox couples are quite important.
- In sodium electrochemical systems, the greatest technical hurdles to overcome are the lack of high-performance electrode and electrolyte materials that are easy to synthesize, safe, and non-toxic, with long calendar and cycling life and low cost.
- Furthermore, fundamental scientific questions need to be elucidated, including (1) the difference in transport and kinetic behaviors between Na and Li in analogous electrodes; (2) Na insertion/extraction mechanism; (3) SEI layer on the electrodes from different electrolyte systems; and (4) charge transfer in the electrolyte–electrode interface and Na⁺ ion transport through the SEI layer.

This task will use the synchrotron based *in situ* X-ray techniques and other diagnostic tools to evaluate new materials and redox couples, to explore fundamental understanding of the mechanisms governing the performance of these materials and provide guidance for new material developments. This task will also be focused on developing advanced diagnostic characterization techniques to investigate these issues, providing solutions and guidance for the problems. The synchrotron based *in situ* X-ray techniques (XRD and hard and soft XAS) will be combined with other imaging and spectroscopic tools such as HRTEM, MS, and TXM.

Task 10.1 – Exploratory Studies of Novel Sodium-Ion Battery Systems (Xiao-Qing Yang and Xiqian Yu, Brookhaven National Laboratory)

Project Objective. The primary objective is to develop new advanced *in situ* material characterization techniques and to apply these techniques to explore the potentials, challenges, and feasibility of new rechargeable battery systems beyond the Li-ion batteries, namely the sodium-ion battery systems for PHEVs. To meet the challenges of powering the PHEV, new rechargeable battery systems with high energy and power density, low cost, good abuse tolerance, and long calendar and cycle life must be developed. This project will use the synchrotron based *in situ* X-ray diagnostic tools developed at BNL to evaluate the new materials and redox couples, exploring the fundamental understanding of the mechanisms governing the performance of these materials.

Project Impact. The VTO Multi Year Program Plan describes the goals for battery: “Specifically, lower-cost, abuse-tolerant batteries with higher energy density, higher power, better low-temperature operation, and longer lifetimes are needed for the development of the next-generation of HEVs, PHEVs, and EVs.” If this project succeeds, the knowledge gained from diagnostic studies and collaborations with U.S. industries and international research institutions will help U.S. industries develop new materials and processes for a new generation of rechargeable battery systems beyond Li-ion batteries, such as Na-ion battery systems in their efforts to reach these VTO goals.

Approach. This project will use the synchrotron based *in situ* X-ray diagnostic tools developed at BNL to evaluate the new materials and redox couples to enable a fundamental understanding of the mechanisms governing the performance of these materials and to provide guidance for new material and new technology development regarding Na-ion battery systems.

Out-Year Goals. Complete the *in situ* XRD and absorption studies of tunnel structured $\text{Na}_{0.66}[\text{Mn}_{0.66}\text{Ti}_{0.34}]\text{O}_2$ with high capacity and $\text{Na}(\text{NiCoFeTi})_{1/4}\text{O}_2$ with high rate and long cycle life capability as cathode materials for Na-ion batteries during charge-discharge cycling.

Collaborations. The BNL team has been working closely with top scientists on new material synthesis at ANL, LBNL, and PNNL, with U.S. industrial collaborators at General Motors, Duracell, and Johnson Control, and with international collaborators.

Milestones

1. Complete the synchrotron-based *in situ* XRD studies of tunnel structured $\text{Na}_{0.44}[\text{Mn}_{0.44}\text{Ti}_{0.56}]\text{O}_2$ as cathode material for Na-ion batteries during charge-discharge cycling. (December 2015 – Complete)
2. Complete *in situ* XRD of the $\text{Na}_{0.66}[\text{Mn}_{0.66}\text{Ti}_{0.34}]\text{O}_2$ high-capacity cathode material for Na-ion half-cell during discharge/charge cycling in a voltage range between 1.5 V and 3.9 V. (March 2016 – Complete)
3. Complete the synchrotron based XANES studies of $\text{Na}(\text{NiCoFeTi})_{1/4}\text{O}_2$ at Ni, Co, Fe, and Ti K-edge as cathode material for Na-ion batteries during charge-discharge cycling. (June 2016 – In Progress)
4. Complete the synchrotron based *in situ* XRD studies of $\text{Na}(\text{NiCoFeTi})_{1/4}\text{O}_2$ as cathode material for Na-ion batteries during charge-discharge cycling (December 2016 – In Progress)

Progress Report

This quarter, the second milestones were completed. BNL has focused on the studies of a new novel sodium rich tunnel-type positive material with a nominal composition of $\text{Na}_{0.66}[\text{Mn}_{0.66}\text{Ti}_{0.34}]\text{O}_2$. When cycled as positive electrode in full cells using $\text{NaTi}_2(\text{PO}_4)_3/\text{C}$ as negative electrode in 1M Na_2SO_4 aqueous electrolyte, this material shows the highest capacity of 76 mAh g^{-1} among the Na insertion oxides with an average operating voltage of 1.2 V at a current rate of 2C. These results demonstrate that $\text{Na}_{0.66}[\text{Mn}_{0.66}\text{Ti}_{0.34}]\text{O}_2$ is a promising positive electrode material for rechargeable aqueous Na-ion batteries. To further understand the structural changes in $\text{Na}_{0.66}[\text{Mn}_{0.66}\text{Ti}_{0.34}]\text{O}_2$ during Na extraction and insertion, *in situ* XRD experiment was performed on a $\text{Na}_{0.66}[\text{Mn}_{0.66}\text{Ti}_{0.34}]\text{O}_2/\text{Na}$ half-cell in a wide voltage range of 1.5-3.9 V, and the results are presented in Figure 92. Most of the XRD reflections [for example, (040), (210), (140), (201)] display continuous peak shift during Na extraction/insertion. There is no evident appearance of a new phase formation upon Na extraction/insertion in a wide Na content range. The main tunnel structure of the $\text{Na}_{0.66}[\text{Mn}_{0.66}\text{Ti}_{0.34}]\text{O}_2$ was maintained during the entire charge/discharge process. In particular, the phase evolution exhibits a symmetric behavior between the charge and discharge processes in the voltage range of 2.7-3.9 V, showing that the phase evolution proceeds through a solid solution reaction upon the initial charge process. It indicates a high structure stability of $\text{Na}_{0.66}[\text{Mn}_{0.66}\text{Ti}_{0.34}]\text{O}_2$ during Na extraction and insertion, which can explain the excellent cycle performance in both nonaqueous and aqueous electrolyte. Furthermore, the solid solution phase transition behavior, which is induced by Ti-substitution, is also expected to enhance the high-rate capability and cycling stability of the $\text{Na}_{0.66}[\text{Mn}_{0.66}\text{Ti}_{0.34}]\text{O}_2$ material..

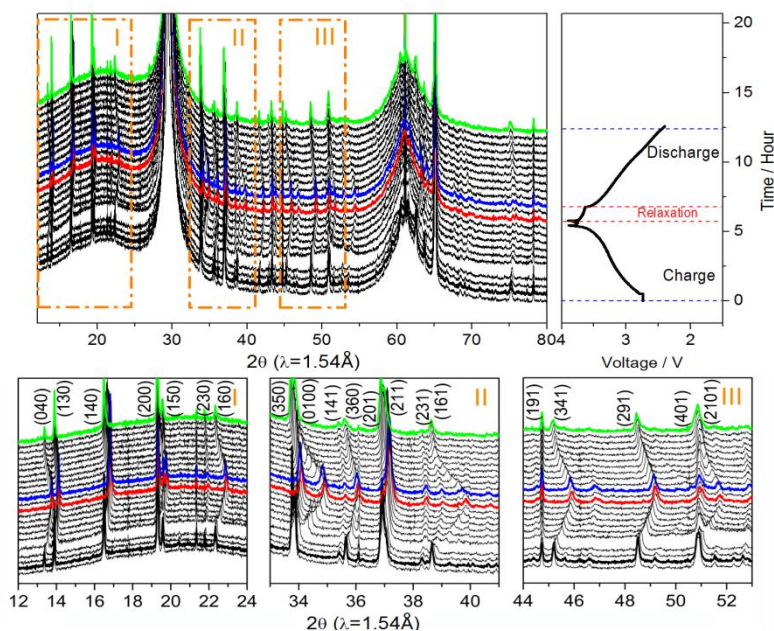


Figure 92. Structure evolution upon Na extraction/insertion. *In situ* X-ray diffraction patterns collected during the first discharge/charge of the $\text{Na}_{0.66}[\text{Mn}_{0.66}\text{Ti}_{0.34}]\text{O}_2/\text{Na}$ half-cell under a current rate of C/10 at a voltage range between 1.5 and 3.9 V. For comparison, the 2θ angle has been converted to values corresponding to the more common laboratory Cu K α radiation ($\lambda = 1.54 \text{ \AA}$).

Patents/Publications/Presentations

Presentation

- 2016 MRS Spring Meeting, Phoenix, Arizona (March 28 – April 1, 2016): “*In situ* Characterization of Advanced Electrode Materials for Na-ion Batteries by Using Synchrotron Based Techniques”; Seongmin Bak, Xiqian Yu, Enyuan Hu, Jue Liu, Hung Sui Lee, Xiao-Qing Yang*, Yong-Sheng Hu, Lin Gu, Hong Li, Xuejie Huang, and Liquan Chen. Invited.